UNIVERSIDADE DA CORUÑA

Programa de Doctorado en Biología Celular y Molecular

TESIS DOCTORAL

Proteomic characterization of the E3 ubiquitin-ligase Hakai: biological insights and new therapeutic strategies

Andrea Díaz Díaz

2020

Directoras:

Dr. Angélica Figueroa Conde-Valvís

Dr. María Esperanza Cerdán Villanueva

The directors of this doctoral thesis, Dr. Angélica Figueroa Conde-Valvís, coordinator of Epithelial Plasticity and Metastasis Group (INIBIC), and Dr. Mª Esperanza Cerdán Villanueva, coordinator of EXPRELA group (UDC),

CERTIFY THAT:

This work, entitled "Proteomic characterization of the E3 ubiquitin-ligase Hakai: biological insights and new therapeutic strategies", was carried out by Andrea Díaz Díaz under our supervision at the Institute of Biomedical Research of A Coruña (INIBIC), and meets the necessary requirements of originality and scientific rigor to be publicly defended and to opt to international PhD in Cellular and Molecular Biology.

And as evidence thereof, we sign this certificate in A Coruña, a 20 de Marzo de 2020

FIGUEROA CONDE-VALVIS ANGELICA - 52988974X

Firmado digitalmente por FIGUEROA CONDE-VALVIS ANGELICA - 52988974X
Fecha: 2020.06.09 12:07:48 +02'00'

Signed: Angélica Figueroa Conde-Valvís

(*Director and tutor*)

CERDAN VILLANUEVA MARIA ESPERANZA - DNI 15811374R

Firmado digitalmente por CERDAN VILLANUEVA MARIA ESPERANZA - DNI 15811374R
Nombre de reconocimiento (DN): c=ES, o=UNIVERSIDAD DE A CORUÑA, ou=CERTIFICADO ELECTRONICO DE EMPLEADO PUBLICO, ou=BIOLOXIA, ou=4845, serialNumber=IDCES-15811374R, sn=CERDAN VILLANUEVA, givenName=MARIA ESPERANZA, cn=CERDAN VILLANUEVA MARIA ESPERANZA - DNI 15811374R
Fecha: 2020.06.09 16:26:00 +02'00'

Signed: Mª Esperanza Cerdán Villanueva

(*Director*)

DIAZ DIAZ, ANDREA (FIRMA)

Firmado digitalmente por DIAZ DIAZ, ANDREA (FIRMA)
Fecha: 2020.06.09 11:11:34 +02'00'

Signed: Andrea Díaz Díaz (*PhD student*)

Part of this research has been carried out during a predoctoral research stay held in 2018 for three months at the Department of Infectious Disease and Immunology at the Institute of Biomedical Sciences of Academia Sinica (Taipei, Taiwan) under the supervision of Dr. Fu-Tong Liu, leader of the group and Vice President of Academia Sinica. This predoctoral research stay was funded by a FPU mobility grant of Ministerio de Educación y Formación Profesional (ID code EST17/00146).

"I was taught that the way of progress is neither swift nor easy."

Marie Curie

A mis padres,

por enseñarme que el esfuerzo transforma sueños en realidades

Siempre pensé que uno de los momentos más deseados a lo largo de una tesis doctoral es este, el escribir los agradecimientos. Cuando el camino se hace largo, este momento se piensa como el principio del final. El trabajo ya está hecho. Pero llegado este momento, empiezas a echar de menos la tempestad que precedió a esta calma y te das cuenta de que, a pesar del largo y duro camino, cada tormenta y huracán han valido la pena, porque ahora sabes que gracias a toda la gente que te encuentras en el camino tú puedes ser más fuerte que el viento.

Qué poco me cuesta ponerme sentimental… y es que, aunque yo soy más bien del estilo "toxo", a mi pequeño corazoncito no le gusta cerrar etapas y dejar buenos momentos atrás. Pero hasta aquí hemos llegado, y ya toca dejar de pensar en uno mismo y en sus agobios y dar las gracias a todos aquellos que han pasado desapercibidos pero que han sido imprescindibles para capear el temporal.

Me gustaría comenzar dando gracias a aquellos que me guiaron en mis primeros pasos. A todos los profesores que a lo largo de mi carrera universitaria me han transmitidos sus conocimientos con tanto cariño y confianza. En especial a María y Javier, los que me "metieron el gusanillo" por la investigación y tienen gran parte de "culpa" de que haya llegado hasta aquí. Y a mi Marta, mi primera mentora en el laboratorio. ¡Qué suerte he tenido de aprender de ti!

Gracias, por supuesto, a mis directoras, la Dra. Angélica Figueroa y la Dra. Esperanza Cerdán. Gracias por depositar en mí toda vuestra confianza y paciencia. Por abrirme las puertas al gratificante mundo de la docencia. Por mantenerme a flote con vuestro optimismo y por celebrar conmigo cada pequeño logro. Este trabajo ha sido fruto de todo vuestro apoyo.

A aquellos que, con gran profesionalidad y mucho cariño, han facilitado el desarrollo de este trabajo: a las plataformas de Proteómica y Genómica del INIBIC, los Servicios de Apoyo a la Investigación de la UDC, y el Servicio de Histomorfología del INIBIC.

I would also like to thank all the people who guided and welcomed me during my predoctoral stay in Taiwan. To Dr. Fu-Tong Liu, Dr. Hung-Ling Chen and Dr. Ming Hsiang Hong for opening their laboratory doors and teaching me everything they knew. To Annie for having that much patience with me and being my shadow. To Poyuan, for his help and being so adorable. And to Jack and Hank, for always lending to help at any time with a big smile. Thanks also to all the good friends that I made there and that made me feel at home. You have all contributed to the

greatest experience of my life. I never thought travelling to the opposite side of the world would become one of the best decisions of my life.

Gracias a todos los compañeros del INIBIC. Todos y cada uno de vosotros habéis hecho mis días más fáciles. Desde las conversaciones en cultivos, las carcajadas durante la comida, hasta las miradas cómplices en el laboratorio los fines de semana. Todos me habéis ayudado con una sonrisa siempre que lo he necesitado y me siento afortunada de haber compartido este tiempo y espacio con vosotros. Sois grandes, como científicos y personas.

Gracias en especial a Sari, por tener una solución para todo y ser como una madre para nosotros, aun cuando solo provocamos desastres. A Vale, Patri, y todas las proteómicas en general, por enseñarme una pequeña parte de su mundo y haber atendido mis múltiples dudas con tanto cariño. A Patri y a Miriam, por permitirme aprender de vosotras a dar el mejor trato posible a los pequeños ratoncillos tan tristemente imprescindibles en investigación. Gracias a Isa, por acogernos a todos bajo su ala y ser una fuente inagotable de experiencia para nosotros. A mis chicas de inflamación, Jenny y Oli, por ser tan sumamente adorables, permitirme esas visitas improvisadas a vuestra poyata y darme conversación durante las tediosas horas de cultivos. Y a Paloma, que me recibió con los brazos abiertos a mi llegada y los sigue abriendo siempre que lo necesito.

Gracias también a mis compis de EXPRELA, a Mónica, Aida, María, Martín y Juanjo. Por hacerme sentir como en casa cada día que he pasado en vuestro laboratorio y por vuestra generosidad compartiendo conmigo vuestros conocimientos. Sois un gran equipo.

Y por supuesto, gracias a todos los miembros integrantes de "Lechs for you". Alba, Dani, Dalmao… Habéis sido imprescindibles en esta odisea y lo seguís siendo. Ese movimiento sensual de rodillas en León me lo llevo para toda la vida. El momento sidras "ti eres malnacida" en Gijón. Muchas mañanas, muchas tardes y algunas noches juntos que han hecho todo más fácil. Tampoco me olvido de mi Martiña, ahora emigrada a Euskadi. Aunque coincidimos poco tiempo, fue el suficiente para que me robaras el corazón y me enseñaras a hacer geles sin pocillos. Os deseo toda la suerte del mundo y sé que os tengo para siempre.

A toda la gente que no forma parte del mundo de la investigación, pero sí del mío. A todos mis amigos, que siempre han confiado en mí y me han hecho olvidar los momentos más bajos con chistes malos (muy malos), múltiples repeticiones de vídeos chorras, grandes conversaciones y

muchos bailes (últimamente sé que no tantos, culpa mía). Xuli, Aitortxu, Francis, Jaco, Paco, Iván, Dani, Miguel, Luis, Buce, Hernán y Jano. Sois todos "la pera" (en las tesis no se pueden decir tacos), y me siento afortunada de que "la casualidad" os haya puesto en mi camino.

Y como no… a esa "casualidad". Mi pequeño y rabudo Jesús. El único capaz de sacarme de quicio, pero también de proporcionarme la calma más completa. Siempre te digo que no sé qué haría sin ti, y es verdad. Has sorteado conmigo todos los baches durante estos casi cinco años y sé que no ha sido fácil. Me has escuchado y me has comprendido, incluso cuando quien más necesitaba ser escuchado eras tú. Has creído en mí siempre y me has alentado a perseguir y conseguir todos mis sueños. Sabes que todo lo que aquí pueda decir es poco, pero sí diré que doy las gracias por tenerte a mi lado y que si hoy me encuentro escribiendo estas líneas es en gran parte gracias a ti.

Y, por último, pero no menos importante, a mi familia, los que me han acompañado desde que la pequeña Andrea echó a andar sin saber muy bien hacia dónde. A todos. A los que por desgracia ya se han ido, me gusta imaginar que estéis donde estéis, estáis orgullosos de mí. A mi hermano, porque siempre me has demostrado lo orgulloso que estás de mí, de tu hermanita, y me has enseñado que en la vida tienes que luchar por lo que te hace feliz. Y por supuesto, Papá, Mamá… Sois mis personas favoritas y mi gran ejemplo a seguir. Probablemente nunca os haya dado las gracias, así que aprovecho este momento y el cobijo del papel para hacerlo. Gracias por pensar siempre en lo mejor para mí. Por esas poesías de Gloria Fuertes y los juegos de la memoria que me han traído hasta aquí. Por perdonar mis errores. Por enseñarme que todo esfuerzo tiene su recompensa y que todo se puede conseguir, solo hay que querer. Gracias por traerme de la mano hasta este momento. Este trabajo es obra vuestra. Os quiero.

A todos y cada uno de vosotros, gracias de corazón.

Os llevo en él para siempre.

Andrea.

INDEX

ABBREVIATIONS

17-AAG	17-N-allylamino-17-demethoxygeldanamycin (Tanespimycin)
17-DMAG	17-Dimethylaminoethylamino-17-demethoxygeldanamycin (Alvespimycin)
3-MA	3-Methyladenine
aa	Amino acid
ADP	Adenosine diphosphate
AJCC	American Joint Committee on Cancer
AMBIC	Ammonium bicarbonate
ATCC	American Type Culture Collection
ATP	Adenosine triphosphate
AUY922	Luminespib
BCA	Bicinchoninic Acid Assay
BSA	Bovine Seroalbumin
CBBL1	C-cbl-like protein gene 1
CDH1	Cadherin 1 gene
cDNA	Complementary DNA
CE	Collision energy employed
CFTR	Cystic fibrosis transmembrane conductance regulator
CHX	Cycloheximide
CID	Collision-induced dissociation
CK1	Casein kinase 1
CMA	Chaperone-mediated autophagy
CQ	Chloroquine
CRD	Carbohydrate-recognition domain
CUR	Curtain gas
DAB	Diaminobenzidine
DDA	Data-dependent acquisition
DEPC	Diethyl pyrocarbonate
DMEM	Dulbecco's Modified Eagle's Medium
DMSO	Dimethyl sulfoxide
DNA	Deoxyribonucleic acid

dNTPs	Deoxynucleotide Triphosphates
DOK-1	Docking protein 1
EBV	Epstein Barr Virus
EDTA	Ethylenediaminetetraacetic acid
EGFR	Epithermal growth factor receptor
EMT	Epithelial-to-mesenchymal transition
ER	Estrogen receptor
ESCRT	Endosomal sorting complex required for transport
FACS	Fluorescence-Activated Cell Sorting
FBS	Fetal Bovine Serum
FDA	Food and Drug Administration
FDR	False discovery rates
G418	Geneticin
GA	Geldanamycin
GAPDH	Glyceraldehyde 3-phosphate dehydrogenase
GO	Gene Ontology database
HCC	Hepatocellular carcinoma
HIF1-α	Hypoxia Inducible Factor 1 alpha
HPLC	High-performance liquid chromatography
HPRT	Hypoxanthine-guanine phosphoribosyl transferase gene
HRP	Horseradish peroxidase
Hsp90	Heat shock protein 90
HYB	Hakai pY-binding domain
INFγ	Interferon gamma
ISVF	Ion spray voltage floating
iTRAQ	Isobaric tag for relative and absolute quantitation
JAM	Junctional adhesion molecules
LC3	C-type lectin 3
LC-MS	Liquid chromatography coupled to mass spectrometry
Lys	Lysine
MET	Mesenchymal-to-epithelial transition
$MgCl_2$	Magnesium chloride
miRNAs	Micro ribonucleic acid

MMLV	Moloney Murine Leukemia Virus
MMPs	Metalloproteinases
MMTS	Methylmethanethiosulfonate
mRNA	Messenger ribonucleic acid
MTT	3-(4,5-dimethylthiazol-2-yl)-2,5-diphenyltetrazolium bromide
MVBs	Multivesicular bodies
nano-LC	nano liquid chromatography
NSCLC	Non-squamous cell lung carcinoma
p120ctn	Adherens junction protein p120
PAGE	Polyacrylamide gels
PBS	Phosphate buffered saline
PCR	Polymerase chain reaction
PFA	Paraformaldehide
PI3K	Phosphatidylinositol 3-kinases
PMSF	Phenylmethanesulphonyl fluoride
PSF	Polypyrimidine tract binding protein associated splicing factor
PVDF	Polyvinylidene fluoride membranes
qPCR	Real-time quantitative PCR
RIPA	Radioimmunoprecipitation assay buffer
RNA	Ribonucleic acid
RP-LC	Reversed-phase liquid chromatography
RT	Room temperature
SDS	Sodium dodecyl sulfate
SEM	Standard error of the mean
Ser	Serine
SH3	Src homology 3
siRNAs	silencing RNA
Src	Proto-oncogene tyrosine-protein kinase Src
STA-9090	Ganetespib
TCEP	Tris(2-carboxyethyl) phosphine
TEAB	Triethylammonium bicarbonate buffer
TEMED	Tetramethylethylenediamine
TGF-β	Transforming growth factor β

TKI	Tyrosine kinase inhibitor
TRAP1	Tumor necrosis factor receptor associated-protein 1
Tyr	Tyrosine
UCB	Urothelial carcinoma of the bladder
UICC	Union for International Cancer Control
VLF	Vinflunine
WTAP	Will's tumor 1-associating protein
ZEB1	Zinc finger E-box-binding homebox 1
ZEB2	Zinc finger E-box-binding homebox 2
ZO-1	Zonula occludens-1 protein

FIGURE INDEX

TABLE INDEX

SUMMARY

RESUMEN

El carcinoma es el tipo más común de cáncer y surge de las células epiteliales. La transición del adenoma al carcinoma se asocia con la pérdida de E-cadherina y, en consecuencia, de los contactos intercelulares. La E-cadherina es un supresor tumoral que está regulado negativamente durante la transición epitelio-mesénquima (EMT) y su pérdida es un marcador de mal pronóstico durante la progresión tumoral. Hakai es una E3 ubiquitina-ligasa que media en la ubiquitinación de la E-cadherina, su endocitosis y consecuente degradación. Aunque la E-cadherina es el sustrato más conocido de Hakai, otras dianas moleculares reguladas por Hakai pueden estar involucradas en la plasticidad celular durante la progresión tumoral. En este trabajo, empleamos la técnica iTRAQ para explorar nuevas rutas moleculares involucradas en la EMT inducida por Hakai. Nuestros resultados muestran que Hakai puede tener una influencia importante sobre proteínas relacionadas con el citoesqueleto, proteínas extracelulares asociadas con el exosoma, proteínas relacionadas con el ARN y proteínas involucradas en metabolismo. Entre las proteínas reguladas por Hakai, describimos la Anexina A2 como un nuevo posible sustrato de Hakai. Además, nuestros resultados revelan que la inhibición farmacológica de Hsp90 con geldanamicina resulta en la degradación de Hakai vía lisosoma. Así, proponemos a Hakai como una nueva proteína cliente de la chaperona Hsp90, destacando un mecanismo novedoso por el cual los inhibidores de Hsp90 pueden influir en el proceso EMT mediado por Hakai y el tratamiento del cáncer.

RESUMO

O carcinoma é o tipo de cancro máis común e xorde das células epiteliais. A transición do adenoma ao carcinoma está asociada á perda de E-cadherina e, en consecuencia, aos contactos intercelulares. A E-cadherina é un supresor tumoral que se encontra regulado negativamente durante a transición epitelio-mesénquima (EMT), e a súa perda é un marcador de mala prognose durante a progresión do tumor. Hakai é unha E3 ubiquitina-ligasa que media a ubiquitinización da E-cadherina, a súa endocitose e a súa conseguinte degradación. Aínda que a E-cadherina é o substrato máis coñecido de Hakai, outras dianas moleculares reguladas por Hakai poden estar implicadas na plasticidade celular durante a progresión tumoral. Neste traballo empregamos a técnica iTRAQ para explorar novas vías moleculares implicadas na EMT inducida por Hakai. Os nosos resultados mostran que Hakai pode ter unha influencia importante sobre proteínas relacionadas co citoesqueleto, proteínas extracelulares asociadas co exosoma, proteínas relacionadas co ARN e proteínas implicadas no metabolismo. Entre as proteínas reguladas por Hakai, describimos a Anexina A2 coma un novo posible substrato de Hakai. Además, describimos una relación entre Hakai e o complexo chaperona da proteína Heat shock protein 90 (Hsp90). Tamén, os nosos resultados revelan que a inhibición farmacolóxica de Hsp90 con geldanamicina resulta na degradación de Hakai vía lisosoma. Así, propoñemos a Hakai como unha nova proteína cliente da chaperona Hsp90, destacando un novo mecanismo polo cal os inhibidores de Hsp90 poden influir no proceso de EMT mediado por Hakai e no tratamento do cancro.

ABSTRACT

Carcinoma is the most common type of cancer and arises from epithelial cells. Transition from adenoma to carcinoma is associated with the loss of E-cadherin and, in consequence, the disruption of cell−cell contacts. E-cadherin is a tumor suppressor which is down-regulated during epithelial-to-mesenchymal transition (EMT), and its loss is a predictor of poor prognosis during tumor progression. Hakai is an E3 ubiquitin-ligase that mediates E-cadherin ubiquitination, endocytosis and consequent degradation. Although E-cadherin is the most established substrate for Hakai activity, other regulated molecular targets for Hakai may be involved in cancer cell plasticity during tumor progression. In this work we employed an iTRAQ approach to explore novel molecular pathways involved in Hakai-driven EMT. Our results show that Hakai may have an important influence on cytoskeleton-related proteins, extracellular exosome-associated proteins, RNA-related proteins and proteins involved in metabolism. Among Hakai-down-regulated proteins, we describe Annexin A2 as a new possible susbtrate for Hakai. Moreover, we also report an interaction between Hakai and the heat shock protein 90 (Hsp90) chaperone complex. Besides, our results reveal that the pharmacological inhibition of Hsp90 with geldanamycin results in the degradation of Hakai in a lysosome-dependent manner. Based on that, we propose Hakai as a new client protein of Hsp90 chaperone highlighting a new mechanism by which Hsp90 inhibitors may influence Hakai-mediated EMT process and cancer treatment.

I. INTRODUCTION

1. Cancer epidemiology

Nowadays, cancer constitutes a high prevalence disease and the second cause of death in the world, showing an increasing rate of mortality due to the aging of population and the modern life acquired habits. According to National Institute of Cancer, the forecast is that the number of new cases of cancer increases from 14,1 million in 2012 up to 23,6 million in 2030. According to the World Health Organization, one out of six deaths in the world is due to cancer disease, and around a third of these deaths are related to five principal risk factors, such as high index of body mass, bad eating habits, alcohol intake, sedentary life and smoking. Besides these risk factors, cancer incidence is also determined by genetic factors and exposure to external agents such as ultraviolet radiation, chemical contaminants (arsenic, aflatoxins, tobacco smoke) and biological factors such as some types of virus, parasites and bacteria. According to data published by GLOBOCAN in 2018, up to date, lung, breast and colorectal cancers constitute the most prevalent types of cancer, and lung, colorectal and stomach cancers, those with a greater mortality in both sexes (Figure 1).

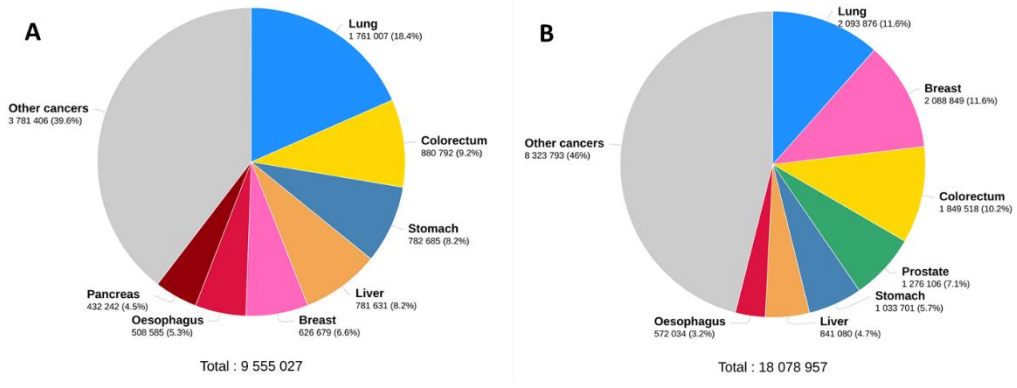

Figure 1. Estimation of new cancer cases and deaths during 2018. Number of estimated deaths (**A**) and number of new cases (**B**) of different types of cancer among global population in the world in 2018. Image obtained from International Agency for Research on Cancer. Source: GLOBOCAN, 2018. https://gco.iarc.fr/today/online-analysis-pie.

According to GLOBOCAN, in 2018, the most common type of cancer in the world among male population is lung cancer (14,5 %), followed by prostate cancer (13,5 %), and colorectal cancer (10,9 %) (Figure 2A). Among worldwide female population, the most incident type of cancer is breast cancer (24,2 %), followed by colorectal cancer (9,5 %) and lung cancer (8,4 %) (Figure 2B). Data of incidence and death cases of cancer vary between continents. Nowadays, Asia is

the continent with the highest incidence due to the exposure to contaminants and to the dietetic habits, followed by Europe with the second highest rate of cancer incidence. According to National Institute of cancer, in 2012 57 % of new cases of cancer and 65 % of death cases were focused in less developed regions, such as Africa and Central America, due to the scarce preventive campaigns and the lack of assistance resources. On the other hand, more developed countries, such as United States, have experimented a marked decrease for the past two decades in the number of cases of cancer deaths. This fact is due to new advances and preventive campaigns, which caused a reduction of 26 % of death cases in 2015 compared to those reported in 1991 by American Cancer Society.

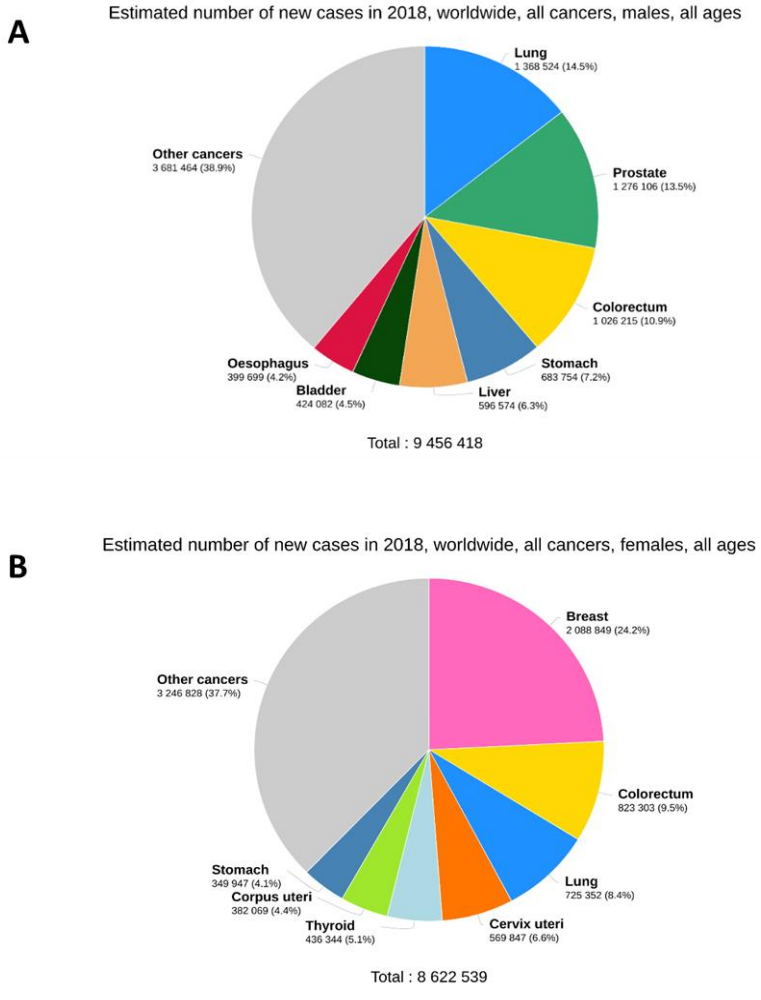

Figure 2. Incidence of different types of cancer in the world. Cancer incidence distribution among male (**A**) and female (**B**) population. Data obtained from International Agency for Research on Cancer. Source: GLOBOCAN, 2018. https://gco.iarc.fr/today/online-analysis-pie.

In Spain, colorectal cancer is the most prevalent in both sexes (13,7 %), followed by breast cancer in women (12,1 %) and prostate cancer in men (11,7 %) [1].

2. Tumors of epithelial origin: carcinomas

2.1. General introduction

Carcinoma is currently the most common type of cancer and it is characterized for emerging from epithelial cells, including those conforming the skin and those conforming the epithelium lining internal organs, such as intestine, lung or breast. Epithelial cells are characterized for being settled down as one or various layers and for being anchored between them and to a basal membrane, thus constituting a polarized and integral tissue. In vertebrates, epithelial cells are connected to each other by four different types of cell junctions, such as: 1) tight junctions, responsible of the impermeability of soluble molecules between epithelial layers and mainly mediated by occludins, claudins and junctional adhesion molecules (JAM); 2) Gap junctions, mainly mediated by connexins, which are responsible of connecting the cytoplasm of adjacent cells allowing molecule exchange; 3) desmosomes, a strong structure specialized in cell-cell adhesion, located in plasma membrane and constituted by different cadherin members, such as desmoglein or desmocollin, which link to intermediate filaments; and 4) adherens junctions, which are adhesive structures regulated in a calcium-dependent manner and constituted by transmembrane proteins, including cadherins and nectins (Figure 3). Cadherins mediating adherens junctions were first described by Takeichi, Kemler and Jacob as a cell-cell adhesion-mediating superfamily of 20 members. Among this superfamily, most described proteins have been classical cadherins, which include epithelial (E), neural (N), placental (P), vascular-endothelial (VE), kidney (K) and retinal (R) cadherins. Extracellular regions of cadherins and nectins mediate adhesion to adjacent cells, while their intracellular regions interact with multiple proteins responsible of the dynamics of adherens junctions by their interaction with actin cytoskeleton and the activation of different signaling pathways [2, 3].

In addition to cell junctions, epithelial cells are also anchored to the extracellular matrix by hemidesmosomes and focal adhesions, which guarantee lateral but not vertical movements, therefore facilitating the maintenance of the epithelium structure and preventing them from crossing the extracellular matrix [4]. Altogether, cell-cell junctions and cell-matrix junctions constitute an impassable protective barrier that protects body surfaces, ducts, gut and glands,

and are essential for the maintenance of a healthy epithelial structure [5]. However, in certain pathologies including cancer, the loss of this characteristic structure may induce the beginning of a carcinogenic process.

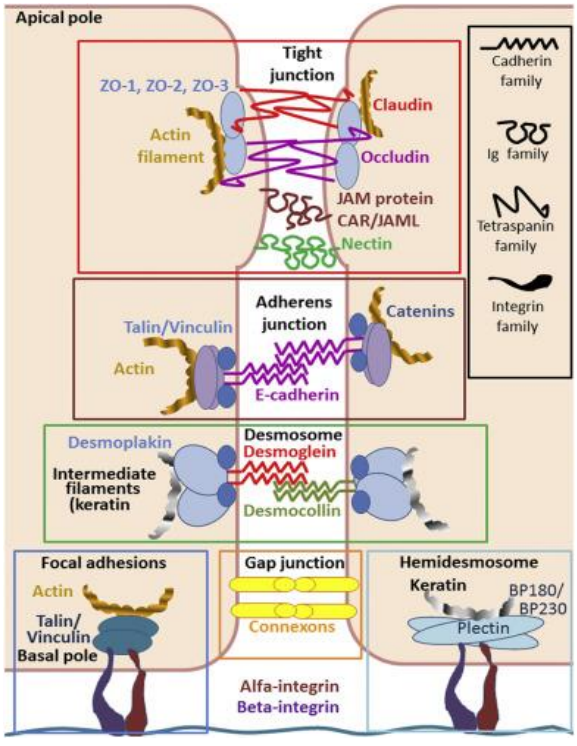

Figure 3. Schematic representation of proteins constituting epithelial cell junctions. Tight junctions, adherens junctions, desmosomes, Gap junctions and hemidesmosomes are conformed by different intracellular and transmembrane proteins represented in the image. Image obtained from Shilova *et al*., 2018.

The emergence of carcinoma is based on the disruption of cell-cell junctions and cell-matrix junctions, thus causing the loss of the characteristic apico-basal polarity of epithelial cells and the architecture of epithelial tissue. Carcinoma usually arises in the basal layer of the epithelium by the appearance of a pre-malign lesion, and remains as a benign located lesion limited to the epithelial cell layer. Over time, carcinoma cells can disrupt the basal membrane and initiate invasion thanks to the acquisition of invasive properties and the ability to degrade the extracellular matrix, turning the benign lesion into a malignant lesion called primary tumor. During this process, tumor and stromal cells secrete different molecules, such as extracellular matrix metalloproteinases (MMPs), which allow them to degrade extracellular matrix and invade. Parallelly, tumor cells secrete angiogenic factors which induce de formation of blood

vessels around the tumor, providing the tumor the oxygen and nutrients necessary for proliferation [6]. This process, known as angiogenesis, gives tumoral cells the ability to intravasate into the bloodstream and migrate to distant organs, where they can extravasate and constitute new micrometastases [7]. These lesions can eventually initiate an uncontrolled proliferation and give rise to secondary tumors called metastases or macrometastases. This event implies a worse prognosis for the patient, since they are currently responsible of 90% of cancer deaths (Figure 4).

These events are caused due to the combination of multiple factors, such as mutations or epigenetic modifications that regulate the expression of different genes, including tumor suppressors, oncogenes or genes related to DNA repair. Taken together, these alterations give cells typical physiological qualities of tumoral cells, such as the ability to evade programmed cell death or apoptosis, to proliferate uncontrollably, to stimulate angiogenesis and to invade and metastasize [8].

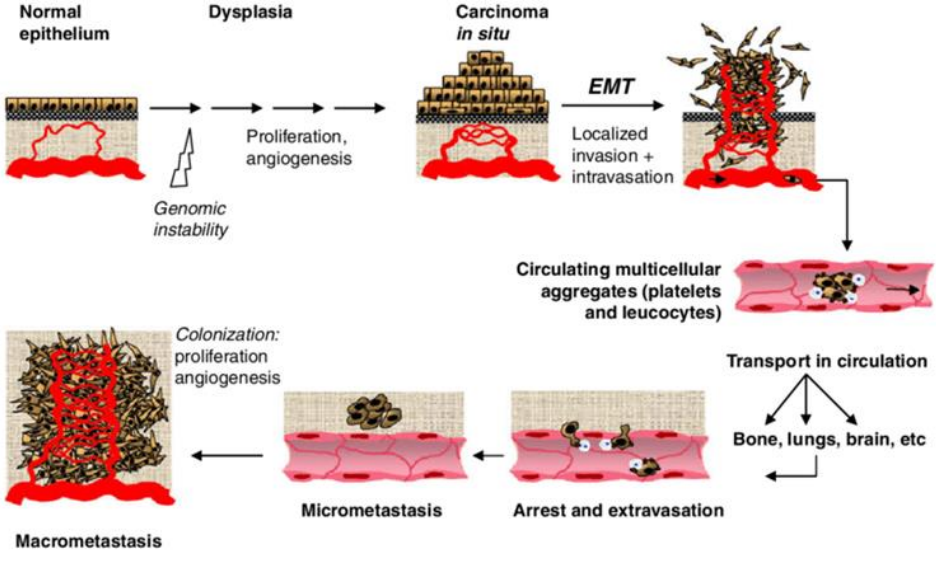

Figure 4. Main steps during carcinoma formation, tumor progression and metastasis. Genetic cell instability may eventually give rise to a neoplastic lesion with high cellular proliferation which can derive in a carcinoma *in situ*. Some of the tumoral cells may acquire the ability to migrate and invade extracellular matrix and to reach blood vessels. Tumoral cells can intravasate and migrate through the bloodstream to distant organs, where they can extravasate and form distant metastasis. Image obtained from Buijs and van der Pluijm, 2009.

2.2. Carcinoma classification systems

There exist different cancer staging systems that can define anatomical extent of cancer. Usually, different stages are referred to the size of the tumor and whether there has been an extension of it from the primary tumor to lymph nodes or secondary organs. The determination of the tumor stage is performed by doctors through the use of diagnostic techniques, such as X-rays, magnetic resonance, imaging, biopsies or other laboratory tests. All these test help to determine not only the existence of a tumor, but also the extent of the disease.

The American Joint Committee on Cancer (AJCC) and the Union for International Cancer Control (UICC) provide TNM system as the common staging classification for stablishing the scope of the disease. TNM system is based on a letter and number classification meaning:

- T: primary tumor
- N: number of affected lymph nodes
- M: presence of metastasis in distant organs

Meaning of each letter and number is summarized in the following table:

Table 1. General TNM classification system.

Tumor	Tx	Tumor cannot be measured
	T0	No evidence of primary tumor
	Tis	Tumor *in situ* growing in the superficial layer of the tissue
	T1, T2, T3, T4	Tumor size and invasion of adjacent tissues. T can be also divided to provide further information (T3a, T3b…)
Nodes	Nx	Lymph nodes cannot be evaluated
	N0	Lymph nodes are not affected
	N1, N2, N3	Number and ubication of affected lymph nodes
Metastasis	M0	No cancer spread to distant organs
	M1	Cancer has been spread to distant organs

This common version can be modified depending on the type of cancer, so the meaning of the letters and numbers can change according to the scope of the disease. Moreover, TNM classification can be simplified in five different numerical stages:

- Stage 0 or carcinoma *in situ*: abnormal cells have not spread to adjacent tissue. Is not considered cancer but may eventually become cancer.
- Stage I, Stage II and Stage III: considered as cancer. Level of spread to adjacent tissues is represented by the stage number.
- Stage IV: Cancer has spread to distant organs.

Besides TNM classification, there exist other classification systems depending on the type of cancer, such as Dukes' or Astler-Coller systems for colorectal cancer. Moreover, TNM classification is not used for brain cancer staging, as it usually spreads to other encephalic organs but not to lymph nodes or distant organs. Also, liquid tumors, such as lymphomas, do not use TNM classification but Ann Arbor staging system [9].

3. Epithelial-to-mesenchymal transition program (EMT)

3.1. Physiological and pathological EMT

During initial phases of carcinoma progression, epithelial tumor cells undergo a series of phenotypic and genotypic transformations encompassed in a process known as epithelial-to-mesenchymal transition (EMT), which is associated with the initial phases of tumor progression and metastasis. During the EMT process, tumor cells experience genetic alterations which lead to the loss of their epithelial characteristics, such as an apical-basal polarity or cell-cell and cell-matrix contacts, and acquire a mesenchymal phenotype characterized by the loss of cell polarity, the absence of cell junctions, the presence of pseudopodia, and the expression of mesenchymal markers, among others. These characteristics, confer tumor cells a greater capability of migration and invasiveness typical of a malignant cellular phenotype [10]. Changes in cell behavior and morphology are responsible of the ability of tumor cells to degrade extracellular matrix and to initiate migration through blood vessels and lymphatic system. This causes dissemination of tumor cells and thus metastases in distant organs, the latter a phenomenon which is facilitated by the activation of the reverse process called mesenchymal-to-epithelial transition (MET). The appearance of secondary epithelial tumors in distant organs and the completion of the metastatic process constitute nowadays the main cause of death during cancer disease [10-12].

The EMT process was first described by Greenburg and Hay in the 1980s in embryonic epithelial cells. They observed that embryonic epithelial cells lost their phenotype and acquired mesenchymal characteristics, such as cytoplasmic projections, that allowed them to desegregate from the primary explant and to migrate individually [13, 14]. Later on, this same process was described during tissue regeneration in wound healing and fibrosis. It was observed that skin resident keratinocytes were able to migrate across the wound to restore epithelial tissue integrity. Finally, as previously mentioned, EMT was associated to tumor progression as a pathological process. In this way, the EMT process has been described in three different biological contexts, among which we can find both physiological and pathological processes. Although all have in common the acquisition of mesenchymal characteristics, the way in which this phenotype is acquired varies among the different types of EMT. Currently, EMT can be classified in three categories according to its related biological process: 1) EMT type I, occurring during embryogenesis; 2) EMT type II, occurring during tissue repair or fibrosis; and 3) EMT type III, occurring during tumoral progression [15].

3.2. EMT and tumor progression

As previously mentioned, the acquisition of mesenchymal phenotype and characteristics by epithelial cells is necessary to start the carcinogenic process. This phenotypic change is determined by the loss of epithelial markers, the loss of cell-cell and cell-matrix junctions, the loss of cell polarity and the ability to degrade local basement membrane, which allows cells to initiate the migration and invasion process and to avoid programmed cell death (Figure 5). Initiation of the EMT process is accompanied by the loss of epithelial markers, such as E-cadherin, cytokeratins, zonula occludens-1 (ZO-1), desmoplakin and laminin. The loss of epithelial markers is accompanied by the appearance of mesenchymal markers, including N-cadherin, Vimentin, Cadherin-11 and other proteins present in the extracellular matrix, such as Collagen or Fibronectin (Figure 5) [12, 16]. Also, accumulation of β-catenin in the nucleus is a characteristic event during EMT. E-cadherin degradation induces β-catenin accumulation in the cytoplasm, which allows its eventual translocation to nucleus under Wnt signaling pathway activation [17]. In nucleus, β-catenin activates genetic expression of different oncogenes such as c-Myc or Cyclin D1, thus contributing to the development of EMT process [18]. Moreover, EMT also entails a change on gene activation, including genes implicated in cell proliferation, cell differentiation, activation of anti-apoptotic pathways, cell movement or proteolytic digestion [19].

Generally, the EMT is a reversible process. Cells which have lost their epithelial phenotype and acquired a mesenchymal phenotype are eventually able to revert that process and get back to its original phenotype during MET. This ability, thanks to which cells are able to differentiate and dedifferentiate, is known as cellular plasticity [20]. Epithelial plasticity allows tumor cells to adapt to the tumor microenvironment and is essential for them to succeed during the metastatic process.

However, cellular plasticity is not experienced by tumor cells at once, and tumors show a lot of heterogeneity during EMT process. In fact, it is possible to find cells within the same tumor at different stages of EMT, showing either epithelial or mesenchymal phenotypes. Given the genetical and phenotypical differences among tumoral cells, intratumoral heterogeneity has been postulated to be the responsible of anticancer drug resistance, and currently represents an important scientific challenge [21, 22].

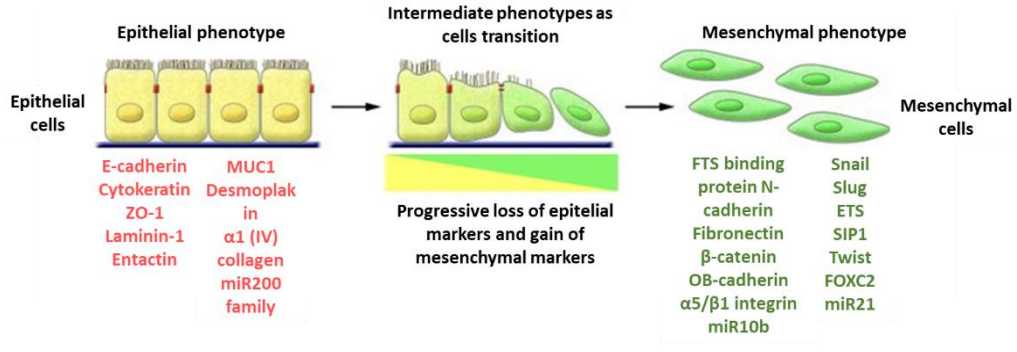

Figure 5. Molecular and phenotypic changes suffered by epithelial cells during EMT. Polarized epithelial cells express a series of epithelial markers which are lost during the initiation of the EMT process. During initial stages of EMT cells express intermediate phenotypes, expressing both epithelial and mesenchymal markers. Once the EMT is completed, cells acquire a mesenchymal phenotype, accompanied by the complete loss of epithelial markers and the expression of mesenchymal markers. Image obtained and modified from Kalluri and Weinberg, 2009.

3.3. EMT regulation during tumor progression

The whole cascades of signaling agents that trigger the initiation of EMT program remain still unclear. However, it is known that, besides protein stability, EMT is modulated at multiple levels, such as epigenetic, transcriptional, post-transcriptional and post-translational level [12].

- Epigenetics: DNA methylation, histone acetylation and phosphorylation, as well as their reverse processes, have been reported during EMT regulation. These changes may affect cell differentiation and proliferation by DNA methylation-induced silencing affecting cell cycle regulator proteins, such as p21 or p53. Furthermore, methylation can also regulate miRNAs expression, important in EMT regulation [23].

- Transcriptional regulation: transcription of genes encoding proteins implicated in cell adhesion is highly regulated during EMT. Some transcription factors, such as Snail, Slug, ZEB1, ZEB2 and Twist, have been described to be activated during EMT and to cause repression of E-cadherin transcription, thus contributing to the loss of the epithelial phenotype [24].

- Post-transcriptional regulation: alternative splicing may regulate protein isoform expression with antagonist functions, and thus regulate the EMT process. CD44 splice isoform switching has been reported to be essential during EMT in breast cancer [25]. In addition, EMT has been widely reported to be regulated by miRNA-mediated control of gene expression. miR-200 and miR-34 have been described to interact with ZEB and SNAI1 mRNA and down-regulate its expression, thus increasing epithelial differentiation [26]. Other miRNAs have been related to poor outcome in cancer progression, such as miR-21, miR-373 or miR200c [27-30].

- Post-translational regulation: modification of transcription factors, such as phosphorylation, SUMOylation, or glycosylation, have also been reported to play a regulatory role during EMT process. Specifically, protein phosphorylation may promote ubiquitin-mediated proteasome degradation of important EMT regulatory proteins. For example, Glycogen synthase kinase 3 beta (GSK-3β) phosphorylates Snail and induces its ubiquitination and proteasome degradation. On the other hand, Snail can also be phosphorylated by the Protein kinase D1 (PKD1), which induces its transcriptional repression [31].

Due to the great complexity and relevance of the EMT process in the progression of cancer disease, the study of those proteins and genes whose expression is altered during the EMT is being deeply studied. Identification of new EMT regulated targets may lead to the design of new possible therapeutic targets for cancer progression treatment and prevention.

3.4. E-cadherin as a hallmark of EMT process

As previously mentioned, E-cadherin is one of the most characterized cadherins in epithelial cells. E-cadherin contributes to cell-cell adhesion and is described as tumor suppressor that plays an anti-invasive and anti-metastatic role. Nowadays, its loss is considered a hallmark of the EMT process.

E-cadherin is a 120 kDa single-pass transmembrane glycoprotein present at the basolateral membrane in adherens junctions of epithelial cells and responsible of the maintenance of Ca^{2+} dependent cell-cell adhesion. It consists of an extracellular domain with five tandem repeated domains, a transmembrane domain and an intracellular domain bound to p120-catenin and β-catenin, which links E-cadherin to actin cytoskeleton through its union to α-catenin (Figure 6) [32, 33].

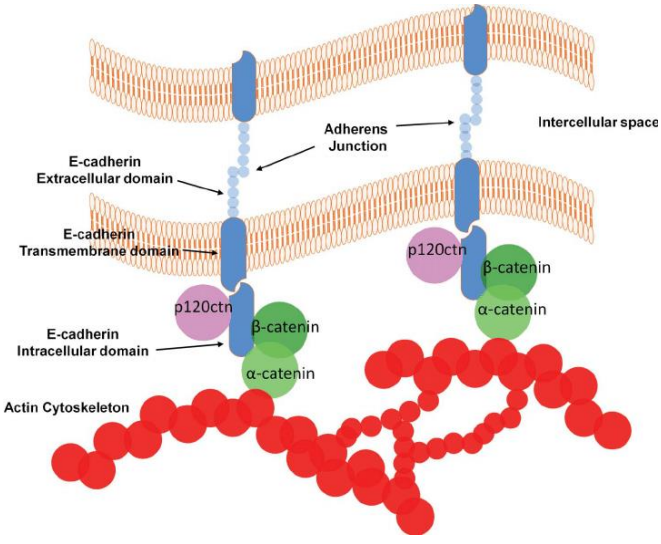

Figure 6. Structure of the E-cadherin complex mediating adherens juntions. Intracellular domain of E-cadherin binds to β-catenin and p120ctn. The complex is linked to actin cytoskeleton through α-catenin. Extracellular domains of adjacent cells bind to each other by calcium activated dimerization. Image obtained from Gall and Frampton, 2013.

Given the importance of E-cadherin in cancer, the mechanisms involved in its inactivation have been extensively studied. Different mechanisms have been described so far for E-cadherin down-regulation, including regulation at a genetic or epigenetic level, transcriptional level and, more recently, post-transcriptional level:

- Genetic and epigenetic regulation: alterations in *CDH1* gene encoding E-cadherin causes the loss of its functionality. *CDH1* was found to experiment somatic mutations in different types of cancer, such as breast cancer and gastric cancer [34]. Germline mutations were also detected in *CDH1* gene for lobular breast cancer and gastric cancer [35]. Moreover, *CDH1* promoter can be methylated in different carcinoma cell lines causing E-cadherin silencing. Prostate, gastric and breast tumor lesions showed a methylated E-cadherin promoter compared to adjacent healthy tissue [36, 37]. In gastric cancer, methylation of E-cadherin promoter was related to *Helicobacter pylori* infection or Epstein Barr Virus (EBV) infection [38, 39]. It has also been suggested that E-cadherin promoter methylation is related to epigenetic regulation caused by Methyl-CpG-binding protein 2 (MECP2) and histone deacetylation [40, 41].

- Transcriptional regulation: control of E-cadherin down-regulation has also been described to occur at transcriptional level. Different transcription factors are responsible of transcriptional regulation of E-cadherin such as, Twist, Snail, ZEB-1, ZEB-2, E47 and Slug. These were described to repress E-cadherin expression through its binding to the E-box situated near *CDH1* promoter [42-48].

- Post-translational regulation: different mechanism of E-cadherin post-translational regulation have also been described such as glycosylation, proteolysis or phosphorylation. E-cadherin N-glycosylation was reported in gastric carcinogenesis to induce tumor cell invasion [49]. Also, proteolytic degradation of E-cadherin was described to occur under the action of different metalloproteases (MMPs), such as MMP2, MMP3, MMP7, MMP9 and MMP14, resulting in a soluble form of E-cadherin of 80 kDa [50]. Phosphorylation is one of the most described posttranscriptional processes to regulate proteins of intercellular junctions [51]. Different kinases were described to participate in E-cadherin regulation, such as Epidermal growth factor receptor (EGFR), Casein kinase 1 (CK1), Insulin-like growth factor 1 receptor (IGF-1R), MET Proto-oncogene receptor tyrosine kinase (c-Met) and Proto-oncogene tyrosine-protein kinase Src (Src) [52-56]. Also, miRNAs such as miR-9, miR-10b, miR-31, miR-192, miR-205, miR-665 and some members of miR-200 family were reported to regulate E-cadherin levels. These miRNAs suppress the activity of the previously

mentioned transcription factors implicated in E-cadherin transcriptional repression, thus inducing E-cadherin recovery [57].

In 2002, Yasuyuki Fujita and collaborators described the first post-translational regulator for E-cadherin. This regulator was named Hakai, which means *destruction* in Japanese. Hakai is an E3 ubiquitin-ligase that is part of the ubiquitination system, whose function is to bind to specific substrates, such as Src-phosphorylated E-cadherin, and to induce its ubiquitination and subsequent lysosomal degradation [56].

4. The ubiquitination system

4.1. Overview of the ubiquitination system

Ubiquitin molecule was firstly discovered in 1975 by Gideon Goldstein and it was described as a 8,6 kDa ubiquitous protein [58]. Later, in 1980s, Avram Hershko, Aaron Ciechanover and Irwin A. Rose described ubiquitin as a component of the ubiquitination pathway, a new mechanism of protein degradation, for which they were awarded with the Nobel Prize in Chemistry in 2004.

Ubiquitination is as an ATP-dependent ubiquitin-mediated protein degradation system. It consists in a two-step degradation system based in the substrate tagging by multiple ubiquitin molecules and its subsequent degradation and recycling of the ubiquitin [59]. Later, Hershko and Ciechanover described three enzymes that collaborate giving rise to a chain process that facilitates the marking and degradation of selected proteins (Figure 7) [60]:

- E1 activating enzyme: responsible of ubiquitin activation in an ATP-dependent reaction.

- E2 conjugating enzyme: responsible of ubiquitin conjugation. The E2 enzyme receives the activated ubiquitin from the E1 enzyme and transports it until it couples with the substrate-specific E3 ubiquitin-ligases.

- E3 ubiquitin-ligase enzyme: responsible of ubiquitin binding to the substrate protein. E3 ubiquitin-ligases receive the activated ubiquitin from E2 enzyme and transfer it to specific signalized substrate molecules in order to induced their targeting for proteasome, lysosome or autophagy degradation. Due to their substrate specificity,

E3 ubiquitin-ligases constitute a big and heterogeneous group of enzymes, existing more than six hundred in humans. Besides its main described role in proteolysis, E3 ubiquitin-ligases were also described to play a role during activation of transcription factors, pointing that they also may play and important role in the nucleus [61]. E3 ubiquitin-ligases are classified according to specific domain contents and mechanisms of ubiquitin transfer in three groups. Domains described in these proteins are: 1) HECT domain, where E3 ubiquitin-ligases receive ubiquitin from E2 enzymes and transfer it directly to the substrate; 2) RING domain, where E3 ubiquitin-ligases set close to E2 enzyme to facilitate ubiquitin transferring to the substrate; and 3) HYB domain, lately discovered, where the dimerization of the E3 ubiquitin-ligases creates a pocket called HYB domain which binds to tyrosine-phosphorylated substrates. This HYB domain is adjacent to RING domain, thus facilitating E2 enzymes positioning [62, 63].

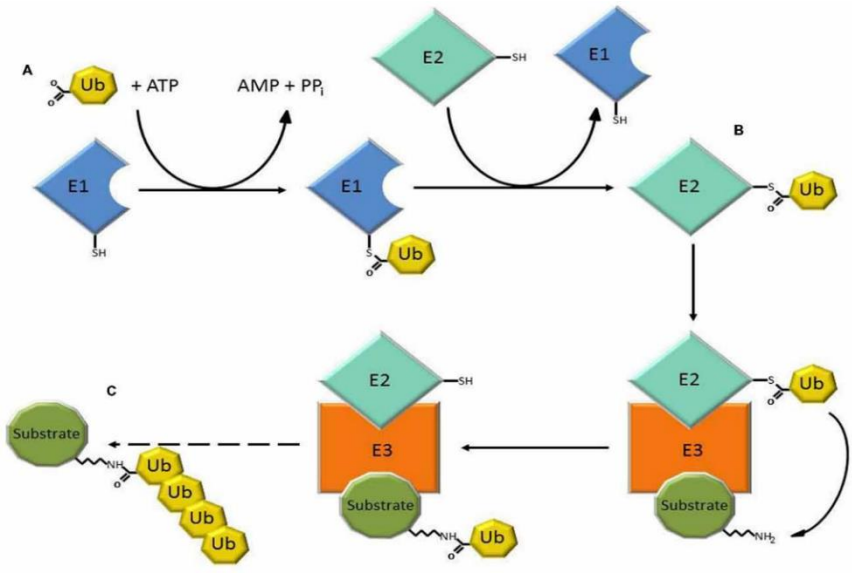

Figure 7. Ubiquitination process. Ubiquitination process is mediated by three different enzymes: E1, responsible of ubiquitin activation; E2, the ubiquitin conjugated enzyme; and E3, responsible of transferring the activated ubiquitin to specific Tyr-phosphorylated substrates and inducing its degradation via proteasome or lysosome. Image obtained from Gong *et al.*, 2016.

4.2. Ubiquitin-mediated degradation pathways

Ubiquitination can trigger different degradation pathways. Ubiquitin is a protein of 76 amino acids containing seven Lys residues that can also bind to other ubiquitin molecules, giving rise to polyubiquitin chains. Usually, most abundant type of ubiquitin chains is composed by ubiquitin monomers or poly-ubiquitin chains of Lys48 residues, which target proteins for proteasomal degradation. Lys63-linked poly-ubiquitin chains were also described as a label for lysosome degradation [64]. Besides, ubiquitin chains linked by Lys63 residues were described to perform different non-degradative roles, such as protein association into complexes to facilitate substrate access or ribosomal protein synthesis [65, 66]. Ubiquitin can not only bind to other ubiquitin molecules, but also suffer other modifications such as SUMOylation, NEDDylation, phosphorylation or acetylation, which target substrates for different metabolic responses [67-70].

Initially, experiments performed by Rudolf Shoenheimer in 1930s suggested that the major part of protein degradation was carried out into the lysosomes. With the discovery of the ubiquitin-proteasome system, this pathway started to be believed as the principal responsible of protein degradation. Nowadays, we know that ubiquitin-tagging of substrate may end in degradation via three possible pathways: proteasome degradation, lysosome degradation and autophagy system (Figure 8) [71]:

- Proteasome degradation: As previously mentioned, usually Lys48 ubiquitination of cytoplasmic proteins targets them proteasome degradation [65]. Mammals have a 26S proteasome, which is constituted by a 20S core particle that contains the proteolytic sites, and two regulatory subunits 19S with multiple ATPase active sites. During proteasome degradation, proteins must be unfolded by an ATPase hexamer and reach the 20S core. Other secondary regulatory molecules contribute to this process, such as Rpn10 and Rpn13 [72]. Proteasome inhibition has been studied for decades to understand protein degradation *in vitro* by using different inhibitors, such as MG132 or lactacystin [73]. Since 1990s many clinical trials were carried out by employing proteasome inhibitors for cancer therapy. These can be divided into first-generation proteasome inhibitors (bortezomib), which target the core of the 20S proteasome subunit, and second-generation proteasome inhibitors (carfilzomib and ixazomib), which bind to the N-terminal domains of catalytic proteasome subunits. At the moment, only bortezomib, ixazomib and carfilzomib have been approved by the

FDA for its use in some liquid cancers treatment, such as multiple myeloma and mantle cell lymphoma. However, they did not show any promising effect for solid tumor treatment. Having that in mind, E3 ubiquitin-ligases have been proposed as an alternative approach for the treatment of solid tumors, which would also prevent side effects derived from the blockage of multiple protein degradation.

- Lysosomal degradation: proteins present in the plasma membrane, such as receptors or channels, can eventually be ubiquitinated and signalized for endocytosis. Lys63-ubiquitinated proteins are internalized into early endosomes under the action of the endosomal sorting complex required for transport (ESCRT). Early endosomes later turn into late endosomes, also known as multivesicular bodies (MVBs), which fuse with lysosomes for degradation. Rab family proteins such as Rab11, Rab4 and Rab7 contribute to this process [72]. Lysosomal degradation can be prevented by employing different lysosomal inhibitors, such as chloroquine and bafilomycin A_1. These drugs have been described to inhibit lysosomal activity by preventing its acidification, thus impairing its enzymatic function [74]. Chloroquine was first used for malaria treatment and constitutes the only inhibitor approved by FDA for its use in clinical trials for treating tumors by late-autophagy inhibition targeting the lysosome [75, 76].

- Autophagy degradation: autophagy is classified in two categories: selective and non-selective autophagy. Selective autophagy has also been described to be dependent on Lys63 ubiquitin tagging. Selective autophagy is based on the presence of specific substrate receptors on the autophagosomal membranes. Ubiquitin-dependent autophagy allows to select specific ubiquitin-tagged cargos into phagosomes for its later fusion and degradation into the lysosome without affecting any other cellular components. Many types of selective autophagy have been reported to be ubiquitin-driven, such as macroautophagy, microautophagy, mitophagy or lysophagy. Autophagy-related protein 8 (Atg8), an ubiquitin-like protein also known as LC3 (and its lipidated form LC3-II), was the first protein identified in phagophores, and plays an important role during autophagic process [77, 78]. Early-autophagy can be inhibited by employing different drugs. Some drugs such as 3-methyladenine (3-MA) have been described to inhibit autophagy by blocking phosphatidylinositol 3-kinase

(PI3K) activity, thus blocking early stages of autophagosome formation [79]. Early-autophagy inhibitors have shown little efficacy *in vivo,* so that late-autophagy inhibitors targeting the lysosome are considered a best alternative [80].

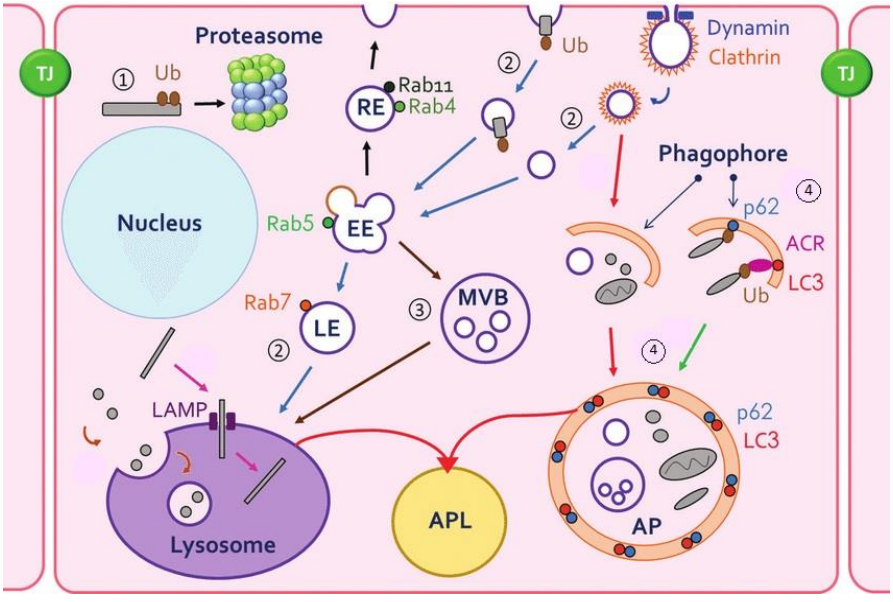

Figure 8. Ubiquitin-dependent degradation pathways. (**1**) Cytosolic proteins are ubiquitinated and tagged for proteasomal degradation. (**2**) Ubiquitinated membrane proteins can be involved into endocytic vesicles and fuse with early endosomes, which develop into late endosomes, multivesicular bodies (**3**) and finally fuse with lysosome. (**4**) Cytosolic organelles or waste material can be ubiquitinated and tagged for selective autophagy. Image obtained and modified from Flores-Maldonado *et al*., 2017.

5. The E3 ubiquitin-ligase Hakai: structure and biological roles

5.1. Hakai discovery

As previously mentioned, the E3 ubiquitin-ligase Hakai, encoded by C-cbl like protein gene *CBBL1*, was discovered in 2002 by Yasuyuki Fujita and collaborators as the first post-translational regulator of E-cadherin stability. Given the importance of the loss of E-cadherin during cancer progression it was vitally important to determine the cause of its degradation. By using a modified yeast-two hybrid screen, they identified one protein which was interacting with E-cadherin in a phosphorylation-dependent manner that they named Hakai, which means *destruction* in Japanese. The mechanism of action of Hakai on E-cadherin consists in the specific recognition of Src-phosphorylated pTyr753 and pTyr754 cytoplasmic residues of E-

cadherin and the transfer of a molecule of activated ubiquitin. E-cadherin ubiquitination targets it for endocytosis through the action of Rab5 and Rab7, and consequent degradation via lysosomes (Figure 9) [56, 81].

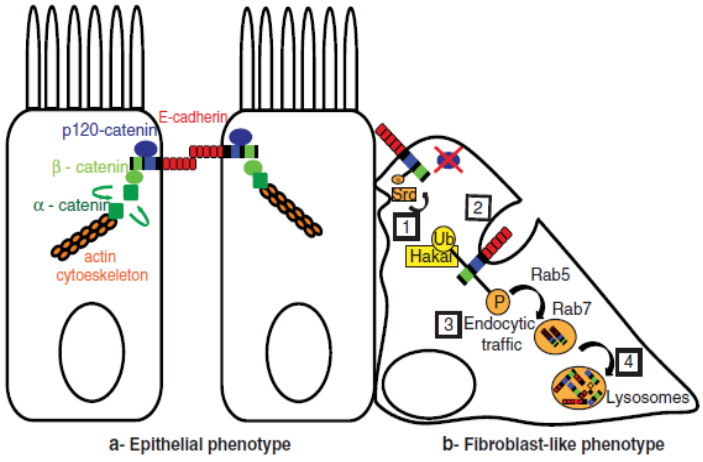

Figure 9. Mechanism of post-translational regulation of E-cadherin by Hakai. E-cadherin is constituted by five extracellular subdomains, a transmembrane domain and an intracellular domain bound to p120- catenin and β-catenin. During mesenchymal transformation, Src-phosphorylated intracellular domain of E-cadherin is ubiquitinated by Hakai and induced to endocytosis through the action of Rab5 and Rab7. Image obtained from Aparicio *et al*., 2012.

Fujita and collaborators observed that, when inducing Src activation, E-cadherin-β-catenin complex was phosphorylated and cell-cell contacts were lost. They also proved that this phenomenon was accompanied by a redistribution of E-cadherin from cellular contacts to intracellular compartments. Further experiments indicated that Src induction caused not only the phosphorylation and internalization of E-cadherin and its binding partner β-catenin into endosomes, but also its ubiquitination [56] (Figure 9). Regulation of E-cadherin degradation through Hakai activity has been described to occur under different molecular regulatory mechanism. For example, Slit-Robo signaling pathway activation, CD147 overexpression, BTB/POZ domain-containing protein 7 (BTBD7) activity or INFγ stimulus have been reported to induce E-cadherin degradation in different types of cancer [82-85]. On the other hand, interaction between Kinesin-like protein KIFC3 and Ubiquitin carboxil-terminal hydrolase 47 (USP47) has been reported to repress E-cadherin degradation [86].

5.2. Hakai structure

E3 ubiquitin-ligase Hakai was firstly described to have a similar structure to Cbl E3 ubiquitin-ligases, consisting in three domains: an N-terminal phosphotyrosine-binding domain, a central RING finger domain and a C-terminal proline-rich domain. Later on, by molecular assays, it was described that Hakai contained the same three domains as Cbl ubiquitin ligases structured in a different order: N-terminal RING finger domain, central p-Tyr binding domain and a C-terminal proline-rich domain (Figure 10A) [56, 62]. A decade after, it was discovered that Hakai and Cbl E3 ubiquitin-ligases were not actually homologues. In 2012, Mukherjee and collaborators reported that Hakai pTyr-binding domain was actually constituted by and homodimer formed by two monomers of zinc-finger domains interacting in an anti-parallel way. Each finger domain was constituted by a N-terminal RING domain and a C-terminal pTyr-binding domain with a coordinated zinc motif. This domain integrated by the RING domain and pTyr-binding domain was called HYB domain (aa 106-206), and constitutes Hakai binding pocket during dimerization [63]. Each HYB monomer is completed with a C-terminal proline-rich domain. Also, zinc coordination to the HYB pTyr-binding domain is essential for Hakai dimerization and binding pocket formation, which is essential for interaction with its phosphorylated targets. In the case of E-cadherin, this interaction is strictly dependent on the recognition of specific phosphorylated Tyr residues by Hakai (Figure 10B) [63, 87]. This fact may be indicative of the preference of Hakai for Src substrates, as Src usually phosphorylates tyrosine residues followed by a specific sequence (Y(p)-E-E-I/V) [88].

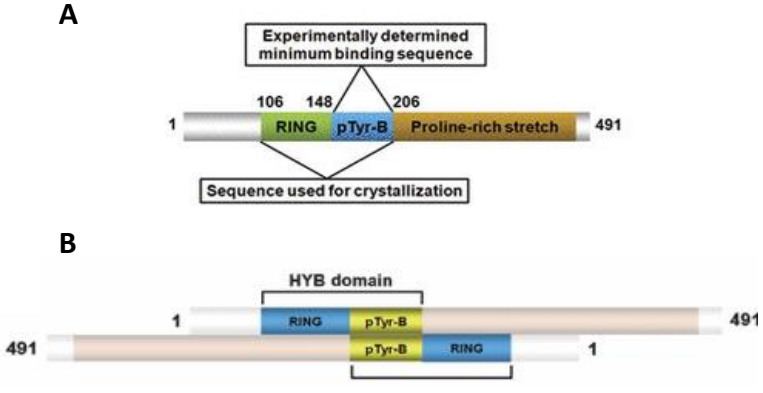

Figure 10. Hakai structure. (**A**) Initially described monomeric structure for Hakai E3 ubiquitin-ligase published by Fujita and collaborators in 2002. (**B**) Homodimeric structure of Hakai described by Mukherjee and collaborators. Images obtained from Mukherjee *et al.,* 2012.

They also found that Hakai shares structure similarities with other RING finger E3 ubiquitin-ligases, but contains a zinc-coordinated pTyr-binding domain structurally unique until the moment. For now, the presence of this unique HYB domain was only found in testis-specific E3 ubiquitin-ligase ZNF645. ZNF645 E3 ubiquitin-ligase was able to interact with E-cadherin but not with other described substrates for Hakai such as Cortactin, suggesting that, despite they structural homology, they may have different subsets of targets [63].

5.3. Hakai functional role: impact on tumor progression

Given Hakai activity on E-cadherin degradation, and the importance of E-cadherin for the maintenance of cell-cell contacts and thus the epithelial phenotype, Fujita and collaborators suggested a possible role of Hakai in tumor progression [56].

In 2009, Figueroa and collaborators firstly described the role of Hakai in cell proliferation and oncogenesis. Hakai stable overexpression in MDCK epithelial cell line showed to have an effect on cellular phenotype, leading to the loss of the epithelial phenotype and cellular contacts characteristic of the wild-type line and to the acquisition of a more fibroblastic phenotype and cellular dynamic protrusions. Expression of E-cadherin in Hakai-overexpressing cells and its localization in cell-cell contacts was lost compared to non-transformed MDCK cells, which suggested that Hakai might be effectively inducing the degradation of E-cadherin and the subsequent acquisition of a mesenchymal phenotype. Hakai overexpression was also responsible of an increase in cellular proliferation by promoting the transition from G0/G1 phase of cell cycle to S phase in an E-cadherin independent manner [89]. Besides, subsequent studies proved that Hakai-overexpressing cells showed oncogenic potential in soft agar, a reduced substratum adhesion and a greater invasiveness compared to parental MDCK cells [90].

Hakai expression was also examined in healthy colon tissue and colon adenocarcinoma human samples. An increased expression of Hakai in both nucleus and cytoplasm was detected in colon cancer compared to healthy tissue [89]. Further results obtained by immunohistochemistry in human colorectal cancer samples proved that Hakai expression increases progressively in different stages of patient samples, and it was proposed as a novel biomarker in colon cancer progression [91, 92]. Hakai expression was also studied in other types of cancer. For example, Hakai was reported to be up-regulated in non-squamous cell lung carcinoma (NSCLC) and to be involved in proliferation, invasion and migration and in the

acquired resistance of NSCLC cells to cisplatin treatment [93, 94]. Indeed, Hakai was related to EGFR inhibitor (TKI) gefitinib resistance in NSCLC with EGFR-activating mutations [95]. Based on this data, authors suggest that Hakai might be a good target to silence when treating NSCLC in order to increase the efficiency of the chemotherapy treatment [94]. Moreover, Hakai was also reported to act as an oncogene in hepatocellular carcinoma (HCC) [83, 96]. For example, Hakai was described to mediate Ajuba neddylation in HCC which, in turn, was reported to act as a tumor suppressor despite its role as an oncogene described in other types of cancer [96].

The role of Hakai was also studied *in vivo* by employing a nude mice model. MDCK non-transformed cells and Hakai-transformed MDCK cells were injected in the flank of nude mice and it was observed that Hakai-transformed MDCK cells were able to form tumors, while MDCK parental cells were not. Histological analysis confirmed that Hakai overexpression increased oncogenic potential *in vivo*, proliferation and mitosis, confirming its role as an oncogene. Besides, Hakai-transformed MDCK cells showed the ability to infiltrate blood vessels and adjacent tissues and to form distant micrometastasis, thus proving the important role of Hakai during carcinoma progression not only *in vitro* but also *in vivo* [91, 92]. Moreover, although not related to an oncogenic activity, Hakai has also been described to play an important role *in vivo* in plant development in *Arabidopsis thaliana* and in embryonic development in *Drosophila melanogaster*, pointing also to a possible role during physiological EMT. [97, 98].

Results obtained so far indicate that Hakai plays a role as an oncogene and that its inhibition could suppose an effective objective for the treatment of different types of cancer. However, Hakai has also been reported to play a role as a tumor suppressor in certain types of cancer. For instance, it was proved in breast cancer cell lines that Hakai acts as a corepressor of estrogen receptors, which are overexpressed in 70% of cases and whose activity induces rapid cell division, proliferation and, therefore, a rapid tumoral cell growth [99].

So far, Hakai regulation has been described by few mechanisms. Hakai expression been reported to be down-regulated by miR-203 and vinflunine (VLF) treatment. As previously mentioned, miRNAs play an important role during carcinogenesis, as they are responsible of regulating important transcription factors activated in the EMT process. In this context, miR-203 has been reported to repress Hakai expression at a post-transcriptional level [100]. On the other hand, VLF treatment was reported to induce Hakai degradation and E-cadherin recovery

in bladder cancer cells [101]. However, finding new mechanisms of Hakai regulation might be an important fact for targeting its oncogenic activity as a cancer therapy.

5.4. Hakai interacting proteins

Most of the E3 ubiquitin-ligases have several substrates to target for their ubiquitination, helping them to interconnect different cellular process [102]. So far, E-cadherin is the best described substrate for Hakai, however, Hakai was described to be ubiquitously expressed, even in those tissues where E-cadherin is not expressed, such as skeletal muscle or spleen. This fact indicates that the role of Hakai may go far beyond E-cadherin degradation by acting on other substrate proteins [89]. Based on this hypothesis, the search for other possible substrates of Hakai has aroused interest in the past few years.

There is experimental evidence that Hakai interacts and induces degradation of other Src-phosphorylated proteins such as Cortactin and DOK-1, suggesting that Hakai might be implicated in their regulation [63]. However, the functional significance of the regulation of Cortactin and DOK-1 remains to be elucidated. Moreover, other Src-phosphorylated proteins were identified in this same study as Hakai-binding proteins by mass spectrometry analysis [63], including Protein phosphatase 1B isoform 1 (PPM1B), Protein phosphatase 1A (PP1A), Protein Phosphatase 1 regulatory subunit 12A (MYPT1), Casein kinase 1 delta (KC1D), Casein Kinase 1 isoform epsilon (KC1E), cAMP-dependent protein kinase type 1-alpha regulatory subunit (KAP0), Interleukin enhancer-binding factor 2 (ILF2), Insulin receptor substrate 4 (IRS4), Interleukin-1 receptor associated kinase 1 isoform 3 (IRAK1), Tyrosine-protein kinase JAK1 (JAK1), Protein kinase C iota (KPCI), Protein kinase C delta (KPCD), Isoform 1 of Nck-associated protein 1 (NCKP1), Rho GTPase activating protein 21 (RHG21), Human Rab GDI (GDIA), LIM domains containing 1 (LIMD1), Phosphoinositide-3-kinase regulatory subunit 4 (PI3R4), Phosphatidylinositol 4-kinase alpha (PI4KA), E3 ubiquitin-protein ligase BRE1B (BRE1B) and E3 ubiquitin-protein ligase BRE1A (BRE1A) [63]. Besides, Hakai was also reported to interact via its HYB domain with Ajuba (a scaffold protein and Wnt signaling pathway regulator) and to regulate its turnover via neddylation [96].

However, Hakai has also been described to interact with and regulate other proteins in a E3 ubiquitin-ligase independent manner. For example, it was reported to interact and positively regulate PTB-associated splicing factor (PSF) RNA-binding activity without detecting any ubiquitination [103, 104]. Also, interaction between Hakai and estrogen receptor (ER)-α-

positive was reported to inhibit ERα activity by blocking the union of coactivators SRC-1 and SRC-2, responsible of ERα transactivation [99]. Similarly, Hakai induces Src stabilization and a consequent increase in δ-catenin Tyr-phosphorylation and stability. This Hakai-mediated δ-catenin stabilization diminishes its affinity to GSK-3β, preventing δ-catenin ubiquitination and degradation and activating β-catenin oncogenic signaling [105].

Hakai has also been reported to interact with mRNA and to play a regulatory role at transcriptional level. Besides its role on regulating PSF RNA-binding activity, interaction between Hakai and splicing regulator Will's tumor 1-associating protein (WTAP) has been described to influence mRNA methylation [106, 107]. Moreover, Hakai has also been described to participate in mRNA methylation in *Arabidopsis thaliana,* thus influencing plant developmental decisions during pattern formation [97]. This fact points to a possible relevance of Hakai during development of eukaryotic organisms.

Given the importance of Hakai during tumor progression and metastasis, it has been proposed as a promising strategy for cancer therapy. So far, only three drugs based on proteasome inhibition have been approved for cancer treatment without successful results in solid tumors. Therefore, focusing on targeting specific E3 ubiquitin-ligases, such as Hakai, is proposed as a new therapeutic strategy for cancer treatment, and it is considered a good alternative to proteasome inhibition. Inhibition of E3 ubiquitin-ligases could reduce side effects derived from non-specific proteasome inhibition therapy and increase its efficacy in carcinoma tumors. In this context, the study of new proteins regulated by Hakai may, therefore, lead to the discovery of new EMT modulators.

6. Galectin-3: structure and impact on tumor progression

6.1. Galectin family and structure

Galectins are mammalian carbohydrate-binding proteins which have the ability to bind to carbohydrates linked to other proteins and lipids, preferentially located in the extracellular matrix or cell surface. Galectins are able to recognize a minimal structure called lactosamine (Galβ1-4GlcNac) contained in N-glycans and O-glycans branches of glycoproteins [108].

Galectin family is constituted by 15 proteins which share similar structure. They are basically constituted by a carbohydrate-recognition domain (CRD domain) of about 130 amino acids

composed by two antiparallel β-sheet, which conform the binding pocket for glycans ligands [109]. This carbohydrate binding site shows a high evolutionary conservation with a slight variation between galectins and it is responsible of the specificity of each galectin binding to different oligosaccharides [110].

Structurally, galectins can be divided into three subfamilies: prototype galectins, chimera galectins and tandem-repeat galectins. Prototype galectins consist in monomer synthesized galectins which can dimerize in an antiparallel manner (e.g Galectin-1). Chimera-type galectins group is only integrated by Galectin-3 and consist in a CRD domain and a N-terminal domain. They can be found as dimers or as multimers linked by their N-terminal domain. Finally, tandem-repeat galectins are constituted by two CRD domains bound by a flexible peptide linker which can oligomerize via their N- and C-terminal domain (Figure 11) [108].

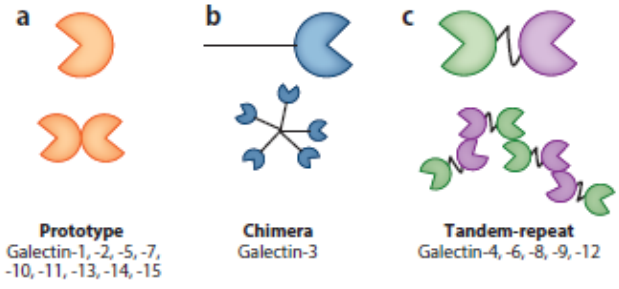

Figure 11. Schematic representation of the three different groups of galectins. (**A**) Prototype galectins constituted by a CRD which can be found in dimers. (**B**) Chimeric Galectin-3 constituted by a CRD domain and an N-terminal domain which can be found in oligomers. (**C**) Tandem-repeat galectins constituted by two different CRDs linked by a flexible linker which can form oligomers through their N- and C-terminal domains. Image obtained from Thiemann and Baum, 2016.

Galectins are synthesized in free ribosomes in the cytoplasm. Once synthesized they can exert intracellular functions or be secreted by non-classical secretory pathways. Extracellularly, Galectins can act by binding to cell-surface and extracellular matrix glycoproteins or glycolipids and activate important signaling pathways [111].

6.2. Galectin-3 implication in cancer

Thanks to their intracellular and extracellular functions, galectins play important roles in different biological processes, including some affecting cancer development. For example, some galectins, such as Galectin-1 and Galectin-3, have been reported to promote tumor cell transformation by interacting with oncogenic Ras. Furthermore, Galectins have been extensively described to play an anti-apoptotic role in different tumor cell lines [112]. Extracellularly, Galectins have also been related to metastatic process thanks to its ability to disrupt cell-cell adhesion and to facilitate the union of tumoral and endothelial cells [113, 114]. Also, galectins favor tumor invasiveness by binding to cell surface receptors implicated in the migration process and by inducing the angiogenic process [115-117].

Specifically, within galectin family, Galectin-3 has been extensively studied in relation to cancer disease. It has been described to be expressed in many types of cancer, however, its expression varies depending on the type of tumor and metastatic state, showing an increased expression in colon, bladder or breast carcinomas among others. So far, Galectin-3 has been extensively related to cell adhesion, apoptosis, proliferation, angiogenesis and metastasis [118].

Regarding its role in cell adhesion, Galectin-3 has the ability to mediate cell-matrix and cell-cell adhesion given its ability to form oligomeric structures in the extracellular space [119, 120]. Extracellular Galectin-3 was reported to bind to integrins, thus promoting their clustering and regulating tumor cell migration [111]. Also, Galectin-3 interaction with β-catenin was reported to activate Wnt signaling pathway and to affect E-cadherin-mediated cell adhesion [121-123]. Moreover, Galectin-3 was reported to interact with Annexin A2 located in the plasma membrane and to promote cell migration [124].

Despite the unquestionable pro-tumoral role of Galectin-3, the down-regulation of this protein has also been linked to the progression of some types of tumors. For example, Galectin-3 down-regulation was reported in cholangiocarcinoma, gastric cancer, endometrial cancer and breast cancer compared to healthy samples [125-128]. Moreover, pro-tumoral or anti-tumoral role of Galectin-3 during cancer progression depends on the type of cancer and the localization of Galectin-3. For example, Galectin-3 cytoplasmic accumulation in prostate cancer is related to cancer progression, however, its nuclear localization is related to metastasis inhibition and increased apoptosis [129]. Also, Galectin-3 localization in the cytoplasm was related to a more

invasive phenotype that when located in both nucleus and cytoplasm in endometrial cancer [127].

So far, a uniform pattern of expression of Galectin-3 in cancer has not been described. Therefore, this protein has been proposed both as a new target for therapeutic strategies and as a biomarker of good prognosis. Having that in mind, deepen the study of Galectin-3 mechanisms of regulation might be interesting in order to understand its controversial behavior and to develop different therapeutic strategies in which Galectin-3 may be involved.

6.3. Galectin-3 mechanisms of regulation

Interestingly, Galectin-3 was reported to suffer different post-translational modifications, such cleavage and phosphorylation, that might regulate its activity and localization. Authors have reported that Galectin-3 can be phosphorylated by three different kinases which are responsible of its functional regulation, such as c-Abl, CK1 and GSK-3β [130]. Specifically, Galectin-3 phosphorylation by c-Abl was reported to prevent it from lysosomal degradation and to affect cell morphology and migration in breast cancer cells [131, 132]. This background evidences that Galectin-3 is actually phosphorylated by multiple kinases in different Ser and Tyr residues, including c-Abl, which shares structural homology with Src.

It is admitted that Galectin-3 degradation mechanisms remain still unclear. However, it is logical to think that Galectin-3 intracellular down-regulation may occur by other degradation mechanisms independent of its extracellular secretion.

7. Heat shock protein 90 chaperone: structure, regulation and implication in cancer disease

7.1. Hsp90 family and structure

Heat shock proteins were unintentionally discovered in 1962 by the scientist Ferruccio Ritossa when he changed by mistake the temperature of an incubator while performing his experiments in *Drosophila melanogaster*. He observed that chromosomes had swollen due to the heat shock. Heat shock activated genes gave rise to stress-induced overexpressed proteins, which he named “heat shock proteins” due to their first observation under elevated temperature conditions [133].

Heat shock protein 90 (Hsp90) is one of the proteins belonging to this family of chaperones. Hsp90 is constitutively expressed in all mammalian cells and is responsible of the folding of its *de novo* synthesized or misfolding client proteins in an ATP-dependent manner, allowing the correct preservation of their activity [134]. In mammals, four different isoforms belonging to the Hsp90 chaperone family have been described according to the cellular compartment where they are located [135]. There exist two major cytoplasmic isoforms of Hsp90, known as Hsp90α (major/inducible form) and Hsp90β (constitutive/minor form), which share 76% homology; the Hsp90 analogue GRP94 (94 kDa glucose-regulated protein), which is located at the endoplasmic reticulum; and the Hsp90 analogue TRAP1 (tumor necrosis factor receptor associated-protein 1), which can be found in the mitochondria [136, 137]. Later, Hsp90N was described as a new isoform of the Hsp90 family implicated in neoplastic transformation. However, its origin remains still unclear [138, 139].

Hsp90 is a highly conserved protein in all the organisms. Its structure was firstly described as an N-terminal ATP-binding domain, a middle domain and a highly conserved C-terminal domain, the latter responsible of the dimerized conformation that allows its activity [140-142]. It was also described that binding of Hsp90 to other molecules, called co-chaperones, was essential for exerting its chaperone activity [143]. Nowadays, Hsp90 is described as a relaxed dimerized protein with an N-terminal ATP binding domain (N-domain), a middle domain (M-domain) involved in ATP hydrolysis, and a C-terminal domain responsible of dimerization (C-domain). N- and M-domains are connected with a charger linker. Protein structure suffers a constriction during ATP-binding on the N-terminal domain, which switches its conformation to prepare the catalytic site for ATP hydrolysis. This switch allows co-chaperone molecules to have access to this pocket and to regulate the chaperone ATPase cycle, thus facilitating the activity of Hsp90 on its client proteins (Figure 12) [144].

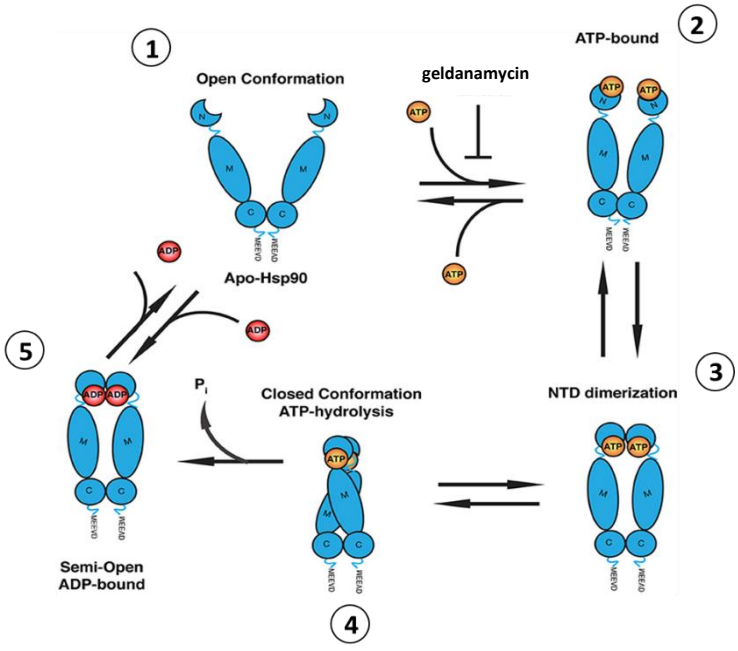

Figure 12. Schematic flow of Hsp90 ATPase cycle. (**1**) Chaperone Hsp90 initially adopts an open conformation favoring the access of the ATP molecule to the N-terminal domain. Hsp90 inhibitors such as geldanamycin can compete with ATP binding at this point. (**2**) Binding of ATP induces a conformational change. (**3**-**4**) Hsp90 adopts a closed structure and recruits the M-domain for the ATP hydrolysis. (**5**) Following hydrolysis, the molecule adopts a semi-open conformation facilitating ADP release. Once the cycle is finished the molecule returns to its open conformation to start a new cycle. Image obtained and modified from Lackie *et al*., 2017.

Hsp90 isoforms are responsible of the stabilization of many client proteins implicated in different aspects of the cellular physiology, such as protein trafficking, DNA damage, signal transduction o innate immunity. The role that Hsp90 plays on its client proteins has not only an impact in many cellular processes and in the maintenance of their homeostasis, but also in different pathological conditions, such as neurodegenerative diseases, infectious diseases and cancer [135, 145].

7.2. Inhibition of Hsp90 activity

Hsp90 plays an important role during protein degradation, either by intervening in the chaperone-mediated autophagy (CMA) process or by inducing the degradation of its client proteins when it cannot exert its chaperone activity. Given Hsp90 chaperone activity on pro-

tumoral proteins [135], the design of compounds that inhibit Hsp90 activity and the correct folding of its client proteins has been deeply studied for the past decades.

The first inhibitor described for Hsp90 was ansamycin antibiotic geldanamycin (GA) in 1994. Geldanamycin was shown to revert the oncogenic phenotype of v-src-transformed cells by binding to Hsp90 and inhibiting its function [146]. Later, structure of Hsp90 was described and, nowadays, geldanamycin mechanism of Hsp90 inhibition is broadly known. Geldanamycin binds to the ATP binding site of the N-terminal domain of Hsp90, blocking ATP binding and preventing ATP-dependent conformational cycling reactions responsible of its action on client proteins (Figure 12) [141]. However, despite its high effectivity on Hsp90 inhibition, geldanamycin was not success in phase I clinical trials due to its high toxicity and low solubility. For these reasons, geldanamycin analogues with lower toxicity and higher solubility were synthesized and are now being tested in different phases of clinical trials for diverse types of cancer. Geldanamycin analogues include tanespimycin (17-*N*-allylamino-17-demethoxygeldanamycin, 17-AAG) and alvespimycin (17-Dimethylaminoethylamino-17-demethoxygeldanamycin, 17-DMAG) [147].

Since the discovery of geldanamycin as the first inhibitor of Hsp90, many inhibitors of this chaperone have been described and subsequently divided in two different groups. The first group includes direct Hsp90 inhibitors, which bind to the ATP-binding site of Hsp90 in the N-terminal domain avoiding ATP hydrolysis and, thus, the correct folding of its client proteins. This group includes geldanamycin (and its analogues), radicicol and the chimeric radamide inhibitors [148, 149]. The second group is constituted by Hsp90/co-chaperone interaction disruptors, such as celastrol or gedunin. These inhibitors act by interrupting the binding of Hsp90 and some co-chaperones, such as Cdc37, thus inducing client protein degradation [150]. This mechanism of action makes these inhibitors to have a more reduced spectrum of action. This kind of inhibition has been extensively studied in the past few years as an alternative to avoid a broad inhibition that could have many side effects when treating cancer disease [151].

More recently, a second generation of inhibitors have been developed from drug screening procedures. These inhibitors showed some advantages compared to previously described inhibitors, such as greater efficiency of inhibition, prolonged inhibition capacity, reduced hepatotoxicity and ability to cross the blood-brain barrier, which makes them clear candidates

for clinical use. Among these inhibitors we can find Luminespib (AUY922), Onalespib (AT13387) and Ganetespib (STA-9090), all in different phases of clinical trials [152].

7.3. Hsp90 client protein degradation systems

As previously mentioned, Hsp90 has been described to exert is chaperone activity on several proteins, including many implicated in tumor progression. Inhibition of Hsp90 chaperone activity prevents the correct folding of its client proteins and eventually causes their degradation. Protein degradation under Hsp90 inhibition has been so far reported to mainly occur via ubiquitin-proteasome system. However, other degradation pathways, such as lysosomal degradation pathway, have also been described for some Hsp90 client proteins [153].

Proteasome degradation of Hsp90 client proteins was firstly described for cytoplasmic Hsp90 client protein Cystic fibrosis transmembrane conductance regulator (CFTR) under geldanamycin treatment [154]. Some authors propose that during its inhibition, Hsp90 facilitates the access of unfolded client proteins to the 20S proteasome, thus promoting their selective degradation [155]. Many pro-tumoral proteins, such as B-Raf proto-oncogene, were reported to be stabilized by Hsp90 and induced to proteasomal degradation in the presence of Hsp90 inhibitors [156]. On the other hand, Hsp90 inhibition with geldanamycin has been reported to induce IκB kinase degradation via non-CMA lysosome degradation pathway, giving rise to new alternative degradation pathway under Hsp90 inhibition [153].

E3 ubiquitin-ligases have been widely described to interact and collaborate with chaperones as part of the chaperone complex [157]. Specifically, Hsp90 interacts with co-chaperones, such as Hsp70, and recruits E3 ubiquitin-ligases to mediate their client protein degradation. This has been demonstrated for Cullin-5 and CHIP, both E3 ubiquitin-ligases that ubiquitinate and induce degradation of Hsp90 client proteins via proteasome in presence of Hsp90 inhibitors (Figure 13) [158, 159]. Given the huge amount of Hsp90 interacting E3 ubiquitin-ligases [160], it is reasonable to assume that many other E3 ubiquitin-ligases might also be taking part in Hsp90 client protein degradation.

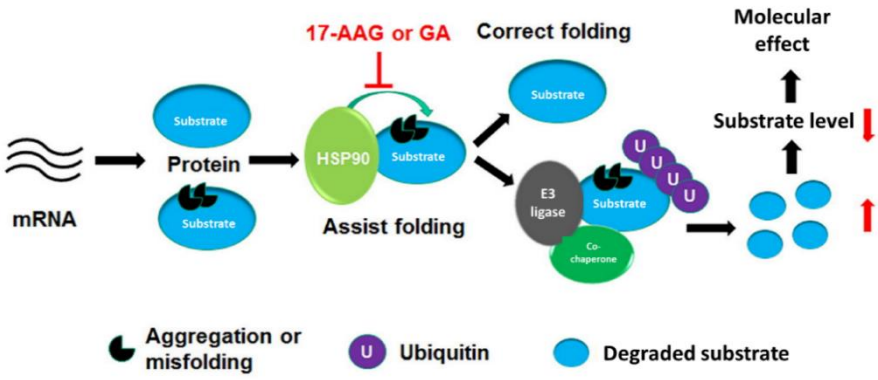

Figure 13. Mechanism of Hsp90 chaperone-mediated degradation. Misfolded or aggregated client proteins of Hsp90 are correctly folded by this chaperone under normal conditions. In presence of Hsp90 inhibitors, such as geldanamycin and derivatives, client proteins are ubiquitinated by specific E3-ubiquitin ligases and induced to degradation. Figure obtained and modified from Zhang *et al.,* 2016.

Besides, proteasome and lysosome degradation, other mechanism of degradation has also been linked to Hsp90 activity. Hsp90 was reported to act as a co-chaperone member of Hsc70 during CMA, thus playing a role during CMA degradation. However, this degradation pathway is usually activated under stress conditions such as starvation, oxidative stress or presence of toxins [161]. For example, cell treatment with oz-apraA Hsp90 inhibitor promotes degradation of some Hsp90 client proteins by CMA. Specifically, membrane receptors belonging to EGFR family, such as ErbB2, are degraded through CMA under oz-apraA treatment. This mechanism of degradation has been reported in cases were proteasome-mediated degradation had been previously described [162].

7.4. Role of Hsp90 in cancer

The role of Hsp90 in cancer has been extensively studied due to its chaperone activity on different proteins implicated in cancer progression. For the past thirty years, numerous proteomic studies employing different biochemical techniques have been carried out on the Hsp90 interactome to discover new client proteins implicated in cancer progression [145, 160]. At present, more than 200 proteins have been identified as Hsp90 client proteins, mostly consisting in transcription factors, kinases and other signaling proteins [145, 163]. Regulation of Hsp90 client proteins plays an important role in different cellular processes, such as cell survival, cell cycle regulation, DNA repair and protein folding. This contributes to the

development of pathological conditions, including neurodegenerative diseases, infectious diseases and cancer [135, 164, 165].

Regarding cancer disease, Hsp90 has been reported to regulate important signaling pathways. For example, AKT (Protein kinase B) is a client protein for Hsp90 involved in PI3K-AKT pathway, which promotes survival of cancer cells by activating different transcription factors [166]. Another important pathway in cancer progression is the Ras-Raf-ERK pathway, where mutated oncogenes N-Ras and B-Raf, both Hsp90 client proteins, participate in promoting proliferation and survival in cancer cells [156]. Moreover, many other Hsp90 client proteins have been proved to be involved in cancer progression, such as tumor suppressor p53, Hypoxia inducible factor HIF1-α, or Tyrosine kinase v-Src [167-169].

Furthermore, E3 ubiquitin-ligases, which play an important role in tumor progression by regulating different substrates implicated in tumorigenesis, have been reported to interact with Hsp90. In fact, a proteomic study carried out by Taipale and collaborators indicated that 31% of the E3 ubiquitin ligases are found between Hsp90 interacting proteins [160, 170]. Although there are few evidences of E3 ubiquitin-ligases as Hsp90 client proteins so far [171], it is reasonable to assume that additional E3 ubiquitin-ligases await to be discovered as new Hsp90 client proteins.

Based in all this data, Hsp90 continues to be widely studied in relation to cancer disease. Specifically, description of new Hsp90 client proteins is gaining great importance with the aim of improving Hsp90 inhibition-based cancer therapy.

8. Annexin A2: structure and impact on cancer progression

8.1. Annexin A2 functions and structure

Annexin family is composed by proteins that bind to negatively charged membrane phospholipids in a calcium-dependent manner. Annexins are expressed in all living organisms and were discovered in animal cells in late 1970s and early 1980s by different research groups. Annexins received this name from the greek word *annex,* which means attachment, due to its function of holding together different structures, such as cellular membranes. Due to this ability, Annexins have been described to participate in different processes involving cellular membranes, such as endo- and exocytosis, vesicular trafficking and redox regulation [172].

In humans, Annexin family is integrated by 13 members, including Annexin A1 to Annexin A13, with different attributed functions [173]. So far, Annexins deregulation was not described to be the cause of any disease, however, altered levels of these proteins have been observed in important human diseases due to their multiple roles in inflammatory response, fibrinolysis and angiogenesis, cell signaling or actin binding and regulation among others [174-179].

Annexins structure is defined as N-terminal domain responsible of the interactions with cytoplasmic proteins, and a C-terminal protein core domain divided into four homologous domains. C-terminal domain is composed by 70 aminoacids responsible of Ca^{2+} and phospholipid binding functions, among others. Annexins N-terminal domain is susceptible to post-translational modifications, which grant a unique function to each annexin [173]. Annexin A2 structure is similar to that previously described, with a modification in its N-terminal domain including an amphipathic region responsible of its bound to S100A10 protein (Figure 14). Annexin A2 is reported to be present in different cellular types in a monomeric or heterotetrameric conformation associated with S100A10 protein. Monomeric and heterotetrameric forms show different biochemical properties. For example, in the heterotetrameric form, Annexin A2 reduces its dependency of Ca^{2+} for its membrane interaction and protects S100A10 from ubiquitin-mediated degradation [172].

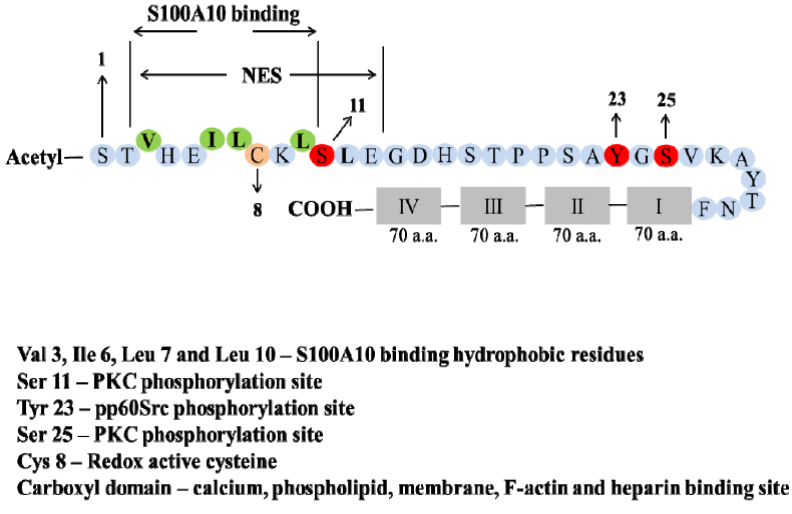

Figure 14. Annexin A2 schematic domain structure. Annexin A2 is composed by an N-terminal domain and a C-terminal domain. N-terminal domain is the site for phosphorylation and other post-translational modifications and also the site for S100A10 binding. The carboxyl-terminal domain is composed by four alpha-helical domains composed by 70 aa and contains binding sites for RNA, heparin, calcium and phospholipid and F-actin. Image obtained from Bharadwaj *et al.,* 2013.

Annexin A2 N-terminal domain was reported to experiment different post-translational modifications, such as acetylation, phosphorylation and glutathionylation, which are responsible its phospholipid-binding activity regulation [180-182]. Ubiquitination and SUMOylation modifications have also been described [183, 184].

Regarding phosphorylation, Annexin A2 was described to be a substrate of Src kinase. Activated form of Src kinase was reported to be responsible of phosphorylation of Tyr23 residue of Annexin A2, causing the regulation of cell shape and motility and restructuration of cytoskeleton, as well as malignant transformation and EMT process [185]. Moreover, Tyr23 Src-phosphorylated Annexin A2 was found to be localized in endomembrane structures, such as endosomes, and to experiment a translocation to the cell surface [181, 186].

8.2. Annexin A2 role in cancer

Deregulation of annexin A2 has been widely described during tumor development and it was related to invasion and metastasis. Annexin A2 has been reported to be up-regulated in many types of cancer, such as colorectal cancer, breast cancer, hepatocellular carcinoma and renal cell carcinoma, where it was found to be implicated in drug resistance, metastasis and invasion. However, Annexin A2 expression during tumor progression is very controversial as it has also been reported to be down-regulated in other types of cancer, such as prostate cancer, nasopharyngeal carcinoma, esophageal squamous carcinoma, intestinal-type sinonasal adenocarcinoma and head and neck squamous cell carcinoma [187-192].

Moreover, heterotetrameric complex constituted by Annexin A2-S100A10 has been described to be implicated in the formation of adherens junctions based on E-cadherin, whose loss is a hallmark of the EMT program. Annexin A2-S100A10 complex has the ability to recruit E-cadherin to adherens junctions, maybe due to its binding ability to the actin cytoskeleton by F-actin-binding protein, also associated with E-cadherin [193].

With this in mind, we can affirm that annexin A2 plays a controversial role in the progression of cancer, as its up-regulation and down-regulation has been described in this disease. Currently, there is still no description of the role of Annexin A2 during EMT process, during which there is a great cellular heterogenicity within the tumor. However, due to the involvement of Annexin A2 in the recovery of E-cadherin, it is possible that this protein might be implicated in cellular plasticity.

8.3. Mechanisms of degradation of Annexin A2

Annexin A2 was described to be degraded via ubiquitin-proteasome pathway. Ubiquitination and consequent degradation of Annexin A2 via proteasome was described as a marker of good prognosis in HCC when Ubiquitin-associated protein 2 (UBAP2) was up-regulated [194]. Furthermore, Annexin A2 was reported to be ubiquitinated in urothelial carcinoma of the bladder (UCB) under E3 ubiquitin-ligase TRIM65 overexpression, causing the induction of the EMT. These data suggest a pro-oncogenic role of Annexin A2 down-regulation under its ubiquitin-proteasome degradation [183].

Other mechanisms such as chaperone-mediated autophagy have also been described for Annexin A2 degradation. Heat shock cognate protein 73 (Hsc73) recognizes KFERQ-related motif present in Annexin A2 when CMA is activated and induces it to degradation. However, this mechanism has only been described *in vitro* under nutrient deprivation conditions [195].

Ubiquitin-proteasome degradation process of Annexin A2 has not been related to Src phosphorylation yet, however, proteasome degradation has often been linked to E3 ubiquitin-ligase recognition after protein phosphorylation.

II. HIPOTHESIS AND OBJECTIVES

As previously mentioned, Hakai plays an important role in tumor progression due to its regulatory activity on E-cadherin. However, Hakai expression has been detected in organs where E-cadherin is absent. This suggests an additional functional role for Hakai independent of that exerted on E-cadherin. So far, few Hakai-regulated proteins have been described, and the functional meaning of these regulation remains to be elucidated.

Based on this and the previously explained background, we propose the following global hypothesis:

- That Hakai E3 ubiquitin-ligase interacts with and/or regulates multiple proteins besides its widely described substrate E-cadherin, on which it can exert an important activity during tumor progression.

To prove our hypothesis, the following objectives were set:

1. To perform a proteomic study in a model of Hakai overexpression to identify new Hakai molecular targets associated with signal pathways implicated in tumor progression.

    1.1. To optimize and perform a comparative study between Hakai-overexpressing MDCK cells and parental MDCK cells by employing iTRAQ technique.
    1.2. To classify the identified proteins based on their biological process and molecular functions.
    1.3. To study the interaction networks of the identified proteins.
    1.4. To validate the regulation of proteins of interest identified in the proteomic study.
    1.5. To analyze the subcellular localization and possible co-localization with Hakai of the identified proteins of interest.

2. To study the mechanism of regulation of Hakai on the identified proteins of interest.

    2.1. To analyze the effect of Hakai transient overexpression and silencing on selected proteins from the proteomic study.
    2.2. To determine the possible interaction between Hakai and the selected proteins.
    2.3. To study Hakai mechanisms of action on the selected proteins.
    2.4. To perform functional studies to determine the impact of Hakai-mediated protein regulation.

III. MATERIALS AND METHODS

1. Cell culture

Madin Darby Canine Kidney (MDCK) cell line is a non-transformed epithelial cell line from dog kidney and was obtained from ATCC and cultured in Dulbecco's Modified Eagle's Medium (DMEM). Hakai overexpressing MDCK cell lines (Hakai-MDCK clon 4, Hakai-MDCK clon 11 and Hakai-MDCK clon 7) were gently provided by Yasuyuki Fujita. These cells were obtained by stable transfection of pcDNA-HA-Hakai in MDCK with Lipofectamin® 2000 and selection with gentamicin antibiotic (G418) at a concentration of 800 ug/µL. These Hakai-overexpressing MDCK clones were indistinctly used as they were probed to have the same phenotype and genotype in different experiments [89]. These clones were cultured in DMEM maintaining G418 antibiotic (Sigma-Aldrich) selection concentration.

Cervix adenocarcinoma HeLa cell line was obtained from ATCC. HEK 293T cell line from human embryonic kidney was obtained from ATCC. HEK 293T-EGFP-C1 and HEK 293T-EGFP-Gal3E were used during a research stay at Dr. Fu-Tong Liu's laboratory in Academia Sinica, Taiwan. All these cell lines were cultured in DMEM.

Renal adenocarcinoma ACHN cell line was obtained from ATCC. Epithelial colorectal cancer cell lines HT29, LoVo and HCT116 were also used. HT29 was cultured in McCoy's 5A (Modified) Medium. LoVo cell line was cultured Kaighn's Modification of Ham's F-12 Medium (F-12K medium). HCT116 cell line was cultured in DMEM.

All culture media were supplemented with 10 % Fetal Bovine Serum (FBS), and 1 % penicillin/streptomycin. All cell lines were maintained at the same culture conditions at 37 °C, 5 % of CO_2 and saturation humidity. Concentration of trypsin employed during cell culture varied depending on the cell line. For MDCK, HT29 and LoVo cell line trypsin 2X was employed diluted from trypsin stock 10X plus EDTA. For the rest of the cell lines trypsin 0,05 % plus EDTA was employed. Culture media, FBS, trypsin and penicillin/streptomycin were provided by Thermo Fisher Scientific.

All cell lines were periodically tested for mycoplasma and used no longer than 3 months after defrosted. Cell line authentication was carried out for HT-29 and LoVo cell lines with the StemElite ID System (Promega).

2. Plasmids, reactives and antibodies

Cell lines were transfected with plasmids pEGFP-Hakai, pEGFP-C1, pcDNA-Flag-Hakai, pcDNA 3.1, pBSSR-HA-Ubiquitin and pSG-v-Src which were kindly provided by Yasuyuki Fujita (Hokkaido University, Japan). P3X-Flag-Gal3 was kindly provided by Dr. Fu-Tong Liu (Academia Sinica, Taiwan). pcDNA-Flag-HA-Hsp90 was kindly provided by Dr. Paweł Bieganowski (Mossakowski Medical Research Centre Polish Academy of Sciences, Poland).

Protein synthesis inhibitor cycloheximide (CHX) (Sigma-Aldrich) was used at 100 µg/mL for the indicated times. Proteasome inhibitor MG132 (Sigma-Aldrich) was employed at 10 µM and 30 µM for 6 h as indicated in figure legends. Lysosome degradation inhibitor chloroquine (CQ) (Sigma-Aldrich) was employed at the indicated concentrations for 24 hours. Autophagy inhibitor 3-methyladenine (3-MA) (Merck) was employed at different concentrations and times, as indicated in figure legends. Hsp90 inhibitor geldanamycin (GA) (TargetMol) was employed at different times and concentrations as indicated in figure legends. In those experiments where these inhibitors were employed, control cells were treated with the indicated vehicle.

Antibodies used for western-blot, immunofluorescence, immunoprecipitation and immunohistochemistry are listed in the following tables:

Table 2. Antibodies used for western-blot.

Antibody	Provider	Species origin	Dilution
Anti-Hakai	Invitrogen	Rabbit	1:1 000
Anti-E-cadherin	BD Transduction Lab	Mouse	1:1 000
Anti-Hsp70	Abcam	Mouse	1:1 000
Anti-Hsp90	Abcam	Mouse	1:1 000
Anti-hsp90	Santa Cruz	Mouse	1:1 000
Anti-Annexin A1	Abcam	Mouse	1:1 000
Anti-Annexin A2	Abcam	Rabbit	1:1 000
Anti-Annexin A2 (C10)	Santa Cruz	Mouse	1:500
Anti-Galectin-3	Abcam	Rabbit	1:1 000
Anti-Galectin-3	Hand-made	Goat	1:1 000
Anti-Stratifin	Sigma-Aldrich	Rabbit	1:500

Anti-IMPDH	Santa Cruz	Rabbit	1:500
Anti-LC3	Cell Signaling	Rabbit	1:1 000
Anti-β-catenin	Cell Signaling	Rabbit	1:1 000
Anti-Flag tag	Sigma Aldrich	Rabbit	1:1 000
Anti-GAPDH	Invitrogene	Mouse	1:10 000
Anti-tubulin	Sigma-Aldrich	Mouse	1:2 000
Anti-tubulin	Proteintech	Rabbit	1:1 000
Anti-mouse IgG HRP	GE Healthcare	Goat	1:10 000
Anti-mouse IgG HRP	Jackson ImmunoResearch	Donkey	1:10 000
Anti-rabbit IgG HRP	GE Healthcare	Donkey	1:10 000
Anti-rabbit IgG HRP	Jackson ImmunoResearch	Goat	1:10 000
Anti-goat IgG HRP	Jackson ImmunoResearch	Rabbit	1:10 000

Table 3. Antibodies used for immunofluorescence.

Antibody	Provider	Species origin	Dilution
Anti-Hakai	Invitrogen	Rabbit	1:100
Anti-Hsp70	Abcam	Mouse	1:100
Anti-Hsp90	Abcam	Mouse	1:100
Anti-Hsp90	Santa cruz	Mouse	1:100
Anti-Annexin A1	Abcam	Mouse	1:100
Anti-E-cadherin	Cell Signaling	Mouse	1:100
Anti-Annexin A2 (3D5)	Santa Cruz	Mouse	1:50
Anti-Galectin-3	Abcam	Rabbit	1:100
Anti-Galectin-3	AbCore	Goat	1:100
Anti-Stratifin	Sigma-Aldrich	Rabbit	1:100
Anti-HA tag	Roche	Mouse	1:100
Anti-Flag tag	Proteintech	Rabbit	1:50
Anti-Mouse IgG-Alexa Fluor® 488	Thermo Fisher Scientific	Goat	1:200
Anti-Rabbit IgG-Alexa Fluor® 568	Thermo Fisher Scientific	Donkey	1:200

Table 4. Antibodies used for immunoprecipitation.

Antibody	Provider	Species origin	Quantity
Anti-Hakai 2498	Dr. Fujita	Rabbit	10 µL
Anti-Hakai	Bethyl	Rabbit	2,5 µg
Anti-Annexin A2 (3D5)	Santa Cruz	Mouse	2,5 µg
Anti-Hsp90	Santa Cruz	Mouse	2,5 µg
Mouse IgG	Santa Cruz	Mouse	2,5 µg
Purified Rabbit IgG	Bethyl	Rabbit	2,5 µg

Table 5. Antibodies used for immunohistochemistry.

Antibody	Provider	Species origin	Dilution
Anti-Hsp90	Abcam	Mouse	1:500

3. Protein extraction and western-blot analysis

3.1. Cell extract preparation

Cells were seeded in 6-well plates or 100 mm dishes at the confluence indicated for each experiment. After transfection or treatment for the indicated times, cells were collected for protein extraction. Cells were placed on ice and washed twice with 5 mL phosphate buffer saline (PBS) pH 7,4 (MP Biomedicals). Once the cells were washed, they were scraped with 1 mL of PBS, transferred to a 1,5 mL tube (Eppendorf) and centrifuged at 4 °C at 5 000 rpm for 5 minutes. The pellets obtained after centrifugation were lysed on ice for 30 min using a variable volume of Triton X-100 lysis buffer (Table 6) with 10 µg/mL leupeptin/aprotinin mix and 1 mM of phenylmethanesulphonyl fluoride (PMSF). Once the lysis was complete, samples were centrifuged for 10 min at 13 000 rpm and 4 °C. The obtained supernatant containing the protein extract was placed in a new tube and proceeded to protein quantification. In the experiments performed at Dr. Fu-Tong Liu's laboratory, cells were placed on ice and washed twice with PBS. For cell lysis, 200 µL of RIPA buffer (Thermo Fisher Scientific) were added to each well and scrapped. Incubation during lysis was performed at 4 °C for 30 min. Samples were centrifuged at 13 000 rpm to remove cellular debris and supernatant was transferred to

a new tube. In both cases, protein quantification was performed by using Pierce™ BCA Protein Assay Kit (Thermo Fisher Scientific).

Table 6. 1% Triton X-100 Lysis buffer composition

Components	Volume
20 mM Tris-Hcl pH 7,5 (Sigma-Aldrich)	1 mL stock 1 M
150 mM NaCl (Sigma-Aldrich)	1,5 mL stock 5 M
1 % Triton X-100 (Sigma-Aldrich)	0,5 mL stock 100X
H_2O	47 L

3.2. Protein quantification

Protein quantification of cell extracts was carried out by performing Bicinchoninic Acid Assay (BCA) method, employing Pierce ™ BCA Protein Assay Kit (Thermo Fisher Scientific) and following manufacturer's instructions. This assay is based in two reactions: reduction of Cu^{2+} ions to Cu^{+} by peptide bonds in a temperature dependent manner, and chelation of bicinchoninic acid with Cu^{+} ions to produce a purple-colored product with a peak of light absorption at 570 nm. This assay was carried out in 96-well plates using a standard gradient curve of Bovine Seroalbumin (BSA) from 0 to 10 µg/µL with two replicates for each point. Two replicates of 2 µL of each sample were placed in the same plate. Solution of BCA reagent was prepared at a 1:50 ratio (reagent B: reactive A) and 200 µL were added to each well followed by and incubation at 37 °C for 30 min. After incubation, absorbance was measured with NanoQuant Infinite M200 (Tecan) at a wavelength of 570 nm. Protein concentration was calculated by performing a linear regression between the absorbance and concentration of the BSA standard curve using Excel Software. The equation obtained was used for calculating protein concentration of the samples.

3.3. Western-blot sample preparation

Western blot samples were prepared with 20 µg or total protein and added of 5X of Laemmli buffer (Table 7) to a final concentration of 1X. Water was added up to a final volume of 20 µL. Samples were boiled at 95 °C for 10 minutes for protein denaturalization and loss of tertiary structure, thus allowing protein resolution in acrylamide gels according to its molecular weight.

Once prepared, samples were directly loaded onto the acrylamide gel or frozen at -20 °C for later use.

Table 7. Laemmli Buffer 5X composition.

Laemmli buffer 5X
200 mM Tris-HCl pH 6,8
10 % sodium dodecyl sulfate (SDS)
50 % glycerol (Sigma-Aldrich)
10 % β-mercaptoethanol
0,1 % bromophenol blue

3.4. Sodium dodecyl sulfate-Acrylamide gel electrophoresis (SDS-PAGE)

Proteins were separated by monodimensional electrophoresis in polyacrylamide gels (PAGE), using denaturing conditions by adding SDS and β-mercaptoethanol and boiling the samples at 95 °C. β-mercaptoethanol acts by cleaving disulfide bonds between cysteines, thus breaking tertiary and quaternary structure of proteins and assuring the presence of monomeric protein molecules. SDS is an anionic detergent which acts by causing the disruption of non-covalent bonds and consequent protein denaturalization. Also, SDS is responsible of granting negative charge to proteins in a charge-to-mass ratio facilitating protein migration from anode to cathode during electrophoresis.

Electrophoresis was performed in Mini-Protean II cuvettes (Bio-Rad) using 1,5 mm acrylamide gels. Gels were prepared at polyacrylamide concentrations of 12 % for chloroquine and 3-MA experiments to allow LC3 better detection, and 10 % for the rest of experiments. Hand-made gels compositions is indicated in Table 8. In those experiments performed at Dr. Fu-Tong Liu's laboratory, SDS-PAGE Mini-PROTEAN® TGX™ pre-cast gels (Bio-Rad) were used. Electrophoresis was performed in running buffer 1X (Table 9) at constant voltage (180 V) during 1 h.

Table 8. Acrylamide gels composition.

Components	Quantity per 10% resolving gel	Quantity per 12% resolving gel	Stacking gel
H_2O	3 mL	2,5 mL	3,2 mL
1,5 M Tris-HCl pH 8,8	2,5 mL	2,5 mL	1,25 mL
Glycerol 50 % (Sigma-Aldrich)	2 mL	2 mL	-
40 % Acrylamide/bisacrylamide 29:1 (Bio-Rad)	2,5 mL	3 mL	0,5 mL
SDS 10 % (Sigma -Aldrich)	100 µL	100 µL	50 µL
Ammonic persulfate (APS) (Sigma-Aldrich)	30 µL	30 µL	50 µL
Tetramethylethylendiamine (TEMED) (NZYTech)	15 µL	15 µL	10 µL

Table 9. Running buffer 10X composition.

Running buffer 10X	Quantity
Trizma base 0,25 M (Sigma-Aldrich)	30,3 g
Glycine 1,92 M (Sigma-Aldrich)	144 g
1 % SDS (Sigma-Aldrich)	10 g
H_2O	1 L

3.5. Western blot and immunodetection

Once the proteins were separated by electrophoresis, they were transferred in transfer buffer 1X (Table 10) to polyvinylidene fluoride membranes (PVDF) (Millipore) with a pore of 0,45 µm Transference was performed at a constant amperage of 200 mA for 1 hour in the previously described cuvettes. After transfer, membranes were blocked for 1 hour under agitation with blocking solution TBS-T 1 % pH 7,4 (Table 10) and 5 % milk powder. After blocking, primary antibodies were diluted in blocking solution at the concentrations indicated in Table 1 and incubated overnight. After primary antibody incubation, membranes were washed three times for 5 min with TBS-T 1 % buffer and incubated for 1 hour at room temperature with secondary

antibodies coupled to horseradish peroxidase (HRP). Antibodies were diluted in blocking solution at the concentrations indicated in table 1. Before image detection, membranes were washed three times for 5 min with TBS-T 1 %. Detection of antigen-antibody complexes corresponding to the experiments of the proteomic study validation was performed with ChemiDoc (Bio-Rad) system. The rest of immunodetections were performed in Amersham Imager 600 system (GE Healthcare Life Sciences). In both cases Luminata™ Crescendo Western HRP Substrate (Millipore) was employed.

Table 10. Transfer buffer and TBS-T 10X composition.

Transfer buffer 1X	TBS-T 1% 10X pH 7,4 (1L)
Trizma base 0,25 M (Sigma-Aldrich)	12,1 g Trizma Base
Glycine 1,92 M (Sigma-Aldrich)	58 g NaCl
20 % Methanol (VWR Chemicals)	10 mL Tween 20
H_2O up to 1 L	H_2O up to 1 L

Same protocol was performed in those experiments carried out at Dr. Fu Tong Liu's laboratory including some modifications. After transfer, membranes were incubated for 1 hour with blocking solution (TBS-T 1 % pH 7,6 supplemented with 5 % BSA). Membrane washing and antibodies dilution was performed in this same blocking buffer. Last washing after incubation with secondary antibodies was performed with TBS-T 1 % buffer without BSA. Detection of antigen-antibody complexes was performed using BioSpectrum Auto Imaging System (UVP) equipment and Luminata™ Crescendo Western HRP Substrate (Millipore).

3.6. Image analysis

Protein levels analysis during proteomic study validation were quantified by using Image Lab Software (Bio-Rad). Protein levels corresponding to the rest of experiments were quantified using the Image J software (National Institutes of Health, US). In both cases, protein levels were normalized against the levels of loading control proteins (GAPDH or Tubulin) and relativized against the control point of the technique. Statistical analysis and graphical representation were performed by employing GraphPad Prism 6 software. Statistical analysis was performed applying unpaired Student's t-test. Results are expressed as Mean ± SEM for the indicated number of experiments. Levels of significance are indicated in figure legends.

4. Cell phenotype analysis

Cell phenotype for non-transformed MDCK cell line and Hakai-overexpressing MDCK cells was evaluated in 6-well plates by employing phase contrast optical microscopy. Images were obtained by employing microscope Nikon Eclipse-Ti microscope. For phenotype evaluation during geldanamycin treatment cell phenotype was evaluated with optical microscope Nikon Eclipse TS100.

5. Proteomic analysis

Proteomic analysis was performed in collaboration with the Proteomics Platform of Instituto de Investigación Biomédica de A Coruña (INIBIC).

5.1. Processing of Protein Samples for iTRAQ Labeling

Before iTRAQ labeling, protein extraction was carried out as follows: MDCK and Hakai-transformed MDCK cells were centrifuged 5 min at 1 200 rpm and cellular pellets were washed twice in phosphate buffer solution. A lysis buffer containing 6 M urea/2 % SDS was employed for protein extraction. Cellular debris was eliminated by centrifugation (10 min at 13 000 rpm) and protein quantification was determined by Bradford assay (Sigma-Aldrich). Samples were cleaned up by precipitation with acetone to eliminate urea residues and protein pellets were dried and resuspended in 25 µL Dissolution Buffer provided with the iTRAQ kit (500 mM triethylammonium bicarbonate buffer, TEAB). 1 µg of each sample was resolved into a 10 % SDS-PAGE gel and then stained by silver nitrate. This technique is valid to ensure proteins integrity after acetone precipitation and to test technical reproducibility of protein precipitation between samples. Then, 25 µg of each condition were resuspended in 25 µL TEAB dissolution buffer yielding to a final protein concentration equal to 1 µg/µL. Then, samples were denatured with 2 % SDS and reduced for 1 h at 60 °C using 50 mM tris(2-carboxyethyl) phosphine (TCEP) (ABSciex) followed by cysteine alkylation with 200 mM methylmethanethiosulfonate (MMTS) (ABSciex) at RT in dark during 30 min. Proteins were digested with trypsin (Gold Mass, Promega) used at 1:20 ratio trypsin/protein for 14 h at 37 °C. Then iTRAQ labeling was performed according to the supplier's instructions (ABSciex). For that, each peptide solution was incubated for 90 min at RT with iTRAQ Reagents. Samples were labeled as follows: MDCK, 114; MDCK, 115; Hakai-transformed MDCK clone 4, 116; Hakai-transformed MDCK clone 11, 117. iTRAQ labeled peptides were mixed and desalted using

reversed phase columns (Pierce C18 Spin Columns, Thermo Fisher Scientific) prior to liquid chromatography coupled to mass spectrometry (LC-MS) analysis.

5.2. Liquid chromatography (LC)

The desalted peptides were fractionated by reversed-phase liquid chromatography (RP-LC) at basic pH (pH = 10) to lower their complexity. Dried labeled peptides were resuspended in 140 µL of buffer A (10 mM ammonium hydroxide, 5% acetonitrile) and injected into a HP 1200 system (Agilent Technologies). Separation was carried out by employing a C18 column (Zorbax extend C18, 100 × 2,1 mm id, 3,5 µm, 300 Å; Agilent). The flow rate used was 0.2 mL/min and the gradient employed was of 90 min. Sixty fractions were pooled every 90 s with FC203B fraction collector (Gilson). Sixteen fractions were pooled post collection based on the peak intensity of the UV trace recorded at 214 nm. Each fraction was dried in a vacuum concentrator and then subjected to a second-dimension separation by resuspending the peptides in 2 % ACN/0,1 % TFA. Then, 5 µL of the peptide solution were desalted and injected into a reversed-phase column (Integrafit C18, ProteopepTM II, New Objetive) for nanoflow LC analysis, using a Tempo nanoLC (Eksigent). Peptides were eluted at a flow rate of 0,35 µL/min during a 90 min linear gradient from 2 to 50 % of buffer B (mobile phase A: 0,1 % TFA/2 % ACN, mobile phase B: 0,1 % TFA/95 % ACN). LC eluate was deposited onto an Opti-TOF LC MALDI target plate (1534-spot format; SCIEX) using the Sun Collect MALDI Spotter/Micro Collector (SunChrom). Before spotting, the LC microfractions were mixed with MALDI matrix (3 mg/mL α-acyano-4-hydroxycinnamic acid in 70 % ACN/0,1 % TFA containing 10 fmol/µL angiotensin as internal standard) at a flow rate of 1,2 µL/min. Fractions were collected every 15 s and spotted onto a matrix-assisted laser desorption/ionization plate for MS analysis.

5.3. MS/MS Analysis

Finally, four plates containing four LC runs per plate were analyzed in a 4800 MALDI-TOF/TOF instrument (ABSciex) with a 200 Hz repetition rate (Nd:YAG laser) and 4000 Series Explorer software version 3.5.1 (ABSciex). MS full-scan spectra were acquired from 800 to 4 000 m/z using a fixed laser intensity of 3 600 kV and 1 500 laser shots/spectrum. Tandem MS mode was operated with 1 kV collision energy with CID gas (air) over a range of 60 to −20 m/z of the precursor mass value. Up to 12 of the most intense precursors per spot with signal/noise ratio (S/N) > 80 were selected for MS/MS acquisition using a fixed laser intensity of 4 400 kV and 2 000 shots/spectrum. Common contaminants such as trypsin autolysis peaks and matrix ion

signals were excluded from the analysis. A second MS/MS was acquired excluding those precursors previously fragmented and using a lower S/N threshold of 50 to detect peptides that were not identified in the previous run.

5.4. Mass spectrometry data analysis

Data from all the MS/MS acquisitions were used for protein identification and quantification using ProteinPilot™ software v.4.5 (Sciex). Each MS/MS spectrum was searched in the Uniprot/Swissprot database (UniProt 2015_05 release version containing 547 599 sequences and 195 014 757 residues, with taxonomy restriction_Homo sapiens). Protein Pilot search parameters were set as follows: trypsin cleavage specificity, methylmethanethiosulfate (MMTS) modified cysteine as fixed modifications, biological modification "ID focus" settings, and a protein minimum confidence score of 95 %. The tolerance used for matching MS/MS peaks to the theoretical fragment ions is based on the information regarding to mass accuracy of the instrument chosen in the Paragon Method dialogue box (4800 MALDI TOF/TOF). ProteinPilot™ software employs two different algorithms: one to perform protein identification (Paragon™ algorithm) and the other one to determine the minimal set of confident protein dentifications (Pro Group™ algorithm). Once the identity of the protein was confirmed (Detected Protein Threshold > 95 %, Unused ProtScore > 1,3), the ratios of the peak areas of iTRAQ reporter ions were calculated in order to compare the relative abundance of the proteins identified in the samples. Data were normalized for loading error by bias, assuming the samples are combined in 1:1 ratio. Peak areas for the iTRAQ reagent(s) and control were also corrected to attempt to remove background ion signal applying the background correction option. Only those changes with a p-value ≤ 0,05 and a ratio ≥ 2 (or ≤ 0,5) were considered statistically significant. Due to the high complexity of the samples, Proteomics System Performance Evaluation Pipeline (PSPEP) software was used independently to calculate false discovery rates (FDR). In order to facilitate the overall analysis, protein classification was carried out using the following bioinformatic tools: Protein Analysis Through Evolutionary Relationships (PANTHER) (http://www.pantherdb.org/about.jsp), Gene Ontology (GO) (http://geneontology.org) and UniProt. Interactive network analysis was performed using the STRING, Search Tool for the Retrieval of Interacting Genes (http://string-db.org).

6. Transfection experiments

6.1. Plasmid overexpression

Transfection experiments were performed by employing Lipofectamine 2000 Transfection Reagent (Invitrogen) and Opti-MEM media following manufacturer's protocol. Cells were plated one day before transfection at a confluence of $2,5 \times 10^5$ cells/well for HeLa and HCT116 cells and $7,5 \times 10^5$ cells/well for HEK 293T cells to reach a confluence of approximately 40-50 % for transfection. The day of transfection, lipofectamine and plasmid were separately diluted in 125 µL of Opti-MEM each for 6-well plates transfection, or 500 µL for 100 mm dish transfection, and incubated for 5 min. The ratio of DNA and Lipofectamine employed for transfection was 1:2. After incubation, lipofectamine 2000 and DNA diluted in Opti-MEM were mixed together by pipetting up and down and incubated for 20 min. Cells were washed carefully twice with sterile saline serum, and Opti-MEM was added to the plate employing a volume of 1,25 mL for 6-well plates and 5 mL for 100 mm dishes. Transfection reaction was added to the cells and incubated for 6 hours. After incubation, cells were washed twice with saline serum and replaced with normal culture medium. Transfection was maintained for the indicated times and proceeded to cell extract preparation. In those cases where transfection was performed using different plasmids in the same experiment, transfection system was completed with empty vector until reaching the same quantity of plasmid at each point of the experiment.

In the experiments performed at Dr. Fu-Tong Liu's laboratory, transfections were performed using Effectene® Transfection Reagent (QIAGEN) following manufacturer's instructions. Cells were seeded in 6-well plate at a confluence of $2,5 \times 10^5$ cells/well for HeLa cells and $7,5 \times 10^5$ cells/well for HEK 293T cells in growth medium containing serum and antibiotics. Transfection was performed once reached 40-60 % of cell confluence. For that, DNA was dissolved in Buffer EC up to a total volume of 100 µL and Enhancer was added keeping a ratio of DNA to enhancer 1:8. The mixture was incubated for 5 min at RT and centrifuged briefly. After incubation, 10 µL of Effectene Transfection Reagent were added to the mixture, which was mixed by vortexing for 10 s and incubated at RT for 10 min. During this incubation, medium was removed from the plate and replaced by 1,6 mL of fresh growth medium. Once finished 10 min of incubation, 600 µL of growth medium were added to the transfection mixture and mixed by pipetting up and down. Total volume of the transfection complexes was carefully dropped onto the cells

and incubated for the indicated times. After time of transfection, cells were scrapped and proceeded to cell extract preparation.

6.2. RNA interference

Hakai silencing was performed by employing siRNA oligonucleotides Hakai 1 (5' CTCGATCGGTCAGTCAGGAAA) and Hakai-2 (5' CACCGCGAACTCAAAGAACTA). Oligonucleotides were transfected into HEK 293T and HCT116 cells by using Lipofectamine 2000 Transfection reagent (Invitrogen). Cells were plated in 6-well plates at a confluence of $7,5 \times 10^5$ cells/well for HEK 293T cells and $2,5 \times 10^5$ cells/well for HCT116. Two microliters of 100 µM stock oligonucleotides (200 pmol) were combined with double amount of lipofectamine and transfected by using the previously described protocol for plasmid transfection. Mission Universal Non-coding siRNA (Sigma-Aldrich) was used as a negative control of transfection by combining 10 µL of 20 µM stock oligonucleotide with 4 µL of lipofectamine. Cells were scrapped 72 hours after transfection and proceeded to cell extract preparation. In those cases where treatment with GA was combined with Hakai silencing, GA was added 48 hours after transfection and maintained for 24 hours.

7. Immunofluorescence

For immunofluorescence experiments, cells were plated in sterile glass coverslips contained in 6-well plates at the previously indicated confluences. Cells were treated as indicated. Cells were washed twice with PBS-Tween 1% and cells were fixed with paraformaldehyde solution 4 % in PBS (Santa Cruz) for 15 min. After fixation, cells were washed twice with PBS pH 7,4 and permeabilized with 0,5 % Triton X-100/PBS pH 7,4 for 15 min. After permeabilization, cells were blocked for 1 hour with culture medium supplemented with 10 % FBS. Cells were washed twice and incubated with primary antibodies diluted in blocking medium for 2 hours at RT at the concentrations indicated in table 2. After primary antibody incubation cells were washed four times with pH 7,4. Secondary antibody was diluted in blocking medium and incubated at RT for 1 h. Cells were washed four times with PBS and incubated with Hoechst (Life Technologies) for nuclear staining employing a 1:10 000 dilution. Finally, ProLong Gold Antifade Mountant (Life Technologies) was employed for coverslips mounting. Images were obtained by using confocal microscope Nikon A1R and analyzed, when needed, using NIS-Elements 3.2 software. Immunofluorescence intensity was evaluated by employing ImageJ software (NIH) for GA experiments. Intensity of ten different areas for two different replicates

were quantified and relativized against the mean control area. Values are indicated as Mean ± SEM of the staining intensity signal per area. Statistical analysis was carried out by using unpaired Student's t-test at the indicated significance levels.

Same protocol was performed during the research stay at Dr. Fu-Tong Liu's laboratory and images were obtained using confocal microscope Olympus # LSM780 using Zen 2011 software.

8. RNA extraction and Real-time PCR

8.1. RNA isolation procedure

RNA was obtained from cultured cells using TRIzol™ Reagent protocol (Life Technologies) following manufacture's indications. Before performing the protocol $2,5 \times 10^4$ cells/well were seeded in 6-well plates and transfected after 24 hours. After 48 hours of transfection, cells were washed twice, scrapped with 1 mL PBS and centrifuged 5 min at 5 000 rpm in 1,5 mL tubes. Once the pellet was obtained, cells were lysed with 1 mL of TRIzol™ Reagent by pipetting the cells up and down until the pellet was dissolved. After homogenization the sample was centrifuged 10 min at 13 000 rpm at 4 °C and transferred to a new tube and incubated 5 min at room temperature. Chloroform was added to the sample following a ratio of 0,2 mL of chloroform per 1 mL of TRIzol, shaked for 15 seconds and incubated at room temperature for 3 min. Samples were centrifuged at 12 000 rpm for 5 min at 4 °C. Aqueous phase was carefully removed from the tube and placed into a new tube. For RNA precipitation 0.5 mL of 100 % isopropanol were added to the aqueous phase, incubated for 10 min at RT and centrifuged at 12 000 g for 10 minutes at 4 °C. Supernatant was removed from the tube and the pellet was washed with 1 mL of 75 % ethanol followed by a 7 500 g for 5 min at 4 °C. The RNA pellet obtained was dried for 20 minutes, resuspended in 50 µL of Nuclease-Free Water (Life Technologies) and quantified using Nanodrop Spectrophotometer ND-1000 (Thermo Fisher Scientific).

8.2. Retrotranscription

Retrotranscription of mRNA was performed by employing NZY First-Strand cDNA Synthesis Kit for RT-PCR (NZYRT Enzyme Mix, NZYRT 2x Master Mix, NZY RNase H and DEPC-treated H_2O). To set the reaction, each sample was prepared up to a final volume of 20 µL as described in table 11.

Table 11. Reactives and volumes for retrotranscription reaction For NZY First-Strand cDNA Synthesis Kit.

Reactive	Volume per reaction
NZY 2x Master Mix	10 µL
NZYRT Enzyme Mix	2 µL
Sample RNA	500 ng
Nuclease-free water	Up to 20 µL

Reactions were incubated in an Applied Biosystems Veriti Thermal Cycler for 96 well plates following the next protocol:

- Priming incubation at 25 °C for 10 min.
- Reverse transcription at 50 °C for 30 min.
- RT Inactivation at 85 °C for 5 min followed by 4 °C incubation.
- Addition of 1 µL of RNase H and incubation at 37 °C for 20 min.

In those experiments performed at Dr. Fu-Ton Liu's laboratory, retrotranscription was performed to obtain cDNA using the iScript™ Reverse Transcription Supermix for RT-qPCR (RNase H + MMLV reverse transcriptase, RNase inhibitor, dNTPs, oligo(dT), random primers, buffer, $MgCl_2$ and stabilizers) (Bio-Rad) following the manufacturer's instructions. To setup each reaction, each sample was prepared in a final volume of 20 µL as indicated in table 12.

Table 12. Reactives and volumes for retrotranscription reaction for iScript™ Reverse Transcription Supermix.

Reactive	Volume per reaction
iScript RT Supermix (Bio-Rad)	4 µL
Sample RNA	500 ng
Nuclease-free water	Up to 20 µL

The reaction was incubated in a thermocycler Verity Thermal Cycler (Applied Biosystems) following the next protocol:

- Priming incubation at 25 °C for 5 min.
- Reverse transcription at 46 °C for 20 min.
- RT Inactivation at 95 °C for 1 min followed by 4 °C incubation.

The cDNA generated in this reaction by following both protocols was directly used for real time quantitative PCR.

8.3. Real-time quantitative PCR (qPCR)

Real time quantitative PCR (qPCR) was carried out by employing LightCycler® 480 SYBR Green I Master Mix (Roche) which is composed by dNTPs, DNA polymerase and SYBR Green dye. This reaction is based in the binding of SYBR Green dye to the DNA molecules and the quantification of its fluorescence emission at 520 nm. The qPCR reaction was settled as indicated in Table 13.

Table 13. Reactives and volumes per SYBR Green qPCR reaction.

Reactive	Volume per reaction
SYBR Green Master Mix	5 µL
Sample cDNA	1 µL
Forward primer	0,7 µL
Reverse primer	0,7 µL
H_2O	Up to 10 µL

Reaction was performed in LightCycler® 480 multiwell plates 96 well (Roche) and accumulating fluorescence was measured employing LightCycler® 480 Instrument II (Roche) using the following program:

- Activation: 1 cycle at 95 °C for 10 min
- Amplification and real-time analysis (45 cycles):
    - 10 s at 95 °C
    - 10 s at 60 °C
    - 5 s at 72 °C
- Melting (1 cycle):
    - 5 s at 95 °C
    - 1 min at 65 °C
- Cooling: samples were maintained at 4 °C after the end of the program.

Data obtained from qPCR was analyzed by employing qbase+ qPCR analysis software (Biogazelle). Primers used for Hakai mRNA were F' TGCTATGACTGTGCATTTTACATGA and R'

ACTGCTAATTCGCTGCAC. *HPRT* gene was used as housekeeping by using primers F' TGACCTTGATTTATTTTGCATACC and R' CGAGCAAGACGTTCAGTCCT.

In those experiments performed at Dr. Fu-Tong Liu's laboratory, qPCR was carried out employing Roche FastStart Universal Probe Master (ROX) kit (Roche) following a modified protocol based on the manufacturer's indications. This reaction is based on the presence of single signal-generating probes with a fluorescence reporter at the 5' end and a quencher at the 3' end. When the hybridation of the probe with cDNA is produced, FastStart Taq DNA Polymerase cleaves the probes with its exonuclease activity and the fluorescent reporter is release. This accumulating fluorescent signal is quantified by the CXF Connect™ Real-Time PCR Detection System (Bio-Rad). Reaction was setup in 0,2 mL tubes as indicated in Table 14.

Table 14. Reactives and volumes for qPCR reaction with Roche FastStart Universal Probe Master.

Reactive	Volume per reaction
cDNA (1:100 dilution)	5 µL
FastStart Universal Probe Master (Ready to use 2X Master Mix) (Roche)	10 µL
Forward-Reverse Primer Mix 5 µM	5 µL
Hydrolysis probe	0,4 µL
Final Volume	24,2 µL

Reaction tubes were placed on instrument to perform the qPCR using a two-step program:

- Activation: 1 cycle at 95 °C for 10 min
- Amplification and real-time analysis (50 cycles):
    - 10 s at 95 °C
    - 30 s at 60 °C
- Cooling: samples were maintained at 4 °C after the end of the program.

Comparative CT Method was used for analyzing qPCR data. Primers used for Galectin-3 mRNA were F' CTTCTGGACAGCCAAGTGC and R' AAAGGCAGGTTATAAGGCACAA. *GAPDH* gene was used as housekeeping by using primers F' AGCCACATCGCTCAGACAC and R' GCCCAATACGACCAAATCC.

9. Protein half-life experiments

Protein half-life experiments were performed by using the protein biosynthesis inhibitor CHX. HEK 293T cells were seeded in 6-well plats at a confluence of $7,5 \times 10^5$ cells/well. Cells were treated with cycloheximide at indicated times and concentration and protein expression was evaluated. E-cadherin was used as a positive control of the technique (data not shown). Transfection was performed 24 hours after seeding the cells and CHX was added 24 hours after transfection for the indicated times. Once time of treatment was completed, cells were collected, lysed and protein levels were analyzed by western blot as previously indicated.

10. Flow cytometry

Flow cytometry was performed using HEK 293T-EGFP and HEK 293T-EGFP-Gal3E cells and auto immunofluorescence produced by EGFP tag was analyzed. For that, cells were seeded in 6-well plates at a confluence of $7,5 \times 10^5$ cells/well and transfected next day for 48 hours with Flag-Hakai plasmid (transfection efficiency was checked before in immunofluorescence experiments). Cells were washed with PBS twice and trypsinized. Then, cells were resuspended in FACS buffer (PBS pH 7,4, 1 % BSA, 0,1 % NaN_3 sodium azide) in cytometry tubes at a concentration of 10^5 cells tube. Three washes were performed by centrifugation with FACS buffer starting at 350 g and increasing 50 g in each centrifugation. Finally, cells were resuspended in FACS Buffer and kept on ice until they were analyzed in the cytometer BD FACSANTO II (BD Biosciences) where the auto immunofluorescence emitted by stable transfection with EGFP was analyzed in each cell line.

11. Immunoprecipitation assays

Cells were plated at $1,5 \times 10^6$ cells/plate in 100 mm dishes (Corning) and grown until reaching 90 % confluence. When needed, cells were treated with 10 µM geldanamycin 24 hours before collecting. Cells were washed twice with PBS-T 1% (PBS supplemented with 1 % of Tween-20), scrapped with 1 mL PBS-T and collected into 1,5 mL tubes. Cell pellets were isolated by a 3 min centrifugation at 4 °C and 4 000 rpm. After centrifugation, cell pellets were incubated with 1 mL lysis buffer (20 mM Tris-HCl pH 7,5, 150 mM NaCl and 1 % Triton X-100, 125 mg/mL N-ethylmaleimide) in rotation at 4 °C for 30 min. Lysis reaction was centrifuged at 14 000 rpm and transferred to a new tube. Pre-clearing was performed to eliminate unspecific interactions. For this, protein extracts were incubated with 60 µL of beads for 1h at 4 °C.

Protein A Agarose Beads (Santa Cruz) were used when using rabbit antibodies for immunoprecipitation and Protein G Plus-Agarose (Santa Cruz) when using mouse antibodies. In parallel, 60 µL of beads were incubated with immunoprecipitation antibody or control IgG (Table 3) in 500 µL of PBS-T for 1 hour in rotation at 4 °C. After pre-clearing, beads were removed by centrifugation at 3 000 rpm, 2 min at 4 °C and 80 µL of supernatant were separated for Input samples. Remaining protein samples were saved for on-bead incubation. Once finished beads-antibody incubation, samples were centrifuged 2 min at 4 °C and 2 000 rpm and washed with lysis buffer once followed by another centrifugation. Protein samples were loaded onto the beads and incubated for 2 hours at 4 °C on rotation. After incubation, beads were washed twice with lysis buffer and supernatant was discarded by centrifugation. Sample preparation for western blotting was carried out by loading 40 µL of Laemmli buffer onto the beads and 20 µL of Laemmli buffer onto the input sample. Samples were heated at 95 °C for 10 min for protein and beads cleavage and denaturalization and proceeded to western blot protocol.

12. Interactome analysis

Hakai interactome analysis was performed in HCT116 cell lines. For that, large scale immunoprecipitation was performed and samples were processed by the Proteomics Platform of Instituto de Investigación de Santiago de Compostela (IDIS).

12.1. Large scale immunoprecipitation

For large scale immunoprecipitation, protein samples were processed as previously described. Briefly, four 150 mm culture dishes were used per point of the experiment (IgG and IP). Cells were placed on ice and washed thrice with filtered PBS, taking care of remaining as much supernatant as possible. LoBind tubes and pipette tips were used (Eppendorf). Protein was extracted as previously described and quantified by BCA method. Parallelly, 40 µL of dynabeads protein A (Thermo Fisher Scientific) were resuspended in 500 µL of filtered PBS-T 0,1 % and incubated with 5 µg of Hakai Bethyl antibody or control IgG (Table 3) 2 h at 4 °C on rotation for beads-antibody coupling. Once finished antibody-beads incubation, beads were washed thrice with filtered PBS-T 0,1 %, and same amount of protein was loaded onto beads for each point of the experiment (approximately 7 mg). Beads and protein sample were incubated overnight at 4 °C on rotation. Following incubation, beads were washed twice with filtered lysis buffer and samples were prepared as previously described. To assure equally

amount of protein on each sample, 10 µL of each sample were loaded in a 10 % SDS-PAGE gel, subjected to electrophoresis as previously described and dyed with silver stain reactive.

12.2. Silver Staining

Gel silver staining was performed following Blum's modified protocol described by Rabilloud and collaborators [196]. Steps performed for gel silver staining were as follows. Reactives' composition is indicated in table 15.

1. Gels were fixed twice during 30 min by employing fixation solution.
2. Gels were washed twice during 10 min with dH_2O.
3. Following washing, gels were sensitized for 1 min with sensitizing solution.
4. Gels were washed twice for 1 min with dH_2O.
5. Gels were dyed with silver nitrate solution for 60 min and washed for 10 s with dH_2O.
6. Dyed gels were revealed by employing revealing solution for 5-10 min.
7. Revealing was stopped by employing stop solution for 30 min.

Table 15. Composition of silver staining protocol reactives.

Reactive	Components	Quantity (up to 50 mL)
Fixation solution	Ethanol 100°	20 mL
	Glacial acetic acid	5 mL
	ddH_2O	25 mL
Sensitizing solution	Sodium thiosulfate solution 10 %	0,1 mL
	ddH_2O	49,9 mL
Silver nitrate solution	$AgNO_3$	0,1 g
	Formaldehide 37 %	37 µL
	ddH_2O	49,63 mL
Revealing solution	K_2CO_3	1,5 g
	Sodium thiosulfate solution 10 %	6,25 µL
	Formaldehide 37 %	12,5 µL
	ddH_2O	49,9 mL
Stop solution	Trizma Base	1,5 g
	Glacial acetic acid	5 mL
	ddH_2O	45 L

12.3. In gel protein digestion

Prepared samples were loaded on a 10 % SDS-PAGE gel and subjected to electrophoresis. The run was stop as soon as the front had penetrated in the resolving gel 3 mm. Band was stained with Sypro-Ruby fluorescent staining (Lonza), excised from the gel and processed for in-gel digestion. For that, samples were reduced in 10 mM dithiothreitol dissolved in 50 mM of ammonium bicarbonate (AMBIC) (Sigma-Aldrich). Then, samples were alkylated with 55 mM iodoacetamide dissolved in 50 mM AMBIC. Rinse of gel pieces was performed with 50 mM AMBIC in 50 % methanol (HPLC grade, Scharlau) and acetonitrile (HPLC grade, Scharlau) was added for dehydration. Gel pieces were dried in a SpeedVac (Thermo Fisher Scientific) and digested with porcine trypsin (Promega) at a final concentration of 20 ng/µL in 20 mM AMBIC and incubated overnight at 37 °C. Peptides were extracted three times in 40 µL of 60 % acetonitrile in 0,5 % formic acid for 20 min, pooled and concentrated in SpeedVac.

12.4. Mass Spectrometric Analysis (DDA acquisition)

Reverse Phase Chromatography was performed for peptide separation. A gradient was created using nano LC 400 micro liquid chromatography system (Eksigent Technologies, ABSciex) coupled to a high-speed Triple TOF 6600 mass spectrometer (ABSciex). Analysis was performed in reversed-phase column C18CL (150 x 0,30 mm, 3 µm, 120 Å) (Eksigent, ABSciex). Trap column YMC-TRIART C18 (3 µm, 120 Å) (YMC Technologies) was matched on-line with the analytical column. Flow rate of loading pump was 10 µL/min of 0.1 % formic acid. Micro-pump flow rate was 5 µL/min under gradient elution conditions (Mobile phase A was 0.1 % formic acid in water; mobile phase B was 0.1 % formic acid in acetonitrile). Peptide separation was performed by employing a gradient of 90 min ranging from 2 % to 90 % of mobile phase B (mobile phase A: 0,1 % formic acid, 2 % acetonitrile; mobile phase B: 0,1 % formic acid, 100 % acetonitrile). Sample volume injected was 4 µL. Data-dependent acquisition was performed in a TripleTOF 6600 system (ABSciex). Ion spray voltage floating (ISVF) was 5 500 V, curtain gas (CUR) was 25, ion source gas 1 (GS1) was 25 and collision energy employed (CE) was 10. Analyst TF 1.7.1 software was employed for instruments operation (ABSciex). A switching criterion was stablished to ions greater than the mass to charge ratio (*m/z)* 350 and smaller than *m/z* 1 400, with a mass tolerance of 250 ppm, a charge state of 2-5 and an abundance threshold over 200 counts (cps). Former target ions were excluded for 15 s. Instruments calibration was automatically performed every 4 h using calibrant peptides from PepCalMix (SCIEX) [197].

12.5. Data analysis

Processing of data files was performed by employing ProteinPilot™ 5.0.1 software (ABSciex) using Parangon™ algorithm for database searching. Data grouping processing was carried out by employing Progroup™ software. Human-specific database from Uniprot was used for data search. Non-linear fitting method was used for false discovery rate, showing only results that reported a 1% Global false discovery rate or better [198]. Hakai specific interacting proteins were identified by employing Venny 2.1 software (CNB-CSIC). Functional description was performed by employing information of Uniprot database.

13. Cell viability assays

Geldanamycin cytotoxicity was analyzed with 3-(4,5-dimethylthiazol-2-yl)-2,5-diphenyltetrazolium bromide (MTT) colorimetric assay developed by Mosmann in 1983 and modified by Denizot and Lang in 1986 [199, 200]. MTT is a compound belonging to the family of tetrazolium salts which has a yellow color and is soluble in water. During the cellular metabolic activity this compound is reduced by dehydrogenases giving rise to a precipitate of formazan insoluble in water and with violet color whose quantity is proportional to the number of living cells. To carry out this test, 10^4 cells were seeded in a 96-well plate and treated with geldanamycin at different concentrations for 24 hours. After incubation with geldanamycin cells were treated with 5 mg/mL of MTT reactive for 3 hours at 37 °C. Following incubation, culture medium was removed, and tetrazolium salts were diluted in 100 µL of DMSO and incubated for 15 minutes with agitation at RT. The absorbance was measured using Multiskan Plus Reader (Nanoquant Infinite M200 Tecan Trading AG, Switzerland) using a wavelength of 570 nm with a reference wavelength of 630 nm. Geldanamycin IC50 was calculated for each cell line by using GraphPad Prism 6 Software in order to determine the concentration at which 50 % of cell population is decreased.

14. Inhibition assays

14.1. Proteasome degradation inhibition with MG132

Proteasome inhibition experiments were performed by using proteasome inhibitor MG132 [201]. Stock solution of MG132 was prepared in DMSO at a 10 mM concentration. Cells were seeded at a confluence of $7{,}5 \times 10^5$ cells/well for HEK 293T. When needed, cells were transfected 24 hours after seeding and MG132 was added 32 hours after transfection during 6 hours at 10 µM and 30 µM concentrations. Once the time of treatment was concluded, cells were collected and proceeded to protein extraction and analysis by western blot. Analysis of β-catenin protein levels were used as a positive control of the effectiveness of MG132 treatment [202]. All the points were completed with DMSO up to the volume of maximum concentration.

14.2. Lysosome degradation inhibition with chloroquine

Lysosomal degradation inhibition was performed by using chloroquine (CQ), initially used as an anti-malarial drug during World War II. Chloroquine inhibits last step of autophagy by raising lysosome pH and avoiding the fusion of autophagosome and lysosome, and thus protein degradation [203]. Chloroquine reagent stock was prepared at a 96 mM concentration in H_2O. Cells were seeded in 6-well plates at a confluence of $7{,}5 \times 10^5$ cells/well for HEK 293T cells and $2{,}5 \times 10^5$ cells/well for HeLa cells. When needed, cells were transfected 24 hours after seeding and incubated at concentrations and times indicated in figure legends. After incubation, cells were collected and proceeded to cell extract preparation and western blot analysis. Analysis of LC3 I/II protein levels were used as a positive control of the effectiveness of chloroquine treatment

14.3. Autophagy inhibition with 3-methyladenine

Autophagy inhibition assays were performed by using 3-methyladenine (3-MA), which inhibits early autophagy and apoptosis by blocking the formation of the autophagosome via PI-3K inhibition [204]. Stock solution of 3-MA was freshly prepared in water at a concentration of 100 mM. To carry out this assay, cells were seeded in 6-well plates at a confluence of $2{,}5 \times 10^5$ cells/well for HeLa cells. When needed, cells were transfected 24 hours after seeding for 48 hours. 3-MA was added to the cells 24 hours after transfection and at the concentration and times indicated in figure legends. Once the treatment time was finished, cells were collected,

and protein levels were analyzed by western blot. Analysis of LC3 I/II protein levels were used as a positive control of the effectiveness of Chloroquine treatment

14.4. Hsp90 activity inhibition with geldanamycin

Hsp90 activity was inhibited by employing ansamycin inhibitor geldanamycin (GA) which acts by blocking ATPase activity of the Hsp90 chaperone. For Hsp90 inhibition experiments, cells were seeded in 6-well plates at a confluence of $7,5 \times 10^5$ cells/well for HEK 293T cells and $2,5 \times 10^5$ cells/well for HCT116 cells, or 100 mm dishes at 3×10^6 cells/dish for HEK 293T $1,5 \times 10^6$ cells/dish for HCT116 cells. Working concentrations for both cell lines were used based on MTT assays as indicated in figure legends. Treatment with GA was maintained for the indicated time. In those cases were GA treatment was combined with siRNA transfection, GA was added after 48 hours after transfection and maintained until reaching 72 hours of transfection. When combined with chloroquine, both treatments were added at the same time for 24 hours. All treated points were completed with DMSO up to the maximum concentration.

15. Migration assay

Cell migration assay was performed in transiently transfected HEK 293T cells employing 24- well Cell Migration Plate 8 µm (12 inserts) (Merck Millipore). For that, cells were seeded and transfected with 8 µg pcDNA 3.1 and pcDNA-Flag-Hakai for 48 hours. Cells were starved by adding serum-free medium 18 hours prior to assay. After 48 hours of transfection, cells were trypsinized, centrifuged 5 min at 1 200 rpm and seeded into migration transwells at a confluence of 3×10^5 cells/insert in 1 % FBS supplemented DMEM medium. To stablish a chemotaxis gradient, 500 µL of 30 % FBS DMEM medium were added to the lower chamber. For geldanamycin treatment, 10 µM of geldanamycin were added to the media in the upper chamber of the transwell. Taking into account the doubling time of this cell line (between 20 and 24 hours), cells were allowed to migrate for 16 hours to avoid the interference of the proliferative capacity in the obtained results. After 16 hours, medium in the upper chamber of the transwell was removed and non-migratory cells were carefully removed from the interior of the insert using a moistened cotton swap. This procedure was repeated three times to ensure the correct removal of the cells. Migratory cells in the bottom of the transwell were fixed with 4 % PFA for 10 minutes and washed three times with PBS pH 7,4. Cells were then stained with crystal violet for 20 min and washed thrice with PBS pH 7,4. Finally, membrane was carefully cut and removed from the transwells and mounted onto slides for image

acquisition with an Olympus BX50 microscope. Data analysis was performed by quantifying the number of migratory cells per 10X microscope field for three different photographs of the same experiment. Statistical analysis was performed with GraphPad Prism 6 by employing Student's t-test. Results were graphically represented as Mean ± SEM.

16. Evaluation of Hsp90 levels in Colorectal Cancer Samples

16.1. Human samples collection

Renal clear cell carcinoma samples were provided by Pathological Anatomy department of Complejo Hospitalario Universitario de A Coruña (CHUAC). All samples were collected under informed consent from the patients and Research Ethics Committee from A Coruña-Ferrol approved their use for investigation according to the standard ethical procedures described in the "Ley Orgánica de Investigación Biomédica" of 14 July 2007 of the Spanish regulation. Paraffin samples were transferred by CHUAC Biobank, which is part of the Spanish Hospital Platform Biobanks Network.

16.2. Immunohistochemistry

Slides containing sections of tumors were deparaffinized for 1 h at 60 °C in the stove. Once dewaxed, the slides were rehydrated by successive incubations in xylol (10 min), xylol (10 min), ethanol 100° (10 min), ethanol 96° (10 min), ethanol 70° (10 min) and water (5 min). Next, antigenic retrieval was performed by boiling the slides in Retriever 2100 (Aptum) using Target Retrieval Solution, Citrate pH 6,1 (10X) (Dako) for 15 min approximately. Slides were allowed to cool and washed with PBS-T 0,1 % (PBS-Tween 20 0,1 % pH 7,6) for 10 min. Endogenous peroxidase activity was inhibited by using peroxidase blocking solution (Dako) for 30 min at RT. Peroxidase blocking solution was discarded and samples were washed again for 10 min with PBS-T 0,1 %. Slides were carefully dried and blocked with blocking solution (0,2 % BSA/0,1 % Triton X-100 in PBS pH 7,6) for 30 min at RT. Incubation with primary antibody was carried out in a wet chamber overnight at 4 °C. Next day, slides were washed three times for 10 min with PBS-T and incubated with secondary antibody (Dako REAL™ Envision™ Detection System) and washed again with PBS-T three times for 5 min. Chromogenic solution of diaminobenzidine (DAB) (Dako REAL™ Envision™ Detection System) was prepared at 1:50 and added to the slides for 2 min to reveal secondary antibody activity. DAB acts as a substrate of HRP bound to secondary antibodies and produces an enzymatic reaction whose product is a brown

precipitate. DAB reaction was stopped by adding distilled water. Finally, slides were counterstained with Gill's Hematoxylin for 20 s to dye the tissue and distinguish DAB dye localization. Sample dehydration was performed following the opposite sequence of alcohols used for rehydration. Samples were left in xylol for 20 min time to ensure the correct dehydration and mounted with the coverslips using DePeX (Serva). A total of four sections of each condition (healthy tissue, adenoma, and adenocarcinoma stages I-IV) were processed. Five pictures of each section were taken with Olympus BX50 microscope with a 20X objective and number of positive staining cells per field were counted by employing Image J program. Statistical analysis was performed by employing GraphPad Prism 6 Software using Kruskal-Wallis with Tukey correction test. Results are represented as Mean ± SEM for each TNM stage in a scatter plot. A representative image is showed for each condition.

IV. RESULTS

1. Proteomic analysis of E3 ubiquitin-ligase Hakai-regulated proteins

1.1. Cell Biological Analysis of Hakai-induced EMT

As previously mentioned, only three substrates have been validated so far for E3 ubiquitin- ligase Hakai: E-cadherin, Cortactin and DOK1. However, as it occurs with other E3 ubiquitin- ligases, many other proteins might be regulated by Hakai E3 ubiquitin-ligase activity. In order to determine the potential role of Hakai upon other possible substrates, we performed a comparative proteomic study in a model of Hakai overexpression employing the previously described MDCK Hakai-overexpressing clones [89]. This cell model consisted in the epithelial MDCK cell line, extensively used in the study of EMT as a non-transformed epithelial cell line [11], which was stably transfected with pcDNA-HA-Hakai plasmid. First, phenotype of parental cell line MDCK and Hakai-overexpressing MDCK clones was examined under phase-contrast microscopy. MDCK cells showed a typical epithelial phenotype characterized by its grown in monolayer forming clusters of tightly connected individual cells. On the other hand, Hakai-transformed MDCK clones showed a mesenchymal phenotype characterized by the absence of intercellular contacts and the presence of cytoplasmic extensions (Figure 15A).

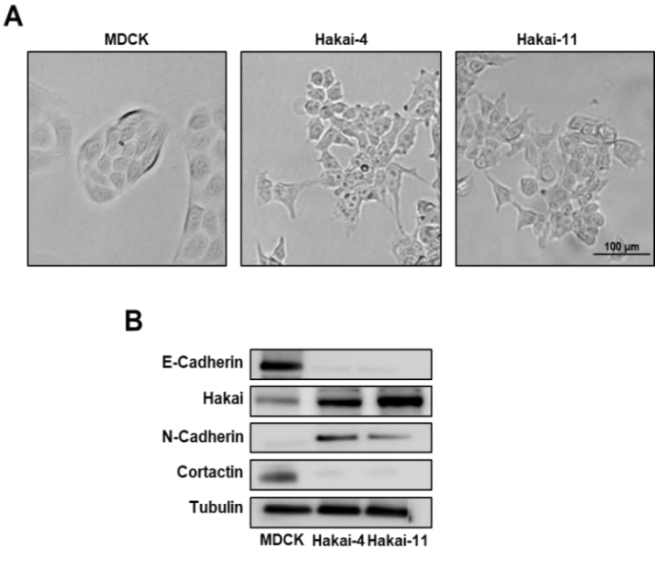

Figure 15. Stable Hakai overexpression in MDCK cells. (**A**) Phenotype of parental MDCK and Hakai-transformed MDCK cells observed with phase contrast microscopy. Both Hakai-transformed clone 4 and clone 11 cells show a loss of epitelial morphology and acquisition of mesenchymal phenotype (scale bar 100 µm). (**B**) Analysis by western blot of the expression levels of Hakai, E-cadherin, N-cadherin and Cortactin in MDCK parental cells and Hakai-transformed MDCK cells. Tubulin was employed as loading control.

Hakai overexpression in clones compared to non-transformed MDCK cells was confirmed by western blot. Given the effect of Hakai overexpression on MDCK cell line phenotype, we decided to support the observed effects by evaluating the expression of the EMT hallmark E-cadherin (target of the E3 ubiquitin-ligase Hakai), the mesenchymal marker N-cadherin, and the recently described susbtrate of Hakai Cortactin [63] (Figure 15B). As previously reported, E-cadherin levels were dramatically down-regulated in Hakai-transformed MDCK cells compared to parental MDCK levels. On the other hand, expression levels of mesenchymal marker N-cadherin were increased in Hakai-transformed MDCK cells and absent in MDCK parental cell line. Moreover, cortactin levels were also studied, confirming a down-regulation in Hakai-transformed MDCK cells compared to non-transformed epithelial MDCK cells in the same way that occurs with Hakai substrate E-cadherin. Altogether, these results confirm the loss of epithelial characteristics present in the MDCK parental line and the acquisition of mesenchymal characteristics in those overexpressing Hakai, supporting the role of Hakai in the induction of EMT process in this MDCK cellular model.

1.2. Strategy for the identification of Hakai-induced differential protein expression

In order to determine the proteomic effect of Hakai overexpression, protein expression profile was determined by HPLC/MS/MS in Hakai-transformed MDCK cells in comparison to MDCK parental cell lines. We performed this approach in collaboration with the Proteomics Platform of INIBIC. For that, total cell extracts from MDCK and Hakai-transformed MDCK cells (clone 4 and clone 11) were obtained from two replicates of each cell line (employing clone 4 and clone 11 as two different replicates). Same amount of total protein of the mentioned samples was loaded in an SDS-PAGE gel in duplicates and resolved by electrophoresis. We confirmed equal amounts or protein loading by silver staining (Figure 16A). Once the protein profile was checked for the different cell lines, we proceeded to sample preparation for the proteomic study. For that, equal amounts of protein from MDCK parental cell line and Hakai-overexpressing MDCK clones were precipitated with acetone and digested with trypsin. Then, peptides resulting from digestion of the 4 different samples were labeled with iTRAQ 4-plex reagent, put together and subjected to a clearing step with a C18 reverse phase column to remove excess of salts and to conditionate the sample. Peptides were subjected to a first separation step by reverse phase liquid chromatography at basic pH. Next, resulting fractions were combined and subjected to a second reverse phase liquid nano liquid chromatography

at acid pH coupled with a mass spectrometer MALDI/TOF-TOF. MS analysis was performed for identification and relative quantification of the present proteins. Schematic workflow of the whole process is represented in figure 16B.

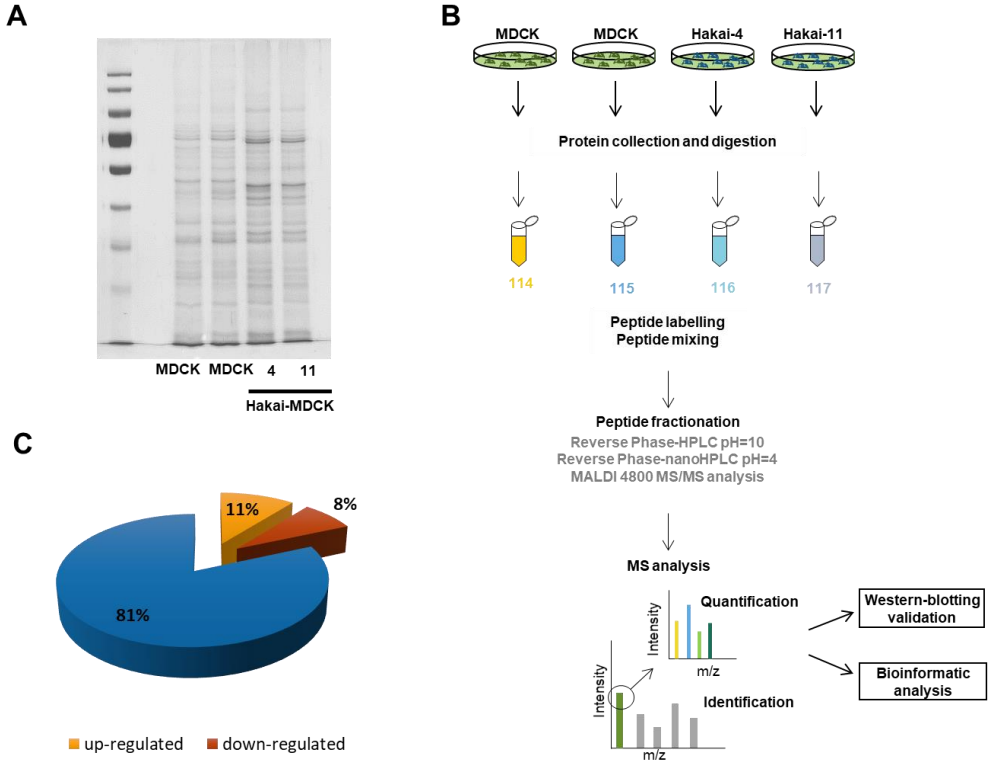

Figure 16. Scheme of experimental design of Hakai proteomic study. (**A**) Protein samples were analyzed by 1D-SDS-PAGE electrophoresis and dyed with silver staining for total protein visualization. (**B**) Experimental workflow. Samples were combined with labeled peptides, fractionated and separated by nano-LC. Separated samples were analyzed by employing MALDI-TOF/TOF mass spectrometry followed by bioinformatic analysis. (**C**) Pie chart diagram of 729 identified proteins. 11 % of proteins were up-regulated (orange) and 8 % were down-regulated (red) in Hakai-transformed cells compared to parental MDCK cells. 81 % of the identified protein were considered as not significatively changed (blue).

A total of 729 proteins were identified by mass spectrometry analysis with a false discovery rate of 1 %, including only proteins with two or more peptides identified with at least 95 % confidence and a protein pilot total score ≥ 2. Relative quantification between Hakai-transformed MDCK cells and MDCK parental cells was performed by using ProteinPilot™ software. In order to study significative differences between samples, bioinformatic analysis was performed and cutoff values for significant fold changes were stablished at > 2 for up-regulated proteins, < 0,5 fold change for down-regulated proteins and *p*-value < 0,05 in both

cases. Taking that into consideration, a total of 145 proteins were considered to be differentially expressed in Hakai-transformed MDCK cells compared to parental MDCK cells. When overexpressing Hakai, 83 proteins (11 %) resulted to be significatively up-regulated whilst 63 proteins (8 %) resulted to be significatively down-regulated (Figure 16C). The rest of the identified proteins (81 %) were considered as not significantly changed. Total identified up and down-regulated proteins with ≥ 2 (≤ 0,5) score are listed in Appendix A.

1.3. Proteomic Profiling of Hakai-transformed MDCK Cells

A classification of the 145 significantly modulated proteins in Hakai-transformed MDCK cells was performed based on the biological process in which they were involved and the molecular function they performed (Figure 17). For biological process classification, UniProt and bibliographic search of the main biological process in which each protein is involved during tumor progression was performed, and different classification categories were established based on the results obtained. Results were graphically represented in pie charts using Excel software (Figure 17A,B). For protein molecular function classification, bioinformatic analysis was carried out using Panther Classification System of Gene Ontology through its search by ID number and its visualization and classification in pie charts. Analysis information obtained with Panther software was collected and subsequently represented in Excel pie charts (Figure 17C,D).

According to biological process classification of up-regulated proteins, they were mainly implicated in metabolic processes (24 %), post-transcriptional regulation (18 %) and cell stress and homeostasis (11 %) (Figure 17A), whereas down-regulated proteins were mainly related to cytoskeleton and cell morphology (24 %), membrane vesicle trafficking (19 %) and metabolic processes (16 %) (Figure 17B). In relation to molecular function based on Gene Ontology classification, proteins were diversely classified in different categories. Proteins included in both classification groups happen to mainly play functions related to catalytic activity (56 % and 33 % for up and down-regulated proteins respectively, Figure 17C,D) and protein binding (32 % and 38 % for up and down-regulated proteins respectively, Figure 17C,D). The implication of Hakai in the processes described in this classification is consistent with the previously published results for Hakai and its involvement in cell migration and invasion [56, 82, 89]. Migration and invasion are both important features during cancer progression, in which many of the processes described in the indicated categories can be found altered, such as adhesion cellular, cytoskeleton reorganization, or increased cellular stress. A representative

subset of selected Hakai significative-down-regulated proteins involved in the described biological processes are listed in Table 16. These proteins were selected according to its classification category's relevance during cancer progression, such as those related to cell adhesion or membrane vesicle trafficking, among other important categories related to cancer progression.

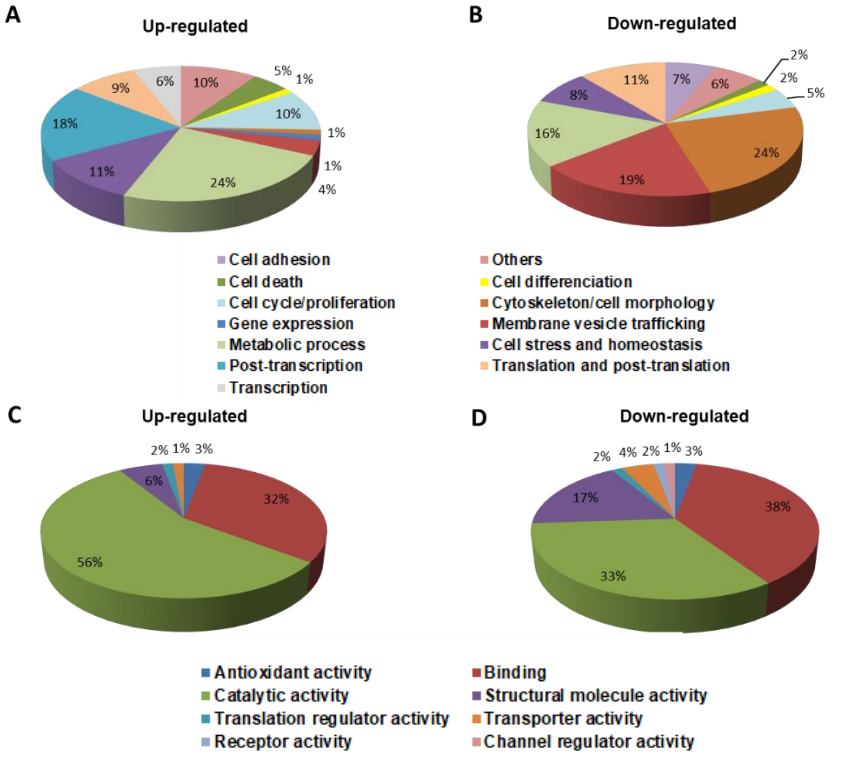

Figure 17. Classification of the identified proteins in diagrams of biological process (A, B) and molecular function (C, D) based on Gene Ontology (GO), Uniprot databases and bibliographic research. This analysis was performed for 145 identified proteins showing a fold-change > 2 and a p-value < 0.05. (**A, C**) Classification of 82 up-regulated proteins in Hakai-transformed MDCK cells compared to MDCK parental cells. (**B, D**) Classification of 62 down-regulated proteins in Hakai-transformed MDCK cells compared to MDCK parental cells.

Among the implicated proteins in cell adhesion, which happens to be reduced during cancer progression, we found Annexin A1, Annexin A2, Galectin-3, Stratifin (14-3-3 protein sigma), S100-A10 (A100 calcium binding protein A10) and Calumenin. Other cytoskeleton-related proteins were also included among Hakai down-regulated proteins, such as Ezrin, Septin-2, Moesin, Alpha-actinin-4, PDZ and LIM domain protein-1 and LIM and SH3 domain protein-1. In addition to the presence of characteristic proteins of the cytoskeleton structure, we also found

cytoskeleton regulatory proteins which happened to be down-regulated in the presence of Hakai overexpression. These proteins play an important role during cytoskeleton remodeling and dynamics, affecting cell contacts, increasing cell plasticity and allowing the creation of cell protrusions which improve migration and invasion ability of cancer cells during tumor progression [205]. Among these cytoskeleton-regulatory proteins we found AHNAK, α-actinin, the Arp2/3 complex, Cofilin and Prelamin-A/C.

Some of the selected significative up-regulated proteins under Hakai overexpression are shown in Table 17. Many of the identified proteins are related to metabolic processes, such as IMPDH1, IMPDH2, LDHB or ALDR, which suggest that Hakai is playing a role in modifying cellular metabolism. Other identified proteins were chaperones Hsp70 and AN32E or post-transcriptional regulators ILF3, RL12, LYAR, PAIRB and ROA1, which were also increased in Hakai-transformed MDCK cells in comparison to parental MDCK cells.

Table 16. List of selected identified down-regulated proteins.

	% coverage	Accession number	Protein symbol	Protein name	Function	Peptide match (95 %)	Fold change (Hakai/wt)	*p* value
1	60,4	P04083	ANXA1	Annexin A1	Cell adhesion molecule involved in cell-to-cell and to extracellular matrix binding. Also involved in proliferation, differentiation, motility, trafficking, apoptosis and tissue architecture	25	0,0137	0
2	33,6	P17931	LEG3	Galectin-3	Galactose-specific lectin which binds IgE. May mediate endothelial cells migration. In the nucleus acts as a pre-mRNA splicing factor. Involved in acute inflammatory responses.	20	0,0198	0,0112
3	84,1	P07355	ANXA2	Annexin A2	Calcium-regulated membrane-binding protein wich plays a role in the regulation of cellular growth and in signal transduction pathways. It binds two calcium ions with high affinity. May be involved in heat-stress response	49	0,0172	0
4	63,9	P60903	S10AA	Protein S100-A10	involved in the regulation of a number of cellular processes such as cell cycle progression and differentiation. This protein may function in exocytosis and endocytosis. Induces the dimerization of ANXA2/p36.	12	0,0211	0,0004
5	49,2	P31947	1433S	14-3-3 protein sigma	Adapter protein implicated in the regulation of different signaling pathways, such as Cell Cycle Checkpoints and p53 Pathway.When bound to KRT17, regulates protein synthesis and epithelial cell growth	11	0,0219	0,0118
6	66	P25786	AHNK	Neuroblast differentiation-associated protein AHNAK	Structural molecule activity conferring elasticity. May be required for neuronal cell differentiation.	88	0,0203	0

	% coverage	Accession number	Protein symbol	Protein name	Function	Peptide match (95 %)	Fold change (Hakai/wt)	*p* value
7	48,5	P02545	LMNA	Prelamin-A/C	Component of the nuclear lamina. Involved in nuclear stability, chromatin structure and gene expression. Required for bone formation. Accelerates smooth muscle senescence.	16	0,0417	0,0015
8	71,4	O43852	CALU	Calumenin	Calcium-binding protein localized in the endoplasmic reticulum (ER) and it is involved in such ER functions as protein folding and sorting. Among its related pathways are Ca, cAMP and Lipid Signaling and Platelet activation, signaling and aggregation	16	0,0912	0
9	41,4	O14818	ACTN4	Alpha-actinin-4	Cytoskeletal protein probably involved in vesicular trafficking via its association with the CART complex. Involved in tight junction assembly in epithelial cells. Is thought to be involved in metastatic processes.	14	0,1306	0
10	75,6	P15311	EZRI	Ezrin	Plays a key role in cell surface structure adhesion, migration and organization, and it has been implicated in various human cancers. In epithelial cells, required for the formation of microvilli and membrane ruffles on the apical pole.	61	0,157	0,0003
11	72,1	P26038	MOES	Moesin	Cross-linker between plasma membranes and actin-based cytoskeletons. Localized membranous protrusions that are important for cell-cell recognition and signaling and for cell movement.	52	0,2109	0,0092
12	89,8	P23528	COF1	Cofilin-1	Important for normal progress through mitosis and normal cytokinesis. Plays a role in the regulation of cell morphology and cytoskeletal organization	23	0,3162	0
13	65,3	P67936	TPM4	Tropomyosin alpha-4 chain	Binds to actin filaments in muscle and non-muscle cells. Plays a central role in the calcium dependent regulation of vertebrate striated muscle contraction	18	0,0794	0,0005

	% coverage	Accession number	Protein symbol	Protein name	Function	Peptide match (95 %)	Fold change (Hakai/wt)	*p* value
14	68,8	P37802	TAGL2	Transgelin-2	The specific function of this protein has not yet been determined, although it is thought to be a tumor suppressor	16	0,1019	0
15	61,8	P52565	GDIR1	Rho GDP-dissociation inhibitor 1	Controls Rho proteins homeostasis. Through the modulation of Rho proteins, may play a role in cell motility regulation. Activity of this protein is important in a variety of cellular processes, and expression of this gene may be altered in tumors.	14	0,227	0,0226
16	60,9	Q15019	SETP2	Septin-2	Required for normal organization of the actin cytoskeleton. Plays a role in the biogenesis of polarized columnar-shaped epithelium, thus facilitating efficient vesicle transport.	12	0,3221	0,0104
17	51,8	P61586	RHOA	Transforming protein RhoA	Rho proteins promote reorganization of the actin cytoskeleton and regulate cell shape, attachment, and motility. Overexpression of this gene is associated with tumor cell proliferation and metastasis.	9	0,3404	0,0133
18	33	P27816	MAP4	Microtubule-associated protein 4	Non-neuronal microtubule-associated protein. Promotes microtubule assembly. Diseases associated with MAP4 include Ovarian Clear Cell Adenocarcinoma	9	0,3767	0,0366
19	53,7	Q9NYL9	TMOD3	Tropomodulin-3	Blocks the elongation and depolymerization of the actin filaments at the pointed end and defines the geometry of the membrane skeleton.	5	0,2014	0,0187
20	32,2	O00151	PDLI1	PDZ and LIM domain protein 1	Cytoskeletal protein that may act as an adapter that brings other proteins (like kinases) to the cytoskeleton.	5	0,0839	0,003
21	30,8	P50552	VASP	Vasodilator-stimulated phosphoprotein	Actin-associated protein involved in cytoskeleton remodeling and cell polarity such as axon guidance, lamellipodial and filopodial dynamics, platelet activation and cell migration	4	0,4742	0,005

	% coverage	Accession number	Protein symbol	Protein name	Function	Peptide match (95 %)	Fold change (Hakai/wt)	*p* value
22	37	O15144	ARPC2	Actin-related protein 2/3 complex subunit 2	Implicated in the control of actin polymerization in cells. Together with an activating nucleation-promoting factor (NPF) mediates the formation of branched actin networks	4	0,263	0,0194
23	26,2	P11234	RALB	Ras-related protein Ral-B	Multifunctional GTPase involved in a variety of cellular processes including gene expression, cell migration, cell proliferation, oncogenic transformation and membrane trafficking.	3	0,3532	0,0261
24	30,7	Q9BPX5	ARP5L	Actin-related protein 2/3 complex subunit 5-like protein	Involved in regulation of actin polymerization and together with an activating nucleation-promoting factor (NPF) mediates the formation of branched actin networks.	3	0,1803	0,0264
25	29,1	Q14847	LASP1	LIM and SH3 domain protein 1	Plays an important role in the regulation of dynamic actin-based, cytoskeletal activities. Involved in ion transmembrane transport activity.	3	0,0711	0,0275

*The selected unique proteins found identified with >95% confidence and score ≤0.5 are indicated. Data in the table include: percentage coverage; Accession number; Symbol; Protein name; Biological roles in references from Gene Cards human database. Number of distinct peptides having at least 95% confidence; Unique peptides; Ratio (Mean ± SD); p-value.

Table 17. List of selected identified up-regulated proteins

	% coverage	Accession number	Protein Symbol	Protein name	Function	Peptide match (95 %)	Fold change (Hakai/wt)	*p* value
1	79,1	P08107	HSP71	Heat shock 70 kDa protein 1A/1B	Chaperone that stabilizes preexistent proteins against aggregation and mediates its folding in the cytosol as well as within organelles. It is also involved in the ubiquitin-proteasome pathway.	111	39,8107	0,0002
2	89,4	P06733	ENOA	Alpha-enolase	Multifunctional enzime which participates in glycolysis, as well as growth control, hypoxia tolerance and allergic responses. Stimulates immunoglobulin production and may play a role as a tumor supressor.	96	32,5087	0,0003
3	88,8	P15531	NDKA	Nucleoside diphosphate kinase A	Protein which plays its major role in synthesis of nucleoside triphosphates. Involved in cell proliferation, differentiation and development, signal transduction and gene expression. NME1 is associated with diseases such as Neuroblastoma and Anal Canal Carcinoma	24	10,5682	0,0009
4	94,1	P22392	NDKB	Nucleoside diphosphate kinase B	Enzime that plays its major role in synthesis of nucleoside triphosphates as well as NME1. Acts as as transcriptional activator of MYC gene and negatively regulates Rho activiy. Diseases associated with NME2 include Myxosarcoma and Lung Sarcoma	30	22,2843	0
5	61,1	P12268	IMDH2	Inosine-5'-monophosphate dehydrogenase 2	Catalyzes the conversion of inosine 5-phosphate (IMP) to xanthosine 5-phosphate, the first limiting step in the sinthesys of guanine nucleotides. It may play a role in the malignancy and progression of some tumors.	21	4,6132	0
6	67,8	P16949	STMN1	Stathmin	Ubiquitous cytosolic phophoprotein involved in the microtubule filament system by destabilizing microtubules. Prevents assembly and promotes disassembly of microtubules.	16	3,4995	0,0001

	% coverage	Accession number	Protein Symbol	Protein name	Function	Peptide match (95 %)	Fold change (Hakai/wt)	*p* value
7	35,6	Q12906	ILF3	Interleukin enhancer-binding factor 3	Protein that regulates gene expression at level of post-transcription. Can act as an inhibitory protein at the initiation phase of RNA translation probably by inhibiting its binding to polysome.	11	2,8054	0,0059
8	71,4	P49773	HINT1	Histidine triad nucleotide-binding protein 1	Protein that hydrolyzes purine nucleotide phosphoramidates substrates. Modulates proteasomal degradation of target proteins by the SCF E3 ubiquitin-protein ligase complex. The HINT1 gene is considered a tumor supressor.	6	15,9956	0,0015
9	23,2	P20839	IMDH1	Inosine-5'-monophosphate dehydrogenase 1	Enzime that catalyzes the conversion of inosine 5-phosphate (IMP) to xanthosine 5-phosphate, the first limiting step in the sinthesys of guanine nucleotides. It may play a role in the malignancy and progression of some tumors.	4	36,6438	0,0006
10	41,6	P07195	LDHB	L-lactate dehydrogenase B chain	B subunit of lactate dehydrogenase enzime which catalyzes the interconversion of pyruvate and lactate with concomitant interconversion of NADH and NAD+. Diseases related to LDHB include urinary bladder urothelial carcinoma.	13	6,9183	0
11	46,5	P15121	ALDR	Aldose reductase	Protein member of aldo/keto reductase superfamily. Catalyzes the NADPH-dependent reduction of aldehydes. It is implicated in the metabolism of steroid hormones and galactose.	4	3,6308	0,024
12	32,1	Q9BTT0	AN32E	Acidic leucine-rich nuclear phosphoprotein 32 family member E	Histone chaperone that specifically mediates the removal of histone H2A.Z/H2AFZ from the nucleosome.	7	4,6989	0,0439
13	43,3	Q9NX58	LYAR	Cell growth-regulating nucleolar protein	Poly(A) RNA binding protein.	7	6,0813	0,0442

	% coverage	Accession number	Protein Symbol	Protein name	Function	Peptide match (95 %)	Fold change (Hakai/wt)	*p* value
14	71,3	Q8NC51	PAIRB	Plasminogen activator inhibitor 1 RNA-binding protein	Poly(A) RNA binding protein and mRNA 3-UTR binding protein. May play a role in the regulation of mRNA stability.	35	8,5507	0
15	70,9	P30050	RL12	60S ribosomal protein L12	Protein component of the ribosomal 60S subunit. This protein binds directly to the 26S rRNA .	13	4,7863	0,0001
16	19,3	P12955	PEPD	Xaa-Pro dipeptidase	The protein forms a homodimer that hydrolyzes dipeptides or tripeptides with C-terminal proline or hydroxyproline residues. The enzyme serves an important role in the recycling of proline, and may be rate limiting for the production of collagen.	3	18,3654	0,0005
17	14,7	Q12765	SCRN1	Secernin-1	Protein that regulates exocytosis in mast cells increasing its secretion and sensitivity to stimulation with calcium.	1	14,8594	0,028
18	31,7	P49321	NASP	Nuclear autoantigenic sperm protein	H1 histone binding protein involved in the transport of histones to the nucleus in dividing cells. Required for DNA replication and normal cell proliferation and cycle progression.	7	4,4875	0,0012
19	40,3	P60891	PRPS1	Ribose-phosphate pyrophosphokinase 1	Enzyme that catalyzes the phosphoribosylation of ribose 5-phosphate to 5-phosphoribosyl-1-pyrophosphate, necessary for nucleotide biosynthesis and purine metabolism.	8	7,2444	0,0008
20	63,7	P09651	ROA1	Heterogeneous nuclear ribonucleoprotein A1	Protein involved in the packaging of pre-mRNA into hnRNP particles, transport of poly(A) mRNA from the nucleus to the cytoplasm and may modulate splice site selection	50	2,8054	0,0011
21	51,6	Q14103	HNRPD	Heterogeneous nuclear ribonucleoprotein D0	Member of the subfamily of ubiquitously expressed heterogeneous nuclear ribonucleoproteins (hnRNPs) which participates in pre-mRNA processing, mRNA metabolism and transport. This protein is implicated in mRNA stability.	18	2,4889	0,0005

*The selected unique proteins found identified with >95% confidence and score ≥2 are indicated. Data in the table include: percentage coverage; Accession number; Symbol; Protein name; Biological roles in references from Gene Cards human database. bNumber of distinct peptides having at least 95% confidence; Unique peptides; Ratio (Mean ± SD); p-value.

1.4. Bioinformatic analysis of Hakai-regulated proteins

In order to evaluate the presence of protein-protein interactions between up and down-regulated proteins in Hakai-transformed MDCK cells, an independent analysis was performed by employing STRING database. STRING database consists in a biological database with web access that can process data from several sources in order to determine and provide information about functional and physical properties [206]. When subjected our identified up- and down-regulated proteins to STRING analysis, we found networks with significantly more interactions than expected, suggesting that our Hakai-regulated proteins are partially connected as a group or, at least, interacting among each other. First, we subjected down-regulated proteins to STRING analysis and evaluated the interaction between proteins for different predetermined categories. The most interesting results were observed for protein metabolism (Figure 18A) and cytoskeleton (Figure 18B), which are related to the main cellular characteristics modified by Hakai protein function. Interestingly, a very delimited cluster of proteins identified as proteasome subunits was observed in STRING analysis for protein metabolism (Figure 18A), suggesting a down-regulation of 26S proteasome catalytic activity in Hakai-transformed cells compared to parental epithelial MDCK cells (Table 18). Similarly, when subjecting up-regulated proteins to STRING analysis (Figure 19), they showed to be mainly gathered in two main groups classified by their RNA-binding properties (Figure 19A) and their association with extracellular exosomes (Figure 19B). Taking into consideration this analysis, proteomic profiling of Hakai suggests its implication in cytoskeleton dynamics, RNA-related proteins, exosome association and protein metabolism. All of these processes are reported to be altered during cancer progression.

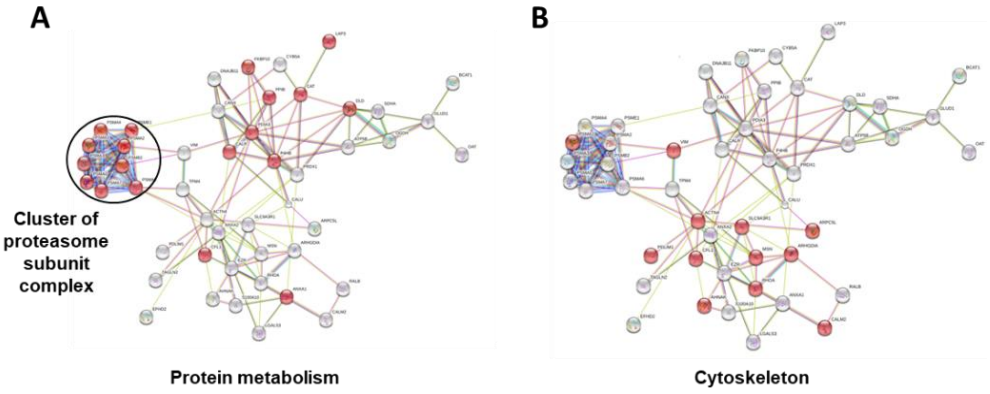

Figure 18. Protein–protein interaction network of the identified down-regulated proteins by Hakai. The STRING database was searched for protein–protein of the connected identified under-regulated proteins in Hakai-transformed MDCK cells compared to normal MDCK ($p < 0.001$). With a confidence cutoff of 0.4, the resulting network contains 138 edges between 63 of the proteins; the proteins with no associations to other proteins in the network were removed. (**A**) Network of proteins involved in protein metabolism are highlighted in red and represented as nodes. Red circle is drawn to indicate the cluster of proteasome subunit complex. Highlighted proteins in red are DLDH, Dihydrolipoyl dehydrogenase, mitochondrial; CATA, Catalase; FKB10, Peptidyl-prolyl cis–trans isomerase FKBP10; PP1B, Serine/threonine-protein phosphatase PP1-beta catalytic subunit; ANXA1, Annexin A1; CALR, Calreticulin; AMPL, Cytosol aminopeptidase; COF1, Cofilin-1; PDIA3, Protein disulfide-isomerase A3; PDIA1, Protein disulfide-isomerase; PSB2, Proteasome subunit beta type 2; PSA2, Proteasome subunit alpha type 2; PSA1, Proteasome subunit alpha type 1; PSA3, Proteasome subunit alpha type 3; PSA7, Proteasome subunit alpha type 7; PSA6, Proteasome subunit alpha type 6; PSA5, Proteasome subunit alpha type 5; PSA4, Proteasome subunit alpha type 4; PSME1, Proteasome activator complex subunit 1. (**B**) Network of cytoskeleton-related proteins are highlighted in red and represented as nodes. ARP5L, Actin-related protein 2/3 complex subunit 5-like protein; CALM, Calmodulin; VIME, Vimentin; PSME1, Proteasome activator complex subunit 1; ACTN4, Alpha-actinin-4; AHNK, Neuroblast differentiation-associated protein AHNAK; COF1, Cofilin-1; MOES, Moesin; GDIR1, Rho GDP-dissociation inhibitor 1; RHOA, Transforming protein RhoA; NHRF1, Na(+)/H(+) exchange regulatory cofactor NHE-RF1; PDLI1, PDZ and LIM domain protein 1.

Table 18. Identified down-regulated proteasome subunits.

	% coverage	Accession number	Protein Symbol	Protein name	Peptide match (95 %)	Fold change (Hakai/wt)	*p* value
1	66,2	P25787	PSA2	Proteasome subunit alpha type-2	12	0,1306	0,0007
2	44,6	Q06323	PSME1	Proteasome activator complex subunit 1	4	0,3251	0,046
3	43,7	P25789	PSA4	Proteasome subunit alpha type-4	8	0,3698	0,0119
4	64,7	P28066	PSA5	Proteasome subunit alpha type-5	7	0,1169	0,0054
5	61,8	P60900	PSA6	Proteasome subunit alpha type-6	13	0,4699	0,0038
6	85,9	O14818	PSA7	Proteasome subunit alpha type-7	12	0,3873	0,0029
7	60,1	P25786	PSA1	Proteasome subunit alpha type-1	12	0,4207	0,0016
8	56,5	P25788	PSA3	Proteasome subunit alpha type-3	10	0,4285	0,0316
9	81,1	P49721	PSB2	Proteasome subunit beta type-2	9	0,3802	0,0462

*Identified subunits involved in 26 proteasome down-regulated in normal MDCK epithelial transformed with Hakai. The table includes percentage coverage; Accession number; Symbol; Protein name. bNumber of distinct peptides having at least 95% confidence; Unique peptides; Ratio (Mean ± SD); p-value.

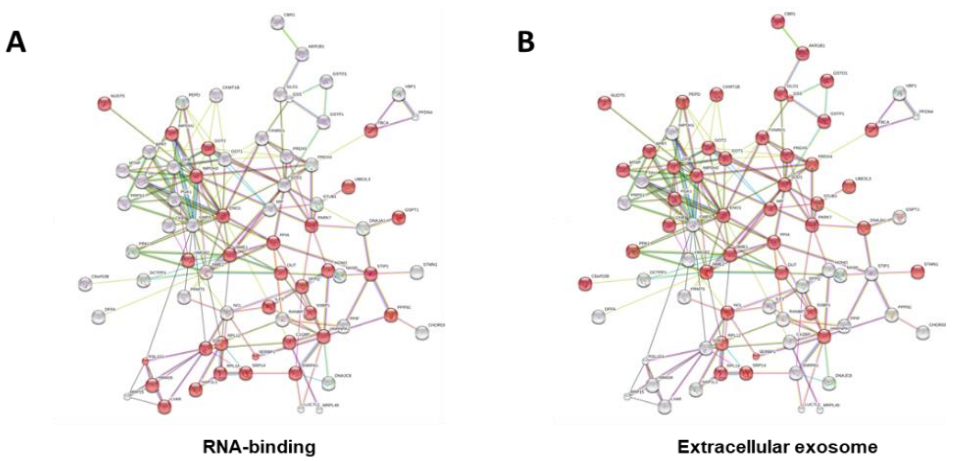

Figure 19. Protein–protein interaction network of the identified up-regulated proteins by Hakai. The STRING database was searched for protein-protein of the connected identified up-regulated proteins in Hakai-transformed MDCK cells compared to normal MDCK ($p < 0.001$). With a confidence cutoff of 0.4, the resulting network contains 179 edges between 82 of the proteins; the proteins with no associations to other proteins in the network were removed. (**A**) Network of proteins with RNA-binding properties are highlighted in red: NUDT5, ADP-sugar pyrophosphatase; IMDH2, Inosine-5′ -monophosphate dehydrogenase 2; NDKA, Nucleoside diphosphate kinase A; DUT, Deoxyuridine 5′ -triphosphate nucleotide hydrolase, mitochondrial; PPIA, Peptidyl-prolyl cis–trans isomerase A; ROA1, Heterogeneous nuclear ribonucleoprotein A1; RL14, 60S ribosomal protein L14; SRP14, Signal recognition particle 14 kDa protein; PAIRB, Plasminogen activator inhibitor 1 RNA-binding protein; RL12, 60S ribosomal protein L12; AATM, Aspartate aminotransferase, mitochondrial; ENOA, Alpha-enolase; PARK7, Protein DJ-1; TBCA, Tubulin-specific chaperone A; IMDH1, Inosine-5′ -monophosphate dehydrogenase 1; HMGB2, High mobility group protein B2; STIP1, Stress induced-phosphoprotein 1; GSTP1, Glutathione S-transferase P; NONO, Non-POU domain-containing octamer-binding protein; SFPQ, Splicing factor, proline- and glutamine-rich; LYAR, Cell growth-regulating nucleolar protein; SSBP, Single-stranded DNA-binding protein, mitochondrial; ILF3, Interleukin enhancer-binding factor 3; UB2L3, Ubiquitin-conjugating enzyme E2 L3; NP1L1, Nucleosome assembly protein 1-like 1; RL1D1, Ribosomal L1 domain-containing protein 1; RBM28, RNA-binding protein 28; RU2A, U2 small nuclear ribonucleoprotein A; C1QBP, Complement component 1 Q subcomponent-binding protein, mitochondrial; LA, Lupus La protein; PPP5, Serine/threonine-protein phosphatase 5. (**B**) Protein–protein interaction of extracellular exosomes-associated proteins are highlighted in red and represented as nodes. NUDT5, ADP-sugar pyrophosphatase; MTAP, S-methyl-5′ -thioadenosine phosphorylase; PGK1, Phosphoglycerate kinase 1; APT, Adenine phosphoribosyltransferase; IMDH2, Inosine-5′ -monophosphate dehydrogenase 2; AATM, Aspartate aminotransferase, mitochondrial; AATC, Aspartate aminotransferase, cytoplasmic; LDHB, L-lactate dehydrogenase B chain; KCRU, Creatine kinase U-type, mitochondrial; STMN1, Stathmin; CBR1, Carbonyl reductase [NADPH] 1; ENOA, Alpha-enolase; NDKB, Nucleoside diphosphate kinase B; NDKA, Nucleoside diphosphate kinase A; RL12, 60S ribosomal protein L12; PRDX4, Peroxiredoxin-4; PRDX5, Peroxiredoxin-5, mitochondrial; GSTO1, Glutathione S-transferase omega-1; GSHB, Glutathione synthetase; GSTP1, Glutathione S-transferase P; LGUL, Lactoylglutathione lyase; ALDR, Aldose reductase; TRXR1, Thioredoxin reductase 1, cytoplasmic; SSBP, Single-stranded DNA-binding protein, mitochondrial; SODC, Superoxide dismutase [Cu–Zn]; TBCA, Tubulinspecific chaperone A; DUT, Deoxyuridine 5-triphosphate nucleotidohydrolase, mitochondrial; PPIA, Peptidyl-prolyl cis–trans isomerase A; PEPD, Xaa-Pro dipeptidase; IPYR, Inorganic pyrophosphatase; KCRB, Creatine kinase B-type; PARK7, Protein DJ-1; DNJA1, DnaJ homologue subfamily A member 1; CHIP, E3 ubiquitin-protein ligase CHIP; UB2L3, Ubiquitin-conjugatin enzyme E2 L3; NUCL, Nucleolin; RCL, Deoxyribonucleoside 5′ -monophosphate N-glycosidase MIF, Macrophage migration inhibitory factor; PAIRB, Plasminogen activator inhibitor 1 RNA-binding protein; RL14, 60S ribosomal protein L14; ROA1, Heterogeneous nuclear ribonucleoprotein A1; SRP14, Signal recognition particle 14 kDa protein.

1.5. Validation of the identified Hakai-regulated proteins by Western blotting

After the classification of the identified proteins in relation to their biological process and molecular function, validation of protein up- or down-regulation was performed for some of the identified proteins which were considered of more interest due to their fold change and their role during cancer development. For that purpose, western blot was performed by using protein extracts of MDCK and two different Hakai-transformed MDCK clones (clone 4 and clone 7) to confirm iTRAQ results (Figure 20). Among down-regulated proteins, Annexin A1, Annexin A2, Calumenin, Stratifin (14-3-3) and Galectin-3 were selected for validation based on their fold-change, *p*-value and the available information about their possible roles during tumor progression.

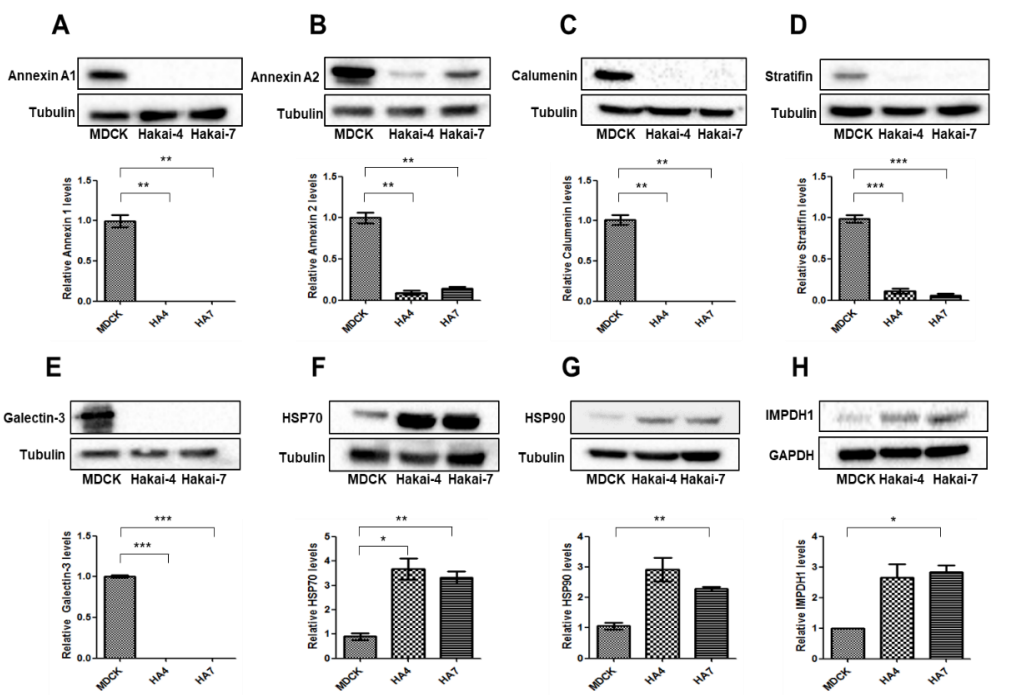

Figure 20. Western blot analysis of selected increased and decreased proteins in Hakai-transformed MDCK cells. Down-regulated proteins (**A-E**) and up-regulated proteins (**F-H**) were selected from iTRAQ analysis identified proteins and validated by western blot by using cell lysates of MDCK parental cell lines and two clones of Hakai-transformed MDCK cells (Hakai-4 and Hakai-7). Densitometric quantification of identified proteins was performed using ImageLab Software by employing Tubulin or GAPDH as housekeeping for normalization. Proteomic study results were validated for all the proteins analyzed. Results are represented as Mean ± SEM from three independent experiments. Statistical analyses indicate a significant difference between Hakai-transformed MDCK cells respect to parental MDCK cells (*p < 0.05, **p < 0.01, ***p < 0.001).

Relative quantification of protein expression levels was performed in relation to housekeeping levels. Hakai-transformed clone 4 and clone 11 quantification values were relativized to control MDCK expression levels. Significant down-regulation of selected proteins was effectively confirmed in Hakai-transformed MDCK clones by statistical analysis (Figure 20A-E). In the same way, a subset of up-regulated proteins was selected for iTRAQ results validation by western blot, including Hsp70 and IMPDH1 based on their fold-change and *p*-value. In addition to these two identified proteins, we decided to include Hsp90 for validation, as it shares important similarities with Hsp70 and has been extensively studied in relation to cancer progression. Statistical significance was confirmed for the up-regulation of selected proteins by western blot in one or both Hakai-transformed MDCK clones in comparison to MDCK parental cells (Figure 20F-H). Altogether, these results support and validate the data obtained through proteomic analysis using iTRAQ approach.

1.6. Analysis of the subcellular localization of Hakai-regulated proteins

In addition to our proteomic study, we further investigated whether subcellular localization of the selected up- and down-regulated proteins was changed in Hakai-transformed MDCK cells compared to MDCK parental cell line. To determine subcellular localization, we performed immunofluorescence assays in MDCK and one of the Hakai-transformed clones for Annexin A1, Annexin A2, Stratifin, Galectin-3, Hsp70 and Hsp90 (Figure 21). As we could observe, Annexin A1 and Annexin A2 (Figure 21A,B) were completely disappeared in Hakai-transformed MDCK cells compared to parental MDCK cell line. No significative changes were observed in localization for Stratifin (Figure 21C) in Hakai-transformed cells compared to MDCK cells. However, a dramatical change in localization for Galectin-3 was observed when overexpressing Hakai (Figure 21D). While Galectin-3 was dispersedly distributed throughout the cytoplasm in parental MDCK cells, it was enriched in specific localizations in the cytoplasm in Hakai-transformed MDCK cells. This enrichment of Galectin-3 seemed to be localized between cellular protrusions and the nuclear area. On the other hand, localization of both chaperones Hsp70 and Hsp90 was also found to be modified when overexpressing Hakai. MDCK parental cells showed a dotted cytoplasmic pattern for Hsp70 while Hakai overexpression apparently induced its translocation to cell-cell contacts (Figure 21E). Regarding Hsp90, localization in MDCK parental cell lines was diffused and cytoplasmatic, however Hakai overexpression induced its translocation to cellular membrane (Figure 21F).

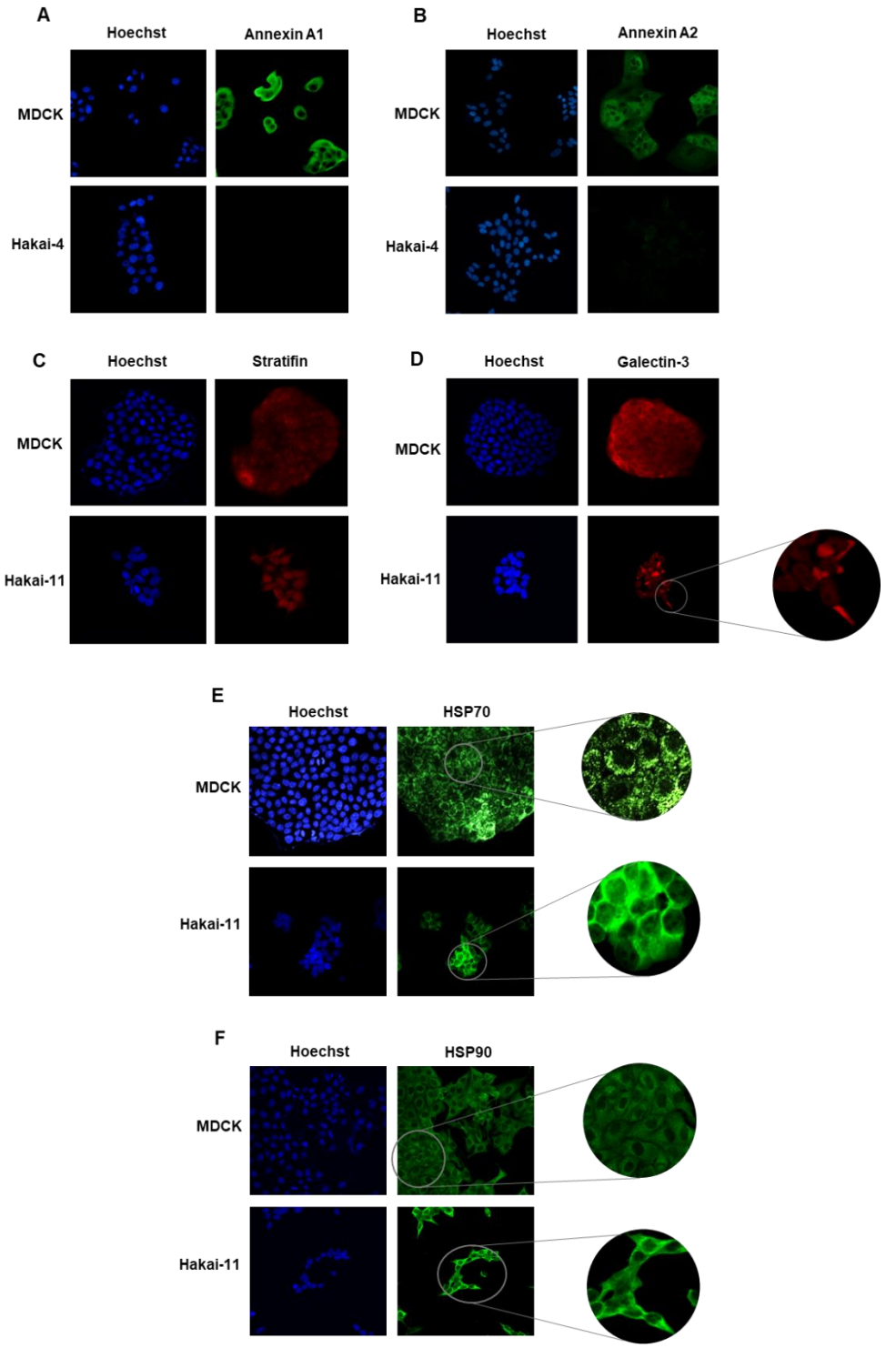

Figure 21. Effect of Hakai overexpression on subcellular localization of selected proteins. Annexin A1 (A), Annexin A2 (B), Stratifin (C), Galectin-3 (D), Hsp70 (E) and Hsp90 (F) subcellular localization was examined by confocal microscopy. Photos were taken with objective of 40X magnification. A zoom was included by amplifying and cutting the images (circle images).

Altogether, these results suggest that, apart from inducing the modulation of their expression levels, Hakai stable overexpression can also modulate the subcellular localization of some selected proteins.

Due to the interesting results obtained for Galectin-3, Hsp70 and Hsp90 regarding their subcellular localization in Hakai-transformed MDCK cells, we decide to evaluate the possible co-localization of Hakai and these mentioned proteins by co-immunofluorescence and confocal microscopy (Figure 22). Immunofluorescence showed a diffuse cytoplasmic localization of Galectin-3 in MDCK parental cell line. Anti-HA tag antibody, only expressed in Hakai-transformed MDCK cells, was used for evaluation of Hakai localization in both cell lines and showed a week unspecific signal in MDCK cells. However, striking co-localization of HA and Galectin-3 was observed in Hakai-transformed MDCK cells in delimited areas localized between cytoplasmic protrusions and nuclear area (Figure 22A). On the other hand, no co-localization was observed for Hsp70 and Hakai, neither in MDCK parental cells nor in Hakai-transformed MDCK cells (Figure 22B). However, co-immunofluorescence performed for Hsp90 and Hakai showed a light cytoplasmic co-localization of both proteins in Hakai-transformed MDCK cells, whereas no co-localization was detected for parental MDCK cell line (Figure 22C). These observations suggest that Hakai may influence the expression or the subcellular localization of Galectin-3 and Hsp90 by directly or indirectly interacting with them.

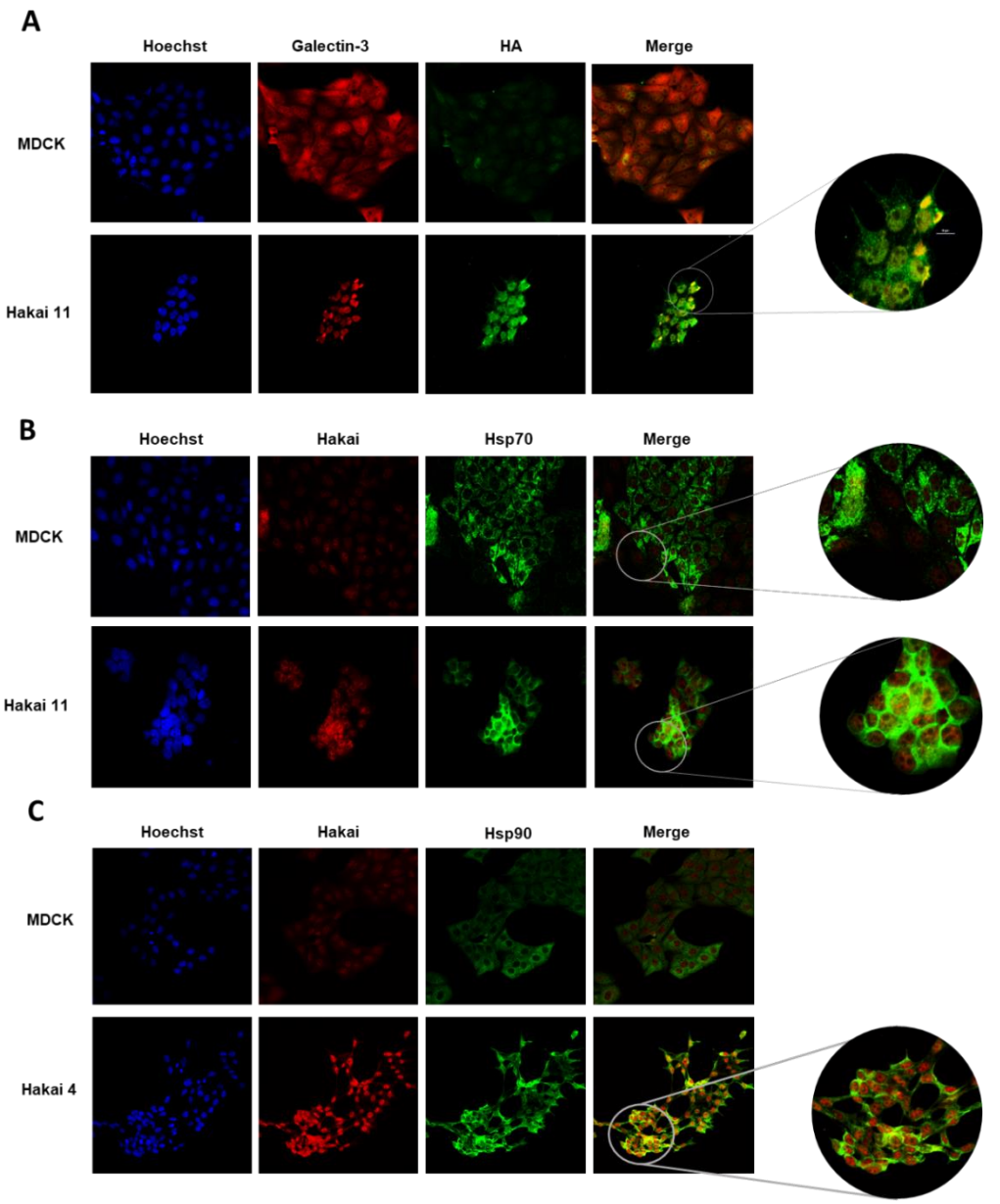

Figure 22. Co-immunofluorescence analysis of Hakai co-localization with selected proteins. Hakai co-localization with Galectin-3 (A), Hsp70 (B) and Hsp90 (C) was examined in Hakai-transformed MDCK cells and MDCK parental cells. Hakai localization was evaluated by employing either anti-Hakai or anti-HA antibody (**A**). Protein localization was examined by confocal microscopy. Photos were taken with objective of 40X magnification. Zoom was included by amplifying and cutting images (circle images).

2. Study of the role of Hakai on Galectin-3 expression

2.1. Analysis of Galectin-3 down-regulation during Hakai transient transfection

Given that Galectin-3 was identified as a down-regulated protein in the proteomic study performed in Hakai-transformed MDCK clones and MDCK parental cell lines, and that immunofluorescence experiments confirmed an interesting colocalization with Hakai in cytoplasmic areas at the base of cellular protrusions, we decided to deeply analyze the possible mechanism of action of Hakai on Galectin-3. Many biological functions for Galectin-3 have been described related to tumor development process such as cell-cell and cell-matrix interaction, cellular proliferation, cellular differentiation and apoptosis [111]. Galectin-3 has been described to be up-regulated in several types of cancer such as colon cancer, ovarian cancer, pancreatic cancer or clear renal cell carcinoma [207-210]. However, its down-regulation has also been described for node-positive breast cancer, thyroid carcinoma, cholangiocarcinoma, cervical carcinoma, small-cell lung cancer, prostate cancer and pancreatic ductal adenocarcinoma [125, 211-216]. Taking into consideration the preliminary results obtained in the proteomic study, and the already reported down-regulation of Galectin-3 in different types of cancer, we decided to evaluate the possible down-regulation of Galectin-3 during Hakai transient overexpression in human cell lines. For that, HEK 293T cells were used given their low expression levels of Galectin-3, and were transiently transfected with increasing amounts of pEGFP-Hakai and constant p3X-Flag-Gal3. Expression levels of both proteins were determined by western blot. Interestingly, Galectin-3 expression levels were markedly decreased in parallel to the increase in Hakai levels (Figure 23).

Given the results obtained, which pointed that Hakai up-regulation induced Galectin-3 down-regulation and that both proteins co-localized, we decided to deepen into the mechanism of this possible regulation by conducting an international research stay at Dr. Fu-Tong Liu's laboratory at Academia Sinica, Taiwan. Dr. Fu-Tong Liu is a worldwide recognized expert in the study of galectins, including Galectin-3, so we considered that carrying out this research stay could be helpful for the completion of this doctoral thesis. All the results shown from now on are about experiments performed in Dr. Fu-Tong Liu's laboratory.

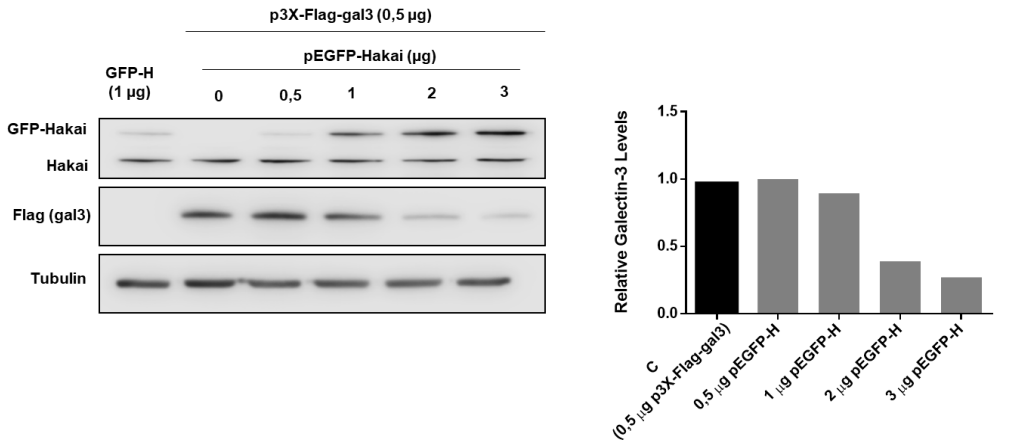

Figure 23. Study of Galectin-3 expression under transfection of increasing amounts of Hakai in HEK 293T cells. HEK 293T cells were transiently co-transfected with constant amount of p3X-Flag-Gal3 (0.5 µg) and increasing amounts of pEGFP-Hakai (0,5 - 3 µg) during 48 h. Cell lysates were subjected to SDS-PAGE electrophoresis and immunoblot with indicated antibodies. Galectin-3 levels are progressively reduced while increasing Hakai expression levels. Relative quantification of expression levels was graphically represented as Mean excluding pEGFP-Hakai control point. Tubulin was used as loading control. Only one replicate of the experiment was performed.

Under Dr. Fu-Tong Liu's supervision, we decided to carry out replicative experiments of our previous results obtained in order to confirm the regulation detected. For that, increasing amounts of pEGFP-Hakai were again co-transfected together with a constant amount of p3X-Flag-Gal3 plasmid in HEK 293T cell line (Figure 24A). In this case, no decrease in Galectin-3 levels was observed under transfection of increasing levels of Hakai. To double-check the effect of Hakai overexpression on Galectin-3, same experiment was performed with only one point for Hakai overexpression. In this case, HEK 293T cells were transfected with same constant amount of p3X-Flag-Gal3 and the highest amount of pEGFP-Hakai employed in previous experiments. As a negative control, cells were transfected with p3X-Flag-Gal3 empty vector (pCDNA 3.1) and pEGFP-Hakai empty vector (pEGFP-C1) (Figure 24B). In this experiment we did not detect any effect on Galectin-3 after Hakai transient overexpression. Different results were observed between experiments performed at Dr. Fu-Tong Liu's laboratory and those performed in our own laboratory. This might be due either to technical differences during plasmid transfection or during cell culture, despite having worked with the same cell line.

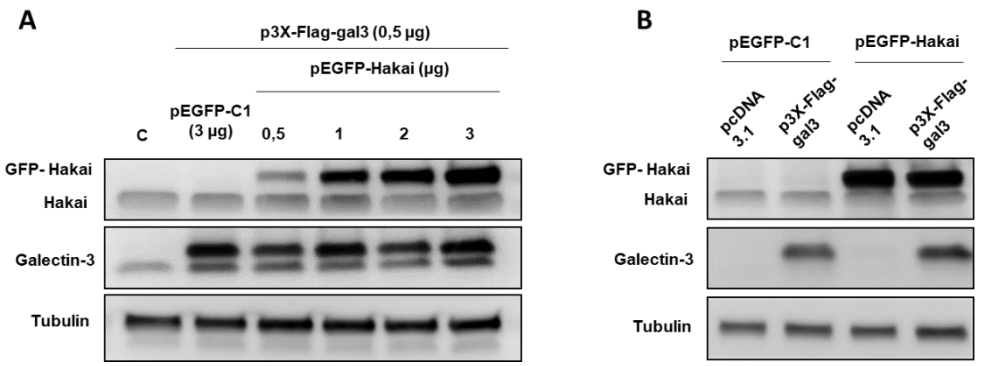

Figure 24. Study of Galectin-3 expression levels during Hakai co-transfection in HEK 293T cells. (**A**) HEK 293T cells were transiently co-transfected with constant amount of p3X-Flag-Gal3 (0,5 µg) and increasing amounts of pEGFP-Hakai (0,5-3 µg) during 48 h. Total amount of transfected plasmid was completed until 3.5 µg with pEGFP-C1 empty vector. (**B**) HEK 239T were transiently co-transfected with 0.5 µg of pFlag-gal3/pcDNA 3.1 and 3 µg of pEGFP-Hakai/pEGFP-C1 for 48 h. Cell lysates were subjected to SDS-PAGE and immunoblot with the indicated antibodies. Tubulin was used as loading control.

In order to further investigate the obtained results, we decided to choose another human cell line expressing higher endogenous levels of Galectin-3. Taking that into account, we selected HeLa cell line, derived from cervical cancer cells, to perform the same experiment and check the possible reproducibility of Galectin-3 down-regulation during Hakai increasing overexpression. For that, HeLa cells were subjected to two different kinetics experiments, one in a time of transfection dependent manner, and other in a concentration dependent manner. In both cases HeLa cells were transfected with pEGFP-Hakai at the indicated concentrations, and endogenous Galectin-3 levels were evaluated by western blot. Time kinetics experiment showed efficient overexpression of Hakai at 24 h, but no effect of Hakai on Galectin-3 expression levels was detected (Figure 25A). Galectin-3 endogenous levels showed an unexpected peak of expression at 4 h after transfection followed by a dramatic decrease up to 75 % of control levels. Galectin-3 endogenous levels were also analyzed in HeLa cells after transfection of increasing levels of Hakai protein (Figure 25B). HeLa cells were transfected with pEGFP-Hakai for 48 h and Galectin-3 endogenous levels were analyzed by western blot. Results

showed a significative down-regulation of Galectin-3 under Hakai overexpression for 1, 2 and 3 µg of pEGFP-Hakai plasmid compared to non-transfected control.

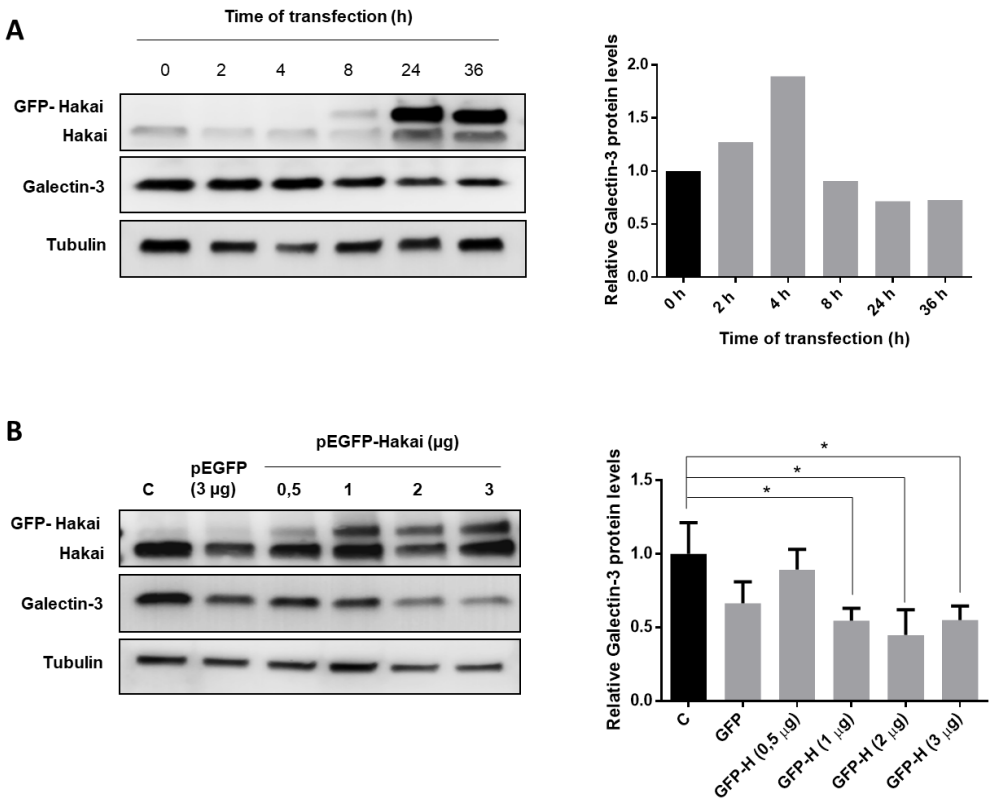

Figure 25. Effect of concentration and time kinetics of Hakai overexpression on Galectin-3 endogenous levels in HeLa cells. (**A**) HeLa cells were transiently transfected with 3 µg of pEGFP-Hakai up to 48 h. Cell lysates were obtained at different times during transfection and subjected to SDS-PAGE electrophoresis and immunoblot with the indicated antibodies (left panel). Relative quantification of Galectin-3 expression levels was graphically represented as Mean for one experiment (right panel). (**B**) HeLa cells were transiently transfected with increasing amounts of pEGFP-Hakai. Total amount of transfected plasmid was completed until 3 µg with pEGFP empty vector. Endogenous levels of Galectin-3 were evaluated (left panel). Relative quantification of Galectin-3 expression levels was represented as Mean ± SEM (right panel) for three independent experiments (*p < 0.05, **p < 0.01, ***p < 0.001).

2.2. Analysis of Galectin-3 protein turnover

Half-life of Galectin-3 protein was also evaluated in order to determine its protein turnover. For this, a time-course experiment was performed by using cycloheximide at the indicated times and concentration in different cell lines (LoVo, HT29 and HEK293T). Figure 26 shows the results obtained for HEK 293T as a representative experiment. No decrease in Galectin-3 levels was detected during treatment with cycloheximide for 8 hours in any of the cell lines used. Effectiveness of cycloheximide was confirmed by evaluation of E-cadherin half-life (data not shown). This result suggests that Galectin-3 has a half-life greater than 8 h.

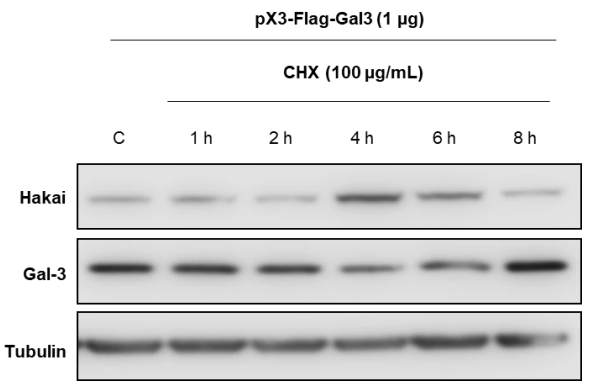

Figure 26. Effect of cycloheximide on Galectin-3 expression in HEK 293T cells. HEK 293T cells were transiently transfected with 1 µg of pFlag-Gal3 for 48 h and treated with 100 µg/mL of CHX, a protein synthesis inhibitor during the indicated times. Cell lysates were obtained and protein expression was evaluated by SDS-PAGE electrophoresis and immunoblot with the indicated antibodies. Tubulin was used as loading control

2.3. Hakai overexpression does not modulate Galectin-3 mRNA levels

Due to the significant decrease of endogenous Galectin-3 protein levels during Hakai overexpression in HeLa cells, we wanted to determine if this modulation was detected at a post-transcriptional or post-translational level. Although the main role for E3 ubiquitin-ligase Hakai has been described to occur at a post-translational level by the ubiquitination of cytosolic proteins, it has also been reported to be mainly localized in the nucleus [89]. Moreover, Hakai has been reported to play a role as transcriptional coregulator in breast cancer (Gong *et al*., 2010), and to interact with PSF splicing factor and promote its binding to different protein transcripts, mainly related to tumorigenesis [99, 103]. Besides, it has been recently described

that Hakai influences mRNA methylation in *Arabidopsis thaliana* [97]. Taking those discoveries into consideration, it is likely to think that Hakai may play additional roles in the mRNA regulation. Based on these facts, we decided to evaluate mRNA expression levels for Galectin- 3 under Hakai overexpression. For that, HeLa cells were transiently transfected as indicated and subjected to mRNA analysis (Figure 27). As shown in figure 27, Hakai overexpression did not significantly modify Galectin-3 expression levels, suggesting that Hakai-dependent Galectin-3 down-regulation may be occurring at post-translational level.

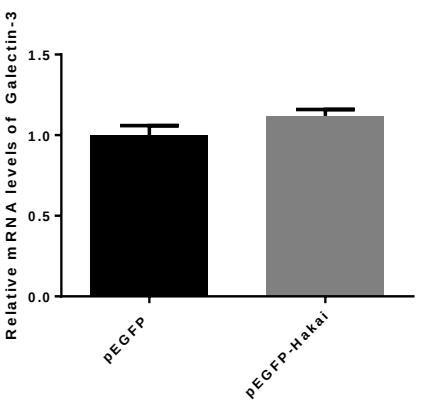

Figure 27. Galectin-3 mRNA expression levels were quantified under Hakai overexpression. HeLa cells were transfected with 3 µg of pEGFP-Hakai/pEGFP for 48 hours. Cells were collected and proceeded to RNA and protein extraction. (A) mRNA levels of Galectin-3 were evaluated by performing RT-qPCR using GAPDH as a housekeeping. Relative quantification of galectin-3 mRNA levels was graphically represented as Mean ± SEM for three independent experiments (*p < 0.05, **p < 0.01, ***p < 0.001).

2.4. Analysis of the effect of autophagy and lysosome inhibitors on Galectin-3 in presence or absence of Hakai

In order to analyze the possible effect of Hakai on Galectin-3 down-regulation, we explored different pathways of degradation. Galectin-3 is mainly described to be secreted during tumor progression and to play extracellular roles, however, little is known about its degradation.

Given the preceding results where Galectin-3 has been related to lysosome degradation [131], we decided to evaluate the effect of autophagy inhibition on the recovery of Galectin-3 protein levels in HeLa cells. For that, HeLa cells were treated with the autophagy inhibitor 3-methyladenine and the lysosome inhibitor chloroquine, which exert their inhibitory function at different stages of autophagy-lysosomal degradation pathway (Figure 28). Galectin-3

endogenous levels were evaluated in HeLa cells under different times and concentrations of CQ (Figure 28A) and 3-MA (Figure 28B). Effectiveness of both inhibitors was confirmed by using LC3 levels as positive control. None of the selected inhibitors showed any effect on Galectin-3 levels, suggesting that Galectin-3 degradation does not occur via autophagy or lysosome degradation pathways in these cell lines. Proteasome inhibition with MG132 was also studied in HEK 293T cells to discard a possible proteasome-mediated down-regulation of Galectin-3, however, no effect was either observed on galectin-3 expression levels (data not shown). Besides, no decrease of Galectin-3 levels was observed in any case during Hakai overexpression. Therefore, we were unable to reproduce our previously reported Galectin-3 down-regulation and to determine the degradation pathway after Hakai overexpression.

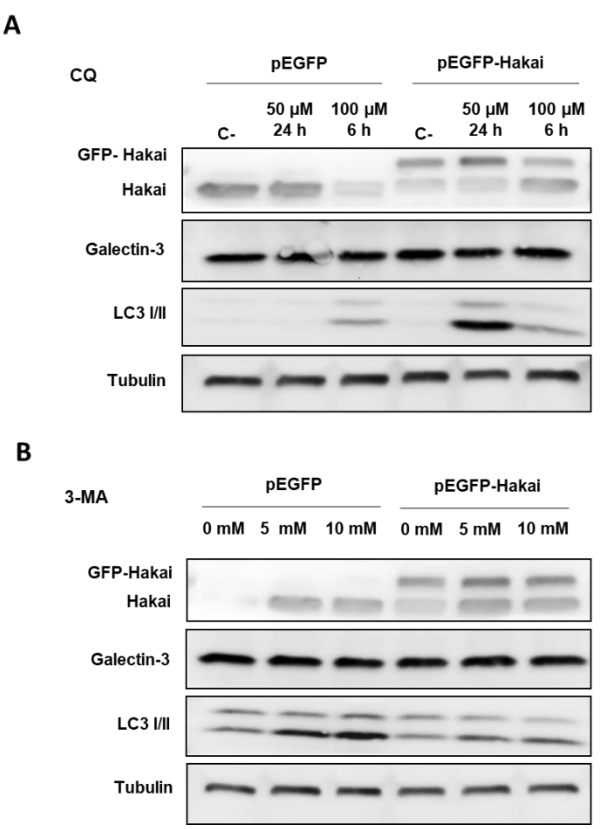

Figure 28. Effect of autophagy inhibition on galectin-3 under Hakai overexpression. HeLa cells were treated with two autophagy inhibitors CQ (**A**) and 3-MA (**B**). Cells were treated with CQ at the indicated times and concentrations and with 3-MA for 24 hours at the indicated concentrations. Autophagy inhibition was studied in presence and absence of Hakai overexpression. Cells were transfected with pEGFP-Hakai or pEGFP empty vector and endogenous levels of Galectin-3 were evaluated. Cell lysates were subjected to SDS-PAGE electrophoresis and immunoblot with the indicated antibodies. LC3 was employed as positive control of the correct functioning of the inhibitors.

2.5. Study of Hakai overexpression on Galectin-3 expression and co-localization in Galectin-3 stable HEK 293T cells

Given the positive results initially obtained for Galectin-3 down regulation in HEK 293T during Hakai and Galectin-3 co-transfection, we decided to re-evaluate Hakai effect on this cell line. For that purpose, we employed HEK 293T stably transfected with GFP-Galectin-3 (HEK 293T-EGFP-Gal3E) and its corresponding control cell line (HEK 293T-EGFP-C1). Taking advantage of Galectin-3 stable transfection linked to GFP fluorophore, we performed flow cytometry and immunofluorescence assays to evaluate Hakai effect on Galectin-3 expression and localization. First, HEK 293T-EGFP-Gal3E cells and their negative control HEK 293T-EGFP-C1 were subjected to flow cytometry (Figure 29). Intensity of GFP endogenous levels was analyzed in both cell lines transiently transfected with pcDNA-Flag-Hakai and pcDNA 3.1. Non-transfected control was also included.

Flow cytometry results were analyzed by calculating the ratio of GFP intensity in Flag-Hakai and pcDNA 3.1 transfected cells to non-transfected control cell line GFP intensity (Figure 29). A <1 ratio indicates GFP intensity down-regulation compared to non-transfected control. pcDNA 3.1 transfected cells were discarded as negative control due to the marked decrease of GFP levels observed in both control and stably transfected cell lines, which indicated a cytotoxic effect during transfection. Regarding Flag-Hakai/Control ratio, Hakai overexpression showed no effect on GFP intensity signal, discarding a down-regulation effect of Hakai on Galectin-3 levels.

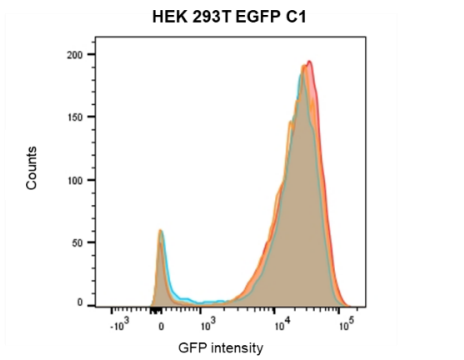

	Sample name	Mean: GFP-A	Ratio
	EGFP-C_1 Flag-Hakai	25001	0.92
	EGFP-C_1 3.1	23237	0.85
	EGFP-C_1 Control	27060	-

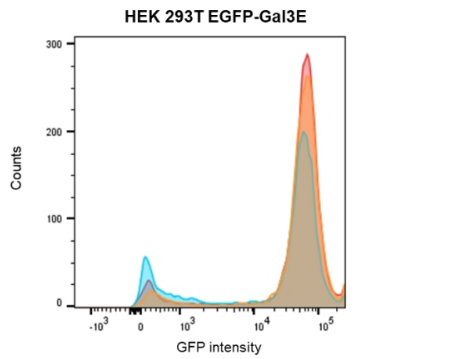

	Sample name	Mean: GFP-A	Ratio
	EGFP-Gal3E Flag-Hakai	62851	1.01
	EGF- Gal3E 3.1	49514	0.79
	EGFP -Gal3E Control	62022	-

Figure 29. Flow cytometry analysis of galectin-3 levels in HEK 293T EGFP-C1 and HEK 293T EGFP-Gal3E under Hakai overexpression. HEK 293T EGFP-C1 (left) and HEK 293T EGFP-Gal3E (right) cells were transfected with pcDNA-Flag-Hakai and pcDNA 3.1 empty vector for 48 h. Non-transfected control was also used to discard cytotoxic effects. Cells were collected and subjected to flow cytometry to evaluate endogenous EGFP levels. Results are shown as ratio of the mean of samples and non-transfected control for one experiment. No differences were found in EGFP-Galectin-3 levels under Hakai overexpression.

Despite the absence of Galectin-3 down-regulation, we decided to evaluate Hakai and Galectin-3 possible co-localization by employing endogenous GFP fluorescence. For that, HEK 293T-EGFP-C1 and HEK 293T-EGFP-Gal3E cells were transiently transfected with pcDNA-Flag-Hakai and pcDNA 3.1 and GFP and Flag localization was determined by confocal microscopy (Figure 30).

We first observed differences in GFP expression between HEK 293T-EGFP-C1 cell lines and HEK 293T-EGFP-Gal3E cell lines. Control cell lines showed a diffuse and uniform pattern of GFP expression, whereas HEK 293T-EGFP-Gal3E cell lines showed a dotted pattern combined with GFP diffuse expression. This fact suggests that Galectin-3 may be partially localized in vesicles. Hakai localization was evaluated by employing Flag antibody and thus, only exogenous Hakai signal was evaluated. Expression pattern of Hakai was found to be irregular, showing a higher expression in some cells compared to those which did not internalize the plasmid. Galectin-3 dotted pattern was not correlated either with Hakai highest or lowest expression, and no clear co-localization of both proteins was observed.

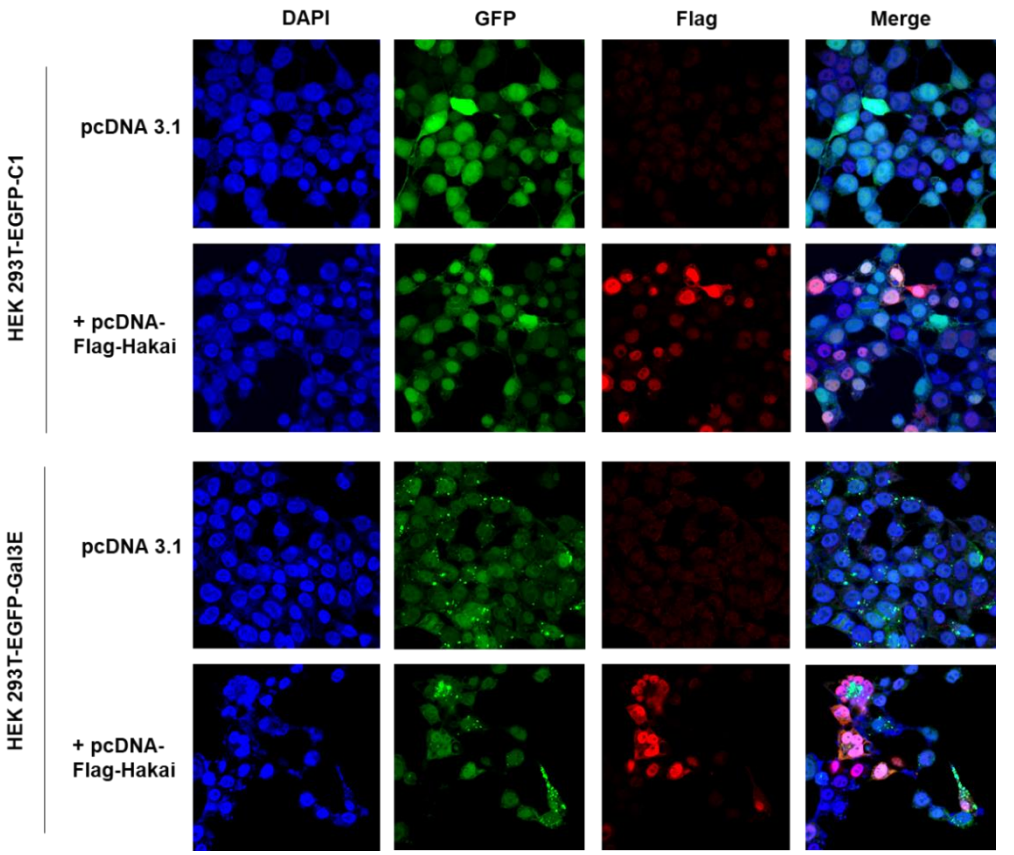

Figure 30. Confocal immunofluorescence analysis of Galectin-3 and Hakai in Galectin-3 stable HEK 293T cells. HEK 293T EGFP-C1 and HEK 293T-EGFP-Gal3E were transfected with pcDNA-Flag-Hakai and pcDNA 3.1 as negative control for 48 h and subjected to immunofluorescence analysis by employing endogenous GFP fluorescence and anti-Flag antibody. No clear co-localization was observed between galectin-3 and Hakai. Images were obtained by confocal microscopy with an objective of 100X magnification.

Altogether, these results do not allow us to conclude if Hakai plays a role on Galectin-3 down-regulation due to the discrepancies observed in the different experiments performed. While the proteomic study showed favorable results for this hypothesis, further experiments could not demonstrate the previous results. Therefore, we decided not to continue with this research line.

3. Study of Heat shock protein 90 regulation of Hakai protein stability

3.1. Analysis of Hakai interactome in HCT116 cells

We decided to further follow another strategy by analyzing Hakai interactome. This type of analysis consists in a proteomic approach which allows to directly identify Hakai-interacting proteins by performing protein immunoprecipitation. This type of approach, unlike the proteomic study in which we detected Hakai-regulated proteins, allows us to narrow the results to only those proteins that are interacting with our protein of interest, either directly or indirectly.

For analyzing Hakai interactome, immunoprecipitation of Hakai endogenous protein levels was optimized in HCT116 until reaching good levels of immunoprecipitation, in order to assure a high probability of co-immunoprecipitated proteins (Figure 31A). Once the immunoprecipitation was optimized, total amount of immunoprecipitated protein was ran in an acrylamide gel and silver stained to observe total immunoprecipitated protein before performing proteomic analysis (Figure 31B). Proteomic analysis was performed by the Proteomic service of IDIS (Instituto de Investigación Sanitaria de Santiago de Compostela) as previously described. Briefly, protein samples, including control IgG and Hakai immunoprecipitation, were loaded into an 10% acrylamide gel and subjected to SDS-PAGE electrophoresis for gel Coomassie staining and subsequent in-gel protein digestion. For protein digestion, gel bands were excised and digested with trypsin for peptide extraction. Digested peptides were subjected to mass spectrometry analysis. First, peptides were separated by Reverse Phase Chromatography and data was obtained in a TripleTOF 6600 System. Raw data analysis was performed by using ProteinPilotTM 5.0.1 software (ABSciex) as previously described.

A total of 48 proteins with a peptide match ≥ 1 were identified in Hakai immunoprecipitated samples, however, only proteins with a peptide match ≥ 2 were considered in this analysis. Hakai-interacting proteins identified with a peptide match ≥ 2 were confronted with those identified in non-specific immunoprecipitation and analyzed by a Venn diagram using Venny 2.1.0 software. Venn diagram showed 13 proteins (16,3 %) exclusively identified in Hakai immunoprecipitated sample, 53 proteins (66,3 %) matching between the IgG control sample and Hakai immunoprecipitated sample, and 14 proteins (17,5 %) identified exclusively in the negative IgG control (Figure 31C). Hakai-interacting proteins are listed in table 19. It should be

noted that, among the identified proteins we can find the Hakai protein immunoprecipitated, thus ensuring the specificity of the developed technique. Among the identified interacting proteins, we could find proteins implicated in cytoskeleton reorganization, such as Keratin type II cytoskeletal 6B (K2C6B), Tubulin β chain (TBB5), Hornerin (HORN) and Keratin type I cytoskeletal 18 (K1C18); proteins involved in ubiquitination, such as Ubiquitin-60S ribosomal protein L40 (RL40), Ubiquitin-40S ribosomal protein S27a (RS27A), Polyubiquitin-C (UBC) and Polyubiquitin-B (UBB); response to stress proteins, such as Heat shock protein 60 (CH60) and Heat shock protein 90 (HS90A); and lipid metabolism proteins, such as Apolipoprotein C-I (APOC1) (Table 19).

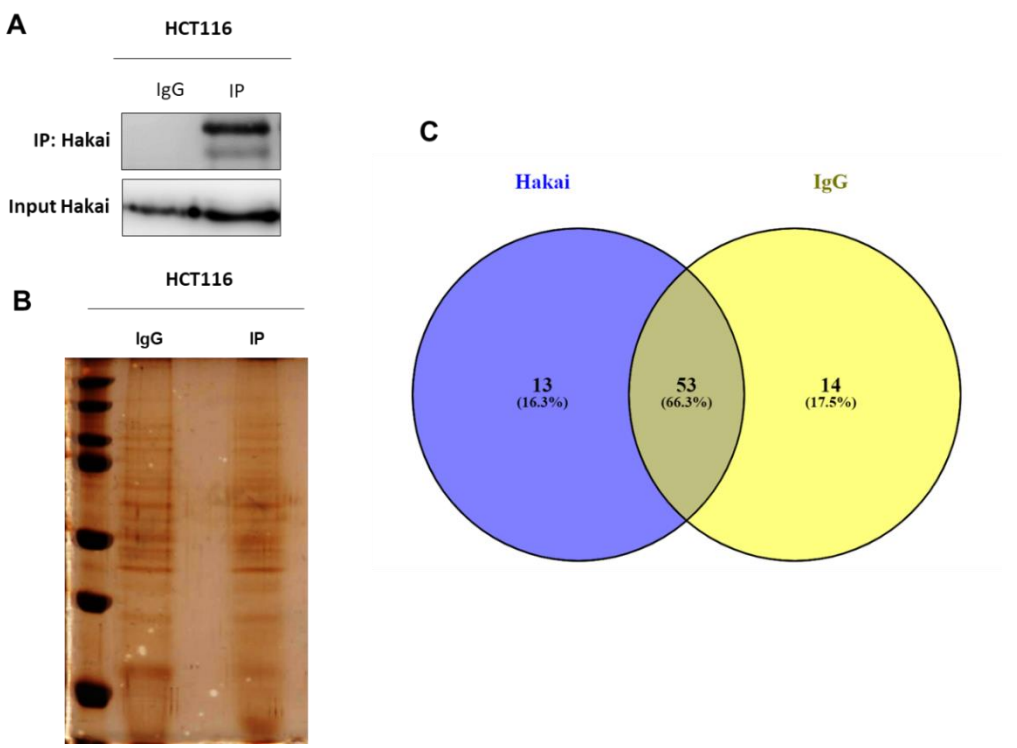

Figure 31. Experimental summary of Hakai interactome analysis. (**A**) Immunoprecipitation of Hakai endogenous levels was optimized until reaching a good level of immunoprecipitation (**B**) Protein samples were analyzed by 1D-SDS-PAGE electrophoresis and dyed with silver staining for total protein visualization. (**C**) Venn diagram of interacting proteins allows to exclude false positive interactions. Hakai interacting proteins are represented in blue. IgG unspecific interacting proteins are represented in yellow. Common interacting proteins between Hakai and IgG are represented in brown. This assay was performed without replicates as a developing experiment.

Table 19. Identified Hakai-interacting proteins in HCT116 cells.

	% Cov(95)	Accesion number	Protein Symbol	Name	Description	Peptide match (95 %)
1	22,87	P04259	K2C6B	Keratin, type II cytoskeletal 6B	Isoform of human type II keratin-6 constituent of cytoskeleton and implicated in cornification, ectoderm development and keratinization.	19
2	18,47	P07437	TBB5	Tubulin beta chain	Major constituent of microtubules. Implicated in cell division, mitotic cell cycle, and other functions involving cytoskeleton reorganization.	6
3	9,77	P10809	CH60	60 kDa heat shock protein	Mitochondrial chaperonin implicated in imported proteins correct folding, apoptotic mitochondrial changes and immune response.	5
4	**4,65**	**P07900**	**HS90A**	**Heat shock protein HSP 90-alpha**	**Molecular chaperone implicated in the structural maintenance of client proteins in an ATP dependent manner. Involved in response to stress, autophagy and ubiquitination.**	**3**
5	5,83	P61978	HNRPK	Heterogeneous nuclear ribonucleoprotein K	Pre-mRNA binding protein. Participates in mRNA splicing, transcription and RNA metabolism.	2
6	3,65	Q86YZ3	HORN	Hornerin OS=Homo sapiens	Component of the epithelial cells. Implicated in keratinization, cell envelope organization and formation of skin barrier.	2
7	**5,91**	**Q75N03**	**HAKAI**	**E3 ubiquitin-protein ligase Hakai**	**E3 ubiquitin-ligase that mediates ubiquitination and degradation of differente Src-phosphorylated proteins sucha as E-cadherin or Cortactin. Implicated in maintenance of cell-cell adhesion, cell migration and mRNA methylation.**	**2**
8	19,53	P62987	RL40	Ubiquitin-60S ribosomal protein L40	Ubiquitin sigle molecule encoded by UBA52 linked to ribosomal protein L40. Implicated in different biological pathways such as protein degradation and endosomal transport.	2
9	16,03	P62979	RS27A	Ubiquitin-40S ribosomal protein S27a	Ubiquitin sigle molecule encoded by RPS27A linked to ribosomal protein S27a. Implicated in different biological pathways such as protein degradation and endosomal transport.	2

	% Cov(95)	Accesion number	Protein Symbol	Name	Description	Peptide match (95 %)
10	32,85	P0CG48	UBC	Polyubiquitin-C	Polyubiquitin precursor encoded by UBC gen with heat-to-tail repeats. Implicated in different biological pathways such as protein degradation, and endosomal transport.	2
11	32,75	P0CG47	UBB	Polyubiquitin-B	Polyubiquitin precursor encoded by UBB gen with heat-to-tail repeats. Implicated in different biological pathways such as protein degradation, and endosomal transport.	2
12	3,72	P05783	K1C18	Keratin, type I cytoskeletal 18	Type I intermediate filament implicated in filament reorganization, morphogenesis, cell cycle and apoptosis. Used as an epithelial marker.	2
13	22,89	P02654	APOC1	Apolipoprotein C-I	Lipoprotein which associates with high density lipoproteins (HDL). Interferes with fatty acid up-take and inhibits cholesteryl ester transfer protein (CETP). Implicated in lipid metabolism.	2

* Hakai-interacting proteins identified in HCT116 cells by immunoprecipitation followed by Triple TOF analysis. Selected proteins were those identified with ≥ 2 peptide match (95 %). % Cov (95), accession number, protein symbol, protein name and functional description of interacting proteins are also included.

Interestingly, Heat shock protein 90 (Hsp90) was identified among Hakai-interacting proteins. Hsp90 is a molecular chaperone implicated in the correct folding of specific client proteins. Hsp90 and Hsp70 proteins were previously validated in the comparative proteomic study performed in Hakai-overexpressing MDCK cells compared to parental MDCK cells. Validation of Hsp90 by western blotting previously confirmed its up-regulation during Hakai stable overexpression (Figure 20). This result, together with its identification among Hakai interacting proteins, suggests a possible relation between both proteins. These facts provided us sufficient evidence to initiate studies in order to determine possible relationship between Hakai and Hsp90.

Hsp90 has been widely described to be implicated in tumor progression by regulating client proteins described as hallmarks of cancer disease. Most of its client proteins are regulators of cellular proliferation, proteins implicated in oxidative stress or cellular differentiation, and well described oncoproteins [217]. Altogether, these facts suggest a clear implication of Hsp90 in cancer evolution and, for this reason, great interest is being generated in the study of this protein as a new target for cancer treatment.

3.2. Study of Hsp90 regulation under Hakai overexpression

In order to study the possible relationship between Hakai and Hsp90, we decided to evaluate whether the previously obtained results in the comparative proteomic study were reproducible by employing a model of Hakai transient transfection. For that, we performed different experiments of Hakai overexpression and evaluated Hsp90 levels in HEK 293T cell line (Figure 32). First, we evaluated the effect of increasing amounts of Hakai overexpression (0-3 μg) on endogenous Hsp90 expression levels (Figure 32A). On the other hand, we performed time course experiments with a constant amount of 3 μg of Hakai plasmid overexpression. This allows to determine possible effects on Hsp90 levels during different times of transfection up to 72 hours (Figure 32B). Non-transfected control was also included. As observed in figure 32, no changes on Hsp90 levels were observed during Hakai transient overexpression in a time or concentration dependent manner.

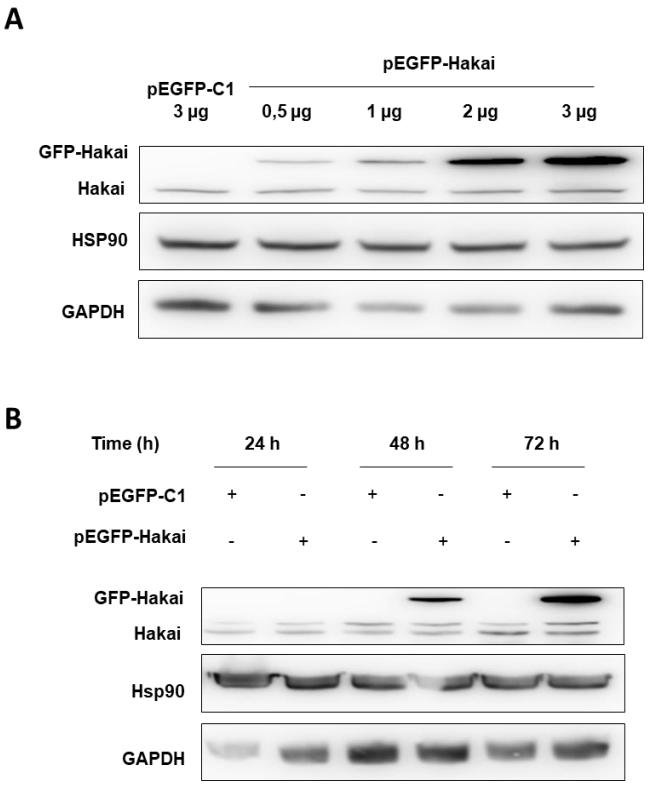

Figure 32. Effect of Hakai overexpression on Hsp90 levels. (**A**) HEK 293T cells were transfected for 48 h with increasing amounts of pEGFP-Hakai plasmid (0 -3 µg) completed with pEGFP-C1 empty vector until reaching maximum concentration of 3 µg. (**B**) HEK 293T were transfected with 3 µg of pEGFP-Hakai and pEGFP-C1 empty vector and lysates were collected at indicated times of transfection. Cell lysates were examined by western blot by employing Hakai, Hsp90 antibodies. GAPDH was employed as loading control.

Similarly, same concentration kinetics experiment was carried out by transient overexpression of Hsp90 in order to determine possible effects on Hakai levels (Figure 33). For this, HEK 293T cell line was transfected with a constant amount of 0,5 µg of Flag-Hakai plasmid and increasing amounts of Flag-HA-Hsp90 plasmid (0–3 µg). Control point of transfection with pcDNA 3.1 was also included. No changes were detected in Hakai expression levels during Hsp90 overexpression.

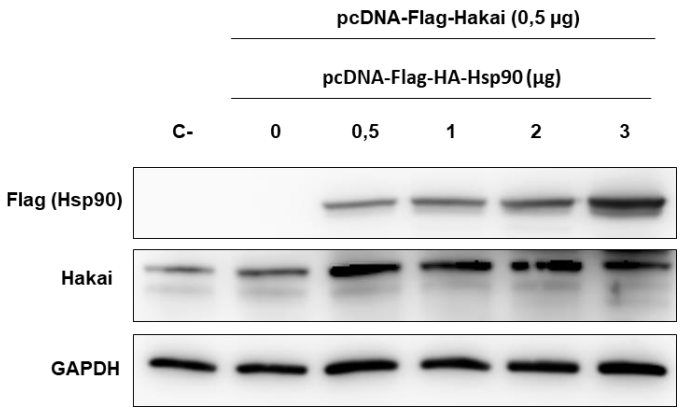

Figure 33. Effect of Hsp90 overexpression on Hakai levels. HEK 293T cells were transfected for 48 h with constant amount of 0,5 µg of pcDNA-Flag-Hakai and increasing amounts of pcDNA-Flag-HA-Hsp90 plasmid (0 – 3 µg). Transfection points were completed with pcDNA 3.1 empty vector until reaching maximum amount of 3 µg. Cell lysates were evaluated by western blot by employing Flag and Hakai antibodies. GAPDH was employed as loading control.

3.3. Confirmation of Hakai and Hsp90 interaction in different cell lines

Despite not observing any effect on Hsp90 during Hakai transient transfection and vice versa, we detected interaction between Hakai and Hsp90 when analyzing Hakai interactome, so we decided to further evaluate the interaction between these two proteins in different cell lines. It has been previously described by a proteomic approach of Hsp90 interactome that, far from expected, about 30 % of the total Hsp90-interacting proteins were E3 ubiquitin ligases [160]. In addition, other works demonstrated the interaction of chaperones Hsp90 or Hsp70 with other E3 ubiquitin-ligases such as Cullin-5 or CHIP. This interacting E3 ubiquitin-ligases help to induce the degradation of those chaperone client proteins that have not been correctly folded [158, 218]. Based on these precedents, it makes sense that Hakai and Hsp90 might be widely interacting regardless of the cell line. To probe this, we performed co-immunoprecipitation experiment in different cell lines, including commonly used HEK 293T cells (Figure 34A) and carcinoma cell lines such as ACHN (Figure 34B), HT29 (Figure 34C) and HCT116 (Figure 34D). Two antibodies of Hakai were used for immunoprecipitation during this experiment. Co-immunoprecipitation of Hakai and Hsp90 was detected in four cell lines tested with either of the two Hakai tested antibodies. Co-immunoprecipitated amount of Hsp90 varied depending on the cell line and the antibody employed for immunoprecipitation. Based on the results showed in figure 34, we can conclude that both proteins Hakai and Hsp90 are either directly or indirectly interacting with each other.

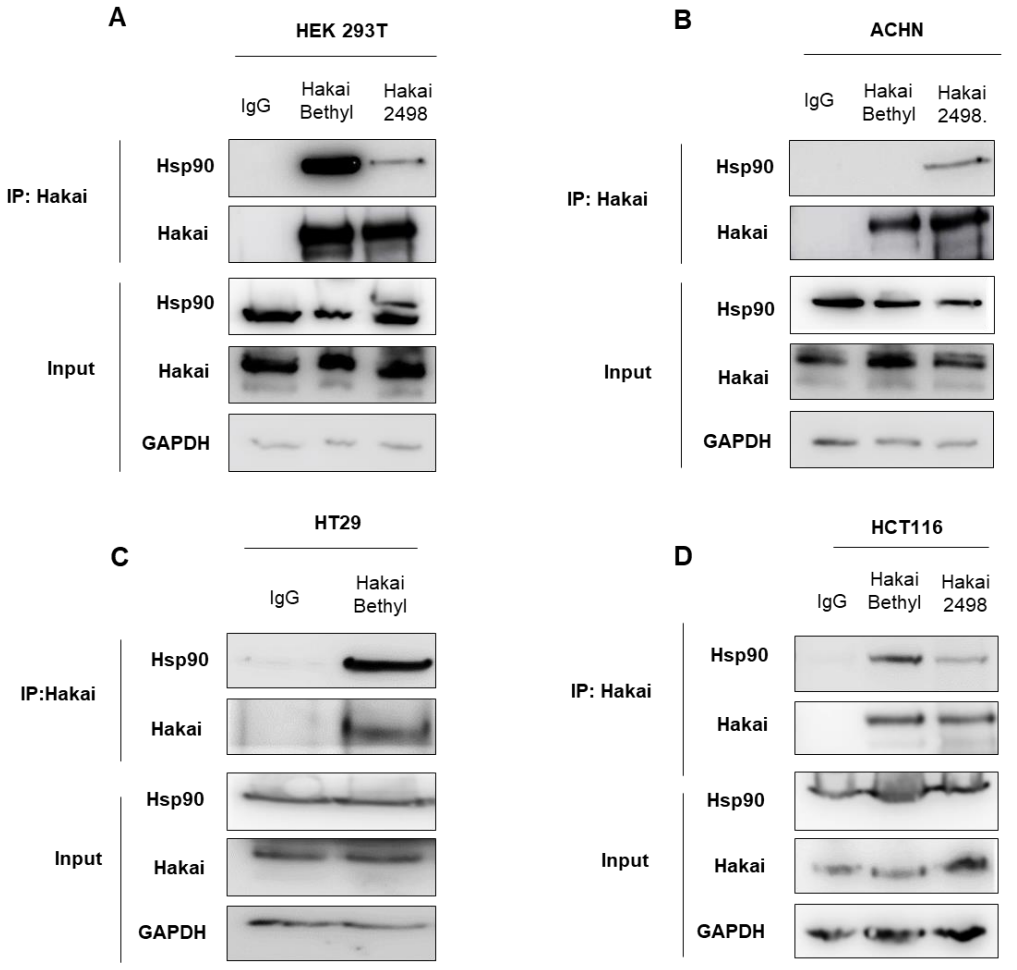

Figure 34. Evaluation of protein-protein interaction between Hakai and Hsp90. Co-immunoprecipitation of Hakai and Hsp90 was detected in different cell lines: HEK 293T (**A**), ACHN (**B**), HT29 (**C**) and HCT116 (**D**). Hakai immunoprecipitation was performed by employing Hakai Bethyl and Hakai 2498 antibodies. GAPDH was used for input loading control.

To support the results obtained by co-immunoprecipitation that confirmed the interaction between Hakai and Hsp90 in different cell lines, we decided to evaluate the possible co- localization of both proteins by immunofluorescence (Figure 35). For that, we performed co- immunofluorescence experiments in different colon carcinoma cell lines and examined subcellular localization of both Hakai and Hsp90 by confocal microscopy. Hakai was mainly localized in the nucleus and, to a lesser extent, in the cytoplasm. On the other hand, Hsp90 was clearly localized throughout the whole cytoplasm. As shown in figure 35, a slight co-localization has been detected in perinuclear areas of the HT29 and LoVo cell lines.

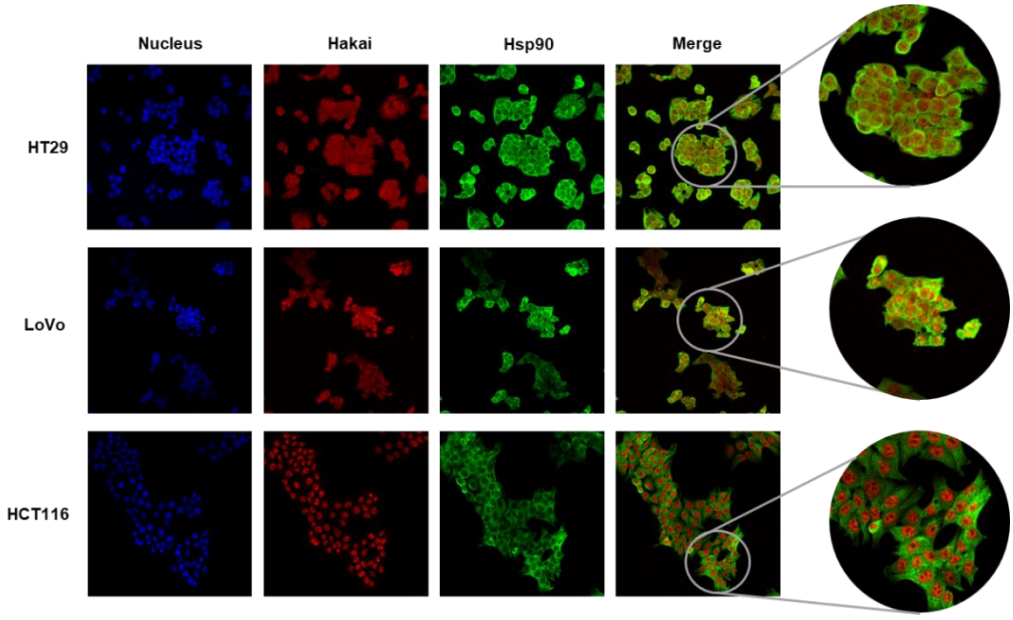

Figure 35. Co-immunofluorescence analysis of Hakai and Hsp90 in HT29, LoVo and HCT116 cell lines. Protein localization was examined by confocal microscopy. Photos were taken with objective of 40X magnification. Zoom images were taken with 80X objective magnification.

Based on the results obtained for co-immunoprecipitation and co-immunofluorescence experiments, we can conclude that Hakai and Hsp90 are effectively interacting with each other either directly or indirectly. It has been extensively reported that, despite being more prevalent in the nucleus, Hakai is also located in the cytosol, where it exerts its E3 ubiquitin-ligase activity. This makes it possible that the weak co-localization observed between both proteins might be due to a detection sensitivity problem.

3.4. Hakai expression levels induce Annexin A2 regulation

Annexin A2 is calcium binding protein which was reported to be expressed in tumoral cells and to be implicated in cytoskeleton dynamics and vesicle trafficking, among others. In addition, Annexin A2 has been extensively studied in relation to its involvement in tumor progression, mainly as a cancer biomarker. However, it has been described both as an up-regulated and down-regulated protein depending on the type of cancer [219].

Annexin A2 was one of the proteins detected in our proteomic study that turned out to be down-regulated in Hakai-overexpressing MDCK cells compared to normal MDCK cell line, suggesting a possible role of this E3 ubiquitin-ligase in its regulation. Besides, Annexin A2 has

been described to be phosphorylated by tyrosine-kinase Src in a similar to E-cadherin, which supports the hypothesis of being a new probable target for the E3 ubiquitin-ligase activity of Hakai. In addition, it has been reported that Annexin A2 co-immunoprecipitates with Hsp90 [220]. Given that Annexin A2 became a new link between Hakai and Hsp90, we decided to deepen in the study of this protein and its relationship with Hakai and Hsp90.

We decided to evaluate the reproducibility of the down-regulation of Annexin A2 in the presence of Hakai overexpression in a different cellular model than the one we used during the proteomic study. To do this, we performed a transient overexpression of Flag-Hakai together with Src and HA-Ubiquitin in HEK 293T cells to favor the activity of the ubiquitin-mediated degradation system. Besides, co-overexpression of Hakai with Src favors the increase of Hakai levels by inducing its stabilization, and helps to observe the effect on Hakai substrates (Figure 36) [56].

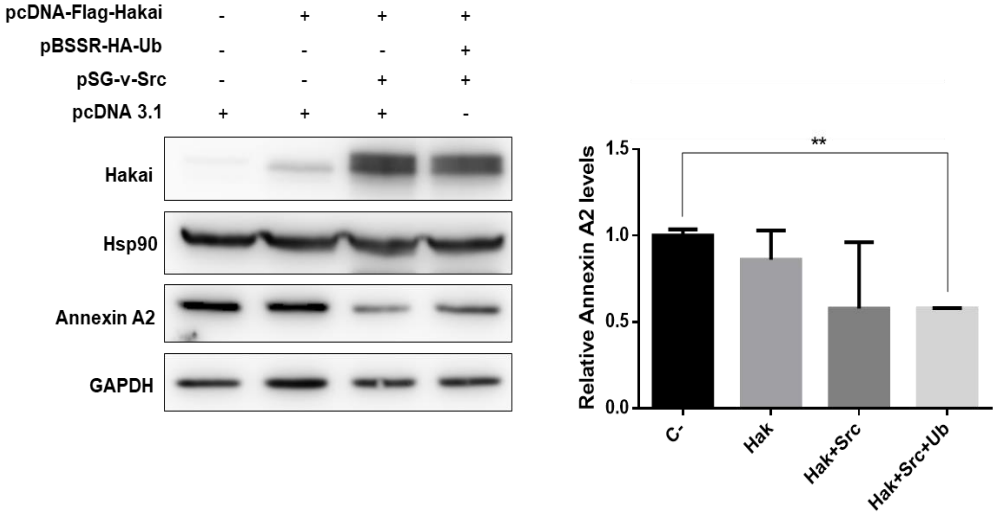

Figure 36. Effect of Hakai overexpression on Annexin A2 levels. HEK 293T cells were transfected with pcDNA-Flag-Hakai (4 µg), pBSSR-HA-Ubiquitin (3 µg) and pSG-v-Src (3 µg) plasmids for 48 h. Cell lysates were evaluated by western blot with the indicated antibodies (left panel). GAPDH was used as loading control. Annexin A2 levels were evaluated when co-transfecting Flag-Hakai, HA-Ubiquitin and Src plasmids. Relative quantification of Annexin A2 expression levels was graphically represented as Mean ± SEM for two independent experiments (*$p < 0.05$, **$p < 0.01$, ***$p < 0.001$) (right panel).

As shown in figure 36, Annexin A2 levels were significatively reduced by co-overexpressing Hakai together with tyrosine kinase Src and Ubiquitin. This observed down-regulation suggests

a role of E3 ubiquitin-ligase Hakai on mediating Annexin A2 degradation. Hsp90 expression levels were also evaluated and, as previously observed in figure 32, no effects were observed.

To further confirm the effect of Hakai on Annexin A2 expression levels we performed Hakai silencing experiments by transiently transfecting two different Hakai siRNAs (Figure 37). HEK 293T and HCT116 cells were transfected with both Hakai siRNA1 and siRNA2 for 72 hours and Annexin A2 levels were evaluated.

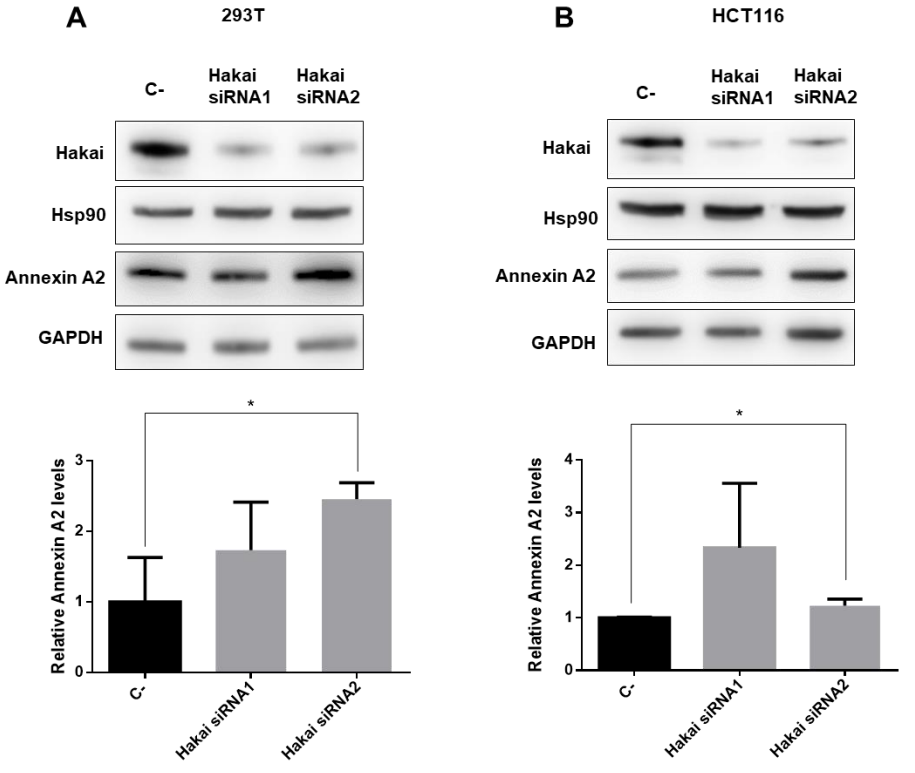

Figure 37. Effect of Hakai silencing Annexin A2 levels. HEK 293T (**A**) and HCT116 (**B**) cells were transiently transfected with Hakai siRNA1 and Hakai siRNA2 for 72 h. Cell lysates were collected and analyzed by western blot with the indicated antibodies (upper panel). GAPDH was employed as loading control. Annexin A2 relative quantification was graphically represented as Mean ± SEM for three independent experiments (lower panel) (*p < 0.05, **p < 0.01, ***p < 0.001).

Hakai expression was 90 % reduced when transfecting with Hakai siRNA1 and siRNA2 (Figure 37A,B). Reduction of Hakai levels was accompanied by an up-regulation of Annexin A2 levels in both cell lines, especially when employing Hakai siRNA2. Hsp90 levels were also evaluated and, as expected, no effects were observed under Hakai silencing. An increase in E-cadherin levels in HEK 293T cell line was also observed during Hakai silencing (data not shown). These

results support those showed in figure 36, suggesting that Hakai may be playing a role on Annexin A2 protein levels.

Taking into account the results obtained during the proteomic study in stable Hakai overexpressing MDCK cells, together with those obtained in HEK 293T and HCT116 during Hakai transient overexpression, we can affirm that Hakai plays an important role in regulating Annexin A2 expression levels, and that Annexin A2 may be a new substrate for E3 ubiquitin-ligase Hakai.

3.5. Hakai, Hsp90 and Annexin A2 interact with each other

As demonstrated so far, Annexin A2 can be a new substrate protein for Hakai E3 ubiquitin- ligase activity. In addition, Annexin A2 has been previously described as an Hsp90 interacting protein, although it has not been probed as a Hsp90 client protein. On the other hand, we have demonstrated the interaction between Hakai and Hsp90 in different cell lines and, to a lesser extent, their subcellular co-localization in colorectal carcinoma cell lines. Based on this, we decided to study the possible interaction of these three proteins in order to determine if they may form a chaperone-substrate-E3 ubiquitin-ligase complex as already described for other Hsp90 client proteins [158].

To probe this, we conducted an interaction study among Hakai, Hsp90 and Annexin A2 by co-immunoprecipitation in HCT116 cell line (Figure 38). HCT116 cell line was selected based on the previous results obtained for Hakai and Hsp90 interaction and Annexin A2 up-regulation during Hakai silencing. During co-immunoprecipitation experiments, endogenous levels of Hakai, Annexin A2 and Hsp90 were immunoprecipitated, and evaluation of co- immunoprecipitation with the other two proteins was performed. Immunoprecipitation of Hakai and consequent co-immunoprecipitation of Hsp90 has been previously described. During this experiment, we confirmed reverse co-immunoprecipitation of Hsp90 and Hakai by performing Hsp90 immunoprecipitation (Figure 38A), co-immunoprecipitation of Hakai and Annexin A2 by performing Hakai immunoprecipitation (Figure 38B), and Annexin A2 and Hsp90 by performing Annexin A2 immunoprecipitation (Figure 38C). These results confirm that Hakai, Hsp90 and Annexin A2 are effectively interacting with each other, either directly or indirectly,

and maybe constitute a complex where Hsp90 is the chaperone responsible of the correct folding of any of these two proteins.

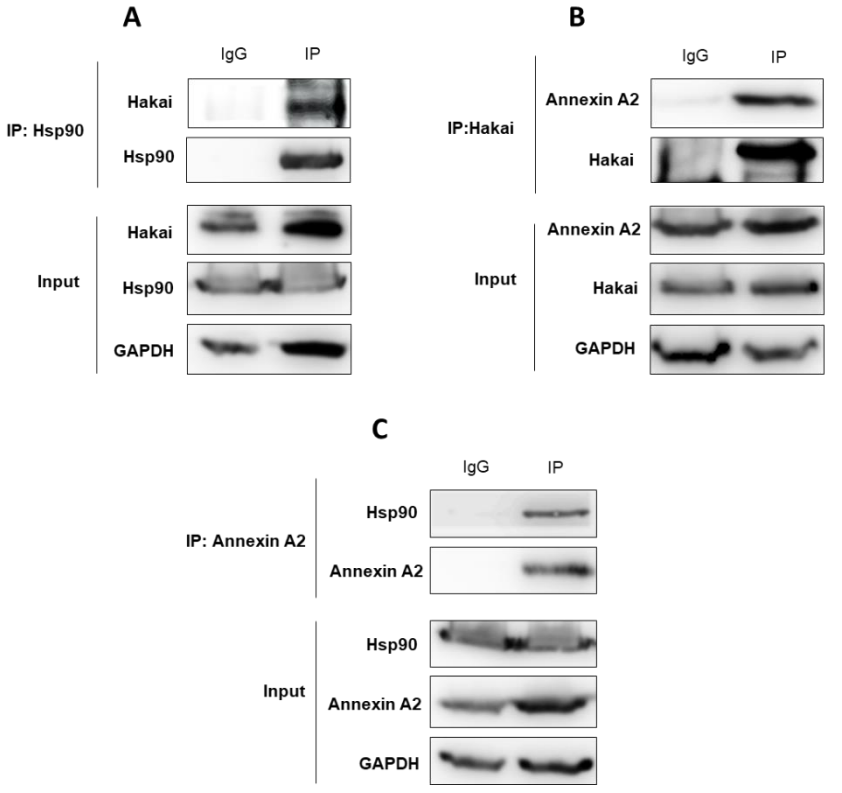

Figure 38. Study of protein-protein interaction between Hakai, Hsp90 and Annexin A2 proteins. Co-immunoprecipitation was performed in HCT116 cell line with Hakai Bethyl (**A**), Hsp90 (**B**) and Annexin A2 (**C**) antibodies. Interaction between the three proteins was evaluated. Co-immunoprecipitation was evaluated by western blot using the indicated antibodies. GAPDH was used for input loading control.

3.6. Effect of Hsp90 inhibitor geldanamycin on cellular phenotype

Geldanamycin (GA) is one of the best described Hsp90 inhibitors so far. It acts by blocking ATP binding site of Hsp90, thus preventing the correct folding of its client proteins. Given the evidence of Hakai, Hsp90 and Annexin A2 interaction, we decided to perform Hsp90 inhibition assays by employing Hsp90 inhibitor geldanamycin in order to probe if Hakai or Annexin A2 may be any of them regulated by Hsp90 activity.

Before starting geldanamycin experiments, we evaluated the cytotoxicity of this inhibitor in the previously used cell lines HEK 293T and HCT116 (Figure 39). Cytotoxicity was evaluated by

performing MTT assay with increasing concentrations of GA up to 200 µM for 24 hours, and IC50 was determined. Both cell lines showed an IC50 close to 10 µM, being 11,83 µM for HEK 293T cells (Figure 39A) and 18,74 µM for HCT116 (Figure 39B). Based on these IC50 concentrations, we chose GA working concentration for the subsequent experiments.

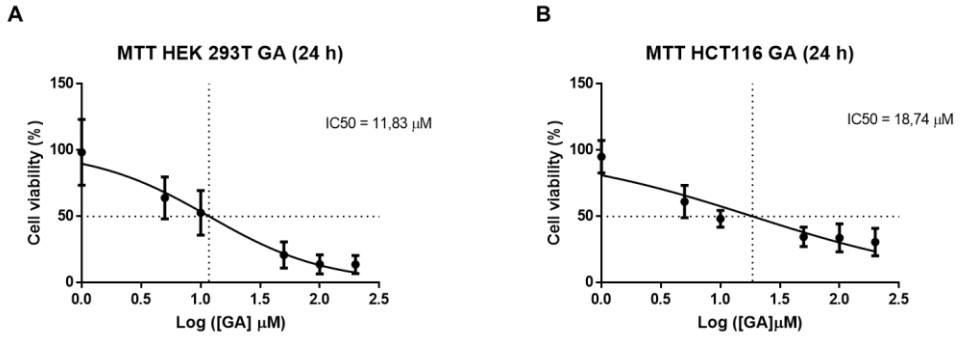

Figure 39. Evaluation of geldanamycin cytotoxicity in HEK 293T and HCT116 cells. Geldanamycin cytotoxicity was evaluated by MTT assay in HEK 293T (**A**) and HCT116 (**B**) cells for 24 h employing increasing concentrations (0-200 µM). Results are represented as Mean ± SEM for three independent experiments employing 6 technical replicates in each experiment. Concentrations of GA were represented in logarithmic scale (log [GA] µM). IC50 was calculated for each cell line.

In parallel to the evaluation of the cytotoxicity of the geldanamycin inhibitor, we decided to evaluate its effect on the cell phenotype in both HEK 293T and HCT116 cell lines. To do this, we treated the cells for 24 hours at two different concentrations: 10 uM, close to the IC50 of the HEK 293T line; and at 20 uM, close to the IC50 of the HCT116 line (Figure 40).

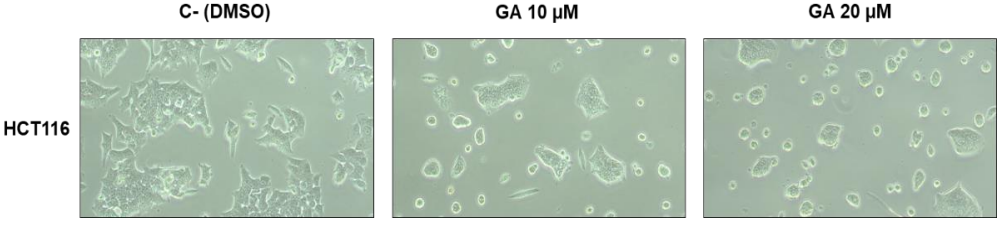

Figure 40. Effect of geldanamycin treatment on HCT116 cell line phenotype. HCT116 phenotype was evaluated after treatment with two different concentrations of geldanamycin (10 and 20 µM) for 24 h. Images were taken with optical microscope by employing objective of 10X magnification.

We were able to verify that the geldanamycin treatment induced a phenotypic change in HCT116 cell line for the two concentrations tested. HCT116 cells showed a loss of its mesenchymal phenotype accompanied by a decrease of cellular protrusions and acquired a more epithelial phenotype, organized in compacted cell clusters. Given the observed phenotypic change, these results led us to hypothesize that geldanamycin could be exerting a reversal effect of the EMT process.

Moreover, we decided to evaluate the localization of Annexin A2 and E-cadherin, by immunofluorescence in presence of geldanamycin in HCT116 cell line (Figure 41).

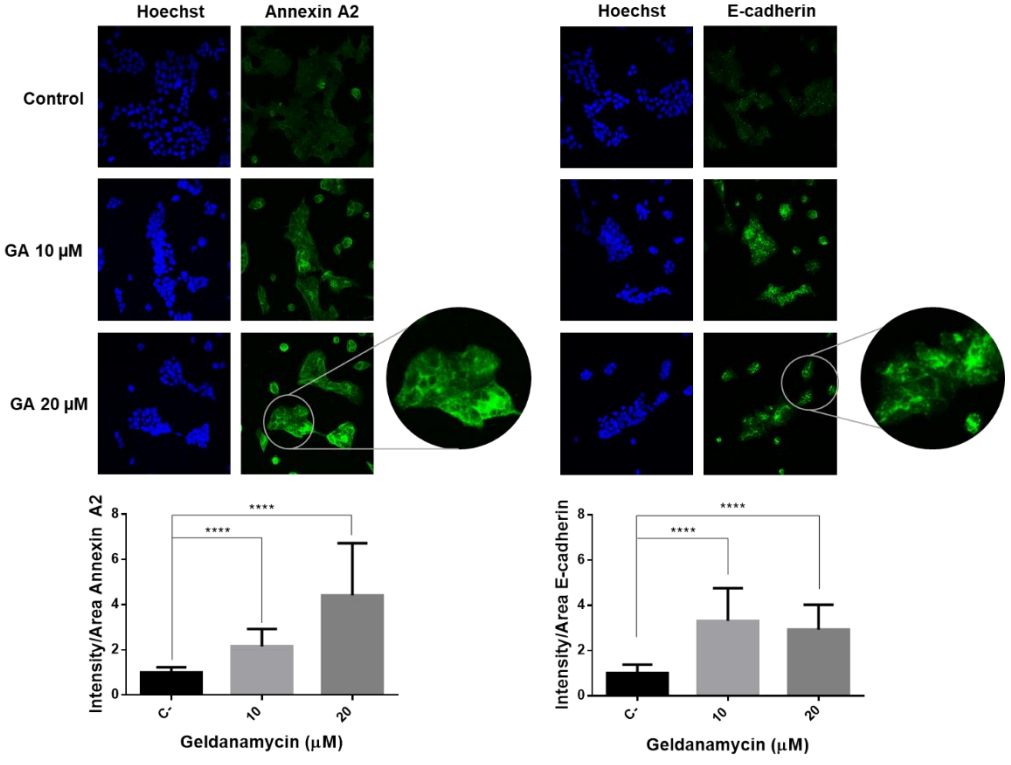

Figure 41. Immunofluorescence evaluation of geldanamycin treatment on Annexin A2 and E-cadherin levels. HCT116 cell line was treated at the indicated concentrations of GA for 24 h. Annexin A2 and E-cadherin subcellular localization was determined by immunofluorescence by employing the same exposition time for all the samples. Images were taken with confocal microscope by employing 40X magnification objective. Intensity quantification was performed by employing ImageJ software. Statistical analysis was performed by employing Student's t-test. Results are represented as Mean ± SEM for two different replicates (*p < 0.05, **p < 0.01, ***p < 0.00,1 ****p < 0.0001).

As shown in figure 41, we observed a four-fold increase of Annexin A2 levels in the presence of geldanamycin inhibitor, showing a statistical enriched pattern in cytoplasm and cell

membrane (Figure 41, left panel). On the other hand, we observed a three-fold increase in E- cadherin at cell-cell contacts in presence of geldanamycin (Figure 41, right panel). All these data support the previously observed effect on cellular phenotype and suggests that geldanamycin inhibitor might be playing a role in the reversal of the EMT process by mediating Hakai down-regulation, which in consequence causes up-regulation of Annexin A2 and E- cadherin. This possible down-regulation of Hakai would propose it as a new client protein for Hsp90.

3.7. Inhibition of Hsp90 induces Hakai down-regulation at post-translational level

Given the previously detected interaction between Hakai, Hsp90 and Annexin A2 and the effect on the recovery of Annexin A2 and E-cadherin in presence of geldanamycin, we decided to study the effect of geldanamycin on Hakai endogenous levels. For that, we analyzed Hakai expression under different time and concentration conditions of geldanamycin in HEK 293T and HCT116 cell lines (Figure 42).

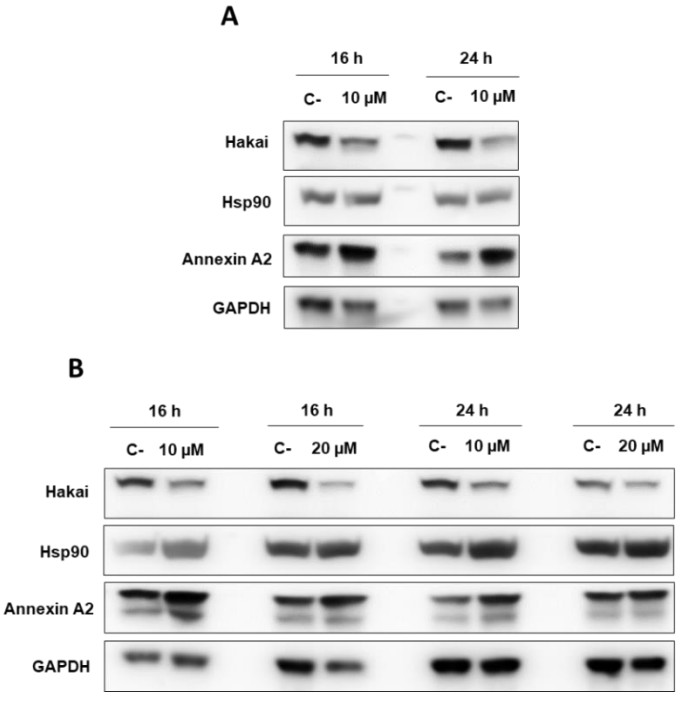

Figure 42. Effect of geldanamycin on Hakai and Annexin A2 expression levels. HEK 293T (**A**) and HCT116 (**B**) cells were treated with GA at the indicated times and concentrations. Cell lysates were subjected to western blot analysis and immunoblot was performed with the indicated antibodies. GAPDH was used as loading control.

As shown in figure 42, Hakai endogenous levels were clearly down-regulated when treating with geldanamycin for all the conditions tested in both cell lines, suggesting that Hakai may be a new client protein for Hsp90. Parallelly to Hakai down-regulation, Annexin A2 levels were up- regulated in all the tested conditions, supporting it as a new substrate for Hakai.

In order to discard the possibility that Hakai down-regulation was taking place at a transcriptional level, endogenous mRNA Hakai levels were determined in presence of geldanamycin for both cell lines HEK 293T and HCT116 (Figure 43).

As shown in figure 43, no significative differences were observed for Hakai mRNA levels after treatment with geldanamycin, neither in HEK 293T nor in HCT116 cell line. This result indicates that down-regulation of Hakai is not occurring at a transcriptional level, and suggests that Hakai down-regulation is effectively taking place at a post-translational level.

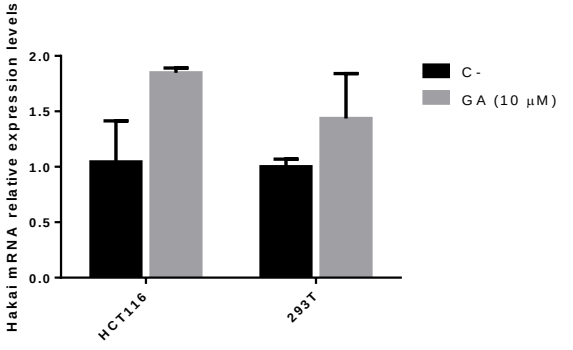

Figure 43. Hakai mRNA expression levels under geldanamycin treatment in HEK 293T and HCT116 cells. HEK 293T and HCT116 cell lines were treated with 10 μM geldanamycin for 24 hours. Cells were collected and proceeded to RNA and protein extraction. Hakai cDNA levels were evaluated by performing RT-qPCR using *HPRT* as a housekeeping. Relative quantification of Hakai mRNA levels was graphically represented as Mean ± SEM for six replicates of the experiment (*p < 0.05, **p < 0.01, ***p < 0.001).

In order to corroborate the results obtained for endogenous protein levels after geldanamycin treatment, we decided to carry out the same experiment under Hakai overexpression in HEK 293T cell line (Figure 44) where Annexin A2 down-regulation had been previously demonstrated (Figure 36).

Hakai down-regulation in presence of geldanamycin was confirmed in a model of Hakai overexpression in HEK 293T cells. As shown in figure 44, Hakai levels were drastically reduced in presence of geldanamycin compared to non-treated control transfected with Hakai, Src and Ubiquitin. Accompanying this reduction in Hakai levels, we observed an increase in Annexin A2 levels, thus confirming the previous results observed by immunofluorescence and western blot.

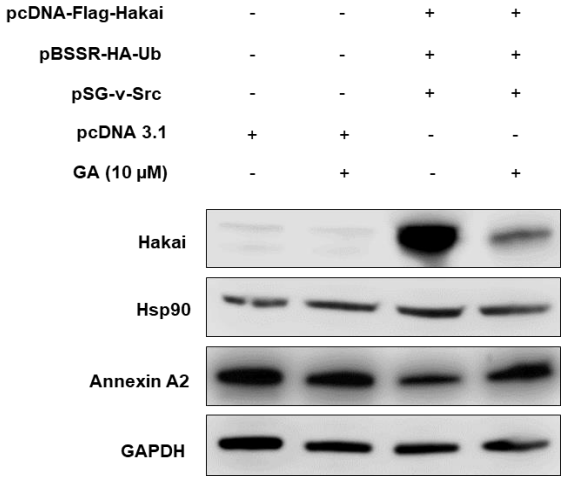

Figure 44. Effect of geldanamycin on Hakai and Annexin A2 levels in a model of Hakai overexpression in HEK 293T cells. HEK 293T cells were transfected with pcDNA 3.1 (10 µg) empty vector or pcDNA-Flag-Hakai (4 µg), pBSSR-HA-ubiquitin (3 µg) and pSG-v-Src (3 µg) plasmids for 48 h. Cell lysates were evaluated by western blot with the indicated antibodies. GAPDH was used for loading control.

To further study the effect of geldanamycin on Hakai and Annexin A2 levels, we performed an experiment combining Hakai silencing with geldanamycin treatment. For that, HCT116 cells were transiently transfected with both Hakai siRNA 1 and Hakai siRNA 2 for 72 hours and treated with 10 µM geldanamycin for 24 hours (Figure 45). As shown in Figure 45, Hakai expression levels in the HCT116 line were drastically reduced in the presence of both siRNAs used. This reduction in Hakai levels was accentuated in combination with geldanamycin treatment, resulting in a synergistic effect that leads to Hakai almost dissapearance. The opposite effect was observed for Annexin A2 levels, which were significantly increased in the presence of Hakai siRNA 2. Statistical signification of regulation of Annexin A2 levels showed an increase in combination of Hakai silencing and geldanamycin treatment for both siRNAs employed.

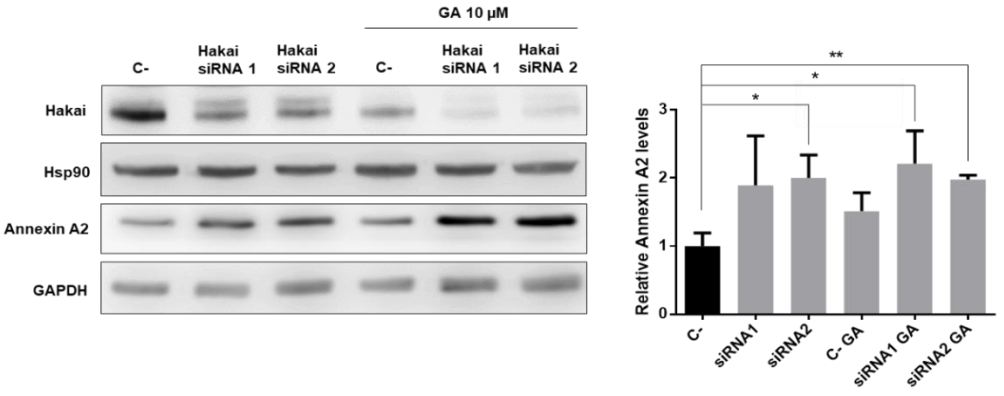

Figure 45. Effect of geldanamycin on Hakai and Annexin A2 levels in a model of Hakai silencing. HCT116 cells were transfected with Hakai siRNA 1 and siRNA 2 for 72 h and treated with 10 µM geldanamycin for the last 24 hours of transfection. Cell lysates were collected and protein expression was evaluated by western blot with the indicated antibodies. GAPDH was employed as loading control. Relative quantification of Annexin A2 expression levels was graphically represented as Mean ± SEM for three independent experiments (*p < 0.05, **p < 0.01, ***p < 0.001).

3.8. Geldanamycin causes the disruption of the interaction between Hakai, Hsp90 and Annexin A2

So far, we have confirmed that Hakai regulates Annexin A2 levels and that Hakai is down-regulated in the presence of an Hsp90 geldanamycin inhibitor. In order to confirm whether Hakai may be an Hsp90 client protein, which in turn regulates Annexin A2 levels, we performed co-immunoprecipitation assays in order to study if geldanamycin treatment may affect this protein interactions. (Figure 46). As shown in figure 46, previously detected interaction between Hakai, Hsp90 and Annexin A2 (Figure 38) was completely disrupted when performing immunoprecipitation with Hakai (Figure 46A) and Annexin A2 antibodies (Figure 46B). These results support the previously shown effect of geldanamycin on Hakai levels, suggesting that Hakai may be degraded after blocking Hakai-Hsp90 interaction. Besides, Annexin A2 interaction with Hakai and Hsp90 was also disrupted. Given that Annexin A2 is proposed as a new substrate for Hakai E3 ubiquitin-ligase activity, and that geldanamycin disrupts interaction between Hakai and Hsp90, it is possible that Hakai might be a direct client protein of Hsp90 chaperone.

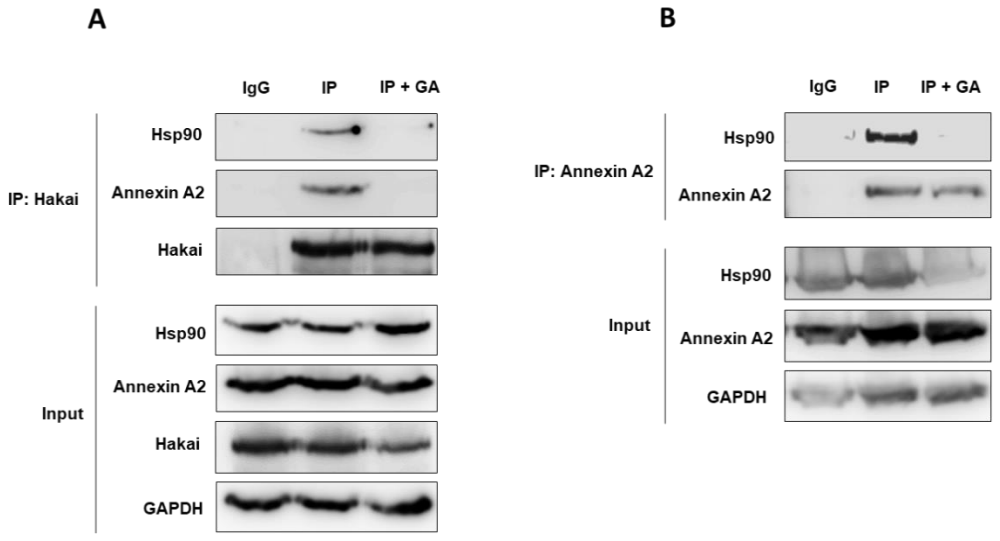

Figure 46. Study of protein-protein interaction disruption after geldanamycin treatment. Co-immunoprecipitation was performed in HCT116 cell line with Hakai Bethyl (**A**) and Annexin A2 (**B**) antibodies. Interaction among the three proteins was evaluated in presence and absence of 10 µM geldanamycin treatment by employing the indicated antibodies. GAPDH was used as input loading control.

3.9. Hsp90 inhibitor geldanamycin induces down-regulation of Hakai protein via lysosome

In order to study the mechanism of Hakai degradation during geldanamycin treatment, we performed inhibition experiments in the previously employed HEK 293T cell line. For that, HEK 293T cells were treated with lysosome degradation inhibitor CQ at different concentrations for 24 hours and with proteasome inhibitor MG132 for 6 hours. Hakai endogenous levels showed a clear recovery when treated with chloroquine, while no effect was observed during MG132 treatment (Figure 47B). This indicates that Hakai down-regulation is occurring in a lysosome-dependent manner (Figure 47A). Besides, Hakai levels recovery was accompanied by a down-regulation of Annexin A2, supporting the previously obtained results and pointing to Annexin A2 as a new possible target protein for Hakai E3 ubiquitin-ligase.

Once Hakai degradation was described to occur via the lysosome pathway, we combined geldanamycin treatment with chloroquine in HEK 293T cells in order to elucidate the mechanism by which Hakai is being degraded in absence of Hsp90 activity. For that, HEK 293T were transiently transfected for 48 hours with Hakai, Src and Ubiquitin in order to better detect

Hakai down-regulation under geldanamycin treatment, as showed in Figure 44. Twenty-four hours after transfection, cells were treated separately with chloroquine, geldanamycin and the combination of both treatments for 24 hours, and protein levels were analyzed by western blot (Figure 47C). In this case, Hakai recovery after chloroquine treatment was not detected, maybe due to the already elevated levels of Hakai after its overexpression. However, a recovery in Hakai levels was observed during combination of both treatments, suggesting that geldanamycin is effectively inducing Hakai degradation in a lysosome-dependent manner. Accordingly, Annexin A2 levels were up-regulated under geldanamycin treatment, while this effect was reverted in combination with chloroquine inhibitor. Moreover, the well-described E3 ubiquitin-ligase Hakai, E-cadherin, showed a similar regulatory pattern to Annexin A2, supporting the expected role of Annexin A2 as a substrate for E3 ubiquitin-ligase Hakai. Altogether, these data support that Hsp90 inhibition induces Hakai lysosome-dependent degradation and suggest the involvement of Hsp90 in the regulation of Hakai specific substrates.

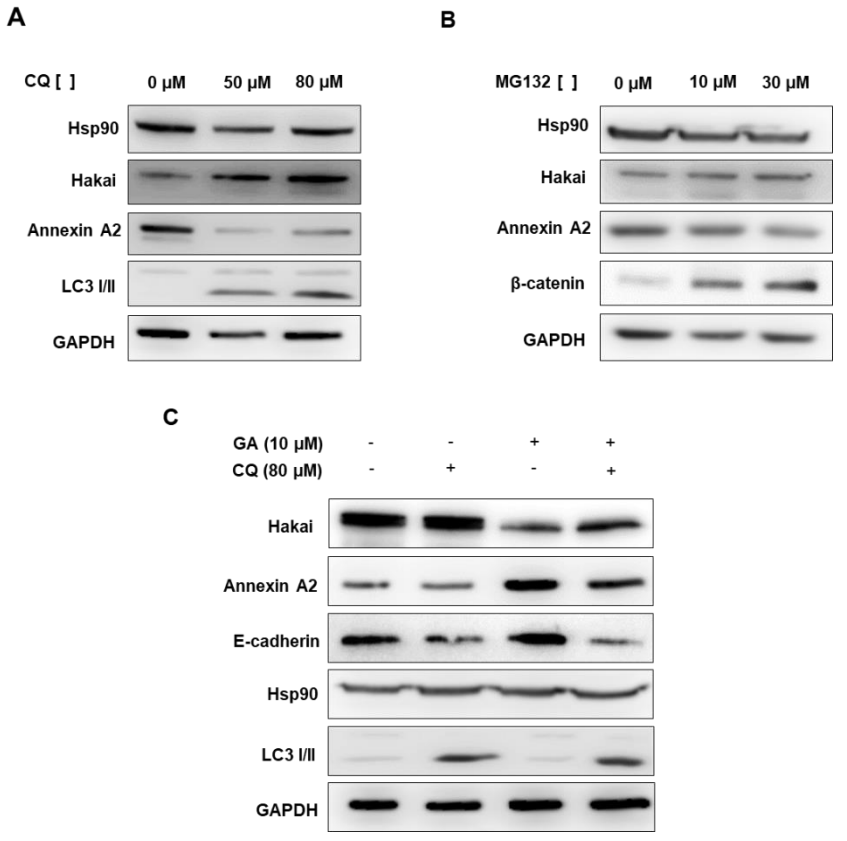

Figure 47. Study of Hakai mechanism of degradation under geldanamycin treatment. (**A**) HEK 293T cells were treated with chloroquine and MG132 at the indicated concentrations. Incubation with chloroquine was performed during 24 h (left panel) and with MG132 for 6 h (right panel). Endogenous protein levels were evaluated. (**B**) HEK 293T cells were transiently transfected with pcDNA-Flag-Hakai (4 μg), pBSSR-HA-Ubiquitin (3 μg) and pSG-v-Src (3 μg) for 48 hours. The day after transfection cells were treated with chloroquine and geldanamycin at the indicated concentrations for 24 hours. Cell lysates were collected and protein expression was evaluated by SDS-PAGE electrophoresis followed by immunoblot with the indicated antibodies. GAPDH was used as loading control. LC3 I/II levels were analyzed as a positive control of chloroquine treatment and β-catenin for MG132 treatment.

3.10. Geldanamycin treatment reduces Hakai-induced migration ability

So far, we demonstrated that geldanamycin-induced Hsp90 inhibition induced Hakai down-regulation and E-cadherin and Annexin A2 recovery, suggesting that Hsp90 plays a role in Hakai stabilization. Hakai was reported to be overexpressed in various cancer, such as lung and colon cancer [89, 91, 93], and to be related to different oncogenic properties such as migration, oncogenic potential, proliferation and invasion [89, 90, 94]. To further confirm the effect of

Hsp90 inhibition on Hakai-induced oncogenic properties, we performed a migration assay in order to determine if the effects observed at a molecular level are affecting Hakai-induced migration ability (Figure 48).

Transwell migration assay was performed for 16 h with HEK 293T cells transiently transfected with pcDNA 3.1 and pcDNA-Flag-Hakai. HEK 293T cells transfected with pcDNA 3.1 empty vector did not show any migration ability, however, Hakai overexpression induced an increase in cell migration when compared to cells transfected with empty vector. This migratory ability was drastically reduced in presence of geldanamycin. This result supports that geldanamycin treatment has an effect on Hakai-mediated cell migration by inhibiting Hsp90 activity, consequently affecting Hakai-induced migration capability.

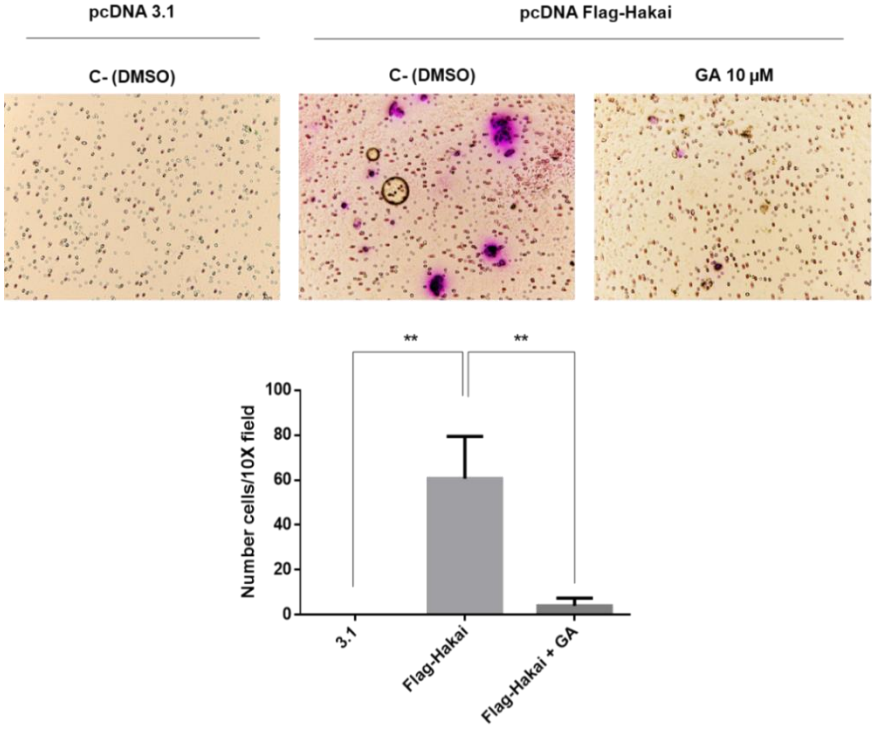

Figure 48. Effect of geldanamycin treatment in Hakai-induced cell migration. HEK 293T cells were transiently transfected with 8 µg empty vector pcDNA 3.1 and pcDNA-Flag-Hakai for 54 h and motility was evaluated by transwell migration assay in presence or absence of geldanamycin. 48 hours after transfection, cells were seeded into migration transwells for 16 h in a gradient concentration of FBS (1%-30%). After incubation, cells in transwells were fixed and stained for microscopy detection. Images were obtained by employing optical microscopy with an objective of 10X¡x magnification. Quantification indicates number of cells per 10x objective field in a total of three different images and was represented as Mean ± SEM for one experiment (*$p < 0.05$, **$p < 0.01$, ***$p < 0.001$).

3.11. Hsp90 is highly expressed in colorectal cancer samples compared to adjacent normal epithelial tissues

As previously mentioned, Hsp90 has been extensively studied in relation to cancer progression. Hsp90 regulates a wide number of down-stream targets which might be implicated in cancer progression, and it is proposed as a potential therapeutic target for cancer treatment. Hsp90 was reported to be implicated in different oncogenic pathways of colorectal cancer, such as mitogen-activated protein kinases (MAPKs) or transforming growth factor β (TGF-β), and different Hsp90 inhibitors are being studied in relation to inhibition of colorectal cancer progression in combination with other chemotherapeutic agents [221]. We previously published that Hakai expression levels are gradually increased according to colorectal tumoral stage in adenoma and different carcinoma TNM stages (I-IV) compared to healthy colon samples [91], thus constituting a novel biomarker of tumor progression. Moreover, in this study we demonstrated a link between Hakai and Hsp90 *in vitro*. In order to determine whether Hsp90 may be implicated in colorectal cancer *in vivo*, we decided to evaluate Hsp90 expression in the same colorectal cancer patient samples were Hakai had been previously evaluated. For that, we performed immunohistochemistry experiments in samples of colorectal cancer patients, including healthy tissue, adenoma, and TNM stages I to IV of colorectal cancer (Figure 49).

As shown in figure 49, Hsp90 expression correlates with the presence of the disease, being practically absent in healthy tissue and adenoma and stably increasing its expression between the different stages of tumor progression. This increased expression further supports the already demonstrated pathological role of Hsp90 in tumor progression and resembles that previously described in our laboratory for Hakai expression *in vivo.* Considering the previously demonstrated regulation of Hakai by Hsp90 *in vitro*, together with this expression pattern in pathological samples, we propose that Hsp90 might be effectively regulating Hakai levels *in vivo* with an important impact on tumor progression.

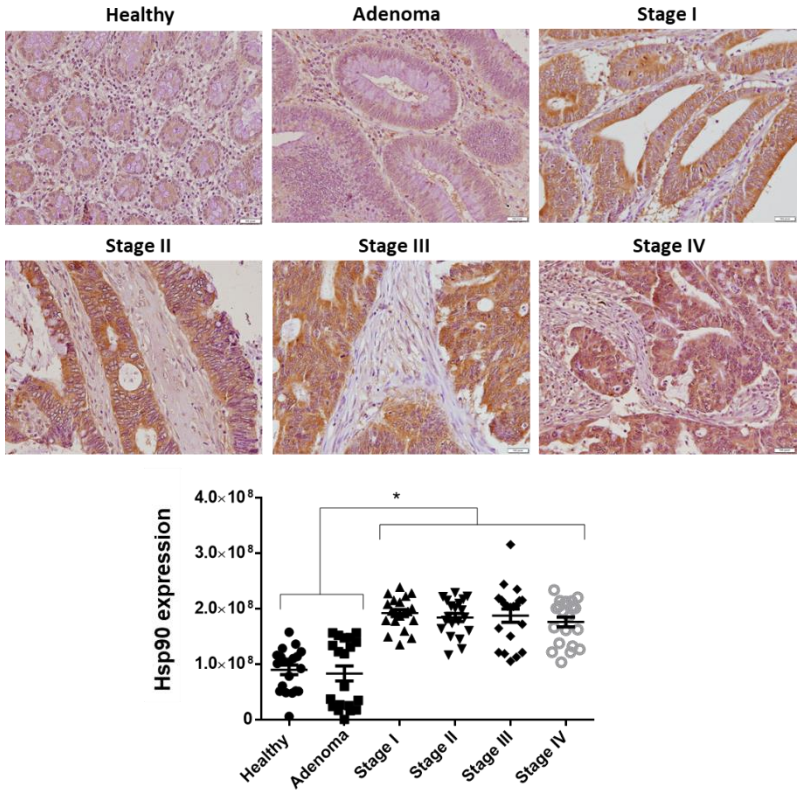

Figure 49. Hsp90 expression levels in colorectal cancer human samples. Representative images of Hsp90 immunoreactivity in healthy tissue, adenoma and TNM stages I – IV of colorectal cancer (upper panel). Images were obtained with 20x objective. Scale bar 125 µm. Statistical analysis of Hsp90 staining intensity in the different samples. Quantification of staining intensity per field of five photographs was performed and represented in a scatter plot. Results are represented as Mean ± SEM for signal intensity (lower panel). Analysis was performed by employing Kruskal-Wallis with Tukey correction test (*$p < 0.05$; **$p < 0,01$; ***$p < 0,001$).

V. DISCUSSION

During the development of this work we performed a proteomic comparative study between Hakai-transformed cells and parental epithelial MDCK cells by employing an iTRAQ technique. Proteomic techniques provide new methods for the identification of molecular pathways that may be regulated during Hakai-driven EMT in tumor progression, and offer a new way to determine new biomarkers related to Hakai overexpression that may be useful during diagnosis, prevention or treatment of cancer and metastatic process. iTRAQ technique is a quantitative method based on isotope labeling of peptides that allows to identified differentially expressed proteins in diverse biological samples or experimental conditions. Here we evaluated differentially expressed proteins during Hakai overexpression and identified one hundred and forty-six deregulated proteins compared to non-transformed epithelial cell line MDCK, out of which 83 happened to be up-regulated and 63 down-regulated. Classification of the identified proteins by employing different databases showed revealed novel molecular pathways were Hakai may be playing a role during tumor progression. By performing bioinformatic analysis employing different bioinformatic tools, we discovered that most up-regulated proteins in Hakai-transformed epithelial cells were implicated in metabolic process and post-transcriptional process. On the other hand, down-regulated proteins in Hakai-transformed epithelial cells were mostly implicated in cytoskeleton morphology and membrane vesicle trafficking, which suggest the clear implication of Hakai during EMT-induced cellular phenotype change and in the mediation of intercellular communication [222]. Besides, among down-regulated proteins implicated in protein metabolism, this analysis also highlighted a broad cluster of 26S proteasome subunit proteins, pointing to a decrease of proteasome activity during Hakai-driven EMT (Banno *et al*., 2016). So far, proteasome inhibitors are being increasingly used for the treatment of hematopoietic malignancies, but showed no successful effect during the treatment of carcinomas [73, 223]. Our results suggest that epithelial cells might be developing escape strategies during carcinoma progression, partly mediated by Hakai overexpression, that could be one of the causes of the lack of effect of treatments based on proteasome inhibition.

Many studies have been published so far explaining that the epithelial plasticity experienced by tumor cells is due to the activation of different key signaling pathways [224, 225]. We currently know that one of these routes involves the E3 ubiquitin ligase Hakai, which binds to the Src-phosphorylated tyrosine residue of the cytoplasmic domain of E-cadherin, thus causing its degradation. We previously reported that Hakai-transformation in MDCK cell line induces the acquisition of a mesenchymal phenotype (Figure 15A) accompanied by a decrease of the

epithelial marker E-cadherin and the increase of mesenchymal markers such as N-cadherin (Figure 15B) which translates into the loss of cell-cell contacts and the acquisition of an increased motility and invasiveness capability [56]. This increased motility and invasiveness capability is a necessary requirement during the metastatic process so that the tumoral cells can initiate their dissemination through the organism and colonize distant organs, causing the appearance of secondary tumors [226]. In the proteomic study conducted in this doctoral thesis, we found numerous down-regulated proteins during Hakai overexpression (Table 16). Among them, we found not only proteins related to cell adhesion, but also related to cytoskeleton dynamics, which play an active role in the acquisition of cellular plasticity, invasion and motility. Cytoskeleton-related proteins such as Annexin A2, Annexin A2, Alpha-actinin-4, Ezrin, Moesin and other are included in this down-regulated group of proteins.

In addition to the changes occurring during the EMT process at a cytoskeleton reorganization level, cells also undergo morphological changes which include the formation of membrane protrusions, such as lamellipodia, phylopodia, podosomes and invadopodia, necessary during the migratory process [226]. Proteins implicated in pseudopodial actin dynamics during cell plasticity in tumor progression were also found among down-regulated proteins during Hakai overexpression, such as AHNAK, Arp2/3 complex, Alpha-actinin-4 and Cofilin [227]. Some of these identified proteins were reported to be down-regulated during the EMT process or cancer invasion. For example, Annexin A1 was reported to attenuate the EMT process and metastatic potential y breast cancer, Annexin A2 was reported to maintain the epithelial phenotype in bladder urothelial carcinoma, Prelamin A was described to prevent tumoral invasiveness and Ahnak was classified as a tumor suppressor through the potentiation of TGF-β1, a crucial factor in the EMT development [183, 228-230].

One of the described down-regulated proteins in this study was Cortactin. Cortactin has been previously reported to be phosphorylated by Src, proposing it as a new possible substrate for Hakai E3 ubiquitin-ligase activity. Cortactin and Hakai interaction has also been confirmed by immunoprecipitation assay, although the physiological meaning of these interaction has not been elucidated [63]. Cortactin has been described to be one of the major substrates for tyrosine kinases including Src, and it exerts its activity as a structural protein implicated in cell motility taking part in lamellipodia and invadopodia formation [231]. Despite not being identified as a down-regulated protein with statistical difference in this proteomic study, we have confirmed Cortactin down-regulation by western blot in Hakai-transformed MDCK cells (Figure 15B). These data suggest that Hakai may be effectively inducing Cortactin down-

regulation, and supports the hypothesis of Cortactin being considered a new substrate for Hakai E3 ubiquitin ligase activity by causing its ubiquitination and consequent degradation. This effect of Hakai on Cortactin may be responsible of the repercussion of Cortactin down-regulation on the EMT process. In this context, previous studies reported a decrease on the tyrosine-phosphorylated Cortactin levels during TGF-β1-driven EMT. Moreover, Cortactin knockdown during TGF-β1-driven EMT lead to the disruption of tight junctions causing thus an increase of the migration ability of AML-12 cells [231]. All these results suggest that Hakai-mediated Cortactin regulation during the metastatic process, however, the mechanism by which Hakai is inducing Cortactin degradation still remains to be elucidated.

Hakai influence on the development of the metastatic process has also been described. By using time-lapse microscopic analysis, it was observed that Hakai-overexpressing MDCK cells experimented a morphological transformation characterized by the appearance of dynamic spiky protrusions which may favor cellular migration and invasiveness [89]. This Hakai influence on cell motility was also reported in *in vivo* assays performed in *Drosophila Melanogaster,* where high levels of Hakai expression were detected in endoderm migratory cells [98]. Given that Hakai was found to be expressed in *Drosophila melanogaster* endoderm tissue where E-cadherin is absent, as well as in other tissues such as spleen, skeletal muscle or lymph nodes, it is believed that Hakai may be involved in the regulation of many other client proteins [56, 63, 89]. This fact would provide a new possible explanation to the phenomena in cell adhesion and migration that arise during embryonic development in *Drosophila melanogaster.* Moreover, Hakai has been recently described to cause micrometastases *in vivo* [91]. Given the described enriched localization of Hakai in cellular protrusions [89], together with the amount of cytoskeleton-related proteins identified in this proteomic study, it is plausible that Hakai may be involved in the turnover of proteins implicated in the maintenance of cellular structure and cell adhesion, thus causing and effect on cell motility and invasiveness.

Besides cytoskeleton-related proteins, an important amount of up-regulated proteins was found to be related to extracellular exosome by employing STRING database (Figure 19). Although Hakai has not yet been related to exosomal content, this result opens a possibility to the investigation of the role of Hakai ubiquitin-ligase E3 in exosomes derived from tumor cells. It has been published that post-translational modifications are involved in the sorting of specific proteins into the exosome content, such as ubiquitin-like modification ISGylation which was reported to control the exosome release *in vitro* and *in vivo* [232, 233]. Despite the indications that point to a possible role of Hakai in the regulation of exosome-related

metabolism, further studies are needed to elucidate whether Hakai may exert and effect on exosome release during the metastatic process.

Our proteomic study also revealed the influence of Hakai on RNA-related proteins. Proteins such as hnRNPA1, PAIRB, ROA1, LYAR or Galectin-3 (Table 17), constitute a network of RNA-binding proteins up-regulated during Hakai overexpression (Figure 19). The importance of the post-transcriptional control by RNA-binding proteins has been previously reported during the EMT process [24, 234]. Regarding this, in 2009 Hakai has been described to promote tumorigenic process by enhancing the RNA-binding activity of PSF splicing factor. Hakai interaction with PSF was described to alter PSF ability to bind to specific cancer-associated mRNAs, however it was not probed that Hakai can induce PSF ubiquitination [89, 103]. These findings, together with the well described presence of Hakai and other E3 ubiquitin-ligases in the nucleus, suggest that Hakai may be playing an E3-ubiquitin-ligase independent role on cellular phenotype by regulating the RNA metabolic process [105].

In addition, our proteomic study also revealed the impact of Hakai on a clear subset of down-regulated proteins implicated in cellular metabolism (Figure 18, Table 16). Interestingly, by protein interaction networks analysis employing STRING database, we identified a specific cluster of interconnected down-regulated proteins constituted by 26S proteasome subunits (Figure 18, Table 18). According to these data, a recent publication demonstrated proteasome activity decrease in epithelial cells during EMT and how this process is induced by the employment of proteasome inhibitors in breast cancer cells [235]. As previously mentioned, proteasome inhibitors such as bortezomib have shown successful results in the treatment of many hematopoietic malignancies in clinical trials, however, the results obtained for the treatment of solid tumors have so far been disappointing [223, 236]. Authors suggest that the use of proteasome inhibitors during breast cancer treatment may be not only inducing EMT process, but also increasing the survival of tumor cells [235]. In addition, although the ubiquitination process has been widely described for the degradation of cytosolic and nuclear proteins via proteasome, we currently know that other membrane proteins are ubiquitinated and degraded via lysosome. This ubiquitin-dependent lysosomal degradation process was first described in *Saccharomyces cerevisiae* [237]. Specifically, this degradation process has been described for E-cadherin in MDCK cells when it is phosphorylated by Src, thus facilitating the loss of cell-cell contacts and allowing cells to acquire mobility capacity [81]. Given that proteasome subunits are specifically down-regulated in Hakai-transformed cells, and that Hakai expression is markedly increased in gastric and colon adenocarcinoma compared to

healthy tissue, our data support the previously reported work where proteasome inhibitors are described as a not effective treatment in tumor subtypes that are subjected to the EMT process [235]. Although further analyses are needed to be carried out in human clinical samples to confirm those obtained in our cellular model system, we first propose that triggering E3 ubiquitin-ligases such as Hakai may be a better strategy during the treatment of solid tumor malignancies in order to prevent carcinoma cells from developing escape strategies during proteasome inhibition-based therapy [238].

In addition to the classification and network analysis of interactions between the identified proteins, some of the up and down-regulated proteins were chosen for validation by western blot based on their implication described in tumor progression. In this case, we chose down-regulated Annexin A1, Annexin A2, Calumenin, Stratifin, Galectin-3 and up-regulated Hsp70, IMPDH and Hsp90 due to their homology with Hsp70 despite not having been identified in the proteomic study (Figure 20). The up and down-regulation observed in the proteomic study was confirmed in all cases by western blot, supporting the hypothesis that they could be new proteins regulated by Hakai. The study of subcellular localization, as well as the study of its co-localization with Hakai, revealed interesting results for some of the identified proteins. Annexin A1 and Annexin A2 showed a membrane expression pattern in MDCK cells and completely disappeared in Hakai-transformed MDCK cells. Given that Annexin A1 and Annexin A2 are cytoskeleton-related proteins, we propose that Hakai-induced EMT has an impact on actin cytoskeleton reorganization in which Annexin A1 and Annexin A2 are implicated [239, 240]. Also, Hsp70 and Hsp90 pattern expression suffered a translocation from cytoplasm in MDCK cells to a higher membrane location in Hakai-transformed cells. This translocation to cell membrane has been previously reported for both chaperones in cancer disease [241, 242]. These results suggest that Hakai overexpression is inducing an EMT process through a global metabolic affectation that includes the dysregulation of the mentioned proteins. Moreover, an interesting result was also observed for the localization of Galectin-3 in cells that overexpress Hakai. While the expression pattern in MDCK lines is diffuse, Hakai-transformed cells showed an interesting localization of Galectin-3 in perinuclear areas located at the base of cellular prolongations accompanied by a clear co-localization with Hakai E3 ubiquitin-ligase.

Galectin-3 is a carbohydrate-binding protein able to recognize and attach to glycoconjugates present on cell surface and extracellular matrices, thus playing an important role in different processes during tumor progression [243, 244]. Galectin-3 has been extensively described to act extracellularly after being secreted during cancer progression however, little is known

about is mechanism of degradation [131, 245]. Besides, most authors describe Galectin-3 as marker of poor prognosis during cancer progression [246-250], however, some others have described a down-regulation of this protein during tumoral progression [125-128].

In order to deepen the mechanism responsible for the results obtained in our stable Hakai-overexpressing model, we carried out experiments of Hakai transient overexpression in other cell lines. These experiments were mostly conducted during a predoctoral stay in Dr. Fu-Tong Liu's laboratory at Academia Sinica. The first results obtained apparently confirmed the down-regulation of Galectin-3 during the transient overexpression of increasing concentrations of Hakai in HEK 293T and HeLa cells (Figure 23 and 25). Since the only evidence of Galectin-3 mechanism of degradation is via lysosome degradation pathway [131], inhibitors of the autophagic and lysosomal pathways were employed in this work to determine the mechanism by which Hakai might be inducing Galectin-3 degradation. In all the cases, previously observed effects of Galectin-3 down-regulation during Hakai overexpression were not replicated, and results were not conclusive. Similarly, the previously observed co-localization between Galectin-3 and Hakai, and the demonstrated Galectin-3 down-regulation in Hakai-overexpressing cells, was not reproduced in stable HEK 293T Galectin-3 overexpressing cells. On the other hand, given that no changes in galectin-3 mRNA levels were detected in presence of Hakai overexpression, it is plausible that the regulation initially observed in the first experiments might be occurring at a protein level. Altogether, despite the signs observed, the results obtained in relation to the regulation of Galectin-3 by Hakai do not allow us to conclude the mechanism by which Hakai is inducing Galectin-3 down-regulation in our Hakai-overexpressing model.

Other proteins identified as a result of the realization of the proteomic study in Hakai-overexpressing cells were Annexin A2 and Hsp90. Hsp90 is a chaperone that has been extensively described related to tumor progression due to the regulation of multiple client proteins directly involved in cancer disease. Most of the proteins described as clients of Hsp90 chaperone are proteins involved in cell proliferation, oxidative stress or cell differentiation, among which we can mostly find kinases and transcription factors [135, 251]. However, a recent study about the Hsp90 interactome has revealed that 31 % of the total tested E3 ubiquitin-ligases interact with this chaperone, out of which a minority has so far been described to interact with this chaperone, such as Cullin-5 or CHIP [158-160]. Here, we first performed a proteomic analysis of Hakai interactome where we identified 13 different proteins, among which we confirmed Hsp90 chaperone as a Hakai-interacting protein (Table

19). Interaction of Hakai and Hsp90 was further confirmed by immunoprecipitation assay followed by western blotting in different cell lines, thus supporting the result obtained in the interactome analysis. Interaction among chaperones and E3 ubiquitin-ligases has been generally stablish to happen as a collaboration as part of the chaperone complex. Usually, E3 ubiquitin-ligases are responsible of ubiquitinating chaperone client proteins which cannot be correctively folded and tagging them for degradation through the proteasome pathway [156, 252, 253]. Regarding Hsp90, the pharmacological inhibition of its folding activity is coupled with the activity of different E3 ubiquitin-ligases such as CHIP or Cullin-5, which are responsible of signalizing its specific client proteins for ubiquitination when they have not been correctly folded [158, 254]. Although this is the best described mechanism for the interaction of chaperones and E3 ubiquitin-ligases, here we demonstrated that Hakai and Hsp90 interaction is due to the nature of Hakai as a client protein of Hsp90. So far, only UHRF1 E3 ubiquitin-ligase has been described as a client protein for Hsp90 [171]. By employing Hsp90 inhibitor geldanamycin, we demonstrated that Hakai is induced to degradation in different cell lines (Figure 42). By combining Hsp90 inhibition with chloroquine, we confirmed that this degradation is taking place in a lysosome-dependent manner (Figure 47), however the exact ubiquitin-ligase mediating Hakai lysosome-dependent degradation upon pharmacological inactivation of Hsp90 remains to be elucidated. To our knowledge, this proteasome-independent degradation of Hsp90 client proteins under geldanamycin treatment has only been described for IκB kinase. A,uthors demonstrate that IκB kinase, an essential activator of NF-κB, is a novel client protein for Hsp90 and is degraded via autophagy when inactivating Hsp90 with geldanamycin [153].

In this work, we previously demonstrated as a result of a proteomic study, that Annexin A2 is down-regulated in Hakai-transformed MDCK epithelial cells compared to parental MDCK cells [238]. Moreover, interaction between Annexin A2 and Hsp90 has been previously reported *in vitro* and *in vivo* in diabetic rat's aorta [220]. Based on these reported results, and the currently confirmed interaction between Hakai and Hsp90 in different cell lines, we were also interested in determining the possible relationship between Annexin A2, Hsp90 and Hakai. In this work, by immunoprecipitation we confirmed interaction between Hakai, Hsp90 and Annexin A2 in HCT116 cell line (Figure 38). Annexin A2 is a calcium-binding protein that belongs to annexin family and is implicated in the dynamic organization of membrane microdomains thus mediating the formation of membrane-cytoskeleton and membrane-membrane contacts [255]. Besides, Annexin A2 has been extensively reported to be tyrosine-phosphorylated by

Src kinase [256]. Moreover, Hakai has been described to interact with different Src tyrosine-phosphorylated proteins and to induce its ubiquitination and consequent degradation. This fact turns Annexin A2 into a new potential substrate for Hakai E3 ubiquitin-ligase. In our work, transient overexpression of Hakai, together with Src and ubiquitin, induced a significative down-regulation of Annexin A2 levels (Figure 36). In the same way, Hakai silencing led to a significative increase in Annexin A2 levels (Figures 37). These data support the results obtained in the comparative proteomic study between Hakai-overexpressing MDCK cells and parental MDCK cells, and suggest that Hakai is directly regulating Annexin A2 levels as a new substrate for its E3 ubiquitin-ligase activity. Furthermore, the previously reported interaction between Hakai, Hsp90 and Annexin A2 was completely disrupted in presence of Hsp90 inhibitor geldanamycin (Figure 46). Also, experiments performed with geldanamycin revealed a down-regulation of Hakai levels accompanied by an up-regulation of Annexin A2 (Figure 44). On the other hand, inhibition of Hsp90 activity in HCT116 cells, which initially show a mesenchymal invasive phenotype, experimented a recovery or the epithelial phenotype, accompanied by an increment of Annexin A2 expression in cell membrane and E-cadherin at cell-cell contacts (Figure 41). Based on this effect, migratory capability of cells was also evaluated in presence of geldanamycin and a clear reduction of Hakai-induced cell migration was observed. Altogether, these data support that Hsp90 inhibition by geldanamycin regulates Hakai stability as a client protein of this chaperone and, in consequence, Hakai substrates such as E-cadherin and Annexin A2 are increased, thus reducing migratory cell ability and causing a reversion of the EMT process. This effect observed in our cellular model matches that previously described where Hsp90 knockdown and inhibition with ganetespib induced a down-regulation of EMT and motility associated molecular pathways [257].

Annexin A2 has been extensively described as a poor-prognosis marker during cancer progression, however it has been recently reported to be induced to degradation by other oncogenic E3 ubiquitin-ligases such as TRIM65 [183]. Besides, as a protein involved in the membrane-cytoskeleton dynamics, Annexin A2 was demonstrated to be implicated in E-cadherin recovery at adherens junctions given its effect on actin cystoskeleton [193], thus supporting the recovery of the epithelial phenotype here observed during geldanamycin treatment. On the other hand, E-cadherin was reported to be stabilized at adherens junctions during geldanamycin treatment due to the degradation of ErbB2. ErbB2 is a tyrosine kinase and Hsp90 client protein responsible of phosphorylating β-catenin and destabilizing the β-catenin-E-cadherin association, necessary for the maintenance of the epithelial phenotype

[258]. This data, together with our observed results suggest that Hsp90 inhibition with geldanamycin might be reverting EMT process at least partially through its effect on Hakai stability and, in consequence, through the stabilization of Hakai substrate E-cadherin and Annexin A2.

In this work, we also evaluated Hsp90 expression in human samples from different colon adenocarcinoma stages in order to study the possible role of this chaperone tumoral progression. Here we demonstrated that Hsp90 expression is increased in human colorectal cancer samples compared to those corresponding to adenoma or adjacent healthy tissue, thus suggesting a role for Hsp90 during tumor malignancy in colorectal cancer. These data agree with those recently published were Hsp90 expression has been related to a poor outcome in colorectal cancer patients [259].

Given the demonstrated interaction between Hakai and Hsp90 *in vitro,* together with the high expression of Hakai oncogene in colorectal cancer [2, 63, 91, 101], further investigations would be needed to elucidate the role of Hsp90 and Hakai interaction *in vivo*. Since the appearance of the first Hsp90 inhibitors such as geldanamycin or radicicol, promotion of Hsp90 client proteins degradation has been extensively studied as an anticancer strategy [217, 260]. In fact, there currently exist numerous clinical trials in progress based on geldanamycin derivative compounds for cancer treatment [151, 261]. Although Hsp90 inhibition has been extensively studied for the treatment of different tumor types, Hsp90 inhibition-based monotherapy has not shown successful results due to the existence of different resistance mechanisms. In fact, only combined therapies based on Hsp90 inhibition and the employment of chemotherapeutic agents have obtained promising results [221]. Given that one of the resistance mechanisms is based on EMT induction, and considering the impact of Hakai during EMT process, the development of therapeutic strategies based on combination of Hsp90 and Hakai inhibition could be and attractive alternative therapy for cancer treatment [262].

VI. CONCLUSIONS

Conclusions related to objective 1:

1. Proteomic analysis shows that Hakai stable overexpression in MDCK cells induces down-regulation of proteins related to cytoskeleton and membrane vesicle trafficking, and up-regulation of proteins implicated in metabolic process and post-transcriptional regulation compared to parental MDCK cells.

2. Hakai stable overexpression in MDCK cells enriches protein-protein interactions related to proteasome subunits.

3. Western blot validation shows that Hakai stable overexpression in MDCK cells effectively induces up-regulation of Hsp70, Hsp90 and IMPDH1 and down-regulation of Annexin A1, Annexin A2, Calumenin, Stratifin and Galectin-3 compared to MDCK parental cells.

4. Hsp70, Hsp90 and Galectin-3 subcellular localization changes during Hakai overexpression in Hakai-overexpressing MDCK cells compared to MDCK parental cells.

Conclusions related to objective 2:

1. Hakai is a novel client protein for Hsp90 chaperone.

2. Annexin A2 is a potential new target for the E3 ubiquitin-ligase Hakai.

3. Geldanamycin treatment induces Hakai degradation in a lysosome-dependent manner, and induces the recovery of epithelial phenotype in HCT116 colon cancer cell line.

4. Geldanamycin treatment reduces Hakai-mediated cell migration.

VII. REFERENCES

1. GLOBOCAN. *Global Cancer Observatory*. Cancer Today 2018; Available from: https://gco.iarc.fr/today/home.

2. Aparicio, L.A., et al., *Biological influence of Hakai in cancer: a 10-year review.* Cancer Metastasis Rev, 2012. **31**(1-2): p. 375-86.

3. Campbell, H.K., J.L. Maiers, and K.A. DeMali, *Interplay between tight junctions & adherens junctions.* Exp Cell Res, 2017. **358**(1): p. 39-44.

4. Yang, J. and R.A. Weinberg, *Epithelial-mesenchymal transition: at the crossroads of development and tumor metastasis.* Dev Cell, 2008. **14**(6): p. 818-29.

5. Lowe, J.S. and P.G. Anderson, *Chapter 3 - Epithelial Cells*. Stevens & Lowe's Human Histology (Fourth Edition), ed. P.G.A. James S. Lowe. 2015: Mosby. ISBN 9780723435020

6. Pezzella, F., et al., *Blood vessels and cancer much more than just angiogenesis.* Cell Death Discov, 2015. **1**:15064.

7. van Zijl, F., G. Krupitza, and W. Mikulits, *Initial steps of metastasis: cell invasion and endothelial transmigration.* Mutat Res, 2011. **728**(1-2): p. 23-34.

8. Hanahan, D. and R.A. Weinberg, *Hallmarks of cancer: the next generation.* Cell, 2011. **144**(5): p. 646-74.

9. NIH. *Cancer Staging - National Cancer Institute*. 2015 03/09/2015 - 08:00 05/02/2020]; Available from: https://www.cancer.gov/about-cancer/diagnosis-staging/staging.

10. Chaffer, C.L. and R.A. Weinberg, *A perspective on cancer cell metastasis.* Science, 2011. **331**(6024): p. 1559-64.

11. Thiery, J.P., *Epithelial-mesenchymal transitions in tumour progression.* Nat Rev Cancer, 2002. **2**(6): p. 442-54.

12. Nieto, M.A., et al., *EMT: 2016.* Cell, 2016. **166**(1): p. 21-45.

13. Greenburg, G. and E.D. Hay, *Epithelia suspended in collagen gels can lose polarity and express characteristics of migrating mesenchymal cells.* J Cell Biol, 1982. **95**(1): p. 333-9.

14. Greenburg, G. and E.D. Hay, *Cytodifferentiation and tissue phenotype change during transformation of embryonic lens epithelium to mesenchyme-like cells in vitro.* Dev Biol, 1986. **115**(2): p. 363-79.

15. Stone, R.C., et al., *Epithelial-mesenchymal transition in tissue repair and fibrosis.* Cell Tissue Res, 2016. **365**(3): p. 495-506.

16. Thiery, J.P., et al., *Epithelial-mesenchymal transitions in development and disease.* Cell, 2009. **139**(5): p. 871-90.

17. Wang, W., et al., *Suppression Of β-catenin Nuclear Translocation By CGP57380 Decelerates Poor Progression And Potentiates Radiation-Induced Apoptosis in Nasopharyngeal Carcinoma.* Theranostics, 2017. **7**(7): p. 2134-49.

18. Jamieson, C., M. Sharma, and B.R. Henderson, *Targeting the beta-catenin nuclear transport pathway in cancer.* Semin Cancer Biol, 2014. **27**: p. 20-9.

19. Heerboth, S., et al., *EMT and tumor metastasis.* Clin Transl Med, 2015. **4**:6.

20. Aparicio, L.A., et al., *Clinical implications of epithelial cell plasticity in cancer progression.* Cancer Lett, 2015. **366**(1): p. 1-10.

21. McGranahan, N. and C. Swanton, *Biological and therapeutic impact of intratumor heterogeneity in cancer evolution.* Cancer Cell, 2015. **27**(1): p. 15-26.

22. Jia, D., et al., *Quantifying Cancer Epithelial-Mesenchymal Plasticity and its Association with Stemness and Immune Response.* J Clin Med, 2019. **8**(5): pii.E725.

23. Skovierova, H., et al., *Molecular regulation of epithelial-to-mesenchymal transition in tumorigenesis (Review).* Int J Mol Med, 2018. **41**(3): p. 1187-1200.

24. Aparicio, L.A., et al., *Posttranscriptional regulation by RNA-binding proteins during epithelial-to-mesenchymal transition.* Cell Mol Life Sci, 2013. **70**(23): p. 4463-77.

25. Brown, R.L., et al., *CD44 splice isoform switching in human and mouse epithelium is essential for epithelial-mesenchymal transition and breast cancer progression.* J Clin Invest, 2011. **121**(3): p. 1064-74.

26. De Craene, B. and G. Berx, *Regulatory networks defining EMT during cancer initiation and progression.* Nat Rev Cancer, 2013. **13**(2): p. 97-110.

27. Su, C., et al., *MiR-21 improves invasion and migration of drug-resistant lung adenocarcinoma cancer cell and transformation of EMT through targeting HBP1.* Cancer Med, 2018. **7**(6): p. 2485-2503.

28. Wang, L.Q., et al., *miR-372 and miR-373 enhance the stemness of colorectal cancer cells by repressing differentiation signaling pathways.* Mol Oncol, 2018. **12**(11): p. 1949-1964.

29. Valladares-Ayerbes, M., et al., *Circulating miR-200c as a diagnostic and prognostic biomarker for gastric cancer.* J Transl Med, 2012. **10**:186.

30. Blanco-Calvo, M., et al., *Circulating levels of GDF15, MMP7 and miR-200c as a poor prognostic signature in gastric cancer.* Future Oncol, 2014. **10**(7): p. 1187-202.

31. Serrano-Gomez, S.J., M. Maziveyi, and S.K. Alahari, *Regulation of epithelial-mesenchymal transition through epigenetic and post-translational modifications.* Mol Cancer, 2016. **15**:18.

32. van Roy, F. and G. Berx, *The cell-cell adhesion molecule E-cadherin.* Cell Mol Life Sci, 2008. **65**(23): p. 3756-88.

33. Hosking, C.R., et al., *The transcriptional repressor Glis2 is a novel binding partner for p120 catenin.* Mol Biol Cell, 2007. **18**(5): p. 1918-27.

34. Berx, G., et al., *Mutations of the human E-cadherin (CDH1) gene.* Hum Mutat, 1998. **12**(4): p. 226-37.

35. Corso, G., et al., *CDH1 germline mutations and hereditary lobular breast cancer.* Fam Cancer, 2016. **15**(2): p. 215-9.

36. Strathdee, G., *Epigenetic versus genetic alterations in the inactivation of E-cadherin.* Semin Cancer Biol, 2002. **12**(5): p. 373-9.

37. Grady, W.M., et al., *Methylation of the CDH1 promoter as the second genetic hit in hereditary diffuse gastric cancer.* Nat Genet, 2000. **26**(1): p. 16-7.

38. Tamura, G., *Genetic and epigenetic alterations of tumor suppressor and tumor-related genes in gastric cancer.* Histol Histopathol, 2002. **17**(1): p. 323-9.

39. Kang, G.H., et al., *Epstein-barr virus-positive gastric carcinoma demonstrates frequent aberrant methylation of multiple genes and constitutes CpG island methylator phenotype-positive gastric carcinoma.* Am J Pathol, 2002. **160**(3): p. 787-94.

40. Darwanto, A., et al., *MeCP2 and promoter methylation cooperatively regulate E-cadherin gene expression in colorectal carcinoma.* Cancer Sci, 2003. **94**(5): p. 442-7.

41. Koizume, S., et al., *Heterogeneity in the modification and involvement of chromatin components of the CpG island of the silenced human CDH1 gene in cancer cells.* Nucleic Acids Res, 2002. **30**(21): p. 4770-80.

42. Yuen, H.F., et al., *Significance of TWIST and E-cadherin expression in the metastatic progression of prostatic cancer.* Histopathology, 2007. **50**(5): p. 648-58.

43. Vesuna, F., et al., *Twist is a transcriptional repressor of E-cadherin gene expression in breast cancer.* Biochem Biophys Res Commun, 2008. **367**(2): p. 235-41.

44. Cano, A., et al., *The transcription factor snail controls epithelial-mesenchymal transitions by repressing E-cadherin expression.* Nat Cell Biol, 2000. **2**(2): p. 76-83.

45. Eger, A., et al., *DeltaEF1 is a transcriptional repressor of E-cadherin and regulates epithelial plasticity in breast cancer cells.* Oncogene, 2005. **24**(14): p. 2375-85.

46. Comijn, J., et al., *The two-handed E box binding zinc finger protein SIP1 downregulates E-cadherin and induces invasion.* Mol Cell, 2001. **7**(6): p. 1267-78.

47. Perez-Moreno, M.A., et al., *A new role for E12/E47 in the repression of E-cadherin expression and epithelial-mesenchymal transitions.* J Biol Chem, 2001. **276**(29): p. 27424-31.

48. Hajra, K.M., D.Y. Chen, and E.R. Fearon, *The SLUG zinc-finger protein represses E-cadherin in breast cancer.* Cancer Res, 2002. **62**(6): p. 1613-8.

49. Carvalho, S., et al., *Preventing E-cadherin aberrant N-glycosylation at Asn-554 improves its critical function in gastric cancer.* Oncogene, 2016. **35**(13): p. 1619-31.

50. Hu, Q.P., et al., *Beyond a tumor suppressor: Soluble E-cadherin promotes the progression of cancer.* Int J Cancer, 2016. **138**(12): p. 2804-12.

51. Maher, P.A., et al., *Phosphotyrosine-containing proteins are concentrated in focal adhesions and intercellular junctions in normal cells.* Proc Natl Acad Sci U S A, 1985. **82**(19): p. 6576-80.

52. Takahashi, K. and K. Suzuki, *Density-dependent inhibition of growth involves prevention of EGF receptor activation by E-cadherin-mediated cell-cell adhesion.* Exp Cell Res, 1996. **226**(1): p. 214-22.

53. Dupre-Crochet, S., et al., *Casein kinase 1 is a novel negative regulator of E-cadherin-based cell-cell contacts.* Mol Cell Biol, 2007. **27**(10): p. 3804-16.

54. Lau, M.T. and P.C. Leung, *The PI3K/Akt/mTOR signaling pathway mediates insulin-like growth factor 1-induced E-cadherin down-regulation and cell proliferation in ovarian cancer cells.* Cancer Lett, 2012. **326**(2): p. 191-8.

55. Kamei, T., et al., *Coendocytosis of cadherin and c-Met coupled to disruption of cell-cell adhesion in MDCK cells--regulation by Rho, Rac and Rab small G proteins.* Oncogene, 1999. **18**(48): p. 6776-84.

56. Fujita, Y., et al., *Hakai, a c-Cbl-like protein, ubiquitinates and induces endocytosis of the E-cadherin complex.* Nat Cell Biol, 2002. **4**(3): p. 222-31.

57. Wong, T.S., W. Gao, and J.Y. Chan, *Interactions between E-cadherin and microRNA deregulation in head and neck cancers: the potential interplay.* Biomed Res Int, 2014. **2014**:126038.

58. Goldstein, G., et al., *Isolation of a polypeptide that has lymphocyte-differentiating properties and is probably represented universally in living cells.* 1975: Proc Natl Acad Sci U S A . **72**(1): p. 11-15.

59. Hershko, A., et al., *Proposed role of ATP in protein breakdown: conjugation of protein with multiple chains of the polypeptide of ATP-dependent proteolysis.* Proc Natl Acad Sci U S A, 1980. **77**(4): p. 1783-6.

60. Hershko, A. and A. Ciechanover, *The ubiquitin system for protein degradation.* Annu Rev Biochem, 1992. **61**: p. 761-807.

61. Lee, D., M. Kim, and K.H. Cho, *A design principle underlying the paradoxical roles of E3 ubiquitin ligases.* Sci Rep, 2014. **4**:5573.

62. Cooper, J.A., T. Kaneko, and S.S. Li, *Cell regulation by phosphotyrosine-targeted ubiquitin ligases.* Mol Cell Biol, 2015. **35**(11): p. 1886-97.

63. Mukherjee, M., et al., *Structure of a novel phosphotyrosine-binding domain in Hakai that targets E-cadherin.* Embo j, 2012. **31**(5): p. 1308-19.

64. Falk, M.M., et al., *Degradation of endocytosed gap junctions by autophagosomal and endo-/lysosomal pathways: a perspective.* J Membr Biol, 2012. **245**(8): p. 465-76.

65. Swatek, K.N. and D. Komander, *Ubiquitin modifications.* Cell Res, 2016. **26**(4): p. 399-422.

66. O'Neill, L.A., *Regulation of signaling by non-degradative ubiquitination.* J Biol Chem, 2009. **284**(13):8209.

67. Galisson, F., et al., *A novel proteomics approach to identify SUMOylated proteins and their modification sites in human cells.* Mol Cell Proteomics, 2011. **10**(2):M110.004796.

68. Ohh, M., et al., *An intact NEDD8 pathway is required for Cullin-dependent ubiquitylation in mammalian cells.* EMBO Rep, 2002. **3**(2): p. 177-82.

69. Swaney, D.L., et al., *Global analysis of phosphorylation and ubiquitylation cross-talk in protein degradation.* Nat Methods, 2013. **10**(7): p. 676-82.

70. Choudhary, C., et al., *Lysine acetylation targets protein complexes and co-regulates major cellular functions.* Science, 2009. **325**(5942): p. 834-40.

71. Nedelsky, N.B., P.K. Todd, and J.P. Taylor, *Autophagy and the ubiquitin-proteasome system: collaborators in neuroprotection.* Biochim Biophys Acta, 2008. **1782**(12): p. 691-9.

72. Clague, M.J. and S. Urbe, *Ubiquitin: same molecule, different degradation pathways.* Cell, 2010. **143**(5): p. 682-5.

73. Manasanch, E.E. and R.Z. Orlowski, *Proteasome inhibitors in cancer therapy.* Nat Rev Clin Oncol, 2017. **14**(7): p. 417-433.

74. Redmann, M., et al., *Inhibition of autophagy with bafilomycin and chloroquine decreases mitochondrial quality and bioenergetic function in primary neurons.* Redox Biol, 2017. **11**: p. 73-81.

75. Slater, A.F., *Chloroquine: mechanism of drug action and resistance in Plasmodium falciparum.* Pharmacol Ther, 1993. **57**(2-3): p. 203-35.

76. Mauthe, M., et al., *Chloroquine inhibits autophagic flux by decreasing autophagosome-lysosome fusion.* Autophagy, 2018. **14**(8): p. 1435-1455.

77. Grumati, P. and I. Dikic, *Ubiquitin signaling and autophagy.* J Biol Chem, 2018. **293**(15): p. 5404-5413.

78. Feng, Y., et al., *The machinery of macroautophagy.* Cell Res, 2014. **24**(1): p. 24-41.

79. Wu, Y.T., et al., *Dual role of 3-methyladenine in modulation of autophagy via different temporal patterns of inhibition on class I and III phosphoinositide 3-kinase.* J Biol Chem, 2010. **285**(14): p. 10850-61.

80. Onorati, A.V., et al., *Targeting autophagy in cancer.* Cancer, 2018. **124**(16): p. 3307-3318.

81. Palacios, F., et al., *Lysosomal targeting of E-cadherin: a unique mechanism for the down-regulation of cell-cell adhesion during epithelial to mesenchymal transitions.* Mol Cell Biol, 2005. **25**(1): p. 389-402.

82. Zhou, W.J., et al., *Slit-Robo signaling induces malignant transformation through Hakai-mediated E-cadherin degradation during colorectal epithelial cell carcinogenesis.* Cell Res, 2011. **21**(4): p. 609-26.

83. Lu, M., et al., *Basolateral CD147 induces hepatocyte polarity loss by E-cadherin ubiquitination and degradation in hepatocellular carcinoma progress.* Hepatology, 2018. **68**(1): p. 317-332.

84. Daley, W.P., et al., *Btbd7 is essential for region-specific epithelial cell dynamics and branching morphogenesis in vivo.* Development, 2017. **144**(12): p. 2200-2211.

85. Smyth, D., et al., *Reduced surface expression of epithelial E-cadherin evoked by interferon-gamma is Fyn kinase-dependent.* PLoS One, 2012. **7**(6): p. e38441.

86. Sako-Kubota, K., et al., *Minus end-directed motor KIFC3 suppresses E-cadherin degradation by recruiting USP47 to adherens junctions.* Mol Biol Cell, 2014. **25**(24): p. 3851-60.

87. Mukherjee, M., et al., *Dimeric switch of Hakai-truncated monomers during substrate recognition: insights from solution studies and NMR structure.* J Biol Chem, 2014. **289**(37): p. 25611-23.

88. Yeatman, T.J., *A renaissance for SRC.* Nat Rev Cancer, 2004. **4**(6): p. 470-80.

89. Figueroa, A., et al., *Novel roles of hakai in cell proliferation and oncogenesis.* Mol Biol Cell, 2009. **20**(15): p. 3533-42.

90. Rodriguez-Rigueiro, T., et al., *Hakai reduces cell-substratum adhesion and increases epithelial cell invasion.* BMC Cancer, 2011. **11**:474.

91. Castosa, R., et al., *Hakai overexpression effectively induces tumour progression and metastasis in vivo.* Sci Rep, 2018. **8**(1):3466.

92. Rodriguez-Rigueiro, T., et al., *A novel procedure for protein extraction from formalin-fixed paraffin-embedded tissues.* Proteomics, 2011. **11**(12): p. 2555-9.

93. Hui, L., et al., *CBLL1 is highly expressed in non-small cell lung cancer and promotes cell proliferation and invasion.* Thorac Cancer, 2019. **10**(6): p. 1479-1488.

94. Liu, Z., et al., *E3 ubiquitin ligase Hakai regulates cell growth and invasion, and increases the chemosensitivity to cisplatin in nonsmallcell lung cancer cells.* Int J Mol Med, 2018. **42**(2): p. 1145-1151.

95. Weng, C.H., et al., *Epithelial-mesenchymal transition (EMT) beyond EGFR mutations per se is a common mechanism for acquired resistance to EGFR TKI.* Oncogene, 2019. **38**(4): p. 455-468.

96. Liu, M., et al., *Ajuba inhibits hepatocellular carcinoma cell growth via targeting of beta-catenin and YAP signaling and is regulated by E3 ligase Hakai through neddylation.* J Exp Clin Cancer Res, 2018. **37**(1):165.

97. Ruzicka, K., et al., *Identification of factors required for m(6) A mRNA methylation in Arabidopsis reveals a role for the conserved E3 ubiquitin ligase HAKAI.* New Phytol, 2017. **215**(1): p. 157-172.

98. Kaido, M., et al., *Essential requirement for RING finger E3 ubiquitin ligase Hakai in early embryonic development of Drosophila.* Genes Cells, 2009. **14**(9): p. 1067-77.

99. Gong, E.Y., E. Park, and K. Lee, *Hakai acts as a coregulator of estrogen receptor alpha in breast cancer cells.* Cancer Sci, 2010. **101**(9): p. 2019-25.

100. Abella, V., et al., *miR-203 regulates cell proliferation through its influence on Hakai expression.* PLoS One, 2012. **7**(12): p. e52568.

101. Aparicio, L.A., et al., *Role of the microtubule-targeting drug vinflunine on cell-cell adhesions in bladder epithelial tumour cells.* BMC Cancer, 2014. **14**:507.

102. Maniatis, T., *A ubiquitin ligase complex essential for the NF-kappaB, Wnt/Wingless, and Hedgehog signaling pathways.* Genes Dev, 1999. **13**(5): p. 505-10.

103. Figueroa, A., Y. Fujita, and M. Gorospe, *Hacking RNA: Hakai promotes tumorigenesis by enhancing the RNA-binding function of PSF.* Cell Cycle, 2009. **8**(22): p. 3648-51.

104. Dong, L., et al., *PTB-associated splicing factor inhibits IGF-1-induced VEGF upregulation in a mouse model of oxygen-induced retinopathy.* Cell Tissue Res, 2015. **360**(2): p. 233-43.

105. Shrestha, H., et al., *Hakai, an E3-ligase for E-cadherin, stabilizes delta-catenin through Src kinase.* Cell Signal, 2017. **31**: p. 135-145.

106. Horiuchi, K., et al., *Identification of Wilms' tumor 1-associating protein complex and its role in alternative splicing and the cell cycle.* J Biol Chem, 2013. **288**(46): p. 33292-302.

107. Yue, Y., et al., *VIRMA mediates preferential m(6)A mRNA methylation in 3'UTR and near stop codon and associates with alternative polyadenylation.* Cell Discov, 2018. **4**:10.

108. Thiemann, S. and L.G. Baum, *Galectins and Immune Responses-Just How Do They Do Those Things They Do?* Annu Rev Immunol, 2016. **34**: p. 243-64.

109. Lobsanov, Y.D., et al., *X-ray crystal structure of the human dimeric S-Lac lectin, L-14-II, in complex with lactose at 2.9-A resolution.* J Biol Chem, 1993. **268**(36): p. 27034-8.

110. Hirabayashi, J., et al., *Oligosaccharide specificity of galectins: a search by frontal affinity chromatography.* Biochim Biophys Acta, 2002. **1572**(2-3): p. 232-54.

111. Liu, F.T. and G.A. Rabinovich, *Galectins as modulators of tumour progression.* Nat Rev Cancer, 2005. **5**(1): p. 29-41.

112. Liu, F.T., R.J. Patterson, and J.L. Wang, *Intracellular functions of galectins.* Biochim Biophys Acta, 2002. **1572**(2-3): p. 263-73.

113. Davidson, P.J., et al., *Shuttling of galectin-3 between the nucleus and cytoplasm.* Glycobiology, 2002. **12**(5): p. 329-37.

114. Glinsky, V.V., et al., *Intravascular metastatic cancer cell homotypic aggregation at the sites of primary attachment to the endothelium.* Cancer Res, 2003. **63**(13): p. 3805-11.

115. Wu, K.L., et al., *Extracellular galectin-3 facilitates colon cancer cell migration and is related to the epidermal growth factor receptor.* Am J Transl Res, 2018. **10**(8): p. 2402-2412.

116. Hittelet, A., et al., *Upregulation of galectins-1 and -3 in human colon cancer and their role in regulating cell migration.* Int J Cancer, 2003. **103**(3): p. 370-9.

117. Dos Santos, S.N., et al., *Galectin-3 acts as an angiogenic switch to induce tumor angiogenesis via Jagged-1/Notch activation.* Oncotarget, 2017. **8**(30): p. 49484-49501.

118. Ahmed, H. and D.M. AlSadek, *Galectin-3 as a Potential Target to Prevent Cancer Metastasis.* Clin Med Insights Oncol, 2015. **9**: p. 113-21.

119. Warfield, P.R., et al., *Adhesion of human breast carcinoma to extracellular matrix proteins is modulated by galectin-3.* Invasion Metastasis, 1997. **17**(2): p. 101-12.

120. Ahmad, N., et al., *Galectin-3 precipitates as a pentamer with synthetic multivalent carbohydrates and forms heterogeneous cross-linked complexes.* J Biol Chem, 2004. **279**(12): p. 10841-7.

121. Shimura, T., et al., *Implication of galectin-3 in Wnt signaling.* Cancer Res, 2005. **65**(9): p. 3535-7.

122. Wu, Z.H. and L. Gan, *[Association of galectin-3 and E-cadherin expressions with lymph node metastasis of colon cancer].* Nan Fang Yi Ke Da Xue Xue Bao, 2007. **27**(11): p. 1731-3.

123. Wang, L.P., et al., *Galectin-3 accelerates the progression of oral tongue squamous cell carcinoma via a Wnt/beta-catenin-dependent pathway.* Pathol Oncol Res, 2013. **19**(3): p. 461-74.

124. Shetty, P., et al., *Cell surface interaction of annexin A2 and galectin-3 modulates epidermal growth factor receptor signaling in Her-2 negative breast cancer cells.* Mol Cell Biochem, 2016. **411**(1-2): p. 221-33.

125. Junking, M., et al., *Decreased expression of galectin-3 is associated with metastatic potential of liver fluke-associated cholangiocarcinoma.* Eur J Cancer, 2008. **44**(4): p. 619-26.

126. Leal, M.F., et al., *Deregulated expression of annexin-A2 and galectin-3 is associated with metastasis in gastric cancer patients.* Clin Exp Med, 2015. **15**(3): p. 415-20.

127. van den Brule, F.A., et al., *Expression of the 67-kD laminin receptor, galectin-1, and galectin-3 in advanced human uterine adenocarcinoma.* Hum Pathol, 1996. **27**(11): p. 1185-91.

128. Castronovo, V., et al., *Decreased expression of galectin-3 is associated with progression of human breast cancer.* J Pathol, 1996. **179**(1): p. 43-8.

129. Califice, S., et al., *Dual activities of galectin-3 in human prostate cancer: tumor suppression of nuclear galectin-3 vs tumor promotion of cytoplasmic galectin-3.* Oncogene, 2004. **23**(45): p. 7527-36.

130. Gao, X., et al., *Cleavage and phosphorylation: important post-translational modifications of galectin-3.* Cancer Metastasis Rev, 2017. **36**(2): p. 367-374.

131. Li, X., et al., *c-Abl and Arg tyrosine kinases regulate lysosomal degradation of the oncoprotein Galectin-3.* Cell Death Differ, 2010. **17**(8): p. 1277-87.

132. Balan, V., et al., *Galectin-3: A novel substrate for c-Abl kinase.* Biochim Biophys Acta, 2010. **1803**(10): p. 1198-205.

133. Oppermann, H., W. Levinson, and J.M. Bishop, *A cellular protein that associates with the transforming protein of Rous sarcoma virus is also a heat-shock protein.* Proc Natl Acad Sci U S A, 1981. **78**(2): p. 1067-71.

134. Obermann, W.M., et al., *In Vivo Function of Hsp90 Is Dependent on ATP Binding and ATP Hydrolysis.* J Cell Biol, 1998. **143**(4): p. 901-10.

135. Hoter, A., M.E. El-Sabban, and H.Y. Naim, *The HSP90 Family: Structure, Regulation, Function, and Implications in Health and Disease.* Int J Mol Sci, 2018. **19**(9): pii. E2560.

136. Sreedhar, A.S., et al., *Hsp90 isoforms: functions, expression and clinical importance.* FEBS Lett, 2004. **562**(1-3): p. 11-5.

137. Kim, K., et al., *Differential expression of HSP90 isoforms and their correlations with clinicopathologic factors in patients with colorectal cancer.* Int J Clin Exp Pathol, 2019. **12**(3): p. 978-986.

138. Grammatikakis, N., et al., *The role of Hsp90N, a new member of the Hsp90 family, in signal transduction and neoplastic transformation.* J Biol Chem, 2002. **277**(10): p. 8312-20.

139. Zurawska, A., J. Urbanski, and P. Bieganowski, *Hsp90n - An accidental product of a fortuitous chromosomal translocation rather than a regular Hsp90 family member of human proteome.* Biochim Biophys Acta, 2008. **1784**(11): p. 1844-6.

140. Young, J.C., C. Schneider, and F.U. Hartl, *In vitro evidence that hsp90 contains two independent chaperone sites.* FEBS Lett, 1997. **418**(1-2): p. 139-43.

141. Grenert, J.P., et al., *The amino-terminal domain of heat shock protein 90 (hsp90) that binds geldanamycin is an ATP/ADP switch domain that regulates hsp90 conformation.* J Biol Chem, 1997. **272**(38): p. 23843-50.

142. Panaretou, B., et al., *ATP binding and hydrolysis are essential to the function of the Hsp90 molecular chaperone in vivo.* Embo j, 1998. **17**(16): p. 4829-36.

143. Dittmar, K.D., et al., *The role of DnaJ-like proteins in glucocorticoid receptor.hsp90 heterocomplex assembly by the reconstituted hsp90.p60.hsp70 foldosome complex.* J Biol Chem, 1998. **273**(13): p. 7358-66.

144. Ali, M.M., et al., *Crystal structure of an Hsp90-nucleotide-p23/Sba1 closed chaperone complex.* Nature, 2006. **440**(7087): p. 1013-7.

145. Wu, Z., A.M. Gholami, and B. Kuster, *Systematic identification of the HSP90 candidate regulated proteome.* Mol Cell Proteomics, 2012. **11**(6):M111.016675.

146. Whitesell, L., et al., *Inhibition of heat shock protein HSP90-pp60v-src heteroprotein complex formation by benzoquinone ansamycins: essential role for stress proteins in oncogenic transformation.* Proc Natl Acad Sci U S A, 1994. **91**(18): p. 8324-8.

147. Eccles, S.A., et al., *NVP-AUY922: a novel heat shock protein 90 inhibitor active against xenograft tumor growth, angiogenesis, and metastasis.* Cancer Res, 2008. **68**(8): p. 2850-60.

148. Roe, S.M., et al., *Structural basis for inhibition of the Hsp90 molecular chaperone by the antitumor antibiotics radicicol and geldanamycin.* J Med Chem, 1999. **42**(2): p. 260-6.

149. Clevenger, R.C. and B.S. Blagg, *Design, synthesis, and evaluation of a radicicol and geldanamycin chimera, radamide.* Org Lett, 2004. **6**(24): p. 4459-62.

150. Zhang, T., et al., *Characterization of celastrol to inhibit hsp90 and cdc37 interaction.* J Biol Chem, 2009. **284**(51): p. 35381-9.

151. Garg, G., A. Khandelwal, and B.S. Blagg, *Anticancer Inhibitors of Hsp90 Function: Beyond the Usual Suspects.* Adv Cancer Res, 2016. **129**: p. 51-88.

152. Butler, L.M., et al., *Maximizing the Therapeutic Potential of HSP90 Inhibitors.* Mol Cancer Res, 2015. **13**(11): p. 1445-51.

153. Qing, G., P. Yan, and G. Xiao, *Hsp90 inhibition results in autophagy-mediated proteasome-independent degradation of IkappaB kinase (IKK).* Cell Res, 2006. **16**(11): p. 895-901.

154. Loo, M.A., et al., *Perturbation of Hsp90 interaction with nascent CFTR prevents its maturation and accelerates its degradation by the proteasome.* Embo j, 1998. **17**(23): p. 6879-87.

155. Whittier, J.E., et al., *Hsp90 enhances degradation of oxidized calmodulin by the 20 S proteasome.* J Biol Chem, 2004. **279**(44): p. 46135-42.

156. Grbovic, O.M., et al., *V600E B-Raf requires the Hsp90 chaperone for stability and is degraded in response to Hsp90 inhibitors.* Proc Natl Acad Sci U S A, 2006. **103**(1): p. 57-62.

157. Kevei, E., W. Pokrzywa, and T. Hoppe, *Repair or destruction-an intimate liaison between ubiquitin ligases and molecular chaperones in proteostasis.* FEBS Lett, 2017. **591**(17): p. 2616-2635.

158. Ehrlich, E.S., et al., *Regulation of Hsp90 client proteins by a Cullin5-RING E3 ubiquitin ligase.* Proc Natl Acad Sci U S A, 2009. **106**(48): p. 20330-5.

159. Quintana-Gallardo, L., et al., *The cochaperone CHIP marks Hsp70- and Hsp90-bound substrates for degradation through a very flexible mechanism.* Sci Rep, 2019. **9**(1):5102.

160. Taipale, M., et al., *Quantitative analysis of HSP90-client interactions reveals principles of substrate recognition.* Cell, 2012. **150**(5): p. 987-1001.

161. Bandyopadhyay, U., et al., *The chaperone-mediated autophagy receptor organizes in dynamic protein complexes at the lysosomal membrane.* Mol Cell Biol, 2008. **28**(18): p. 5747-63.

162. Shen, S., et al., *Cyclodepsipeptide toxin promotes the degradation of Hsp90 client proteins through chaperone-mediated autophagy.* J Cell Biol, 2009. **185**(4): p. 629-39.

163. Sharma, K., et al., *Quantitative proteomics reveals that Hsp90 inhibition preferentially targets kinases and the DNA damage response.* Mol Cell Proteomics, 2012. **11**(3): p. M111.014654.

164. Schopf, F.H., M.M. Biebl, and J. Buchner, *The HSP90 chaperone machinery.* Nat Rev Mol Cell Biol, 2017. **18**(6): p. 345-360.

165. Lackie, R.E., et al., *The Hsp70/Hsp90 Chaperone Machinery in Neurodegenerative Diseases.* Front Neurosci, 2017. **11**:254.

166. Sato, S., N. Fujita, and T. Tsuruo, *Modulation of Akt kinase activity by binding to Hsp90.* Proc Natl Acad Sci U S A, 2000. **97**(20): p. 10832-7.

167. Hagn, F., et al., *Structural analysis of the interaction between Hsp90 and the tumor suppressor protein p53.* Nat Struct Mol Biol, 2011. **18**(10): p. 1086-93.

168. Minet, E., et al., *Hypoxia-induced activation of HIF-1: role of HIF-1alpha-Hsp90 interaction.* FEBS Lett, 1999. **460**(2): p. 251-6.

169. Brugge, J.S., E. Erikson, and R.L. Erikson, *The specific interaction of the Rous sarcoma virus transforming protein, pp60src, with two cellular proteins.* Cell, 1981. **25**(2): p. 363-72.

170. Senft, D., J. Qi, and Z.A. Ronai, *Ubiquitin ligases in oncogenic transformation and cancer therapy.* Nat Rev Cancer, 2018. **18**(2): p. 69-88.

171. Ding, G., et al., *Regulation of Ubiquitin-like with Plant Homeodomain and RING Finger Domain 1 (UHRF1) Protein Stability by Heat Shock Protein 90 Chaperone Machinery.* J Biol Chem, 2016. **291**(38): p. 20125-35.

172. Bharadwaj, A., et al., *Annexin A2 heterotetramer: structure and function.* Int J Mol Sci, 2013. **14**(3): p. 6259-305.

173. Gerke, V. and S.E. Moss, *Annexins: from structure to function.* Physiol Rev, 2002. **82**(2): p. 331-71.

174. Parente, L. and E. Solito, *Annexin 1: more than an anti-phospholipase protein.* Inflamm Res, 2004. **53**(4): p. 125-32.

175. Choi, K.S., et al., *Annexin II tetramer inhibits plasmin-dependent fibrinolysis.* Biochemistry, 1998. **37**(2): p. 648-55.

176. Kwon, M., et al., *Identification of annexin II heterotetramer as a plasmin reductase.* J Biol Chem, 2002. **277**(13): p. 10903-11.

177. Grewal, T. and C. Enrich, *Annexins--modulators of EGF receptor signalling and trafficking.* Cell Signal, 2009. **21**(6): p. 847-58.

178. Hayes, M.J., et al., *Annexin-actin interactions.* Traffic, 2004. **5**(8): p. 571-6.

179. Rescher, U. and T. Grewal, *Highlight: annexins in health and disease.* Biol Chem, 2016. **397**(10): p. 947-8.

180. Nazmi, A.R., et al., *N-terminal acetylation of annexin A2 is required for S100A10 binding.* Biol Chem, 2012. **393**(10): p. 1141-50.

181. Grindheim, A.K., J. Saraste, and A. Vedeler, *Protein phosphorylation and its role in the regulation of Annexin A2 function.* Biochim Biophys Acta Gen Subj, 2017. **1861**(11 Pt A): p. 2515-2529.

182. Caplan, J.F., et al., *Regulation of annexin A2 by reversible glutathionylation.* J Biol Chem, 2004. **279**(9): p. 7740-50.

183. Wei, W.S., et al., *TRIM65 supports bladder urothelial carcinoma cell aggressiveness by promoting ANXA2 ubiquitination and degradation.* Cancer Lett, 2018. **435**: p. 10-22.

184. Caron, D., et al., *Annexin A2 is SUMOylated on its N-terminal domain: regulation by insulin.* FEBS Lett, 2015. **589**(9): p. 985-91.

185. de Graauw, M., et al., *Annexin A2 phosphorylation mediates cell scattering and branching morphogenesis via cofilin Activation.* Mol Cell Biol, 2008. **28**(3): p. 1029-40.

186. Deora, A.B., et al., *An annexin 2 phosphorylation switch mediates p11-dependent translocation of annexin 2 to the cell surface.* J Biol Chem, 2004. **279**(42): p. 43411-8.

187. Zhang, X., et al., *The association of annexin A2 and cancers.* Clin Transl Oncol, 2012. **14**(9): p. 634-40.

188. Yee, D.S., et al., *Reduced annexin II protein expression in high-grade prostatic intraepithelial neoplasia and prostate cancer.* Arch Pathol Lab Med, 2007. **131**(6): p. 902-8.

189. Chan, C.M., et al., *Proteomic comparison of nasopharyngeal cancer cell lines C666-1 and NP69 identifies down-regulation of annexin II and beta2-tubulin for nasopharyngeal carcinoma.* Arch Pathol Lab Med, 2008. **132**(4): p. 675-83.

190. Qi, Y.J., et al., *[Dysregulation of Annexin II expression in esophageal squamous cell cancer and adjacent tissues from a high-incidence area for esophageal cancer in Henan province].* Ai Zheng, 2007. **26**(7): p. 730-6.

191. Rodrigo, J.P., et al., *Down-regulation of annexin A1 and A2 protein expression in intestinal-type sinonasal adenocarcinomas.* Hum Pathol, 2011. **42**(1): p. 88-94.

192. Pena-Alonso, E., et al., *Annexin A2 localizes to the basal epithelial layer and is down-regulated in dysplasia and head and neck squamous cell carcinoma.* Cancer Lett, 2008. **263**(1): p. 89-98.

193. Yamada, A., et al., *Involvement of the annexin II-S100A10 complex in the formation of E-cadherin-based adherens junctions in Madin-Darby canine kidney cells.* J Biol Chem, 2005. **280**(7): p. 6016-27.

194. Bai, D.S., et al., *UBAP2 negatively regulates the invasion of hepatocellular carcinoma cell by ubiquitinating and degradating Annexin A2.* Oncotarget, 2016. **7**(22): p. 32946-55.

195. Cuervo, A.M., et al., *Selective degradation of annexins by chaperone-mediated autophagy.* J Biol Chem, 2000. **275**(43): p. 33329-35.

196. Rabilloud, T., et al., *Modified silver staining for immobilized pH gradients.* Electrophoresis, 1992. **13**(4): p. 264-6.

197. Alvarez, J.V., et al., *Proteomic Analysis in Morquio A Cells Treated with Immobilized Enzymatic Replacement Therapy on Nanostructured Lipid Systems.* Int J Mol Sci, 2019. **20**(18): pii. E4610.

198. Shilov, I.V., et al., *The Paragon Algorithm, a next generation search engine that uses sequence temperature values and feature probabilities to identify peptides from tandem mass spectra.* Mol Cell Proteomics, 2007. **6**(9): p. 1638-55.

199. Denizot, F. and R. Lang, *Rapid colorimetric assay for cell growth and survival. Modifications to the tetrazolium dye procedure giving improved sensitivity and reliability.* J Immunol Methods, 1986. **89**(2): p. 271-7.

200. Mosmann, T., *Rapid colorimetric assay for cellular growth and survival: application to proliferation and cytotoxicity assays.* J Immunol Methods, 1983. **65**(1-2): p. 55-63.

201. Tsubuki, S., et al., *Purification and characterization of a Z-Leu-Leu-Leu-MCA degrading protease expected to regulate neurite formation: a novel catalytic activity in proteasome.* Biochem Biophys Res Commun, 1993. **196**(3): p. 1195-201.

202. Sun, Z., et al., *Inhibition of beta-catenin signaling by nongenomic action of orphan nuclear receptor Nur77.* Oncogene, 2012. **31**(21): p. 2653-67.

203. Kumamoto, T., et al., *Expression of lysosome-related proteins and genes in the skeletal muscles of inclusion body myositis.* Acta Neuropathol, 2004. **107**(1): p. 59-65.

204. Kaushik, S., et al., *Constitutive activation of chaperone-mediated autophagy in cells with impaired macroautophagy.* Mol Biol Cell, 2008. **19**(5): p. 2179-92.

205. Lauffenburger, D.A. and A.F. Horwitz, *Cell migration: a physically integrated molecular process.* Cell, 1996. **84**(3): p. 359-69.

206. Franceschini, A., et al., *STRING v9.1: protein-protein interaction networks, with increased coverage and integration.* Nucleic Acids Res, 2013. **41**(Database issue): p. D808-15.

207. Huang, Z., et al., *Over expression of galectin-3 associates with short-term poor prognosis in stage II colon cancer.* Cancer Biomark, 2016. **17**(4): p. 445-455.

208. Kim, M.K., et al., *Overexpression of Galectin-3 and its clinical significance in ovarian carcinoma.* Int J Clin Oncol, 2011. **16**(4): p. 352-8.

209. Song, S., et al., *Overexpressed galectin-3 in pancreatic cancer induces cell proliferation and invasion by binding Ras and activating Ras signaling.* PLoS One, 2012. **7**(8):e42699.

210. Sakaki, M., et al., *Clinical significance of Galectin-3 in clear cell renal cell carcinoma.* J Med Invest, 2010. **57**(1-2): p. 152-7.

211. Ilmer, M., et al., *Low expression of galectin-3 is associated with poor survival in node-positive breast cancers and mesenchymal phenotype in breast cancer stem cells.* Breast Cancer Res, 2016. **18**(1):97.

212. Selemetjev, S.A., et al., *Changes in the expression pattern of apoptotic molecules (galectin-3, Bcl-2, Bax, survivin) during progression of thyroid malignancy and their clinical significance.* Wien Klin Wochenschr, 2015. **127**(9-10): p. 337-44.

213. Lee, J.W., et al., *Decreased galectin-3 expression during the progression of cervical neoplasia.* J Cancer Res Clin Oncol, 2006. **132**(4): p. 241-7.

214. Buttery, R., et al., *Galectin-3: differential expression between small-cell and non-small-cell lung cancer.* Histopathology, 2004. **44**(4): p. 339-44.

215. Merseburger, A.S., et al., *Involvement of decreased Galectin-3 expression in the pathogenesis and progression of prostate cancer.* Prostate, 2008. **68**(1): p. 72-7.

216. Shimamura, T., et al., *Clinicopathological significance of galectin-3 expression in ductal adenocarcinoma of the pancreas.* Clin Cancer Res, 2002. **8**(8): p. 2570-5.

217. Chatterjee, S. and T.F. Burns, *Targeting Heat Shock Proteins in Cancer: A Promising Therapeutic Approach.* Int J Mol Sci, 2017. **18**(9): pii. E1978.

218. Jiang, J., et al., *CHIP is a U-box-dependent E3 ubiquitin ligase: identification of Hsc70 as a target for ubiquitylation.* J Biol Chem, 2001. **276**(46): p. 42938-44.

219. Wang, C.Y. and C.F. Lin, *Annexin A2: its molecular regulation and cellular expression in cancer development.* Dis Markers, 2014. **2014**:308976.

220. Lei, H., G. Romeo, and A. Kazlauskas, *Heat shock protein 90alpha-dependent translocation of annexin II to the surface of endothelial cells modulates plasmin activity in the diabetic rat aorta.* Circ Res, 2004. **94**(7): p. 902-9.

221. Kryeziu, K., et al., *Combination therapies with HSP90 inhibitors against colorectal cancer.* Biochim Biophys Acta Rev Cancer, 2019. **1871**(2): p. 240-247.

222. Becker, A., et al., *Extracellular Vesicles in Cancer: Cell-to-Cell Mediators of Metastasis.* Cancer Cell, 2016. **30**(6): p. 836-848.

223. Rosenberg, J.E., et al., *Phase II study of bortezomib in patients with previously treated advanced urothelial tract transitional cell carcinoma: CALGB 90207.* Ann Oncol, 2008. **19**(5): p. 946-50.

224. Thiery, J.P. and J.P. Sleeman, *Complex networks orchestrate epithelial-mesenchymal transitions.* Nat Rev Mol Cell Biol, 2006. **7**(2): p. 131-42.

225. Gotzmann, J., et al., *Molecular aspects of epithelial cell plasticity: implications for local tumor invasion and metastasis.* Mutat Res, 2004. **566**(1): p. 9-20.

226. Yilmaz, M. and G. Christofori, *EMT, the cytoskeleton, and cancer cell invasion.* Cancer Metastasis Rev, 2009. **28**(1-2): p. 15-33.

227. Shankar, J., et al., *Pseudopodial actin dynamics control epithelial-mesenchymal transition in metastatic cancer cells.* Cancer Res, 2010. **70**(9): p. 3780-90.

228. Maschler, S., et al., *Annexin A1 attenuates EMT and metastatic potential in breast cancer.* EMBO Mol Med, 2010. **2**(10): p. 401-14.

229. de la Rosa, J., et al., *Prelamin A causes progeria through cell-extrinsic mechanisms and prevents cancer invasion.* Nat Commun, 2013. **4**: p. 2268.

230. Lee, I.H., et al., *Ahnak functions as a tumor suppressor via modulation of TGFbeta/Smad signaling pathway.* Oncogene, 2014. **33**(38): p. 4675-84.

231. Zhang, K., D. Wang, and J. Song, *Cortactin is involved in transforming growth factor-beta1-induced epithelial-mesenchymal transition in AML-12 cells.* Acta Biochim Biophys Sin (Shanghai), 2009. **41**(10): p. 839-45.

232. Villarroya-Beltri, C., et al., *Sorting it out: regulation of exosome loading.* Semin Cancer Biol, 2014. **28**: p. 3-13.

233. Villarroya-Beltri, C., et al., *ISGylation controls exosome secretion by promoting lysosomal degradation of MVB proteins.* Nat Commun, 2016. **7**:13588.

234. Burk, U., et al., *A reciprocal repression between ZEB1 and members of the miR-200 family promotes EMT and invasion in cancer cells.* EMBO Rep, 2008. **9**(6): p. 582-9.

235. Banno, A., et al., *Downregulation of 26S proteasome catalytic activity promotes epithelial-mesenchymal transition.* Oncotarget, 2016. **7**(16): p. 21527-41.

236. Aghajanian, C., et al., *A phase II evaluation of bortezomib in the treatment of recurrent platinum-sensitive ovarian or primary peritoneal cancer: a Gynecologic Oncology Group study.* Gynecol Oncol, 2009. **115**(2): p. 215-20.

237. Hicke, L. and H. Riezman, *Ubiquitination of a yeast plasma membrane receptor signals its ligand-stimulated endocytosis.* Cell, 1996. **84**(2): p. 277-87.

238. Diaz-Diaz, A., et al., *Proteomic Analysis of the E3 Ubiquitin-Ligase Hakai Highlights a Role in Plasticity of the Cytoskeleton Dynamics and in the Proteasome System.* J Proteome Res, 2017. **16**(8): p. 2773-2788.

239. Patel, D.M., et al., *Annexin A1 is a new functional linker between actin filaments and phagosomes during phagocytosis.* J Cell Sci, 2011. **124**(Pt 4): p. 578-88.

240. Grieve, A.G., S.E. Moss, and M.J. Hayes, *Annexin A2 at the interface of actin and membrane dynamics: a focus on its roles in endocytosis and cell polarization.* Int J Cell Biol, 2012. **2012**:852430.

241. Elmallah, M.I.Y., et al., *Membrane-anchored heat-shock protein 70 (Hsp70) in cancer.* Cancer Lett, 2020. **469**: p. 134-141.

242. Snigireva, A.V., et al., *[The Role of Membrane-Bound Heat Shock Proteins Hsp90 in Migration of Tumor Cells in vitro and Involvement of Cell Surface Heparan Sulfate Proteoglycans in Protein Binding to Plasma Membrane].* Biofizika, 2016. **61**(2): p. 328-36.

243. Fortuna-Costa, A., et al., *Extracellular galectin-3 in tumor progression and metastasis.* Front Oncol, 2014. **4**:138.

244. Funasaka, T., A. Raz, and P. Nangia-Makker, *Galectin-3 in angiogenesis and metastasis.* Glycobiology, 2014. **24**(10): p. 886-91.

245. Lobry, T., et al., *Interaction between galectin-3 and cystinosin uncovers a pathogenic role of inflammation in kidney involvement of cystinosis.* Kidney Int, 2019. **96**(2): p. 350-362.

246. Song, Y.K., T.R. Billiar, and Y.J. Lee, *Role of galectin-3 in breast cancer metastasis: involvement of nitric oxide.* Am J Pathol, 2002. **160**(3): p. 1069-75.

247. Tao, L., et al., *Galectin-3 Expression in Colorectal Cancer and its Correlation with Clinical Pathological Characteristics and Prognosis.* Open Med (Wars), 2017. **12**: p. 226-230.

248. Canesin, G., et al., *Galectin-3 expression is associated with bladder cancer progression and clinical outcome.* Tumour Biol, 2010. **31**(4): p. 277-85.

249. Wang, C., et al., *Galectin-3 may serve as a marker for poor prognosis in colorectal cancer: A meta-analysis.* Pathol Res Pract, 2019. **215**(10):152612.

250. Wang, Y., et al., *Prognostic role of galectin-3 expression in patients with solid tumors: a meta-analysis of 36 eligible studies.* Cancer Cell Int, 2018. **18**:172.

251. Mahalingam, D., et al., *Targeting HSP90 for cancer therapy.* Br J Cancer, 2009. **100**(10): p. 1523-9.

252. Schneider, C., et al., *Pharmacologic shifting of a balance between protein refolding and degradation mediated by Hsp90.* Proc Natl Acad Sci U S A, 1996. **93**(25): p. 14536-41.

253. Saibil, H., *Chaperone machines for protein folding, unfolding and disaggregation.* Nat Rev Mol Cell Biol, 2013. **14**(10): p. 630-42.

254. Zhou, P., et al., *ErbB2 degradation mediated by the co-chaperone protein CHIP.* J Biol Chem, 2003. **278**(16): p. 13829-37.

255. Hitchcock, J.K., A.A. Katz, and G. Schafer, *Dynamic reciprocity: the role of annexin A2 in tissue integrity.* J Cell Commun Signal, 2014. **8**(2): p. 125-33.

256. Hayes, M.J. and S.E. Moss, *Annexin 2 has a dual role as regulator and effector of v-Src in cell transformation.* J Biol Chem, 2009. **284**(15): p. 10202-10.

257. Nagaraju, G.P., et al., *Heat shock protein 90 promotes epithelial to mesenchymal transition, invasion, and migration in colorectal cancer.* Mol Carcinog, 2015. **54**(10): p. 1147-58.

258. Bonvini, P., et al., *Geldanamycin abrogates ErbB2 association with proteasome-resistant beta-catenin in melanoma cells, increases beta-catenin-E-cadherin association, and decreases beta-catenin-sensitive transcription.* Cancer Res, 2001. **61**(4): p. 1671-7.

259. Zhang, S., et al., *High expression of HSP90 is associated with poor prognosis in patients with colorectal cancer.* PeerJ, 2019. **7**:e7946.

260. Barrott, J.J. and T.A. Haystead, *Hsp90, an unlikely ally in the war on cancer.* Febs j, 2013. **280**(6): p. 1381-96.

261. Sidera, K. and E. Patsavoudi, *HSP90 inhibitors: current development and potential in cancer therapy.* Recent Pat Anticancer Drug Discov, 2014. **9**(1): p. 1-20.

262. Diaz-Diaz, A., et al., *Heat Shock Protein 90 Chaperone Regulates the E3 Ubiquitin-Ligase Hakai Protein Stability.* Cancers (Basel), 2020. **12**(1): pii. E215.

VIII. APPENDIXES

APPENDIX A

Identified regulated proteins in the comparative proteomic study:

- Table A1: List of total identified Hakai-down-regulated proteins with score ≤0.5.
- Table 2A: List of total identified Hakai-down-regulated proteins with score ≥2.

Table A1. List of total identified Hakai-down-regulated proteins with score ≤0.5.

Accesion number	Protein symbol	Protein name	Peptides (95%)	114:115	PVal 114:115	115:114	PVal 115:114	116:115	PVal 116:115	116:114	PVal 116:114	117:115	PVal 117:115	117:114	PVal 117:114
Q09666	AHNK	Neuroblast differentiation-associated protein AHNAK	88	1,2589	0,0004	0,7798	0,0004	**0,0254**	**0**	**0,0213**	**0**	**0,0203**	**0**	**0,0175**	**0**
P15311	EZRI	Ezrin	61	1,028	0,7296	0,955	0,7296	**0,1905**	**0,0004**	**0,1888**	**0,0004**	**0,157**	**0,0003**	**0,1528**	**0,0002**
P26038	MOES	Moesin	52	1,4454	0,0175	0,6792	0,0175	**0,3162**	**0,0965**	**0,2109**	**0,0092**	**0,1995**	**0,0829**	**0,1355**	**0,0108**
P07355	ANXA2	Annexin A2	49	0,4446	0,045	2,208	0,045	**0,0172**	**0**	**0,0256**	**0,3955**	**0,0146**	**0**	**0,0223**	**0,2509**
P07237	PDIA1	Protein disulfide-isomerase	34	1	0,7675	0,9817	0,7675	**0,4966**	**0,084**	**0,4966**	**0,0609**	**0,2228**	**0,0055**	**0,2228**	**0,0024**
P04181	OAT	Ornithine aminotransferase, mitochondrial	34	0,6138	0,0362	1,5996	0,0362	**0,0157**	**0,0027**	**0,0198**	**0,005**	**0,0189**	**0**	**0,0227**	**0,0001**
P27797	CALR	Calreticulin	29	0,912	0,5922	1,0765	0,5922	**0,4831**	**0**	**0,5248**	**0,0001**	**0,4613**	**0**	**0,5012**	**0**
Q06830	PRDX1	Peroxiredoxin-1	28	1,3552	0,0036	0,7244	0,0036	**0,3311**	**0**	**0,2399**	**0**	**0,3565**	**0**	**0,2582**	**0**
P04083	ANXA1	Annexin A1	25	1,1376	0,3795	0,863	0,3795	**0,0137**	**0**	**0,0126**	**0**	**0,011**	**0**	**0,0108**	**0**
P30101	PDIA3	Protein disulfide-isomerase A3	24	1,1482	0,6458	0,8551	0,6458	**0,492**	**0,0871**	**0,4487**	**0,08**	**0,3162**	**0,0402**	**0,2754**	**0,0334**
P23284	PPIB	Peptidyl-prolyl cis-trans isomerase B	24	0,673	0,1964	1,4588	0,1964	**0,2965**	**0,0039**	**0,4285**	**0,0078**	**0,3251**	**0,0054**	**0,4699**	**0,0122**
P23528	COF1	Cofilin-1	23	0,8395	0,3168	1,1695	0,3168	**0,3162**	**0**	**0,3698**	**0,0002**	**0,4875**	**0,0004**	**0,5702**	**0,0034**
P24534	EF1B	Elongation factor 1-beta	20	1,0864	0,6653	0,9036	0,6653	**0,4831**	**0,0172**	**0,4365**	**0,0092**	**0,4699**	**0,0127**	**0,4285**	**0,0069**
P17931	LEG3	Galectin-3	20	1,406	0,3584	0,6982	0,3584	**0,0171**	**0,0111**	**0,0153**	**0,0088**	**0,0198**	**0,0112**	**0,0167**	**0,0088**
P67936	TPM4	Tropomyosin alpha-4 chain	18	1,9409	0,2368	0,5058	0,2368	**0,2188**	**0,0017**	**0,1169**	**0,0009**	**0,1585**	**0,0008**	**0,0794**	**0,0005**
P37802	TAGL2	Transgelin-2	16	1,1803	0,347	0,8318	0,347	**0,4365**	**0,003**	**0,3664**	**0,0008**	**0,1202**	**0,0001**	**0,1019**	**0**
P09622	DLDH	Dihydrolipoyl dehydrogenase, mitochondrial	16	1,4997	0,0354	0,6546	0,0354	**0,1459**	**0,0498**	**0,1191**	**0,0132**	**0,7943**	**0,364**	**0,4966**	**0,0405**
O43852	CALU	Calumenin	16	0,7943	0,2466	1,2359	0,2466	**0,0912**	**0**	**0,1127**	**0**	**0,1644**	**0**	**0,2032**	**0**

P02545	LMNA	Prelamin-A/C	16	0,6026	0,0033	1,6293	0,0033	**0,0417**	**0,0015**	**0,0679**	**0,0084**	**0,0441**	**0**	**0,0692**	**0,0001**
P62158	CALM	Calmodulin	15	1,1066	0,5876	0,8872	0,5876	**0,166**	**0,0032**	**0,1486**	**0,0019**	**0,3802**	**0,0099**	**0,3404**	**0,0055**
P31040	DHSA	Succinate dehydrogenase [ubiquinone] flavoprotein subunit, mitochondrial	14	1,1803	0,8785	0,8318	0,8785	**0,3981**	**0,0249**	**0,3373**	**0,0113**	**0,4018**	**0,0794**	**0,3373**	**0,0502**
P52565	GDIR1	Rho GDP-dissociation inhibitor 1	14	1,2589	0,1936	0,7798	0,1936	**0,2938**	**0,0331**	**0,227**	**0,0226**	**0,4325**	**0,0867**	**0,3373**	**0,0438**
O43707	ACTN4	Alpha-actinin-4	14	0,8472	0,2672	1,1588	0,2672	**0,166**	**0**	**0,1959**	**0**	**0,1306**	**0**	**0,1528**	**0**
P60900	PSA6	Proteasome subunit alpha type-6	13	1,2706	0,2247	0,7727	0,2247	**0,597**	**0,0304**	**0,4699**	**0,0038**	**0,7244**	**0,1501**	**0,5598**	**0,0238**
P06576	ATPB	ATP synthase subunit beta, mitochondrial	13	0,3767	0,0008	2,6062	0,0008	**0,0437**	**0**	**0,0863**	**0,0003**	**0,0391**	**0**	**0,0855**	**0,0025**
P25786	PSA1	Proteasome subunit alpha type-1	12	1,5417	0,0216	0,6368	0,0216	**0,6792**	**0,1428**	**0,4325**	**0,0021**	**0,6546**	**0,1053**	**0,4207**	**0,0016**
O14818	PSA7	Proteasome subunit alpha type-7	12	1,7219	0,0297	0,5702	0,0297	**0,6546**	**0,232**	**0,3873**	**0,0029**	**0,7311**	**0,422**	**0,4285**	**0,0057**
Q15019	SEPT2	Septin-2	12	1,3552	0,2541	0,7244	0,2541	**0,4285**	**0,0692**	**0,3221**	**0,0104**	**0,5754**	**0,2087**	**0,4246**	**0,0318**
P25787	PSA2	Proteasome subunit alpha type-2	12	1,5704	0,1021	0,6252	0,1021	**0,2089**	**0,0082**	**0,1306**	**0,0007**	**0,4285**	**0,0254**	**0,2704**	**0,0018**
P60903	S10AA	Protein S100-A10	12	0,8017	0,4375	1,2246	0,4375	**0,0211**	**0,0004**	**0,0233**	**0,0011**	**0,0209**	**0,0002**	**0,0233**	**0,0003**
P49748	ACADV	Very long-chain specific acyl-CoA dehydrogenase, mitochondrial	11	0,8395	0,3655	1,1695	0,3655	**0,0955**	**0,0015**	**0,1148**	**0,0026**	**0,0429**	**0,0007**	**0,0501**	**0,0038**
O14745	NHRF1	Na(+)/H(+) exchange regulatory cofactor NHE-RF1	11	1,7539	0,1032	0,5598	0,1032	**0,0698**	**0,0045**	**0,0425**	**0,0018**	**0,0667**	**0,0037**	**0,0409**	**0,0018**
P31947	1433S	14-3-3 protein sigma	11	0,9462	0,9771	1,0375	0,9771	**0,0219**	**0,0118**	**0,0236**	**0,0119**	**0,0483**	**0,0212**	**0,0506**	**0,0214**

P25788	PSA3	Proteasome subunit alpha type-3	10	1,5996	0,1367	0,6138	0,1367	**0,7516**	**0,5215**	**0,4613**	**0,0534**	**0,7112**	**0,3248**	**0,4285**	**0,0316**
P28838	AMPL	Cytosol aminopeptidase	10	1,028	0,836	0,955	0,836	**0,3373**	**0,1353**	**0,3342**	**0,0466**	**0,2704**	**0,1551**	**0,263**	**0,0489**
P00367	DHE3	Glutamate dehydrogenase 1, mitochondrial	10	0,6982	0,1352	1,406	0,1352	**0,1406**	**0**	**0,1923**	**0,0001**	**0,2606**	**0,0002**	**0,3664**	**0,0012**
Q96AY3	FKB10	Peptidyl-prolyl cis-trans isomerase FKBP10	10	0,7178	0,145	1,3677	0,145	**0,1096**	**0**	**0,1514**	**0,0023**	**0,0592**	**0**	**0,0745**	**0**
P49721	PSB2	Proteasome subunit beta type-2	9	1,9231	0,1127	0,5105	0,1127	**0,7943**	**0,6719**	**0,4246**	**0,0619**	**0,7112**	**0,4266**	**0,3802**	**0,0462**
P61586	RHOA	Transforming protein RhoA	9	1,1272	0,7006	0,871	0,7006	**0,4786**	**0,0379**	**0,4207**	**0,0237**	**0,3837**	**0,0205**	**0,3404**	**0,0133**
Q15102	PA1B3	Platelet-activating factor acetylhydrolase IB subunit gamma	9	1,0965	0,7391	0,8954	0,7391	**0,2559**	**0,0087**	**0,2291**	**0,0181**	**0,3192**	**0,0514**	**0,2965**	**0,0108**
Q02818	NUCB1	Nucleobindin-1	9	0,8872	0,5699	1,1066	0,5699	**0,0964**	**0**	**0,1076**	**0**	**0,0929**	**0**	**0,1038**	**0**
P25789	PSA4	Proteasome subunit alpha type-4	8	1,4859	0,1943	0,6607	0,1943	**0,5495**	**0,0647**	**0,3698**	**0,0119**	**0,6138**	**0,0944**	**0,4093**	**0,0162**
P28066	PSA5	Proteasome subunit alpha type-5	7	2,5586	0,3113	0,3837	0,3113	**0,5702**	**0,5811**	**0,2109**	**0,0062**	**0,3499**	**0,5073**	**0,1169**	**0,0054**
P04040	CATA	Catalase	7	1,5136	0,2254	0,6486	0,2254	**0,3767**	**0,0342**	**0,2535**	**0,0136**	**0,3467**	**0,029**	**0,2312**	**0,012**
Q9UBS4	DJB11	DnaJ homolog subfamily B member 11	7	0,7586	0,2349	1,2942	0,2349	**0,3133**	**0,0049**	**0,3981**	**0,0235**	**0,1837**	**0,001**	**0,2355**	**0,0036**
Q14914	PTGR1	Prostaglandin reductase 1	7	0,8954	0,9802	1,0965	0,9802	**0,0122**	**0,0443**	**0,0137**	**0,0443**	**0,0105**	**0,0576**	**0,0106**	**0,0575**
P54687	BCAT1	Branched-chain-amino-acid aminotransferase, cytosolic	6	0,7047	0,5185	1,3932	0,5185	**0,078**	**0,1201**	**0,1057**	**0,1457**	**0,0305**	**0,0453**	**0,036**	**0,0486**
Q9NYL9	TMOD3	Tropomodulin-3	5	0,6486	0,2536	1,5136	0,2536	**0,3532**	**0,0792**	**0,5445**	**0,3288**	**0,2014**	**0,0187**	**0,3048**	**0,0475**
P08670	VIME	Vimentin	5	2,4889	0,0174	0,3945	0,0174	**0,2377**	**0,0325**	**0,0973**	**0,0021**	**0,1871**	**0,0147**	**0,0824**	**0,0013**

O00151	PDLI1	PDZ and LIM domain protein 1	5	0,7656	0,3493	1,2823	0,3493	**0,0839**	**0,003**	**0,1107**	**0,0059**	**0,1629**	**0,004**	**0,2109**	**0,0081**
P40121	CAPG	Macrophage-capping protein	5	1,406	0,324	0,6982	0,324	**0,0661**	**0,0182**	**0,0515**	**0,0132**	**0,037**	**0,0071**	**0,0302**	**0,0058**
Q13510	ASAH1	Acid ceramidase	5	1,2246	0,3877	0,8017	0,3877	**0,0387**	**0,0027**	**0,0331**	**0,0021**	**0,0331**	**0,0661**	**0,027**	**0,0561**
Q06323	PSME1	Proteasome activator complex subunit 1	4	1,0375	0,913	0,9462	0,913	**0,5445**	**0,1324**	**0,4831**	**0,2919**	**0,3251**	**0,046**	**0,278**	**0,1034**
Q96C19	EFHD2	EF-hand domain-containing protein D2	4	1,0186	0,9262	0,9638	0,9262	**0,2421**	**0,0224**	**0,2333**	**0,0211**	**0,2559**	**0,0223**	**0,2489**	**0,0209**
Q6NZI2	PTRF	Polymerase I and transcript release factor	4	0,3837	0,0424	2,5586	0,0424	**0,1343**	**0,0067**	**0,3311**	**0,169**	**0,1393**	**0,003**	**0,3532**	**0,0672**
Q02218	ODO1	2-oxoglutarate dehydrogenase, mitochondrial	4	0,8166	0,4611	1,2023	0,4611	**0,0545**	**0,0032**	**0,0637**	**0,0043**	**0,0608**	**0,0033**	**0,0718**	**0,0045**
P27824	CALX	Calnexin	3	0,9376	0,7509	1,0471	0,7509	**0,4285**	**0,1292**	**0,4529**	**0,1655**	**0,1**	**0,0437**	**0,1038**	**0,051**
P11234	RALB	Ras-related protein Ral-B	3	0,9817	0,7793	1	0,7793	**0,3945**	**0,031**	**0,3981**	**0,0347**	**0,3532**	**0,0261**	**0,3565**	**0,0289**
P62072	TIM10	Mitochondrial import inner membrane translocase subunit Tim10	3	0,8872	0,6818	1,1066	0,6818	**0,3221**	**0,0249**	**0,3597**	**0,0291**	**0,4018**	**0,0452**	**0,4529**	**0,0554**
Q9BPX5	ARP5L	Actin-related protein 2/3 complex subunit 5-like protein	3	1,2359	0,528	0,7943	0,528	**0,3076**	**0,062**	**0,2466**	**0,0445**	**0,2208**	**0,0341**	**0,1803**	**0,0264**
Q15046	SYK	Lysyl-tRNA synthetase	3	1,0666	0,6419	0,9204	0,6419	**0,1977**	**0,0144**	**0,1837**	**0,011**	**0,1977**	**0,0158**	**0,1871**	**0,012**
Q14847	LASP1	LIM and SH3 domain protein 1	3	1,2359	0,4804	0,7943	0,4804	**0,1644**	**0,0412**	**0,1306**	**0,0301**	**0,0887**	**0,0372**	**0,0711**	**0,0275**
P00167	CYB5	Cytochrome b5	3	0,9908	0,9432	0,9908	0,9432	**0,0863**	**0,0276**	**0,0847**	**0,0283**	**0,0787**	**0,026**	**0,078**	**0,0266**
P52943	CRIP2	Cysteine-rich protein 2	1	1,0666	0,9726	0,9204	0,9726	**0,0586**	**0,0595**	**0,0555**	**0,0592**	**0,0461**	**0,0368**	**0,0437**	**0,0367**

*114 and 115 indicate MDCK labeled replicates. 116 indicates Hakai-transforming clone 4. 117 indicates Hakai-transforming clone 11. Hakai-transforming clones-related values are indicated in bold font.

Table A2. List of total identified Hakai-down-regulated proteins with score ≥2.

Accesion number	Protein symbol	Protein name	Peptides (95%)	114:115	PVal 114:115	115:114	PVal 115:114	116:115	PVal 116:115	116:114	PVal 116:114	117:115	PVal 117:115	117:114	PVal 117:114
P08107	HSP71	Heat shock 70 kDa protein 1A/1B	111	2,0893	0,7688	0,4325	0,7688	**32,8095**	**0,0003**	**20,893**	**0,0012**	**39,8107**	**0,0002**	**27,0396**	**0,0008**
P06733	ENOA	Alpha-enolase	96	5,5976	0,0031	0,1871	0,0031	**27,0396**	**0,0005**	**7,5162**	**0**	**32,5087**	**0,0003**	**10**	**0**
P19338	NUCL	Nucleolin	63	0,2399	0,0286	4,0926	0,0286	**2,9648**	**0,8082**	**9,1201**	**0,1408**	**10,4713**	**0**	**26,3027**	**0**
P31948	STIP1	Stress-induced-phosphoprotein 1	54	1,7378	0,0668	0,5649	0,0668	**5,445**	**0**	**3,1623**	**0**	**4,7863**	**0**	**2,8576**	**0**
P09651	ROA1	Heterogeneous nuclear ribonucleoprotein A1	50	0,52	0,0272	1,888	0,0272	**1,2246**	**0,2**	**2,3335**	**0,004**	**1,4588**	**0,0383**	**2,8054**	**0,0011**
P62937	PPIA	Peptidyl-prolyl cis-trans isomerase A	48	0,3698	0,5842	2,6546	0,5842	**2,0701**	**0,0696**	**4,5709**	**0,0292**	**2,2699**	**0,0877**	**5,2481**	**0,035**
P60174	TPIS	Triosephosphate isomerase	46	3,1333	0,0948	0,3133	0,0948	**5,3951**	**0,0024**	**1,8535**	**0,0496**	**8,6298**	**0**	**3,0479**	**0,0005**
P12277	KCRB	Creatine kinase B-type	40	1,9409	0,6134	0,4875	0,6134	**36,3078**	**0,0004**	**22,4905**	**0,0009**	**37,325**	**0,0004**	**23,9883**	**0,0009**
Q8NC51	PAIRB	Plasminogen activator inhibitor 1 RNA-binding protein	35	0,4656	0,4066	2,1086	0,4066	**3,767**	**0**	**7,3114**	**0**	**4,5709**	**0**	**8,5507**	**0**
P00558	PGK1	Phosphoglycerate kinase 1	33	1,5136	0,2926	0,631	0,2926	**16,293**	**0,0022**	**13,9316**	**0**	**14,4544**	**0,0043**	**12,2462**	**0**
P22392	NDKB	Nucleoside diphosphate kinase B	30	2,5119	0,2355	0,2805	0,2355	**24,2103**	**0,0643**	**17,2187**	**0**	**30,1995**	**0,0535**	**22,2843**	**0**
P05455	LA	Lupus La protein	26	0,7516	0,385	1,3062	0,385	**6,792**	**0**	**9,0365**	**0**	**6,1376**	**0**	**8,091**	**0**
Q07021	C1QBP	Complement component 1 Q subcomponent-	25	0,4699	0,0545	2,0701	0,0545	**20,5116**	**0,0025**	**33,4195**	**0,0152**	**22,6987**	**0,0012**	**36,3078**	**0,0153**

		binding protein, mitochondrial												
P15531	NDKA	Nucleoside diphosphate kinase A	24	1,0568	0,6166	0,879	0,6166	**9,6383**	**0,0136**	**11,1686**	**0,0026**	**9,3756**	**0,0024**	**10,5682**	**0,0009**
P23246	SFPQ	Splicing factor, proline- and glutamine-rich	23	0,871	0,9104	1,1272	0,9104	**2,5823**	**0,0391**	**2,704**	**0,0095**	**4,7863**	**0**	**4,9204**	**0**
P12268	IMDH2	Inosine-5'-monophosphate dehydrogenase 2	21	0,4487	0,0017	2,1878	0,0017	**1,556**	**0,0368**	**3,4041**	**0,0007**	**2,1281**	**0,0001**	**4,6132**	**0**
Q15233	NONO	Non-POU domain-containing octamer-binding protein	17	1,1376	0,8517	0,863	0,8517	**2,421**	**0,0086**	**2,1878**	**0,0374**	**3,5645**	**0**	**3,2509**	**0,0001**
P16949	STMN1	Stathmin	16	1,4859	0,0803	0,6607	0,0803	**2,8576**	**0,0017**	**1,977**	**0,0147**	**3,4995**	**0,0001**	**2,421**	**0,0014**
P00505	AATM	Aspartate aminotransferase, mitochondrial	16	0,3162	0,1557	3,0761	0,1557	**2,2491**	**0,002**	**6,792**	**0,0017**	**2,5823**	**0,0005**	**7,7983**	**0,0001**
P26583	HMGB2	High mobility group protein B2	16	0,9817	0,6884	1	0,6884	**1,5276**	**0,2953**	**1,5136**	**0,1719**	**2,4889**	**0,0209**	**2,4889**	**0,0133**
Q99497	PARK7	Protein DJ-1	14	1,2359	0,9739	0,7943	0,9739	**6,6681**	**0,006**	**5,7016**	**0,0037**	**7,3114**	**0,0075**	**6,1376**	**0,0064**
Q15181	IPYR	Inorganic pyrophosphatase	14	1,0471	0,6801	0,9376	0,6801	**4,4875**	**0**	**3,9811**	**0,0002**	**4,2855**	**0**	**3,8726**	**0**
P31689	DNJA1	DnaJ homolog subfamily A member 1	14	0,3105	0,0005	2,8576	0,0005	**1,6596**	**0,0042**	**4,5709**	**0**	**1,4588**	**0,0153**	**4,0551**	**0**
P07195	LDHB	L-lactate dehydrogenase B chain	13	1,9231	0,2574	0,5058	0,2574	**6,9183**	**0**	**3,4995**	**0,005**	**6,1944**	**0,0001**	**2,9648**	**0,0355**
Q04837	SSBP	Single-stranded DNA-binding protein, mitochondrial	13	1,1482	0,5931	0,8551	0,5931	**4,1687**	**0,0004**	**3,6983**	**0,0247**	**5,2481**	**0,0001**	**4,6559**	**0,0015**
P43487	RANG	Ran-specific GTPase-	13	1,4588	0,79	0,673	0,79	**3,6644**	**0,087**	**2,5119**	**0,1199**	**5,9156**	**0,021**	**4,0926**	**0,0271**

		activating protein													
P30050	RL12	60S ribosomal protein L12	13	0,5445	0,1829	1,7865	0,1829	**2,1086**	**0,0064**	**3,4356**	**0,0003**	**2,8054**	**0,0008**	**4,7863**	**0,0001**
P14174	MIF	Macrophage migration inhibitory factor	12	2,1281	0,0524	0,3664	0,0524	**29,6483**	**0,0214**	**20,7014**	**0,1066**	**39,4457**	**0,0205**	**29,1072**	**0,0883**
P09211	GSTP1	Glutathione S-transferase P	12	1,4454	0,6035	0,6792	0,6035	**14,8594**	**0,1793**	**11,9124**	**0,0289**	**29,9226**	**0,1501**	**24,6604**	**0,0044**
Q9Y383	LC7L2	Putative RNA-binding protein Luc7-like 2	12	0,7586	0,5106	1,2589	0,5106	**4,8306**	**0,0002**	**5,7016**	**0,0001**	**3,9446**	**0,001**	**4,529**	**0,0002**
O75937	DNJC8	DnaJ homolog subfamily C member 8	12	0,7178	0,2328	1,3677	0,2328	**2,2909**	**0,0259**	**3,1046**	**0,0007**	**2,7797**	**0,0027**	**3,8019**	**0,0003**
P55209	NP1L1	Nucleosome assembly protein 1-like 1	12	0,8551	0,4642	1,1482	0,4642	**2,1878**	**0,0461**	**2,5351**	**0,0186**	**1,8197**	**0,1034**	**2,0701**	**0,0389**
Q13162	PRDX4	Peroxiredoxin-4	11	0,5152	0,5016	1,9055	0,5016	**5,1051**	**0,0004**	**8,8716**	**0,0002**	**3,281**	**0,0032**	**5,8076**	**0,0026**
Q12906	ILF3	Interleukin enhancer-binding factor 3	11	0,955	0,5995	1,028	0,5995	**2,466**	**0,0711**	**2,4889**	**0,0195**	**2,8054**	**0,0245**	**2,8054**	**0,0059**
P07741	APT	Adenine phosphoribosyl transferase	10	0,8017	0,3023	1,3062	0,3023	**17,378**	**0,0002**	**15,5597**	**0,115**	**18,5353**	**0,0002**	**16,7494**	**0,1086**
O75347	TBCA	Tubulin-specific chaperone A	10	2,1478	0,303	0,4571	0,303	**15,7036**	**0,3179**	**6,9183**	**0,6914**	**23,3346**	**0,1313**	**11,1686**	**0,0049**
P16152	CBR1	Carbonyl reductase [NADPH] 1	10	0,631	0,2427	1,4723	0,2427	**8,0168**	**0,0003**	**9,7275**	**0,0001**	**10,3753**	**0,0001**	**12,5892**	**0,0001**
P12532	KCRU	Creatine kinase U-type, mitochondrial	9	1,7539	0,4185	0,5598	0,4185	**4,7424**	**0,031**	**2,7797**	**0,0116**	**4,0551**	**0,0889**	**2,3768**	**0,0697**
Q04760	LGUL	Lactoylglutathione lyase	8	2,4889	0,3008	0,2168	0,3008	**25,5859**	**0,1177**	**23,7684**	**0**	**24,6604**	**0,1229**	**22,6987**	**0**
P00441	SODC	Superoxide dismutase [Cu-Zn]	8	1,5849	0,404	0,6194	0,404	**13,9316**	**0,0001**	**8,6298**	**0,0042**	**27,5423**	**0**	**18,7068**	**0,0002**
P60891	PRPS1	Ribose-phosphate	8	0,4656	0,3014	2,0137	0,3014	**3,4356**	**0,0321**	**6,6681**	**0,0012**	**3,767**	**0,0066**	**7,2444**	**0,0008**

		pyrophosphokinase 1													
P33316	DUT	Deoxyuridine 5'-triphosphate nucleotidohydrolase, mitochondrial	8	1,0375	0,7491	0,955	0,7491	**2,6062**	**0,0106**	**2,5823**	**0,103**	**3,3113**	**0,0036**	**3,1915**	**0,0087**
P61758	PFD3	Prefoldin subunit 3	8	1,0666	0,5802	0,9204	0,5802	**2,1281**	**0,0173**	**2,0512**	**0,0382**	**2,1878**	**0,0091**	**2,0324**	**0,0167**
P37108	SRP14	Signal recognition particle 14 kDa protein	7	1,7865	0,5948	0,4742	0,5948	**12,1339**	**0,0006**	**8,1658**	**0,0009**	**15,1356**	**0,0003**	**10,3753**	**0,0004**
Q9BTT0	AN32E	Acidic leucine-rich nuclear phosphoprotein 32 family member E	7	1,2706	0,7491	0,7727	0,7491	**6,3096**	**0,0512**	**4,6989**	**0,0439**	**3,5645**	**0,1097**	**2,6303**	**0,0886**
Q9NX58	LYAR	Cell growth-regulating nucleolar protein	7	1,8197	0,5559	0,5346	0,5559	**6,2517**	**0,2452**	**2,3335**	**0,3017**	**12,942**	**0,1797**	**6,0813**	**0,0442**
Q16881	TRXR1	Thioredoxin reductase 1, cytoplasmic	7	2,6546	0,1414	0,3698	0,1414	**4,6132**	**0,074**	**1,556**	**0,6355**	**7,4473**	**0,0103**	**2,355**	**0,3222**
P49321	NASP	Nuclear autoantigenic sperm protein	7	2,5823	0,0681	0,3532	0,0681	**3,5318**	**0,0023**	**1,5276**	**0,2921**	**4,4875**	**0,0012**	**1,9055**	**0,0377**
O00273	DFFA	DNA fragmentation factor subunit alpha	7	0,4571	0,3833	2,1281	0,3833	**2,9648**	**0,0489**	**5,4954**	**0,0052**	**2,3988**	**0,136**	**4,4463**	**0,0097**
P15170	ERF3A	Eukaryotic peptide chain release factor GTP-binding subunit ERF3A	7	0,5248	0,0436	1,8197	0,0436	**2,3121**	**0,0028**	**3,9446**	**0,0001**	**1,803**	**0,015**	**3,0761**	**0,0003**
P53999	TCP4	Activated RNA polymerase II transcriptional coactivator p15	6	1	0,6177	1,4322	0,6177	**28,0543**	**0,0001**	**23,7684**	**0,0001**	**31,6228**	**0**	**25,8226**	**0**
Q9NQP4	PFD4	Prefoldin subunit 4	6	0,4018	0,6562	2,5351	0,6562	**9,2045**	**0,0394**	**18,8799**	**0,0326**	**7,3114**	**0,0405**	**15,2757**	**0,0334**

Q9H773	DCTP1	dCTP pyrophosphatase 1	6	0,4699	0,2406	2,1878	0,2406	**8,0168**	**0,0034**	**14,3219**	**0,0014**	**10,7647**	**0,0011**	**18,3654**	**0,0004**
P07108	ACBP	Acyl-CoA-binding protein	6	1,4322	0,4406	0,631	0,4406	**7,3114**	**0,007**	**6,0256**	**0,0105**	**8,1658**	**0,0057**	**6,7298**	**0,0083**
Q9UKK9	NUDT5	ADP-sugar pyrophosphatase	6	0,2466	0,307	3,9811	0,307	**6,3096**	**0,0996**	**18,3654**	**0,0127**	**4,8753**	**0,1946**	**14,7231**	**0,0351**
P49773	HINT1	Histidine triad nucleotide-binding protein 1	6	0,2168	0,0032	4,3251	0,0032	**4,0179**	**0,0164**	**11,8032**	**0,0016**	**5,445**	**0,0159**	**15,9956**	**0,0015**
P09661	RU2A	U2 small nuclear ribonucleoprotein A'	6	0,6486	0,751	1,5136	0,751	**1,4859**	**0,2356**	**2,0137**	**0,1215**	**2,2491**	**0,0474**	**2,9376**	**0,0317**
P78417	GSTO1	Glutathione S-transferase omega-1	5	1,5849	0,131	0,6081	0,131	**6,1376**	**0,154**	**3,9811**	**0,3597**	**6,5464**	**0,0382**	**4,2855**	**0,1611**
P68036	UB2L3	Ubiquitin-conjugating enzyme E2 L3	5	0,871	0,6677	1,1272	0,6677	**3,6983**	**0,0139**	**4,0551**	**0,0097**	**2,7797**	**0,065**	**3,1046**	**0,0404**
P30405	PPIF	Peptidyl-prolyl cis-trans isomerase F, mitochondrial	5	1,1066	0,8151	0,8872	0,8151	**3,1623**	**0,0455**	**2,8576**	**0,0509**	**2,6546**	**0,0596**	**2,3988**	**0,0678**
P49915	GUAA	GMP synthase [glutamine-hydrolyzing]	5	0,0904	0,0121	7,656	0,0121	**2,6062**	**0,0067**	**18,0302**	**0,0005**	**2,1677**	**0,0158**	**15,7036**	**0,0007**
P48637	GSHB	Glutathione synthetase	4	1,2823	0,9823	0,7656	0,9823	**14,3219**	**0,004**	**11,3763**	**0,0041**	**16,1436**	**0,0033**	**10,9648**	**0,0033**
P20839	IMDH1	Inosine-5'-monophosphate dehydrogenase 1	4	0,0417	0,0007	21,8776	0,0007	**2,9107**	**0,0509**	**40,9261**	**0,0006**	**2,5119**	**0,0653**	**36,6438**	**0,0006**
P53041	PPP5	Serine/threonine-protein phosphatase 5	4	0,3221	0,2276	2,5119	0,2276	**2,2284**	**0,1456**	**5,3951**	**0,0404**	**2,729**	**0,0797**	**6,4863**	**0,0259**
P15121	ALDR	Aldose reductase	4	0,7447	0,4725	1,3183	0,4725	**1,7701**	**0,4649**	**2,4889**	**0,4034**	**2,7797**	**0,0419**	**3,6308**	**0,024**
P12955	PEPD	Xaa-Pro dipeptidase	3	2,7542	0,045	3,5975	0,045	**19,0546**	**0,0006**	**13,0617**	**0,0005**	**18,3654**	**0,0005**	**17,2187**	**0,0005**

Q13428	TCOF	Treacle protein	3	3,5975	0,0685	0,2188	0,0685	**14,3219**	**0,0247**	**6,9823**	**0,1311**	**18,5353**	**0,024**	**9,3756**	**0,1151**
Q13126	MTAP	S-methyl-5'-thioadenosine phosphorylase	3	3,4041	0,1393	0,3048	0,1393	**13,5519**	**0,024**	**4,1687**	**0,0585**	**9,2045**	**0,0447**	**2,3768**	**0,1615**
Q9H2W6	RM46	39S ribosomal protein L46, mitochondrial	3	1,3677	0,8285	0,7311	0,8285	**8,5507**	**0,0492**	**8,2414**	**0,0548**	**9,9083**	**0,0374**	**9,0365**	**0,0411**
P17174	AATC	Aspartate aminotransferase, cytoplasmic	3	1,8707	0,3783	0,3945	0,3783	**7,8705**	**0,0284**	**5,4954**	**0,0426**	**10,3753**	**0,0226**	**6,9823**	**0,0325**
P30044	PRDX5	Peroxiredoxin-5, mitochondrial	3	1,0666	0,8156	0,9204	0,8156	**5,5976**	**0,0279**	**5,0119**	**0,0305**	**5,445**	**0,0282**	**5,2966**	**0,0308**
P50914	RL14	60S ribosomal protein L14	3	0,2421	0,1024	3,9446	0,1024	**2,355**	**0,1946**	**9,2045**	**0,0407**	**1,5417**	**0,569**	**6,1944**	**0,0708**
O43598	RCL	Far upstream element-binding protein 2	2	7,3114	0,0627	0,057	0,0627	**38,3707**	**0,0224**	**14,8594**	**0,0977**	**27,0396**	**0,0236**	**8,9536**	**0,1243**
O76021	RL1D1	Ribosomal L1 domain-containing protein 1	2	2,6792	0,0076	0,3281	0,0076	**18,197**	**0,001**	**8,091**	**0,0135**	**18,5353**	**0,001**	**7,5858**	**0,0141**
Q9H910	HN1L	Hematological and neurological expressed 1-like protein	2	3,5975	0,058	0,2729	0,058	**16,9044**	**0,0249**	**4,8306**	**0,2128**	**18,5353**	**0,0267**	**4,2462**	**0,4564**
Q969H8	CS010	UPF0556 protein C19orf10	2	3,5318	0,0891	0,2938	0,0891	**12,5892**	**0,0286**	**4,2855**	**0,1166**	**16,1436**	**0,0296**	**4,2855**	**0,1249**
Q9UNE7	CHIP	E3 ubiquitin-protein ligase CHIP	2	3,8019	0,2415	0,2228	0,2415	**10,9648**	**0,0472**	**3,6983**	**0,1079**	**6,6681**	**0,0861**	**2,3988**	**0,2641**
O14744	ANM5	Protein arginine N-methyltransferase 5	2	1,0965	0,7137	0,8954	0,7137	**4,2462**	**0,0283**	**3,8371**	**0,0219**	**4,4875**	**0,0269**	**3,9446**	**0,0209**
Q9H3K6	BOLA2	BolA-like protein 2	2	0,7586	0,5973	1,2706	0,5973	**3,4041**	**0,0626**	**4,1687**	**0,0474**	**3,6644**	**0,0551**	**4,4463**	**0,0423**
Q9Y3B9	RRP15	RRP15-like protein	2	1,5704	0,5244	0,5598	0,5244	**2,9648**	**0,1034**	**2,0137**	**0,1707**	**7,1121**	**0,0305**	**5,0582**	**0,0403**

Q9UHD1	CHRD1	Cysteine and histidine-rich domain-containing protein 1	2	0,5445	0,2003	1,7539	0,2003	**2,208**	**0,0735**	**3,767**	**0,0226**	**2,0893**	**0,0903**	**3,5645**	**0,0262**
Q9NW13	RBM28	RNA-binding protein 28	2	0,8091	0,7241	1,2134	0,7241	**2,0512**	**0,2147**	**2,421**	**0,1588**	**4,2855**	**0,0569**	**5,0119**	**0,0476**
Q12765	SCRN1	Secernin-1	1	6,5464	0,0962	0,1355	0,0962	**14,8594**	**0,028**	**3,02**	**0,142**	**13,9316**	**0,0282**	**2,8054**	**0,1482**

*114 and 115 indicate MDCK labeled replicates. 116 indicates Hakai-transforming clone 4. 117 indicates Hakai-transforming clone 11. Hakai-transforming clones-related values are indicated in bold font.

APPENDIX B

Summary of the thesis in Spanish: required summary of a minimum of 3000 words for thesis that have been written in English.

El carcinoma surge en las células epiteliales y es el tipo de cáncer más común que existe. Durante la progresión tumoral las células activan un programa denominado proceso de transición epitelio-mesénquima (EMT), mediante el cual sufren un cambio fenotípico y adquieren características tales como la alteración de los contactos célula-célula y de unión al sustrato, y adquieren capacidades de invasión y migración que facilitan el avance del proceso tumoral. El proceso de transición epitelio-mesénquima se caracteriza por la pérdida de características epiteliales de las células y adquisición de características mesenquimales. Uno de los sellos más importantes del proceso de EMT es la pérdida de E-cadherina presente en las uniones adherentes, la cual es considerada un supresor tumoral y cuya pérdida supone un marcador de mal pronóstico. Este proceso de transición epitelio-mesénquima también se caracteriza por la pérdida de otros marcadores epiteliales como las citoqueratinas y el aumento de marcadores mesenquimales como la N-cadherina o la Vimentina (Chaffer and Weinberg, 2011; Nieto *et al*., 2016).

Dada la importancia de la E-cadherina durante la plasticidad epitelial, los mecanismos mediante los cuales esta proteína es regulada durante la progresión tumoral fueron ampliamente estudiados. El primer regulador post-traduccional conocido para la E-cadherina fue la E3 ubiquitin-ligasa Hakai, y fue descrito por Fujita y colaboradores en 2002. Hakai media la ubiquitinización de la E-cadherina cuando ésta se encuentra fosforilada por Src en su dominio citoplasmático. La E-cadherina fosforilada es reconocida y ubiquitinizada por Hakai, provocando así su consecuente endocitosis y degradación y, por lo tanto, la pérdida de los contactos intercelulares, uno de los fenómenos más característicos del comienzo del proceso de transición epitelio-mesénquima (Fujita *et al*., 2002). Además de la E-cadherina, otros sustratos fosforilados por Src como Cortactina o DOK-1 han sido descritos para Hakai, sin embargo, su significado funcional no ha sido descrito hasta el momento (Figueroa *et al*., 2009).

Por otro lado, la expresión de Hakai ha sido detectada en tejidos donde la E-cadherina no se encuentra presente, por lo que se sugiere que Hakai se encuentra en ellos regulando otras proteínas todavía desconocidas (Figueroa *et al*., 2009). Además, se ha descrito que la sobreexpresión de Hakai no afecta solo a la adhesión y plasticidad celular, sino también al potencial oncogénico y a la invasión y migración celular (Figueroa *et al*., 2009; Rodríguez-Rigueiro *et al*., 2011; Castosa *et al*., 2018). Dado que no todos los cambios celulares descritos bajo la actividad de Hakai pueden ser debidos a su actividad sobre la E-cadherina, en esta tesis doctoral nos hemos propuesto identificar nuevas dianas moleculares relacionadas con Hakai

que puedan estar implicadas en la plasticidad celular y la progresión tumoral, y para ello nos hemos propuesto los siguientes objetivos:

1. Realizar un estudio proteómico en un modelo de sobreexpresión de Hakai con el fin de identificar nuevas dianas moleculares asociadas con rutas de señalización implicadas en la progresión tumoral.
    1.1. Optimizar y realizar un estudio comparativo entre líneas MDCK que sobreexpresan Hakai y líneas MDCK sin transformar empleando la técnica iTRAQ.
    1.2. Clasificar las proteínas identificadas en base al proceso biológico en el que están implicadas y su función molecular.
    1.3. Estudiar las distintas redes de interacción existentes entre las proteínas identificadas.
    1.4. Validar la regulación de algunas proteínas de interés seleccionadas de entre las identificadas en el estudio proteómico.
    1.5. Analizar la localización subcelular y la posible co-localización de Hakai con las proteínas identificadas seleccionadas.
2. Estudiar el mecanismo de regulación de Hakai sobre las proteínas de interés identificadas.
    2.1. Analizar el efecto de la sobreexpresión y silenciamiento transitorios de Hakai sobre las proteínas seleccionadas del estudio proteómico.
    2.2. Determinar la posible interacción de Hakai y las proteínas seleccionadas
    2.3. Estudiar el mecanismo de acción de Hakai sobre las proteínas seleccionadas
    2.4. Realizar estudios funcionales para determinar el impacto de la regulación proteica mediada por Hakai.

Tal y como se detalla en los objetivos, el desarrollo de esta tesis doctoral se inició con la realización de un estudio proteómico comparativo entre dos líneas celulares: la línea epitelial de riñón de perro MDCK y dicha línea sobreexpresando Hakai de forma estable (Díaz-Díaz *et al*., 2017). El estudio proteómico se llevó a cabo mediante la técnica proteómica iTRAQ seguida de cromatografía líquida y análisis por espectrometría de masas MALDI-TOF/TOF. El desarrollo de esta parte técnica del estudio proteómico se realizó en colaboración con la plataforma de proteómica del Instituto de Investigación Biomédica de A Coruña (INIBIC). Las proteínas identificadas fueron clasificadas en función de su expresión *up* o *down*-regulada en la línea transformada con Hakai en comparación con la línea control, y se seleccionaron aquellas que se modulaban de forma más significativa en base a criterios estadísticos. Una vez seleccionadas las proteínas más relevantes, éstas fueron clasificadas en base a su función molecular y

proceso biológico en el que se encuentran principalmente implicadas teniendo en cuenta la información obtenida de la bibliografía y las bases de datos Uniprot, Gene Ontology y PANTHER. Los resultados evidenciaron que la mayor parte de las proteínas *up*-reguladas bajo la sobreexpresión de Hakai se encontraban principalmente implicadas en procesos metabólicos o regulación post-transcripcional**,** mientras que aquellas cuya expresión estaba *down*-regulada se encontraban principalmente implicadas en el citoesqueleto y el tráfico de vesículas de membrana.

Además de la clasificación de las proteínas identificadas en base a su función molecular y proceso biológico, se analizó también la interacción entre las proteínas identificadas mediante la base de datos STRING- Esto nos permite determinar posibles rutas metabólicas especialmente activas durante la sobreexpresión de Hakai. Entre las redes de interacciones identificadas, destacó aquella constituida por subunidades del proteasoma identificadas entre las proteínas down-reguladas. La down-regulación del proteasoma ha sido recientemente descrita en células epiteliales durante el proceso de transición epitelio-mesénquima (Banno *et al*., 2016).

Posteriormente, las proteínas identificadas como *up* y *down*-reguladas bajo la sobreexpresión estable de Hakai, fueron sometidas a un proceso de selección basado en su interés e implicación en el desarrollo del cáncer. En base a ello, 10 proteínas fueron seleccionadas finalmente para su validación mediante western blot, entre las cuales se encontraban 5 proteínas down-reguladas (Annexin A1, Annexin A2, Galectin-3, Stratifin y Calumenin) y 3 proteínas up-reguladas (Hsp90, Hsp70 e IMPDH). En todos los casos, los resultados obtenidos mediante western blot validaron aquellos obtenidos en el estudio proteómico.

Una vez validadas las proteínas seleccionadas, se determinó la localización subcelular de las mismas en líneas MDCK y MDCK transformadas con Hakai, así como su posible co-localización con Hakai. Para ello, se realizaron ensayos de co-inmunofluorescencia y se tomaron imágenes mediante microscoscopía confocal, que permitieron determinar la presencia o ausencia de co-localización entre Hakai y las proteínas validadas. Se obtuvieron resultados interesantes para Annexin A1 y Annexin A2, cuya expresión en membrana desapareció por completo en presencia de sobreexpresión de Hakai; Hsp70 y Hsp90, las cuales mostraron un patrón mayoritariamente citoplasmático en la línea parental MDCK y una traslocación a membrana en las células transformadas con Hakai. La localización de Hsp90 y Hsp70 en membrana ha sido

previamente descrita en líneas de cáncer colorrectal (Elmallah *et al*., 2020; Snigireva *et al*., 2016); una co-localización perinuclear entre Hakai y Hsp90 en las células transformadas con Hakai; y finalmente, una destacada co-localización entre Hakai y Galectin-3 en la zona base de las prolongaciones de membrana en las células transformadas con Hakai.

En base al interesante resultado obtenido para la localización de Galectin-3 y Hakai, se realizó una estancia predoctoral en el laboratorio del Dr. Fu-Tong Liu, donde se decidió profundizar en el estudio de la posible implicación de Hakai en la regulación de Galectin-3. Galectin-3 es una proteína de unión a carbohidratos que tiene la habilidad de unirse a lípidos y proteínas glicosiladas presentes en la matriz extracelular y en la superficie de la membrana celular. Concretamente, la Galectina-3 es el único tipo de galectina quimérica existente, lo cual facilita sus importantes funciones durante la progresión tumoral (Liu and Rabinovich, 2015).

Se comenzó con la realización de ensayos de cinética de expresión, en los cuales se evaluaron los niveles de expresión de Galectin-3 en función de la cantidad de Hakai transfectada en las líneas celulares HEK 293T y HeLa. En primera instancia se obtuvieron resultados interesantes que mostraron una clara *down*-regulación de Galectin-3 en función de los niveles de expresión de Hakai que posteriormente no se lograron reproducir. La posible regulación de Galectin-3 fue también evaluada mediante citometría de flujo en la línea celular HEK 293T transfectada de forma estable con Galectin-3 y de forma transitoria con Hakai. En este caso tampoco se detectó una modulación en los niveles de Galectina-3 cuando Hakai se encontraba sobreexpresado. Además, se realizaron ensayos de vida media de Galectin-3 en presencia y ausencia de Hakai que no mostraron resultados concluyentes.

En base a la *down*-regulación experimentada por Galectina-3 en presencia de sobreexpresión de Hakai en los primeros experimentos realizados, se decidió evaluar el mecanismo por el cual se estaba llevando a cabo la degradación de Galectina-3 en presencia de Hakai. Para ello se realizaron ensayos de inhibición de la vía de degradación del proteasoma, lisosoma y autofagia mediante el empleo de los inhibidores MG132, cloroquina y 3-metiladenina, respectivamente. En ninguno de los casos se observó una recuperación de los niveles de Galectin-3 en presencia o ausencia de Hakai en las condiciones experimentales testadas.

Debido a la escasez de resultados positivos obtenidos durante esta estancia, se decidió abandonar esta línea de investigación y se inició una nueva basada en el estudio de la relación de Hakai con otras proteínas identificadas en el estudio proteómico inicial.

Previamente, mediante el estudio proteómico realizado al inicio de esta tesis, se identificaron Annexin A2 y Hsp90 como proteínas reguladas por Hakai. Annexin A2 es una proteína de unión a fosfolípidos de forma dependiente de calcio. Su expresión durante la progresión tumoral es muy controvertida, ya que ha sido descrita en distintos tipos de cáncer como marcador de mal y buen pronóstico (Zhang *et al*., 2012; Yee *et al*., 2007; Rodrigo *et al*., 2011; Pena-Alonso *et al*., 2008). Por otro lado, Hsp90 es una chaperona que ha sido ampliamente relacionada con la progresión tumoral debido a su acción sobre proteínas cliente implicadas en la progresión tumoral (Qing *et al*., 2006). Existen numerosos inhibidores de la actividad chaperona de Hsp90, entre los cuales se incluye la geldanamicina. El tratamiento con inhibidores de Hsp90 induce la degradación de sus proteínas cliente. Este proceso ocurre gracias a la presencia de E3 ubiquitin-ligasas en el complejo chaperona, encargadas de la ubiquitinización e inducción a la degradación vía proteasoma de las proteínas cliente que no han sido correctamente plegadas (Ehrlich *et al*., 2008; Quinatan-Gallardo *et al*., 2019).

Distintos estudios publicados demostraron que Annexin A2 es una proteína fosforilada por Src, convirtiéndola en un posible sustrato de la actividad E3 ubiquitin-ligasa de Hakai. Además, un estudio en aorta de rata ha demostrado la interacción de Annexin A2 y Hsp90, convirtiendo a Annexin A2 en una posible proteína sustrato de esta chaperona (Lei *et al*., 2004). Por otro lado, un estudio del interactoma de Hsp90 reveló que un 37% de las E3 ubiquitin-ligasas testadas se encontraban interaccionando directamente con esta chaperona (Taipale *et al*., 2012). Esto implica la existencia de un gran número de E3 ubiquitin-ligasas, entre las cuales podría encontrarse Hakai, que podrían interaccionar con Hsp90, bien colaborando en el complejo chaperona para la degradación de aquellos sustratos que no han sido correctamente plegados, o bien como proteínas cliente. Actualmente, la interacción de E3 ubiquitin-ligasas como proteínas cliente de Hsp90 sólo se ha descrito para la E3 ubiquitin-ligasa UHRF1 (Ding *et* al., 2016). Este descubrimiento, abre otra posibilidad en relación al papel de Hakai con respecto a Hsp90. En base a estos indicios que apuntan a la existencia de una posible relación entre estas tres proteínas, se decidió profundizar en el estudio de Hakai y su relación con Hsp90 y Annexin A2.

Para comenzar esta línea de investigación, se realizó una prueba piloto consistente en la puesta a punto de un estudio del interactoma de Hakai mediante técnicas proteómicas. Para ello, se llevó a cabo una inmunoprecipitación a gran escala de esta proteína en la línea celular de cáncer de colon HCT116. Una vez puesta a punto la inmunoprecipitación, se analizó la calidad de la inmunoprecipitación mediante una tinción de plata y se procedió a realizar el estudio del interactoma. Para ello, las muestras de la inmunoprecipitación de Hakai con sus respectivos controles fueron analizadas mediante cromatografía líquida seguida de espectrometría de masas TripleTOF en colaboración con la plataforma de proteómica del IDIS (Santiago de Compostela). Los datos fueron analizados con el software ProteinPilot™. Entre las proteínas identificadas se encontraba nuestra proteína Hakai (confirmando así la especificidad de la inmunoprecipitación) y la chaperona Hsp90, previamente validada en el estudio proteómico. En base a este conjunto de resultados, se decidió profundizar en el estudio de esta interacción.

Para determinar la posible relación entre Hakai, Hsp90 y Annexin A2, se realizaron distintos experimentos en los que se estudió la posible regulación de las tres proteínas citadas durante la sobreexpresión transitoria de alguna de ellas. En primer lugar, se estudió el posible efecto de la sobreexpresión de Hakai en líneas HEK 293T sobre los niveles de Hsp90 y viceversa, sin detectar modulación de los niveles de expresión de ambas proteínas en ninguno de los casos. Por otro lado, se evaluó el efecto de la sobreexpresión transitoria de Hakai sobre Annexin A2, confirmando en este caso una *down*-regulación de Annexin A2 cuando sobreexpresamos Hakai junto con ubiquitina y la tirosina kinasa Src. Este efecto de Hakai sobre Annexin A2 fue confirmado mediante el silenciamiento transitorio de Hakai, tras el cual se detectó, como era de esperar, un incremento de los niveles de Annexin A2 en las líneas células HCT116 y 293T y ausencia de efecto sobre los niveles de Hsp90. Estos resultados sugieren que Annexin A2 puede ser una nueva proteína sustrato de Hakai.

Por otro lado, decidimos confirmar los resultados obtenidos en la prueba piloto del interactoma entre Hakai y Hsp90 y determinar la posible interacción entre éstas y Annexin A2. Para ello, se realizó la imunoprecipitación de Hakai y Hsp90 en las líneas celulares HEK 293T, HT29 y ACHN, confirmando en todos los casos la interacción positiva previamente observada en la línea HCT116. Además, se realizaron ensayos de co-inmunoprecipitación para determinar la posible interacción entre las tres proteínas. En este caso, se confirmó la interacción entre Hakai y Hsp90 y Annexin A2, la interacción entre Annexin A2 y Hsp90 y la interacción entre

Hsp90 y Hakai. Estos resultados sugirieren que las tres proteínas se encontraban formando parte del complejo chaperona constituido por Hsp90.

Una vez confirmada la interacción entre las tres proteínas, realizamos los ensayos de interacción en presencia del inhibidor de Hsp90 geldanamicina. Este inhibidor se une de forma competitiva al sitio de unión de ATP de la chaperona impidiendo que ejerza su actividad de plegamiento sobre sus proteínas clientes (Grenert *et al.,*1997). En primer lugar, se demostró que la interacción previamente detectada en la línea celular HCT116 entre las tres proteínas desaparec en presencia de este inhibidor, sugiriendo que al menos una de ellas, bien Hakai o Annexin A2, se encuentra interaccionando con Hsp90 como proteína cliente. Por otro lado, se realizaron ensayos de inhibición con geldanamicina en cultivo celular en las líneas HEK 293T y HCT116, los cuales revelaron una disminución de los niveles de Hakai en paralelo al aumento de los niveles de Annexin A2. Estos resultados sugieren que Hakai constituye una nueva proteína cliente de Hsp90 y que, en consecuencia, Annexin A2 se regularía como proteína sustrato de Hakai, aumentando sus niveles en presencia de geldanamicina y perdiendo su interacción con Hsp90 debido a la degradación de Hakai. Por otro lado, comprobamos mediante ensayos fenotípicos y de inmunofluorescencia que, en presencia de geldanamicina, la línea celular HCT116 adquiría un fenotipo más epitelial y menos invasivo propio de la reversión del proceso de EMT. Este cambio fenotípico fue acompañado del incremento de los niveles de Annexin A2 en membrana y del marcador epitelial E-cadherina en contactos celulares. La estabilización de E-cadherina en presencia de geldanamicina ha sido previamente demostrada debido a la degradación de ErbB2, una kinasa cliente de Hsp90 responsable de causar la degradación de β-catenina y desestabilizar su asociación con E-cadherina (Bonvini *et* al., 2001). Por otro lado, Annexin A2 se ha relacionado con la recuperación de E-cadherina en uniones adherentes (Yamada *et al.,*2005). Estos resultados sugieren que el tratamiento con geldanamicina podría estar revertiendo el proceso de EMT mediante la regulación de Hakai.

Con el fin de determinar el mecanismo por el cual se produce la regulación de Hakai en presencia de geldanamicina, se llevaron a cabo ensayos combinados con inhibidores de degradación lisosomal (cloroquina) y degradación vía proteasoma (MG132). En este caso, se confirmó que la degradación de Hakai se estaba produciendo vía lisosoma, dada la recuperación de los niveles experimentada durante el tratamiento con cloroquina y la ausencia de efecto con otros inhibidores de proteasoma como MG132. Además, la recuperación de los niveles de Hakai en presencia de cloroquina fue acompañada de una regulación inversa de la

proteína sustrato E-cadherina y Annexin A2. La degradación independiente de proteasoma de proteínas cliente de Hsp90 sólo había sido descrita hasta el momento para kinasa IκB (Qing *et al*., 2006).

Por otro lado, se llevó a cabo un ensayo funcional de migración para estudiar la implicación de dicha degradación de Hakai en presencia de geldanamicina. Para ello, se sobreexpresó Hakai de forma transitoria en la línea celular HEK 293T y se realizó un ensayo de migración en transwell en presencia y ausencia de geldanamicina. Con este ensayo comprobamos que la sobreexpresión de Hakai aumenta la capacidad de migración de esta línea celular, inicialmente ausente en el control sin sobreexpresión y que, una vez tratada con geldanamicina, dicha capacidad de migración se ve significativamente disminuida. Este resultado concuerda con la previamente observada recuperación de E-cadherina y del fenotipo epitelial en la línea celular HCT116, y sugiere que la inhibición de la actividad de Hsp90 tiene un impacto en la migración celular de células tumorales mediada, al menos en parte, por su acción sobre Hakai como proteína cliente de esta chaperona.

Paralelamente, se evaluó la expresión de la chaperona Hsp90 en muestras de pacientes con cáncer colorrectal correspondientes a tejido sano y distintos estadios tumorales. En este caso se comprobó que Hsp90 se encuentra incrementada en muestras tumorales en comparación con el tejido sano, sugiriendo una clara implicación de dicha chaperona en la progresión tumoral. Estos datos concuerdan con los recientemente publicados por Zhang y colaboradores, en los que describen Hsp90 como un marcador de mal pronóstico en cáncer colorrectal (Zhang *et al*., 2019).

Todos los resultados obtenidos a lo largo del desarrollo de esta tesis doctoral indican que Hakai ejerce un importante papel en la progresión tumoral, afectando no sólo a su ampliamente conocido sustrato descrito E-cadherina, sino también a otras proteínas implicadas en el mantenimiento del fenotipo epitelial y en la promoción de la progresión tumoral. En concreto, aquí describimos la Annexin A2 como una nueva potencial proteína sustrato para la E3 ubiqutin-ligasa Hakai. No obstante, todavía se requiere profundizar en el estudio de este mecanismo de regulación. Por otro lado, los resultados obtenidos respecto a la interacción entre Hakai y Hsp90, así como la regulación de su expresión y actividad en presencia de geldanamicina, sugieren que Hakai y Hsp90 podrían estar jugando conjuntamente un papel

importante durante la progresión tumoral *in vivo,* y se abre así una nueva ventana terapéutica basada en la combinación de fármacos antitumorales dirigidos a la inhibición de Hsp90 y de Hakai.

APPENDIX C

Publications related to the present doctoral thesis:

- Article 1: Diaz-Diaz, A., Casas-Pais, A., Calamia, V., Castosa, R., Martinez-Iglesias, O., Roca-Lema, D., Santamarina, I., Valladares-Ayerbes, M., Calvo, L., Chantada, V. and Figueroa, A. *Proteomic Analysis of the E3 Ubiquitin-Ligase Hakai Highlights a Role in Plasticity of the Cytoskeleton Dynamics and in the Proteasome System.* J Proteome Res, 2017. **16**(8): p. 2773-2788. PMID:28675930. DOI: 10.1021/acs.jproteome.7b00046.

- Article 2: Diaz-Diaz, A., Roca-Lema, D., Casas-Pais, A., Romay, G., Colombo, G., Concha, A., Graña, B. and Figueroa, A. *Heat Shock Protein 90 Chaperone Regulates the E3 Ubiquitin-Ligase Hakai Protein Stability.* Cancers (Basel), 2020. **12**(1). PMID: 31952268. DOI: 10.3390/cancers12010215.

Journal of proteome research

Article

pubs.acs.org/jpr

Proteomic Analysis of the E3 Ubiquitin-Ligase Hakai Highlights a Role in Plasticity of the Cytoskeleton Dynamics and in the Proteasome System

Andrea Díaz-Díaz,[†] Alba Casas-Pais,[†] Valentina Calamia,[‡] Raquel Castosa,[†] Olaia Martinez-Iglesias,[†] Daniel Roca-Lema,[†] Isabel Santamarina,[†] Manuel Valladares-Ayerbes,[§] Lourdes Calvo,[∥] Venancio Chantada,[†] and Angélica Figueroa*[,†]

[†]Epithelial Plasticity and Metastasis Group, Instituto de Investigación Biomédica de A Coruña (INIBIC), Complexo Hospitalario Universitario de A Coruña (CHUAC), Sergas, Universidade da Coruña (UDC), 15006 A Coruña, Spain

[‡]Proteomics Group-ProteoRed PRB2/ISCIII, INIBIC−CHUAC, UDC, 15006 A Coruña, Spain

[§]Clinical and Translational Oncology Group, Hospital Universitario Virgen del Rocio, Instituto de Investigación Biomédica de Sevilla (IBIS), 41013 Sevilla, Spain

[∥]Clinical and Translational Oncology Group, Complexo Hospitalario Universitario de A Coruña (CHUAC), Sergas, 15006 A Coruña, Spain

Supporting Information

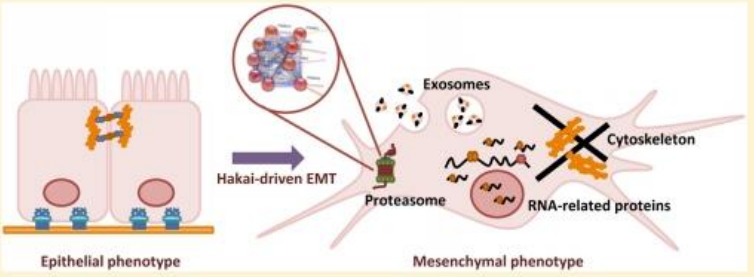

ABSTRACT: Carcinoma, the most common type of cancer, arises from epithelial cells. The transition from adenoma to carcinoma is associated with the loss of E-cadherin and, in consequence, the disruption of cell−cell contacts. E-cadherin is a tumor suppressor, and it is down-regulated during epithelial-to-mesenchymal transition (EMT); indeed, its loss is a predictor of poor prognosis. Hakai is an E3 ubiquitin-ligase protein that mediates E-cadherin ubiquitination, endocytosis and finally degradation, leading the alterations of cell−cell contacts. Although E-cadherin is the most established substrate for Hakai activity, other regulated molecular targets for Hakai may be involved in cancer cell plasticity during tumor progression. In this work we employed an iTRAQ approach to explore novel molecular pathways involved in Hakai-driven EMT during tumor progression. Our results show that Hakai may have an important influence on cytoskeleton-related proteins, extracellular exosome-associated proteins, RNA-related proteins and proteins involved in metabolism. Moreover, a profound decreased expression in several proteasome subunits during Hakai-driven EMT was highlighted. Since proteasome inhibitors are becoming increasingly used in cancer treatment, our findings suggest that the E3 ubiquitin-ligase, such as Hakai, may be a better target than proteasome for using novel specific inhibitors in tumor subtypes that follow EMT.

KEYWORDS: *epithelial-to-mesenchymal transition, E-cadherin, E3 ubiquitin-ligase, Hakai, proteasome*

INTRODUCTION

Most human malignant tumors are carcinomas, and almost 90% of cancer-associated mortality is due to metastasis. Carcinoma arises from the transformation of epithelial cells.[1] During epithelial tumor progression, cells activate a program named epithelial-to-mesenchymal transition (EMT) that is frequently observed in human cancer. EMT is an essential and tightly controlled developmental process that plays a critical role during embryogenesis, wound healing and tissue repair.[2] Pathological EMT has also been described in organ fibrosis and in tumor progression.[3,4] EMT process is an early step during carcinoma metastasis characterized by the loss of apical-basal polarity and acquisition of migratory and invasive abilities.

Received: January 24, 2017
Published: July 4, 2017

DOI: 10.1021/acs.jproteome.7b00046
J. Proteome Res. XXXX, XXX, XXX−XXX

These features are accompanied by a loss of epithelial morphology and the acquisition of mesenchymal characteristics, resulting from the alteration of cell−cell contacts and cell−substrate adhesions.[4,5] A critical molecular hallmark of EMT is the functional loss of the E-cadherin at adherens junctions. E-cadherin is a tumor suppressor, and its loss is associated with the transition from adenoma to carcinoma. It has also been reported as a clinical predictor of poor prognosis in many types of cancer.[6−8] In parallel to the down-regulation of E-cadherin, EMT is characterized by the acquisition of mesenchymal markers, such as N-cadherin.[9,10]

Given the important impact of E-cadherin during epithelial plasticity and carcinoma metastasis, the molecular mechanisms involved in its down-regulation have been extensively studied.[11−14] One of the most crucial regulators of E-cadherin described at post-translational level is the E3 ubiquitin-ligase Hakai. Tyrosine phosphorylation of the E-cadherin complex by receptor or nonreceptor kinases promotes the interaction of Hakai. Hakai mediates E-cadherin ubiquitination, endocytosis and degradation, leading the disruption of cell−cell contacts.[15,16] Indeed, it has been postulated that Hakai participates in the regulation of epithelial-to-mesenchymal transition by modulating E-cadherin cell−cell adhesions during colorectal malignant transformation.[15,17] Although most of the substrates for the E3 ubiquitin-ligases are targets for destruction via 26S proteasome, it has been reported that ubiquitin-tagged E-cadherin is degraded into lysosomes.[15,16,18]

Since Hakai was identified in 2002, many authors highlighted its crucial role in EMT during carcinogenesis. Moreover, Hakai abundance was shown markedly higher in human colon and gastric adenocarcinoma compared to normal tissues[19,20] and it was proposed as an attractive molecular target for cancer therapy.[17,19,21−25] Several drugs, such as vinflunin or silibinin, were reported to exert anti-invasive effect accompanied by an E-cadherin increase and Hakai decrease protein levels.[26,27] The publication of Hakai molecular structure in 2012 opened the possibility to design novel specific antitumor compounds against this target for cancer treatment.[28,29] However, not all cellular changes described for Hakai activity can be attributed to its action on E-cadherin substrate. Indeed, several lines of evidence suggest additional roles for Hakai. First, Hakai is ubiquitously expressed, even in tissues that do not express E-cadherin, such as lymph nodes or skeletal muscle.[15,19,30] Second, Hakai was reported to exert a control on cell proliferation in an E-cadherin independent manner suggesting its role in different cellular processes.[20,31,32] Moreover, many E3 ubiquitin-ligases are reported to have several substrates for ubiquitination. Indeed, novel potential substrates, such as Cortactin and DOK1, were described as novel Hakai-interacting proteins in Src-phosphorylation-dependent manner, however, up to date the physiological significance of these interactions is not defined.[28] Finally, Hakai localizes not only in the cytoplasm but also in the nucleus, suggesting its involvement in novel functional roles and cellular processes.[19] According to this, it has been described that Hakai interacts with RNA-binding proteins elucidating its implication in post-transcriptional regulation.[31,32]

Given that the normal epithelial MDCK cell line has been extensively used as an in vitro model system to study EMT,[33] in the present investigation, we aim to determine how protein expression is altered during epithelial-to-mesenchymal transition in a Hakai-dependent manner. For this purpose, we perform, for the first time, a proteomic analysis using a gel-free approach and employing isobaric tags for relative and absolute quantitation (iTRAQ) methodology, in order to compare protein expression from MDCK normal epithelial cells with protein profiles from Hakai-transformed MDCK cells, whereby the EMT program is induced.[19,25] As part of the experimental design, some of the identified Hakai-regulated proteins using iTRAQ technique were validated independently by Western blotting. Moreover, by bioinformatics we reveal the impact of Hakai on cytoskeleton dynamics, post-transcriptional regulation, protein metabolism, and exosome-associated proteins. We highlight a specific down-regulation of proteasome subunits suggesting that targeting E3 ubiquitin-ligase Hakai may be a more effective therapeutic strategy rather than using proteasome inhibitors in specific tumors subtypes that follow EMT.

■ EXPERIMENTAL SECTION

Antibodies and Materials

Antibody to cytoplasmic domain of E-cadherin was from BD Transduction Laboratories. The rabbit polyclonal anti-Hakai antibody (Hakai-2498) was kindly provided by Professor Yasuyuki Fujita. Anti-α-tubulin and anti-Stratifin (14-3-3 sigma) antibodies were from Sigma-Aldrich (St. Louis, MO). N-cadherin, Anti-HSP70, anti-HSP90, anti-Galectin-3, anti-Calumenin, anti-Annexin A1 and anti-Annexin A2 antibodies were from Abcam (Cambridge, UK). Anti-IMPDH-1 was from Santa Cruz Biotechnology (Santa Cruz, CA), anti-Cortactin antibody was from Millipore (Darmstadt, Germany). Anti-GAPDH antibody was from Thermo Fisher Scientific (Rockford, IL). HRP-rabbit and mouse polyclonal antibodies were from GE Healthcare (Uppsala, Sweden). All primary antibodies were used at dilution 1:1000 for Western Blot analysis, except anti-stratifin and IMPDH-1 antibodies, which were used at 1:500 and 1:100 respectively dilution, and anti-α-tubulin antibody that was used at a 1:2000 dilution. Secondary antibodies for Western Blot were used at a dilution of 1:5000. For immunofluorescence, all primary antibodies were used at a dilution 1:100, Alexa-Fluor 488-conjugated or Alexa-Fluor 568-conjugated secondary antibodies (Thermo Fisher Scientific) were used at a dilution 1:200.

Cell Culture

MDCK cells were cultured in Dulbecco's Modified Eagles Medium (DMEM) containing 1% of penicilin/streptomycin, 1% of glutamine and 10% of FBS at 37 °C and ambient air supplemented with 5% of CO_2. Hakai-transformed MDCK cells were kindly provided by Yasuyuki Fujita.[19] Hakai-transformed MDCK cells clones were selected in a medium containing 800 μg/mL of G418 (Sigma-Aldrich). In the present work, all clones used were interchangeably (clon 4, clon 7, and clon 11), representing comparable phenotypes and results.[19] Cell culture phenotype was analyzed in a 6-well plate by phase contrast images using Nikon Eclipse-Ti microscope.

Western Blot Analysis

For protein extraction, cell lysates were obtained by using 1% Triton X-100 buffer (20 mM Tris/HCl [pH 7.5], 150 mM NaCl and 1% Triton X-100) containing 1 mM phenylmethylsulfonyl fluoride, and a 1× protease inhibitor cocktail dilution from 100× stock (AEBSF at 104 mM, Aprotinin at 80 μM, Bestatin at 4 mM, E-64 at 1.4 mM, Leupeptin at 2 mM and Pepstatin A at 1.5 mM). After 20 min incubation at 4 °C and centrifugation at 14, 000 × g for 10 min, protein concentration

DOI: 10.1021/acs.jproteome.7b00046
J. Proteome Res. XXXX, XXX, XXX−XXX

Table 1. Identified Down-Regulated Proteins in Hakai-Transformed MDCK Cells[a]

N	% coverage	accession number	symbol	protein name	biological roles involved in references from GeneCards human gene database	peptides[b] (95%)	unique peptides	ratio (mean ± SD)	p-value	MW[c]
1	60.4	P04083	ANXA1	Annexin A1	Cell adhesion molecule involved in cell-to-cell and to extracellular matrix binding. Involved in proliferation, differentiation, motility, trafficking, apoptosis and tissue architecture	25	25	0.012 ± 0.001	<0.001	54389.71
2	33.6	P17931	LEG3	Galectin-3	Galactose-specific lectin which binds IgE. May mediate endothelial cells migration. In the nucleus acts as a pre-mRNA splicing factor. Involved in acute inflammatory responses.	20	20	0.017 ± 0.002	0.011	26021.14
3	84.1	P07355	ANXA2	Annexin A2	Calcium-regulated membrane-binding protein wich plays a role in the regulation of cellular growth and in signal transduction pathways. May be involved in heat-stress response.	49	49	0.020 ± 0.005	<0.001	38472.85
4	66.0	P25786	AHNK	Neuroblast differentiation-associated protein AHNAK	Structural molecule activity conferring elasticity. May be required for neuronal cell differentiation.	88	88	0.021 ± 0.003	<0.001	629101.22
5	63.9	P60903	S10AA	Protein S100-A10	Involved in the regulation processes such as cell cycle progression and differentiation. It may function in exocytosis and endocytosis. Induces the dimerization of ANXA2/p36.	12	12	0.022 ± 0.001	<0.001	11071.91
6	49.2	P31947	14335	14-3-3 protein sigma	Adapter protein implicated in the regulation Cell Cycle Checkpoints and p53 Pathway. Bound to KRT17, regulates protein synthesis and epithelial cell growth	11	6	0.036 ± 0.015	0.012	27774.06
7	48.5	P02545	LMNA	Prelamin-A/C	Component of the nuclear lamina. Involved in nuclear stability, chromatin structure and gene expression. Required for bone formation. Accelerates smooth muscle senescence.	16	15	0.055 ± 0.005	0.002	74139.49
8	29.1	Q14847	LASP1	LIM and SH3 domain protein 1	Plays an important role in the regulation of dynamic actin-based, cytoskeletal activities. Involved in ion transmembrane transport activity.	3	3	0.114 ± 0.042	0.028	29717.16
9	32.2	O00151	PDLI1	PDZ and LIM domain protein 1	Cytoskeletal protein that may act as an adapter that brings other proteins (like kinases) to the cytoskeleton.	5	5	0.142 ± 0.056	0.003	35940.52
10	71.4	O43852	CALU	Calumenin	Calcium-binding protein localized in the endoplasmic reticulum (ER) and it is involved in such ER functions as protein folding and sorting. Among its related pathways are Ca_2 cAMP and Lipid Signaling and Platelet activation, signaling and aggregation.	16	16	0.143 ± 0.051	<0.001	34961.15
11	65.3	P67936	TPM4	Tropomyosin alpha-4 chain	Binds to actin filaments in muscle and nonmuscle cells. Plays a central role in the calcium dependent regulation of vertebrate striated muscle contraction	18	10	0.143 ± 0.060	<0.001	28390.62
12	41.4	O14818	ACTN4	Alpha-actinin-4	Cytoskeletal protein probably involved in vesicular trafficking via its association with the CART complex. Involved in tight junction assembly in epithelial cells. Is thought to be involved in metastatic processes.	14	14	0.161 ± 0.027	<0.001	104854.04
13	75.6	P15311	EZRI	Ezrin	Plays a key role in cell surface structure adhesion, migration and organization, and it has been implicated in various human cancers. In epithelial cells, required for the formation of microvilli and membrane ruffles on the apical pole.	61	35	0.172 ± 0.020	<0.001	69281.61
14	72.1	P26038	MOES	Moesin	Cross-linker between plasma membranes and actin-based cytoskeletons. Localized membranous protrusions that are important for cell–cell recognition and signaling and for cell movement.	52	27	0.216 ± 0.075	0.009	67688.85
15	30.7	Q9BPX5	ARPSL	Actin-related protein 2/3 complex subunit 5-like protein	Involved in regulation of actin polymerization and together with an activating nucleation-promoting factor (NPF) mediates the formation of branched actin networks.	3	3	0.239 ± 0.053	0.026	16941.19
16	68.8	P37802	TAGL2	Transgelin-2	The specific function of this protein has not yet been determined, although it is thought to be a tumor suppressor.	16	16	0.256 ± 0.170	<0.001	22260.25
17	61.8	P52565	GDIR1	Rho GDP-dissociation inhibitor 1	Controls Rho proteins homeostasis. Through the modulation of Rho proteins, may play a role in cell motility regulation. Activity of this protein is important in a variety of cellular processes, and expression of this gene may be altered in tumors.	14	14	0.322 ± 0.086	0.023	23075.92
18	53.7	Q9NYL9	TMOD3	Tropomodulin-3	Blocks the elongation and depolymerization of the actin filaments at the pointed end and defines the geometry of the membrane skeleton.	5	5	0.351 ± 0.144	0.019	39594.77
19	26.2	P11234/ P11233	RALB/A	Ras-related protein Ral-B/A	Multifunctional GTPase involved in a variety of cellular processes including gene expression, cell migration, cell proliferation, oncogenic transformation and membrane trafficking.	3	0	0.375 ± 0.024	0.026	23079.09
20	51.8	P61586	RHOA	Transforming protein RhoA	Rho proteins promote reorganization of the actin cytoskeleton and regulate cell shape, attachment, and motility. Overexpression of this gene is associated with tumor cell proliferation and metastasis.	9	9	0.406 ± 0.059	0.013	21442.68
21	89.8	P23528	COF1	Cofilin-1	Important for normal progress through mitosis and normal cytokinesis. Plays a role in the regulation of cell morphology and cytoskeletal organization.	23	23	0.436 ± 0.115	<0.001	18371.3
22	60.9	Q15019	SEPT2	Septin-2	Required for normal organization of the actin cytoskeleton. Plays a role in the biogenesis of polarized columnar-shaped epithelium, thus facilitating efficient vesicle transport.	12	12	0.438 ± 0.104	0.010	41487.47

DOI: 10.1021/acs.jproteome.7b00046
J. Proteome Res. XXXX, XXX, XXX−XXX

Table 1. continued

[a]Statistically significant identified down-regulated proteins by iTRAQ analysis of normal MDCK epithelial transformed with Hakai. The selected unique proteins found identified with >95% confidence and score ≤0.5 are indicated. Data in the table include: percentage coverage; Accession number; Symbol; Protein name; Biological roles in references from Gene Cards human database. [b]Number of distinct peptides having at least 95% confidence; Unique peptides; Ratio (Mean ± SD); *p*-value. [c]MW: Molecular Weight in Dalton.

was measured using Pierce BCA Protein Assay Kit (Thermo Fisher Scientific). Twenty micrograms of the supernatant were loaded in 12%, 10% or 8% polyacrilamide SDS-PAGE, as needed. Western blotting was performed as previously described.[13] Densitometric quantification of Western Blot images was performed by ImageLab software.

Immunofluorescence

Immunofluorescence was performed as described previously.[26] Briefly, cells were plated in sterile glass coverslip to each well of 6-well dish, fixed with 4% PFA for 15 min and permeabilized with 0.5% Triton-X-phosphate buffered saline (PBS) for 15 min. Primary antibodies were incubated for 2 h and secondary antibodies for 1 h. Hoechst (LifeTech) was used for nucleus staining at a dilution 1:10 000. Finally, the mounting media used was ProLong Gold Antifade Mountant (LifeTech) and images were taken with confocal microscope Nikon A1R and were analyzed using NIS-Elements 3.2 software.

Processing of Protein Samples for iTRAQ Labeling

Before iTRAQ labeling, protein extraction was carried out as follow: cells were centrifugated 5 min at 1200 rpm and cellular pellets were washed twice in phosphate buffer solution. A lysis buffer containing 6 M urea/2% SDS was employed for protein extraction. Cellular debris was eliminated by centrifugation (10 min at 13 000 rpm). Samples were cleaned up by precipitation with acetone and pellets were dried and resuspended in 25 μL Dissolution Buffer provided with the iTRAQ kit (500 mM triethylammonium bicarbonate buffer, TEAB). Protein concentration was determined by Bradford assay (Sigma-Aldrich, St. Louis, MO, USA) before acetone precipitation. Twenty-five μg of each condition were resuspended in 25 μL TEAB yielding to a final protein concentration equal to 1 μg/μL. One μg of each sample was resolved by 1D-SDS-PAGE. The gel was then stained by silver nitrate to ensure proteins integrity after acetone precipitation and to test technical reproducibility of proteins precipitation. Equal amounts of proteins (25 μg) were reduced, alkylated, and digested with trypsin. Then iTRAQ labeling was performed according to the supplier's instructions (ABSciex, Foster City, CA, USA). The samples were labeled as follows: MDCK, 114; MDCK, 115; Hakai-transformed MDCK clon 4, 116; Hakai-transformed MDCK clon 11, 117. iTRAQ-labeled peptides were mixed and desalted using reversed phase columns (Pierce C18 Spin Columns, Thermo Fisher Scientific, Rockford, IL, USA) prior to liquid chromatography coupled to mass spectrometry (LC-MS) analysis.

LC-MALDI-MS Analysis

The desalted peptides were fractionated by reversed-phase liquid chromatography (RP-LC) at basic pH (pH = 10) on a HP 1200 system (Agilent Technologies, Santa Clara, CA, USA) employing a C18 column (Zorbax extend C18, 100 × 2.1 mm id, 3.5 μm, 300 Å; Agilent). The flow rate used was 0.2 mL/min and the gradient was as in supplemental Figure S1. Sixteen fractions were pooled postcollection (FC203B fraction collector, Gilson, Middleton, WI, USA) based on the peak intensity of the UV trace recorded at 214 nm. Each fraction was dried in a vacuum concentrator and then the peptides were resuspended in 2% ACN/0.1% TFA. Five μL of the peptides solution were injected into a reversed-phase column (Integrafit C18, ProteopepTM II, New Objetive) for nanoflow LC analysis, using a Tempo nanoLC (Eksigent). Peptides were eluted at a flow rate of 0.35 μL/min during a 90 min linear gradient from 2 to 50%B (mobile phase A: 0.1% TFA/2%

DOI: 10.1021/acs.jproteome.7b00046
J. Proteome Res. XXXX, XXX, XXX−XXX

Table 2. Identified Up-Regulated Proteins in Hakai-Transformed MDCK Cells[a]

N	% coverage	accession number	symbol	protein name	biological roles involved in references from GeneCards human gene database	peptides[b] (95%)	unique peptides	ratio (mean ± SD)	p-value	MW[c]
1	79.1	P08107	HSP71	Heat shock 70 kDa protein 1A/1B	Chaperone that stabilizes preexistent proteins against aggregation and mediates its folding in the cytosol as well as within organelles; It is also involved in the ubiquitin-proteasome pathway	111	65	30.138 ± 8.078	<0.001	69921.04
2	94.1	P22392	NDKB	Nucleoside diphosphate kinase B	Enzime that plays its major role in synthesis of nucleoside triphosphates as well as NME1; Acts as as transcriptional activator of MYC gene and negatively regulates Rho activity; Diseases associated with NME2 include Myxosarcoma and Lung Sarcoma	30	18	19.751 ± 3.582	<0.001	17298.04
3	23.2	P20839	IMDH1	Inosine-5′-monophosphate dehydrogenase 1	Enzime that catalyzes the conversion of inosine 5-phosphate (IMP) to xanthosine 5-phosphate, the first limiting step in the sinthesys of guanine nucleotides; It may play a role in the malignancy and progression of some tumors	4	3	38.785 ± 3.028	<0.001	55274.60
4	89.4	P06733	ENOA	Alpha-enolase	Multifunctional enzime which participates in glycolysis, as well as growth control, hypoxia tolerance and allergic responses; Stimulates immunoglobulin production and may play a role as a tumor suppressor	96	77	19.266 ± 12.379	<0.001	47037.77
5	19.3	P12955	PEPD	Xaa-Pro dipeptidase	The protein forms a homodimer that hydrolyzes dipeptides or tripeptides with C-terminal proline or hydroxyproline residues; The enzyme serves an important role in the recycling of proline, and may be rate limiting for the production of collagen	3	3	16.925 ± 2.685	<0.001	54416.98
6	88.8	P15531	NDKA	Nucleoside diphosphate kinase A	Protein which plays its major role in synthesis of nucleoside triphosphates; Involved in cell proliferation, differentiation and development, signal transduction and gene expression; NME1 is associated with diseases such as Neuroblastoma and Anal Canal Carcinoma	24	12	10.188 ± 0.830	<0.001	17017.53
7	71.4	P49773	HINT1	Histidine triad nucleotide-binding protein 1	Protein that hydrolyzes purine nucleotide phosphoramidates substrates; Modulates proteasomal degradation of target proteins by the SCF E3 ubiquitin-protein ligase complex; The HINT1 gene is considered a tumor suppressor	6	6	9.315 ± 5.593	0.002	13670.72
8	43.3	Q9NX58	LYAR	Cell growth-regulating nucleolar protein	Poly(A) RNA binding protein	7	7	2.796 ± 0.344	0.044	43614.80
9	71.3	Q8NC51	PAIRB	Plasminogen activator inhibitor 1 RNA-binding protein	Poly(A) RNA binding protein and mRNA 3-UTR binding protein; May play a role in the regulation of mRNA stability	35	35	6.050 ± 2.254	<0.001	44834.20
10	40.3	P60891	PRPS1	Ribose-phosphate pyrophosphokinase 1	Enzyme that catalyzes the phosphoribosylation of ribose 5-phosphate to 5-phosphoribosyl-1-pyrophosphate, necessary for nucleotide biosynthesis and purine metabolism	8	8	5.279 ± 1.956	<0.001	34703.04
11	41.6	P07195	LDHB	L-lactate dehydrogenase B chain	B subunit of lactate dehydrogenase enzime which catalyzes the interconversion of pyruvate and lactate with concomitant interconversion of NADH and NAD+; Diseases related to LDHB include urinary bladder urothelial carcinoma	13	13	4.894 ± 1.954	<0.001	36507.30
12	32.1	Q9BTT0	AN32E	Acidic leucine-rich nuclear phosphoprotein 32 family member E	Histone chaperone that specifically mediates the removal of histone H2AZ/H2AFZ from the nucleosome	7	7	4.301 ± 1.384	0.044	30692.49
13	70.9	P30050	RL12	60S ribosomal protein L12	Protein component of the ribosomal 60S subunit; It binds directly to the 26S rRNA	13	13	3.284 ± 1.139	<0.001	17818.59
14	61.1	P12268	IMDH2	Inosine-5′-monophosphate dehydrogenase 2	Catalyzes the conversion of inosine 5-phosphate (IMP) to xanthosine 5-phosphate, the first limiting step in the sinthesys of guanine nucleotides; It may play a role in the malignancy and progression of some tumors	21	20	2.925 ± 1.365	<0.001	55673.79
15	31.7	P49321	NASP	Nuclear autoantigenic sperm protein	H1 histone binding protein involved in the transport of histones to the nucleus in dividing cells; Required for DNA replication and normal cell proliferation and cycle progression	7	7	3.308 ± 1.305	0.001	85106.53
16	67.8	P16949	STMN1	Stathmin	Ubiquitous cytosolic phosphoprotein involved in the microtubule filament system by destabilizing microtubules; Prevents assembly and promotes disassembly of microtubules	16	16	2.689 ± 0.649	<0.001	17171.32
17	46.5	P15121	ALDR	Aldose reductase	Protein member of aldo/keto reductase superfamily; Catalyzes the NADPH-dependent reduction of aldehydes; It is implicated in the metabolism of steraid hormones and galactose	4	3	3.205 ± 0.602	0.024	35722.21
18	35.6	Q12906	ILF3	Interleukin enhancer-binding factor 3	Protein that regulates gene expression at level of post-transcription; Can act as an inhibitory protein at the initiation phase of RNA translation probably by inhibiting its binding to polysome	11	11	2.699 ± 0.183	0.006	95338.37
19	63.7000	P09651	ROA1	Heterogeneous nuclear ribonucleoprotein A1	Protein involved in the packaging of pre-mRNA into hnRNP particles, transport of poly(A) mRNA from the nucleus to the cytoplasm and may modulate splice site selection	50	44	2.199 ± 0.683	0.001	38746.65

DOI: 10.1021/acs.jproteome.7b00046
J. Proteome Res. XXXX, XXX, XXX−XXX

Table 2. continued

[a]Statistically significant identified up-regulated proteins by iTRAQ analysis of normal MDCK epithelial transformed with Hakai. The selected unique proteins found identified with >95% confidence and score >2.0 are indicated. The table includes percentage coverage; Accession number; Symbol; Protein name; Biological roles in references from Gene Cards human database. [b]Number of distinct peptides having at least 95% confidence; Unique peptides; Ratio (Mean ± SD); *p*-value. [c]MW: Molecular Weight in Dalton.

ACN, mobile phase B: 0.1% TFA/95% ACN). LC eluate was deposited onto an Opti-TOF LC MALDI target plate (1534-spot format; Sciex, Framingham, MA, USA) using the Sun Collect MALDI Spotter/Micro Collector (SunChrom Wissenschaftliche Geräte GmbH, Germany). Before spotting, the LC microfractions were mixed with MALDI matrix (3 mg/mL a-cyano-4-hydroxycinnamic acid in 70% ACN/0.1% TFA containing 10 fmol/μL angiotensin as internal standard). Finally, 4 plates containing 4 LC runs per plate were analyzed in a 4800 MALDI-TOF/TOF instrument (ABSciex) with a 200 Hz repetition rate (Nd:YAG laser). MS full-scan spectra were acquired from 800 to 4000 m/z using a fixed laser intensity of 3600 kV and 1500 shots/spectrum. Tandem MS mode was operated with 1 kV collision energy with CID gas (air) over a range of 60 to −20 m/z of the precursor mass value. Up to 12 of the most intense precursors per spot with signal/noise ratio (S/N) > 80 were selected for MS/MS acquisition using a fixed laser intensity of 4400 kV and 2000 shots/spectrum. Common contaminants such as trypsin autolysis peaks and matrix ion signals were excluded from the analysis. A second MS/MS was acquired excluding those precursors previously fragmented and using a lower S/N threshold of 50 to detect peptides that were not identified in the previous run.[34,35]

Data Analysis

Data from all the MS/MS acquisitions were used for protein identification and quantification using ProteinPilot software v.4.5 (Sciex). Each MS/MS spectrum was searched in the Uniprot/Swissprot database (UniProt 2015_05 release version containing 547 599 sequences and 195 014 757 residues, with taxonomy restriction_*Homo sapiens*). Protein Pilot search parameters were set as follows: trypsin cleavage specificity, methylmethanethiosulfate (MMTS) modified cysteine as fixed modifications, biological modification "ID focus" settings, and a protein minimum confidence score of 95%. The tolerance used for matching MS/MS peaks to the theoretical fragment ions is based on the information regarding to mass accuracy of the instrument chosen in the Paragon Method dialogue box (4800 MALDI TOF/TOF).[36] The ProteinPilot software employs two different algorithms: one to perform protein identification (ParagonTM algorithm) and the other one to determine the minimal set of confident protein identifications (Pro GroupTM algorithm). Once the identity of the protein was confirmed (Detected Protein Threshold >95%, Unused ProtScore >1.3), the ratios of the peak areas of iTRAQ reporter ions were calculated in order to compare the relative abundance of the proteins identified in the samples. Data were normalized for loading error by bias, assuming the samples are combined in 1:1 ratios. Peak areas for the iTRAQ reagent(s) and control are also corrected to attempt to remove background ion signal applying the background correction option. Only those changes with a *p*-value ≤0.05 and a ratio ≥2 (or ≤0.5) were considered statistically significant. Due to the high complexity of the samples, Proteomics System Performance Evaluation Pipeline (PSPEP) software was used independently to calculate false discovery rates (FDR). In order to facilitate the overall analysis, protein classification was carried out using the following bioinformatic tools: PANTHER, Protein ANalysis THrough Evolutionary Relationships (http://www.pantherdb.org/about.jsp) and GO, Gene Ontology (http://geneontology.org). Interactive network analysis was performed using the STRING, Search Tool for the Retrieval of Interacting Genes (http://string-db.org) .

DOI: 10.1021/acs.jproteome.7b00046
J. Proteome Res. XXXX, XXX, XXX−XXX

Table 3. Identified down-Regulated Proteasome Subunits in Hakai-Transformed MDCK Cells[a]

N	% coverage	accession number	symbol	protein name	peptides (95%)[b]	unique peptides	ratio (mean ± SD)	p-value	MW[c]
1	60.1	P25786	PSA1	Proteasome subunit alpha type-1	12	12	0.500 ± 0.452	0.002	29555.59
2	66.2	P25787	PSA2	Proteasome subunit alpha type-2	12	12	0.131 ± 0.126	<0.001	25767.39
3	56.5	P25788	PSA3	Proteasome subunit alpha type-3	10	10	0.478 ± 0.532	0.032	28302.04
4	43.7	P25789	PSA4	Proteasome subunit alpha type-4	8	8	0.486 ± 0.167	0.012	29483.81
5	64.7	P28066	PSA5	Proteasome subunit alpha type-5	7	7	0.312 ± 0.197	0.005	26411.03
6	61.8	P60900	PSA6	Proteasome subunit alpha type-6	13	13	0.492 ± 0.398	0.004	27399.45
7	85.9	O14818	PSA7	Proteasome subunit alpha type-7	12	12	0.478 ± 0.600	0.003	27886.85
8	44.6	Q06323	PSME1	Proteasome activator complex subunit 1	4	4	0.408 ± 0.127	0.046	28723.10
9	81.1	P49721	PSB2	Proteasome subunit beta type-2	9	9	0.560 ± 0.184	0.046	22836.28

[a]Identified subunits involved in 26 proteasome down-regulated in normal MDCK epithelial transformed with Hakai. The table includes percentage coverage; Accession number; Symbol; Protein name. [b]Number of distinct peptides having at least 95% confidence; Unique peptides; Ratio (Mean ± SD); p-value. [c]MW: Molecular Weight in Dalton.

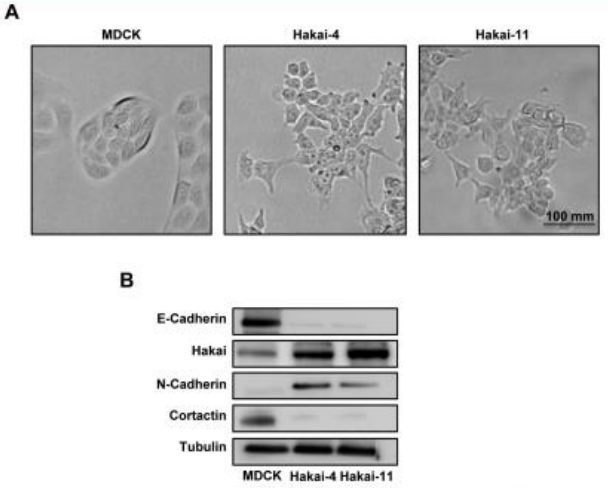

Figure 1. Effect of Hakai-transformation in MDCK cells. (A) Cell morphology of Hakai-transformed and parental MDCK cells was analyzed by phase contrast. Hakai-MDCK cells exhibit elongated cell morphology during EMT (Scale Bar 100 μm). (B) Expression levels of Hakai, E-cadherin, Cortactin and N-cadherin in Hakai-transformed and parental MDCK cells. Cell lysates of the indicated Hakai-transformed clones were examined by western-blotting with the indicated antibodies, using α-tubulin as loading control for normalization.

Statistical Analysis

Proteomics data were analyzed employing normalization tools and statistical package from ProteinPilot. The results obtained were exported to Microsoft Excel for further analyses. Where appropriate, results are expressed as the mean ± standard error (Tables 1, 2 and 3). For western-blotting analyses, it was used Student's *t*-test to evaluate two-sample comparisons at the indicated significance level. GraphPad Prism 5 was used for data management in the statistical analyses.

■ RESULTS

Cell Biological Analysis of Hakai-Induced EMT

The normal epithelial MDCK cell line has been extensively used as an in vitro model system to study EMT.[33] In keeping with previous reports,[19] under phase-contrast microscopy, MDCK cells showed a typical epithelial morphology forming an epithelial cell sheet where individual cells are tightly connected to surrounding cells. In contrast, Hakai-transformed MDCK cells showed a fibroblastic-like phenotype, elongated spindle-shaped morphology, and reduced intercellular contacts (Figure 1A).[19] Given that the EMT hallmark E-cadherin is a target for the E3 ubiquitin-ligase Hakai, as previously reported, we confirmed the down-regulation of E-cadherin in the Hakai-transformed MDCK epithelial cells. As shown in Figure 1B, the expression of E-cadherin epithelial marker decreased dramatically in Hakai-transformed MDCK cells compare to non-transformed MDCK cells. Moreover, the recently described target, Cortactin, for the E3-ubiquitin-ligase Hakai was also down-regulated in this model system (Figure 1B). Conversely, expression of the N-cadherin mesenchymal marker was recovered in Hakai-transformed MDCK cells compared to nontransformed epithelial MDCK cells. Taken together, these results support the implication of Hakai during EMT in MDCK cells.

DOI: 10.1021/acs.jproteome.7b00046
J. Proteome Res. XXXX, XXX, XXX−XXX

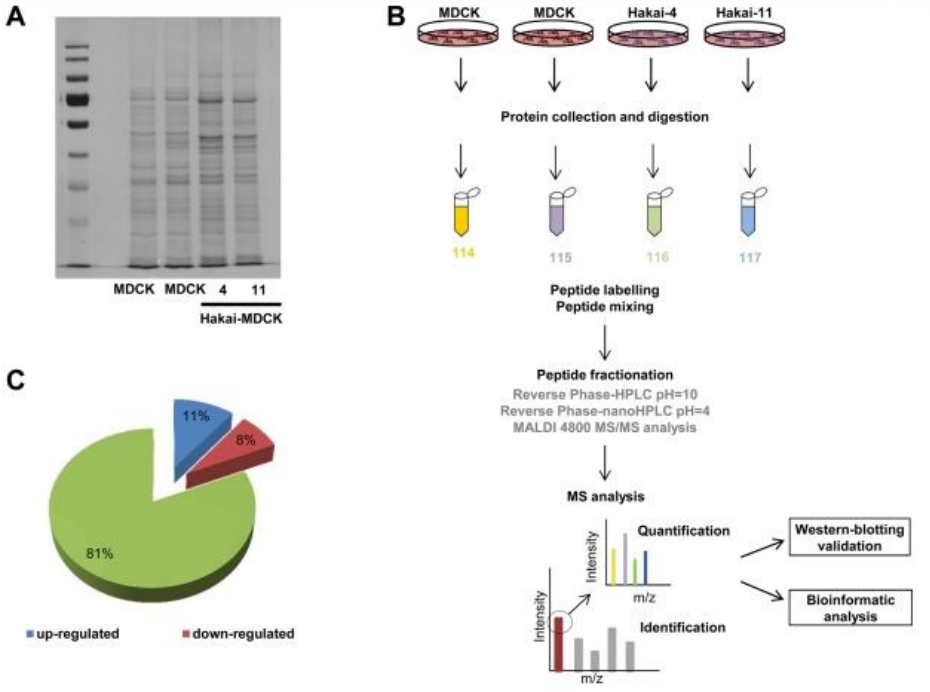

Figure 2. Experimental design. (A) Protein content of sample preparations was analyzed by 1D-SDS-PAGE and bands were visualized using silver staining. (B) Experimental workflow of the proteomic study for MDCK and Hakai-transformed MDCK cells. Labeled peptides were combined and fractionated and collected fractions were separated by nano-LC and analyzed by MALDI-TOF/TOF mass spectrometry. Western-blotting and bioinformatic analysis were performed. (C) A pie chart diagram with the 729 identified human proteins, reveals 11% proteins up-regulated and 8% proteins down-regulated in Hakai-transformed MDCK compared to wild-type MDCK cells (Table S1). The rest of the proteins (81%) were considered not significantly changed.

Strategy for the Identification of Hakai-Induced Differential Protein Expression

We profiled the proteome upon Hakai overexpression in normal epithelial MDCK cell lines. We used total protein from two MDCK replicates and two different clones previously established for Hakai-overexpression MDCK cells. Same amount of extracted protein, from MDCK (in duplicates) and from two different clones (Hakai-4 and Hakai-11), was resolved by SDS-PAGE, as shown by silver staining (Figure 2A). A schematic workflow is represented in Figure 2B. Equal amounts of proteins from Hakai-transformed MDCK and wild-type MDCK cells were digested with trypsin, and the resulting tryptic peptides were labeled with four-plex iTRAQ. Peptides were combined and separated using reversed phase LC prior to MS analysis for the identification and relative quantification of the corresponding proteins. Two biological replicates per experimental group were analyzed.[37] A total of 729 proteins were identified after combining the results (false discovery rate at 1%) with two or more peptides with 95% confidence and total score ≥2, and quantified (Table S1). Data from the proteomic measurement were subjected to bioinformatics analysis for protein classification, network and pathway analysis using Gene Ontology, PANTHER and STRING databases. Hakai-induced differential proteins were identified and subsets of them were validated by western-blotting. Among the 729 proteins identified, 145 were found to be differential regulated by Hakai (Table S1). Upon Hakai overexpression, 83 proteins (11%) appear to be significantly increased (>2-fold change, *p*-value <0.05). Similarly, 63 proteins (8%) were found decreased (or ≤0.5-fold change, *p*-value <0.05) under Hakai-transformed MDCK cells compared to wild-type MDCK cells. The remaining proteins were considered as not significantly changed (81%), (Figure 2C).

Proteomic Profiling of Hakai-Transformed MDCK Cells

The functional annotation of the 145 identified Hakai-regulated proteins was subjected to GO analysis using Panther Classification System. As shown in Figure 3, two main types of annotations were analyzed from gene ontology: the enrichment in biological process (Figure 3A,B) and in molecular function (Figure 3C,D) of the Hakai-regulated protein. Notably, in GO term, the molecular function of increased proteins are mainly annotated in metabolic processes (24%), post-transcriptional regulation (18%) and cell-stress and homeostasis (11%, Figure 3A), whereas decreased proteins are mainly annotated in cytoskeleton and cell morphology (24%), membrane vesicle trafficking (19%) and metabolic processes (16%, Figure 3B). The ontology analysis of the identified proteins indicated the relevance and diversity of molecular

DOI: 10.1021/acs.jproteome.7b00046
J. Proteome Res. XXXX, XXX, XXX−XXX

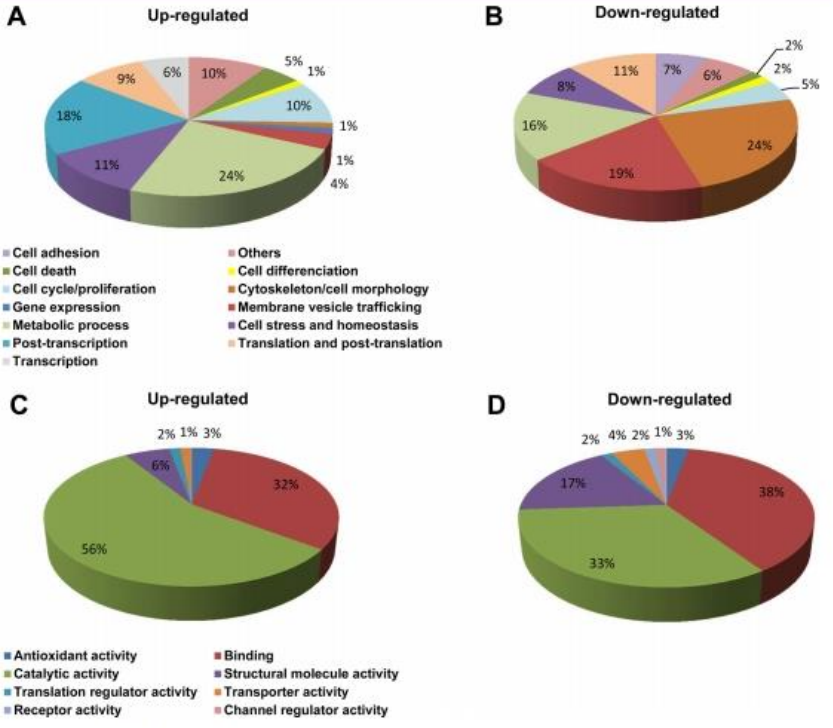

Figure 3. Classification of identified proteins based on their functional annotations using gene ontology (GO) biological process (A, B) and molecular function (C, D). These analyses were performed with the 145 identified regulated proteins considering a fold change >2 and *p*-value <0.05. This analysis was based on Gene Ontology classification categories using Panther system. (A, C) Classification of the 82 increased proteins in Hakai-transformed MDCK cells compared to wild-type MDCK. (B, D) Classification of the 62 decreased proteins in Hakai-transformed MDCK cells compared to wild-type MDCK.

functions, such as catalytic activity (56% and 33% for Hakai identified up and down-regulated proteins, Figure 3C,D, respectively) or protein binding (32% and 38% for Hakai identified up and down-regulated proteins, Figure 3C,D, respectively). The data in Figure 3 support the previously reported in vitro functional role of Hakai overexpression impact on cellular reorganization affecting migration and invasion, two important features during metastatic process.[15,17,19]

Among Hakai-regulated proteins identified, a representative subset of under-regulated proteins involved in the above-mentioned biological process is shown in Table 1. Several important decreased proteins were found related to processes such as cell adhesion and membrane vesicle trafficking. Some of these proteins include Annexin A1 and A2, Galectin-3, Stratifin (14-3-3 protein sigma), Protein S100-A10 and Calumenin. Cytoskeleton related-proteins such as Ezrin, Moesin, Septin-2, Alpha-actinin-4, PDZ and LIM domain protein-1 or LIM and SH3 domain protein were also included. Moreover, many of these proteins are important regulators of actin cytoskeleton dynamics in cell plasticity, remodelling substrate contacts that drive protrusions and represent the basic mechanism by which cells migrate and invade during tumor progression.[38] The expression of protein regulators of local actin reorganization critical for pseudopod protrusion, such as AHNAK, the Arp2/3 complex, α-Actinin, Cofilin and Prelamin-A/C, was also decreased in Hakai-transformed MDCK cells. A subset of up-regulated proteins by Hakai overexpression is shown in Table 2. Interestingly, in Hakai-transformed cells important proteins such as IMPDH1, IMPDH2, LDHB, ALDR are implicated in protein metabolism suggesting the role of Hakai in this process. Other relevant proteins such as chaperones HSP70 and AN32E or the post-transcriptional regulators as ILF3, LYAR, RL12, ROA1 and PAIRB are also found increased in Hakai-transformed cells compared to normal.

Validation of the Identified Regulated Proteins by Western-Blotting

As part of the validation analyses of the identified proteins in the iTRAQ experiments, western-blotting analyses was performed by using protein extracts from two different clones of Hakai-overexpressing MDCK cells (Figure 4). The results verified differential down-regulation of Annexin A1, Annexin A2, Calumenin, Stratifin (14-3-3) and Galectin-3 upon Hakai-transformed MDCK cells. On the other hand, Hsp70, Hsp90 and IMPDH1 were confirmed to be up-regulated in Hakai-overexpressing cells. Together these results further support the protein identification found using iTRAQ approach.

DOI: 10.1021/acs.jproteome.7b00046
J. Proteome Res. XXXX, XXX, XXX−XXX

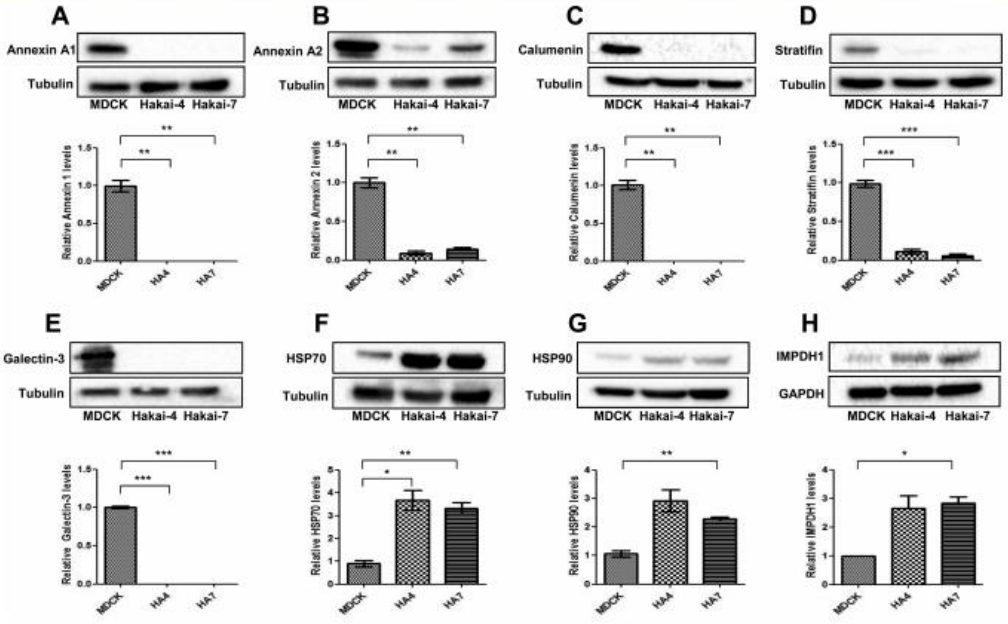

Figure 4. Verification analyses of differential expression of identified proteins by western-blotting. A validation of the iTRAQ results of a subset of selected proteins by western-blotting analysis using protein extracts from two different clones of Hakai transformed MDCK cells (Hakai-4 and Hakai-7). (A–E) Western blotting analysis (Top) and quantification by densitometry (Bottom) confirmed a differential down-regulation of Annexin A1, Annexin A2, Calumenin, Stratifin and Galectin-3 upon Hakai-overexpression. (F–H) Western blotting analysis (Top) and quantification by densitometry (Bottom) confirmed differential up-regulation of HSP70, HSP90 and IMPDH 1. Values (A–H) are the means ± SEM from three independent experiments. Statistical analyses indicate the significant difference in the indicated Hakai-transformed MDCK cells with respect to nontransformed MDCK cells (*$p < 0.05$, **$p < 0.01$, ***$p < 0.001$). The Western blotting data are representative of three independent experiments.

Subcellular Localization of Annexin A1, Galectin-3 and HSP70

We further investigated whether the subcellular localization of several identified regulated-proteins was changed in Hakai-transformed cells compared to normal cells. For this purpose, we performed an immunofluorescence analysis for Annexin A1, Galectin-3 and HSP70. As shown in Figure 5, Annexin A1 was completely disappeared in Hakai-transformed cells compared to normal (Figure 5A), while localization of Galectin-3 (Figure 5B) and HSP70 (Figure 5C) was dramatically changed. Interestingly, in Hakai-transformed cells, Galectin-3 is enriched at specific localizations closed to the nucleus and to the beginning of the protrusions. However, in MDCK cells, Galectin-3 cytoplasmic staining was detected. On the other hand, in MDCK cells, HSP70 was found in a speckle pattern in the cytoplasm and absent in the nucleus, while in Hakai-transformed cells, it was strongly enriched at cell–cell contacts. These results suggest that Hakai may exert an action on the modulation of subcellular localizations of specific proteins in different conditions.

Bioinformatic Analysis of the Regulated Proteins

An independent analysis was performed to search for protein–protein interaction between up- or down-regulated proteins in Hakai-transformed MDCK cells by using STRING database. STRING database allows to integrate interaction data from several sources and provide information about functional and physical properties.[39] Our STRING network shows significantly more interactions than expected indicating that proteins are, at least, partially connected as a group. First, we subjected the down-regulated proteins to a bioinformatic analysis. As shown in Figure 6, most of interacting proteins are integrated in two big networks: protein metabolism (Figure 6A) and cytoskeleton (Figures 6B), which are involved in two main characteristic processes of Hakai protein function. Interestingly, a significant cluster of proteasome subunit complex is highlighted (Figures 6A) further suggesting a selective down-regulation of 26S proteasome catalytic activity in Hakai-transformed cells compared to nontransformed epithelial cells (Table 3). In a similar way, we subjected the up-regulated proteins to a bioinformatic analysis by STRING (Figure 7). These proteins are mainly gathered into two main groups including proteins with RNA-binding properties (Figure 7A) and extracellular exosomes-associated proteins (Figure 7B). Taken together, proteomic profiling of Hakai reveals its implication in cytoskeleton-associated proteins, RNA-related proteins, exosomes proteins and protein metabolism (Figure 8).

■ DISCUSSION

The originality of this study deals with the application of an iTRAQ technique to analyze the molecular pathways associated with Hakai overexpression in normal epithelial MDCK cells. This proteomic technique is a powerful method for the

DOI: 10.1021/acs.jproteome.7b00046
J. Proteome Res. XXXX, XXX, XXX−XXX

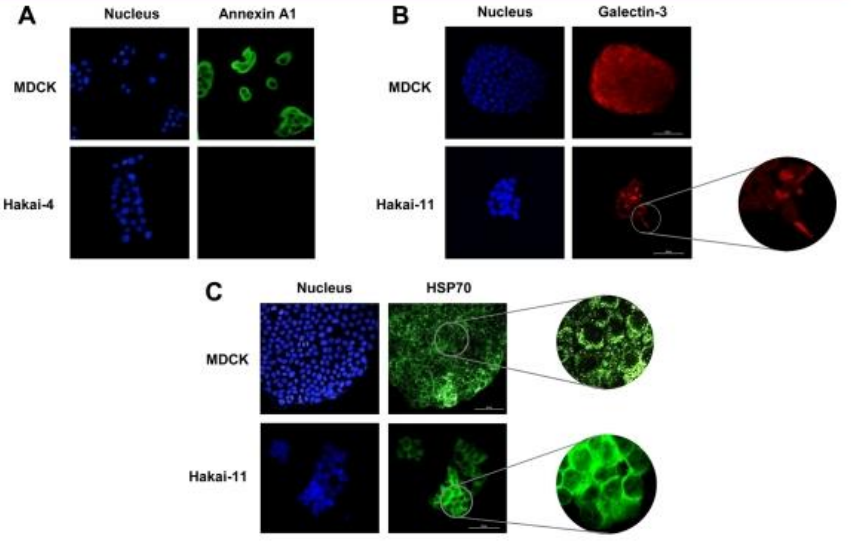

Figure 5. Effect of Hakai overexpression on subcellular localization of Annexin A1, Galectin-3 and HSP70. Parental and Hakai-transformed MDCK cells were examined by confocal microscopy using anti-Annexin A1 (A), anti-Galectin-3 (B) and HSP70 antibodies (C). Photos were observed at 40× optical magnification, including a zoom. Scale bar, 50 μm.

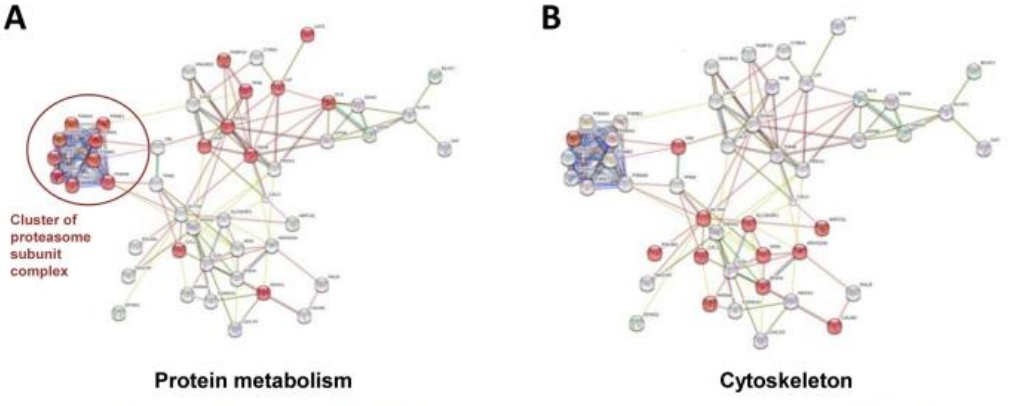

Figure 6. Protein−protein interaction network of the identified under-regulated proteins by Hakai. The STRING database was searched for protein−protein of the connected identified under-regulated proteins in Hakai-transformed MDCK cells compared to normal MDCK ($p < 0.001$). With a confidence cutoff of 0.4, the resulting network contains 138 edges between 63 of the proteins; the proteins with no associations to other proteins in the network were removed. (A) Network of proteins involved in protein metabolism are highlighted in red and represented as *nodes*. Red circle is drawn to indicate the cluster of proteasome subunit complex. Highlighted proteins in red are DLDH, Dihydrolipoyl dehydrogenase, mitochondrial; CATA, Catalase; FKB10, Peptidyl-prolyl cis−trans isomerase FKBP10; PP1B, Serine/threonine-protein phosphatase PP1-beta catalytic subunit; ANXA1, Annexin A1; CALR, Calreticulin; AMPL, Cytosol aminopeptidase; COF1, Cofilin-1; PDIA3, Protein disulfide-isomerase A3; PDIA1, Protein disulfide-isomerase; PSB2, Proteasome subunit beta type 2; PSA2, Proteasome subunit alpha type 2; PSA1, Proteasome subunit alpha type 1; PSA3, Proteasome subunit alpha type 3; PSA7, Proteasome subunit alpha type 7; PSA6, Proteasome subunit alpha type 6; PSA5, Proteasome subunit alpha type 5; PSA4, Proteasome subunit alpha type 4; PSME1, Proteasome activator complex subunit 1. (B) Network of cytoskeleton-related proteins are highlighted in red and represented as nodes. ARP5L, Actin-related protein 2/3 complex subunit 5-like protein; CALM, Calmodulin; VIME, Vimentin; PSME1, Proteasome activator complex subunit 1; ACTN4, Alpha-actinin-4; AHNK, Neuroblast differentiation-associated protein AHNAK; COF1, Cofilin-1; MOES, Moesin; GDIR1, Rho GDP-dissociation inhibitor 1; RHOA, Transforming protein RhoA; NHRF1, Na(+)/H(+) exchange regulatory cofactor NHE-RF1; PDLI1, PDZ and LIM domain protein 1.

DOI: 10.1021/acs.jproteome.7b00046
J. Proteome Res. XXXX, XXX, XXX−XXX

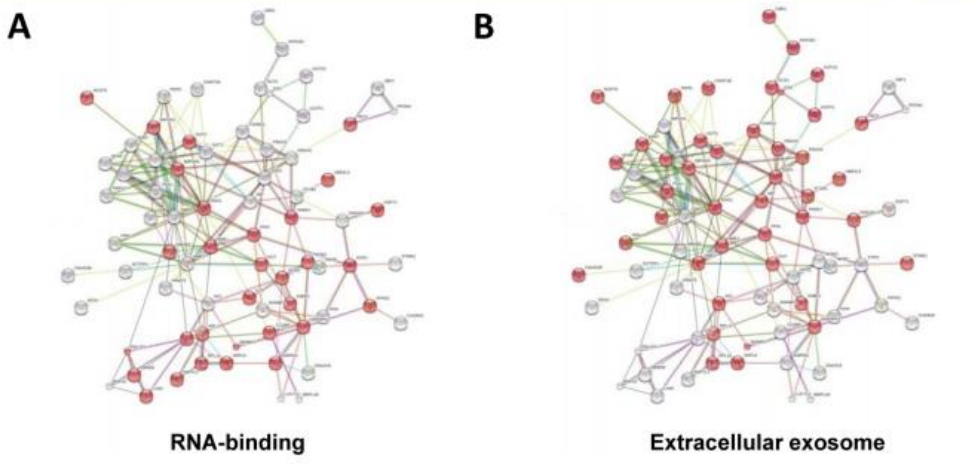

Figure 7. Protein−protein interaction network of the identified up-regulated proteins by Hakai. The STRING database was searched for protein−protein of the connected identified up-regulated proteins in Hakai-transformed MDCK cells compared to normal MDCK ($p < 0.001$). With a confidence cutoff of 0.4, the resulting network contains 179 edges between 82 of the proteins; the proteins with no associations to other proteins in the network were removed. (A) Network of proteins with RNA-binding properties are highlighted in red: NUDT5, ADP-sugar pyrophosphatase; IMDH2, Inosine-5′-monophophate dehydrogenase 2; NDKA, Nucleoside diphosphate kinase A; DUT, Deoxyuridine 5′-triphosphate nucleotidohydrolase, mitochondrial; PPIA, Peptidyl-prolyl cis−trans isomerase A; ROA1, Heterogeneous nuclear ribonucleoprotein A1; RL14, 60S ribosomal protein L14; SRP14, Signal recognition particle 14 kDa protein; PAIRB, Plasminogen activator inhibitor 1 RNA-binding protein; RL12, 60S ribosomal protein L12; AATM, Aspartate aminotransferase, mitochondrial; ENOA, Alpha-enolase; PARK7, Protein DJ-1; TBCA, Tubulin-specific chaperone A; IMDH1, Inosine-5′-monophophate dehydrogenase 1; HMGB2, High mobility group protein B2; STIP1, Stress-induced-phosphoprotein 1; GSTP1, Glutathione S-transferase P; NONO, Non-POU domain-containing octamer-binding protein; SFPQ, Splicing factor, proline- and glutamine-rich; LYAR, Cell growth-regulating nucleolar protein; SSBP, Single-stranded DNA-binding protein, mitochondrial; ILF3, Interleukin enhancer-binding factor 3; UB2L3, Ubiquitin-conjugating enzyme E2 L3; NP1L1, Nucleosome assembly protein 1-like 1; RL1D1, Ribosomal L1 domain-containing protein 1; RBM28, RNA-binding protein 28; RU2A, U2 small nuclear ribonucleoprotein A′; C1QBP, Complement component 1 Q subcomponent-binding protein, mitochondrial; LA, Lupus La protein; PPP5, Serine/threonine-protein phosphatase 5. (B) Protein−protein interaction of extracellular exosomes-associated proteins are highlighted in red and represented as nodes. NUDT5, ADP-sugar pyrophosphatase; MTAP, S-methyl-5′-thioadenosine phosphorylase; PGK1, Phosphoglycerate kinase 1; APT, Adenine phosphoribosyltransferase; IMDH2, Inosine-5′-monophosphate dehydrogenase 2; AATM, Aspartate aminotransferase, mitochondrial; AATC, Aspartate aminotransferase, cytoplasmic; LDHB, L-lactate dehydrogenase B chain; KCRU, Creatine kinase U-type, mitochondrial; STMN1, Stathmin; CBR1, Carbonyl reductase [NADPH] 1; ENOA, Alpha-enolase; NDKB, Nucleoside diphosphate kinase B; NDKA, Nucleoside diphosphate kinase A; RL12, 60S ribosomal protein L12; PRDX4, Peroxiredoxin-4; PRDX5, Peroxiredoxin-5, mitochondrial; GSTO1, Glutathione S-transferase omega-1; GSHB, Glutathione synthetase; GSTP1, Glutathione S-transferase P; LGUL, Lactoylglutathione lyase; ALDR, Aldose reductase; TRXR1, Thioredoxin reductase 1, cytoplasmic; SSBP, Single-stranded DNA-binding protein, mitochondrial; SODC, Superoxide dismutase [Cu−Zn]; TBCA, Tubulin-specific chaperone A; DUT, Deoxyuridine 5′-triphosphate nucleotidohydrolase, mitochondrial; PPIA, Peptidyl-prolyl cis−trans isomerase A; PEPD, Xaa-Pro dipeptidase; IPYR, Inorganic pyrophosphatase; KCRB, Creatine kinase B-type; PARK7, Protein DJ-1; DNJA1, DnaJ homologue subfamily A member 1; CHIP, E3 ubiquitin-protein ligase CHIP; UB2L3, Ubiquitin-conjugatin enzyme E2 L3; NUCL, Nucleolin; RCL, Deoxyribonucleoside 5′-monophosphate N-glycosidase MIF, Macrophage migration inhibitory factor; PAIRB, Plasminogen activator inhibitor 1 RNA-binding protein; RL14, 60S ribosomal protein L14; ROA1, Heterogeneous nuclear ribonucleoprotein A1; SRP14, Signal recognition particle 14 kDa protein.

identification of the molecular pathways involved in Hakai-driven EMT during tumor progression, which provides an accessible way to discover potential related targets and biomarkers that could be used as a tool for diagnosis, prevention or treatment metastatic disease. We believe that this is the first study using iTRAQ to determine the influence of Hakai in epithelial cells during EMT and to find out novel possible molecular pathways whereby Hakai could be involved. The advantage of iTRAQ allows us to identify and quantify the differentially expressed proteins between the experimental conditions. One hundred and forty five proteins were found differentially expressed in a significant manner in Hakai-transformed MDCK cells. A subset of proteins was confirmed to be regulated by an independent semiquantitative method, the western-blotting. By using bioinformatics we have discovered novel molecular pathways on which Hakai may play an important role during tumor progression. Our results confirmed a broad spectrum of identified proteins regulated in Hakai-transformed epithelial cells confirming the crucial impact of Hakai on cytoskeleton-related proteins and RNA-related proteins. Moreover, Hakai was found to regulate many reported extracellular exosome-associated proteins, which are critical mediators of intercellular communication between tumor and stromal cells in local and distant microenvironment, suggesting an implication of Hakai on this process.[40] Finally, Hakai has been found to play an important role in the regulation of cellular metabolism, evidencing a profound decreased expression in many 26S proteasome subunits during Hakai-driven EMT. Given that proteasome inhibitors are increasingly used in cancer treatment for hematopoietic malignancies, our findings highlight a potential risk of these therapeutic approaches in

DOI: 10.1021/acs.jproteome.7b00046
J. Proteome Res. XXXX, XXX, XXX−XXX

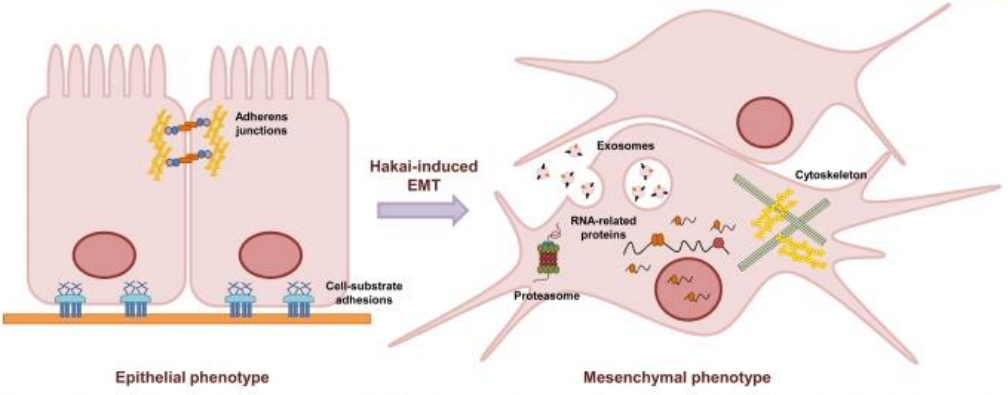

Figure 8. Schematic diagram of altered protein roles by Hakai during transformation of normal epithelial cells. Hakai-induced EMT in MDCK cells may impact on plasticity of the cytoskeleton dynamics, RNA-related protein function, intercellular communication by exosomes, and protein metabolism affecting proteasome system.

carcinoma, as epithelial cells may develop strategies to escape from proteasome inhibitor-based therapy.

Our current understanding of epithelial plasticity has been defined by the discovery of key signaling pathways that regulate the process in several lines and development studies.[5,41] Hakai is an E3 ubiquitin-ligase for E-cadherin that binds to its cytoplasmic domain in a tyrosin phosphorylated dependent manner, driven by v-Src.[15] Our results confirmed that Hakai-transformation in MDCK cells induced a mesenchymal phenotype (Figures 1A), accompanied to a decrease of E-cadherin and an increase of N-cadherin EMT markers (Figure 1B), which in turn it causes a disruption of cell−cell contacts and increase motility.[15] During metastatic process, cancer cells acquire migratory and invasive capabilities for the dissemination through the body to seed secondary tumors at distant sites.[42] Our proteomic results show that an important amount of Hakai down-regulated proteins are related not only to cell−cell adhesion but also to actin-cytoskeleton dynamics, which have an impact on cell plasticity, motility and invasion. Proteins such as Annexin A1, Annexin A2, alpha-actinin-4, Ezrin, Moesin and others are included in these groups of regulated proteins (Figure 5B, Table 1). Moreover, during EMT, besides changing their adhesive repertoire and the actin-cytoskeleton reorganization, cancer cells form membrane protrusion (lamellipodia, filopodia, invadopodia and podosomes) required for invasive growth to gain migratory and invasive properties.[42] Arp2/3 complex, Ahnak, α-actinin and cofilin are also down-regulated proteins in Hakai-overexpressing cells which are critical regulators of pseudopodial actin dynamics control during cell plasticity in tumor progression.[43] Several of these identified down-regulated proteins were reported to be down-regulated during EMT or cancer invasion. For example, Annexin A1 attenuates EMT and metastatic potential in breast cancer, Prelamin A prevents cancer cell invasiveness and accelerates aging syndromes and Anhak functions as tumor suppressor through potentiation of TGF-β1, an important regulator of EMT.[44−46]

In our proteomic study, we have also identified Cortactin. This protein was previously reported as Hakai-interacting protein phosphorylated by Src suggesting that Hakai could act as an E3 ubiquitin-ligase for this substrate. Hakai and Cortactin interaction was also confirmed by immunoprecipitation, although the physiological meaning of these interaction is still unknown.[29] Cortactin is one of the major substrates for tyrosine kinases such as Src and is mainly distributed in cell motility structures such as lamellipodia and invadopodia.[47] Although, in our proteomic study we did not detect statistical difference, we confirmed a down-regulation of Cortactin protein in Hakai-transformed MDCK cells. These data suggest that Hakai may induce Cortactin ubiquitination and degradation in a phosphorylation-dependent manner. Previous results showed a decrease in the levels of tyrosine-phosphorylated Cortactin during EMT driven by TGF-β1. Moreover, knock-down of Cortactin led to a disruption of tight and adherent junctions, causing an enhancement of TGF-β1-induced EMT and increased the migratory capacity of AML-12 cells.[47] In Hakai-overexpressing MDCK cells it is shown by time-lapse microscopic analyses a spiky protrusions, dynamically extended and retracted.[19] Furthermore, Hakai influence on motility was also reported in vivo.[22] In *D. melanogaster* high levels of Hakai were detected in migrating endoderm cells. Given that endoderm epithelia do not express E-cadherin, it was proposed that additional *Drosophila* Hakai targets should be involved in cell adhesion and migration during embryonic development. Given that Hakai is enriched at the end of the protrusions it is plausible that Hakai modulate the turnover of adhesion and cytoskeleton-related proteins in different localizations exerting an influence in cell motility and invasion.[19]

On the other hand, an increase of proteins associated with extracellular exosomes is detected by using STRING database (Figure 7B). This fact opens an interesting possibility to research the role of the E3 ubiquitin-ligase Hakai in cancer exosomes. It has been published that post-translational modifications are involved in the sorting of specific proteins into exosomes.[48] Indeed, an ubiquitin-like modification ISGylation, controls exosome release in vitro and in vivo studies.[49] Further studies are needed to elucidate whether Hakai may exert an effect on exosome release during cancer metastasis. Importantly, our study also reveals a significant Hakai influence on RNA-related proteins (Figure 1A). Proteins such as hnRNPA1, PAIRB, LYAR, ROA1 or Galectin-3 (Table 2) constitute a network of upregulated RNA binding-proteins

DOI: 10.1021/acs.jproteome.7b00046
J. Proteome Res. XXXX, XXX, XXX−XXX

by Hakai overexpression (Figure 7A). It was previously reported the importance of post-transcriptional control by RNA-binding proteins on EMT.[11,50] In 2009 it was described that Hakai promotes tumorigenesis by enhancing RNA-binding functions of the polypyrimidine tract-binding protein-associated splicing factor (PSF). Hakai altered PSF ability to bind specific cancer-associated mRNAs, however, it is not demonstrated that Hakai can induce ubiquitination of PSF.[19,31] Given that Hakai is localized in the nucleus and that other E3 ubiquitin-ligases have been shown to play a role in the nucleus, our findings suggest that Hakai may influence cell phenotype, independent of its E3 ubiquitin-ligase activity, and may play different role in the nucleus or in the cytoplasm, as previously shown.[51]

Finally, our proteomic study identified a subset of down-regulated proteins involved in cellular metabolism (Table 1). Interestingly, STRING database highlights an specific and well interconected cluster of proteasome subunits (Figure 6A), including 9 proteins belonging to the 26 proteasome (Table 3). According to this data, a recent publication demonstrate that epithelial cells decrease their proteasome activity during EMT and how proteasome inhibitors induce EMT.[52] While many patients with hematopoietic malignancies respond to the proteasome inhibitor bortezomib, clinical trials investigating the use of proteasome inhibitors for solid tumors have thus far been disappointing.[53,54] Authors results also suggest the possibility that pharmacologic inhibition of the proteasome may not only induce EMT in breast cancer cells, but may also endow them with an enhanced capacity to survive.[52] Although the ubiquitination is one of the main mechanisms to target cytosolic or nuclear proteins for degradation via proteasome, many membrane proteins have triggered for degradation into lysosomes. Degradation into lysosomes in a ubiquitination-dependent manner was first published in *Saccharomyces cerevisiae*.[55] Ubiquitin-tagged E-cadherin is essential for its sorting into lysosome under Src activation in MDCK cells, facilitating the dissolution of adherens junctions and ensuring cells remain motile.[16] Given the specific downregulation of proteasome subunits found in Hakai-transformed cells, and that Hakai expression is markedly higher in human gastric and colon adenocarcinoma compared to normal tissues, our data reinforce the previous reported work[52] supporting that proteasome inhibitors may not be the effective treatment in tumor subtypes that follow EMT. Although our work has been developed in a cellular model system and further analysis need to be performed in human clinical specimens, we propose that the E3 ubiquitin-ligases, such as Hakai, may be a better target than proteasome for an effective therapeutic strategy in tumor subtypes that follow EMT which allow to avoid carcinoma cells to develop strategies to escape from proteasome inhibitor-based therapy.

■ CONCLUSIONS

Hakai-driven EMT plays an important role in plasticity of the cytoskeleton dynamics, post-transcriptional regulation, protein metabolism, and exosome-associated proteins. Moreover, Hakai-transformed epithelial cells specifically down-regulate proteasome subunits suggesting that targeting E3 ubiquitin-ligase Hakai may be a more effective therapeutic strategy for solid tumors rather than using proteasome inhibitors in specific tumors subtypes that follow EMT.

■ ASSOCIATED CONTENT

Supporting Information

The Supporting Information is available free of charge on the ACS Publications website at DOI: 10.1021/acs.jproteome.7b00046.

Figure S1: HPLC setup (PDF)

Table S1: List of identified proteins (XLSX)

■ AUTHOR INFORMATION

Corresponding Author

*Phone: +34-981-176399. E-mail: angelica.figueroa.conde-valvis@sergas.es.

ORCID

Angélica Figueroa: 0000-0001-5530-5213

Notes

The authors declare no competing financial interest.

■ ACKNOWLEDGMENTS

This work has been supported by Plan Estatal I + D + I 2013−2016, cofunded by the Instituto Carlos III (ISCIII, Spain)—Fondo Europeo de Desarrollo Regional (FEDER) "A way of Making Europe" (PI13/00250) and by Red Gallega de Investigación sobre Cáncer Colorrectal (REGICC), Consellería de Cultura, Educación e Ordenación Universitaria (R2014/039), Xunta de Galicia. Diaz−Diaz has been supported by FPU contract (FPU014/02837) from Ministerio de Educación, Cultura y Deporte from Spain.

■ REFERENCES

(1) Hanahan, D.; Weinberg, R. A. The hallmarks of cancer. *Cell* **2000**, *100* (1), 57−70.

(2) Nieto, M. A. Epithelial plasticity: a common theme in embryonic and cancer cells. *Science* **2013**, *342*, 1234850.

(3) Zeisberg, M.; Yang, C.; Martino, M.; Duncan, M. B.; Rieder, F.; Tanjore, H.; Kalluri, R. Fibroblasts derive from hepatocytes in liver fibrosis via epithelial to mesenchymal transition. *J. Biol. Chem.* **2007**, *282*, 23337−47.

(4) Aparicio, L. A.; Blanco, M.; Castosa, R.; Concha, Á.; Valladares, M.; Calvo, L.; Figueroa, A. Clinical implications of epithelial cell plasticity in cancer progression. *Cancer Lett.* **2015**, *366*, 1−10.

(5) Thiery, J. P.; Sleeman, J. P. Complex networks orchestrate epithelial-mesenchymal transitions. *Nat. Rev. Mol. Cell Biol.* **2006**, *7*, 131−42.

(6) Umbas, R.; Isaacs, W. B.; Bringuier, P. P.; Schaafsma, H. E.; Karthaus, H. F.; Oosterhof, G. O.; Debruyne, F. M.; Schalken, J. A. Decreased E-cadherin expression is associated with poor prognosis in patients with prostate cancer. *Cancer Res.* **1994**, *54*, 3929−33.

(7) Li, B.; Shi, H.; Wang, F.; Hong, D.; Lv, W.; Xie, X.; Cheng, X. Expression of E-, P- and N-Cadherin and Its Clinical Significance in Cervical Squamous Cell Carcinoma and Precancerous Lesions. *PLoS One* **2016**, *11*, e0155910.

(8) Tsanou, E.; Peschos, D.; Batistatou, A.; Charalabopoulos, A.; Charalabopoulos, K. The E-cadherin adhesion molecule and colorectal cancer. A global literature approach. *Anticancer Res.* **2008**, *28*, 3815−26.

(9) Perl, A. K.; Wilgenbus, P.; Dahl, U.; Semb, H.; Christofori, G. A causal role for E-cadherin in the transition from adenoma to carcinoma. *Nature* **1998**, *392*, 190−3.

(10) Kalluri, R.; Weinberg, R. A. The basics of epithelial-mesenchymal transition. *J. Clin. Invest.* **2009**, *119*, 1420−8.

(11) Aparicio, L. A.; Abella, V.; Valladares, M.; Figueroa, A. Posttranscriptional regulation by RNA-binding proteins during

DOI: 10.1021/acs.jproteome.7b00046
J. Proteome Res. XXXX, XXX, XXX−XXX

epithelial-to-mesenchymal transition. *Cell. Mol. Life Sci.* **2013**, *70*, 4463−4477.
(12) Batlle, E.; Sancho, E.; Francí, C.; Domínguez, D.; Monfar, M.; Baulida, J.; García De Herreros, A. The transcription factor snail is a repressor of E-cadherin gene expression in epithelial tumour cells. *Nat. Cell Biol.* **2000**, *2*, 84−9.
(13) Cano, A.; Pérez-Moreno, M. A.; Rodrigo, I.; Locascio, A.; Blanco, M. J.; del Barrio, M. G.; Portillo, F.; Nieto, M. A. The transcription factor snail controls epithelial-mesenchymal transitions by repressing E-cadherin expression. *Nat. Cell Biol.* **2000**, *2*, 76−83.
(14) Chaffer, C. L.; San Juan, B. P.; Lim, E.; Weinberg, R. A. EMT, cell plasticity and metastasis. *Cancer Metastasis Rev.* **2016**, *35*, 645−654.
(15) Fujita, Y.; Krause, G.; Scheffner, M.; Zechner, D.; Leddy, H.; Behrens, J.; Sommer, T.; Birchmeier, W. Hakai, a c-Cbl-like protein, ubiquitinates and induces endocytosis of the E-cadherin complex. *Nat. Cell Biol.* **2002**, *4*, 222−31.
(16) Palacios, F.; Tushir, J.; Fujita, Y.; D'Souza-Schorey, C. Lysosomal targeting of E-cadherin: a unique mechanism for the down-regulation of cell-cell adhesion during epithelial to mesenchymal transitions. *Mol. Cell. Biol.* **2005**, *25*, 389−402.
(17) Zhou, W. J.; Geng, Z. H.; Chi, S.; Zhang, W.; Niu, X. F.; Lan, S. J.; Ma, L.; Yang, X.; Wang, L. J.; Ding, Y. Q.; Geng, J. G. Slit-Robo signaling induces malignant transformation through Hakai-mediated E-cadherin degradation during colorectal epithelial cell carcinogenesis. *Cell Res.* **2011**, *21*, 609−26.
(18) Cooper, J. A.; Kaneko, T.; Li, S. S. Cell regulation by phosphotyrosine-targeted ubiquitin ligases. *Mol. Cell. Biol.* **2015**, *35*, 1886−97.
(19) Figueroa, A.; Kotani, H.; Toda, Y.; Mazan-Mamczarz, K.; Mueller, E.; Otto, A.; Disch, L.; Norman, M.; Ramdasi, R.; Keshtgar, M.; Gorospe, M.; Fujita, Y. Novel roles of hakai in cell proliferation and oncogenesis. *Mol. Biol. Cell* **2009**, *20*, 3533−42.
(20) Abella, V.; Valladares, M.; Rodriguez, T.; Haz, M.; Blanco, M.; Tarrio, N.; Iglesias, P.; Aparicio, L. A.; Figueroa, A. miR-203 Regulates Cell Proliferation through Its Influence on Hakai Expression. *PLoS One* **2012**, *7*, e52568.
(21) Janda, E.; Nevolo, M.; Lehmann, K.; Downward, J.; Beug, H.; Grieco, M. Raf plus TGFbeta-dependent EMT is initiated by endocytosis and lysosomal degradation of E-cadherin. *Oncogene* **2006**, *25*, 7117−30.
(22) Kaido, M.; Wada, H.; Shindo, M.; Hayashi, S. Essential requirement for RING finger E3 ubiquitin ligase Hakai in early embryonic development of Drosophila. *Genes Cells* **2009**, *14*, 1067−77.
(23) Rodríguez-Rigueiro, T.; Valladares-Ayerbes, M.; Haz-Conde, M.; Aparicio, L. A.; Figueroa, A. Hakai reduces cell-substratum adhesion and increases epithelial cell invasion. *BMC Cancer* **2011**, *11*, 474.
(24) Swaminathan, G.; Cartwright, C. A. Rack1 promotes epithelial cell-cell adhesion by regulating E-cadherin endocytosis. *Oncogene* **2012**, *31*, 376−89.
(25) Aparicio, L. A.; Valladares, M.; Blanco, M.; Alonso, G.; Figueroa, A. Biological influence of Hakai in cancer: a 10-year review. *Cancer Metastasis Rev.* **2012**, *31*, 375−386.
(26) Aparicio, L. A.; Castosa, R.; Haz-Conde, M.; Rodríguez, M.; Blanco, M.; Valladares, M.; Figueroa, A. Role of the microtubule-targeting drug vinflunine on cell-cell adhesions in bladder epithelial tumour cells. *BMC Cancer* **2014**, *14*, 507.
(27) Deep, G.; Gangar, S.; Agarwal, C.; Agarwal, R. Role of E-cadherin in anti-migratory and anti-invasive efficacy of silibinin in prostate cancer cells. *Cancer Prev. Res.* **2011**, *4*, 1222−32.
(28) Mukherjee, M.; Jing-Song, F.; Ramachandran, S.; Guy, G. R.; Sivaraman, J. Dimeric switch of Hakai-truncated monomers during substrate recognition: insights from solution studies and NMR structure. *J. Biol. Chem.* **2014**, *289*, 25611−23.
(29) Mukherjee, M.; Chow, S. Y.; Yusoff, P.; Seetharaman, J.; Ng, C.; Sinniah, S.; Koh, X. W.; Asgar, N. F.; Li, D.; Yim, D.; Jackson, R. A.; Yew, J.; Qian, J.; Iyu, A.; Lim, Y. P.; Zhou, X.; Sze, S. K.; Guy, G. R.; Sivaraman, J. Structure of a novel phosphotyrosine-binding domain in Hakai that targets E-cadherin. *EMBO J.* **2012**, *31*, 1308−19.
(30) Rodriguez-Rigueiro, T.; Valladares-Ayerbes, M.; Haz-Conde, M.; Blanco, M.; Aparicio, G.; Fernandez-Puente, P.; Blanco, F. J.; Jose Lorenzo, M.; Aparicio, L. A.; Figueroa, A. A novel procedure for protein extraction from formalin-fixed paraffin-embedded tissues. *Proteomics* **2011**, *11*, 2555−2559.
(31) Figueroa, A.; Fujita, Y.; Gorospe, M. Hacking RNA: Hakai promotes tumorigenesis by enhancing the RNA-binding function of PSF. *Cell Cycle* **2009**, *8*, 3648−51.
(32) Horiuchi, K.; Kawamura, T.; Iwanari, H.; Ohashi, R.; Naito, M.; Kodama, T.; Hamakubo, T. Identification of Wilms' tumor 1-associating protein complex and its role in alternative splicing and the cell cycle. *J. Biol. Chem.* **2013**, *288*, 33292−302.
(33) Thiery, J. P. Epithelial-mesenchymal transitions in tumour progression. *Nat. Rev. Cancer* **2002**, *2*, 442−54.
(34) Calamia, V.; Rocha, B.; Mateos, J.; Fernández-Puente, P.; Ruiz-Romero, C.; Blanco, F. J. Metabolic labeling of chondrocytes for the quantitative analysis of the interleukin-1-beta-mediated modulation of their intracellular and extracellular proteomes. *J. Proteome Res.* **2011**, *10*, 3701−11.
(35) Fernández-Puente, P.; Mateos, J.; Fernández-Costa, C.; Oreiro, N.; Fernández-López, C.; Ruiz-Romero, C.; Blanco, F. J. Identification of a panel of novel serum osteoarthritis biomarkers. *J. Proteome Res.* **2011**, *10*, 5095−101.
(36) Shilov, I. V.; Seymour, S. L.; Patel, A. A.; Loboda, A.; Tang, W. H.; Keating, S. P.; Hunter, C. L.; Nuwaysir, L. M.; Schaeffer, D. A. The Paragon Algorithm, a next generation search engine that uses sequence temperature values and feature probabilities to identify peptides from tandem mass spectra. *Mol. Cell. Proteomics* **2007**, *6*, 1638−55.
(37) Gan, C. S.; Chong, P. K.; Pham, T. K.; Wright, P. C. Technical, experimental, and biological variations in isobaric tags for relative and absolute quantitation (iTRAQ). *J. Proteome Res.* **2007**, *6*, 821−7.
(38) Lauffenburger, D. A.; Horwitz, A. F. Cell migration: a physically integrated molecular process. *Cell* **1996**, *84*, 359−69.
(39) Franceschini, A.; Szklarczyk, D.; Frankild, S.; Kuhn, M.; Simonovic, M.; Roth, A.; Lin, J.; Minguez, P.; Bork, P.; von Mering, C.; Jensen, L. J. STRING v9.1: protein-protein interaction networks, with increased coverage and integration. *Nucleic Acids Res.* **2013**, *41*, D808−15.
(40) Becker, A.; Thakur, B. K.; Weiss, J. M.; Kim, H. S.; Peinado, H.; Lyden, D. Extracellular Vesicles in Cancer: Cell-to-Cell Mediators of Metastasis. *Cancer Cell* **2016**, *30*, 836−848.
(41) Gotzmann, J.; Mikula, M.; Eger, A.; Schulte-Hermann, R.; Foisner, R.; Beug, H.; Mikulits, W. Molecular aspects of epithelial cell plasticity: implications for local tumor invasion and metastasis. *Mutat. Res., Rev. Mutat. Res.* **2004**, *566*, 9−20.
(42) Yilmaz, M.; Christofori, G. EMT, the cytoskeleton, and cancer cell invasion. *Cancer Metastasis Rev.* **2009**, *28*, 15−33.
(43) Shankar, J.; Messenberg, A.; Chan, J.; Underhill, T. M.; Foster, L. J.; Nabi, I. R. Pseudopodial actin dynamics control epithelial-mesenchymal transition in metastatic cancer cells. *Cancer Res.* **2010**, *70*, 3780−90.
(44) Maschler, S.; Gebeshuber, C. A.; Wiedemann, E. M.; Alacakaptan, M.; Schreiber, M.; Custic, I.; Beug, H. Annexin A1 attenuates EMT and metastatic potential in breast cancer. *EMBO Mol. Med.* **2010**, *2*, 401−14.
(45) de la Rosa, J.; Freije, J. M.; Cabanillas, R.; Osorio, F. G.; Fraga, M. F.; Fernández-García, M. S.; Rad, R.; Fanjul, V.; Ugalde, A. P.; Liang, Q.; Prosser, H. M.; Bradley, A.; Cadiñanos, J.; López-Otín, C. Prelamin A causes progeria through cell-extrinsic mechanisms and prevents cancer invasion. *Nat. Commun.* **2013**, *4*, 2268.
(46) Lee, I. H.; Sohn, M.; Lim, H. J.; Yoon, S.; Oh, H.; Shin, S.; Shin, J. H.; Oh, S. H.; Kim, J.; Lee, D. K.; Noh, D. Y.; Bae, D. S.; Seong, J. K.; Bae, Y. S. Ahnak functions as a tumor suppressor via modulation of TGFβ/Smad signaling pathway. *Oncogene* **2014**, *33*, 4675−84.
(47) Zhang, K.; Wang, D.; Song, J. Cortactin is involved in transforming growth factor-beta1-induced epithelial-mesenchymal

DOI: 10.1021/acs.jproteome.7b00046
J. Proteome Res. XXXX, XXX, XXX−XXX

transition in AML-12 cells. *Acta Biochim. Biophys. Sin.* **2009**, *41*, 839–45.
(48) Villarroya-Beltri, C.; Baixauli, F.; Gutiérrez-Vázquez, C.; Sánchez-Madrid, F.; Mittelbrunn, M. Sorting it out: regulation of exosome loading. *Semin. Cancer Biol.* **2014**, *28*, 3–13.
(49) Villarroya-Beltri, C.; Baixauli, F.; Mittelbrunn, M.; Fernández-Delgado, I.; Torralba, D.; Moreno-Gonzalo, O.; Baldanta, S.; Enrich, C.; Guerra, S.; Sánchez-Madrid, F. ISGylation controls exosome secretion by promoting lysosomal degradation of MVB proteins. *Nat. Commun.* **2016**, *7*, 13588.
(50) Burk, U.; Schubert, J.; Wellner, U.; Schmalhofer, O.; Vincan, E.; Spaderna, S.; Brabletz, T. A reciprocal repression between ZEB1 and members of the miR-200 family promotes EMT and invasion in cancer cells. *EMBO Rep.* **2008**, *9*, 582–9.
(51) Shrestha, H.; Ryu, T.; Seo, Y. W.; Park, S. Y.; He, Y.; Dai, W.; Park, E.; Simkhada, S.; Kim, H.; Lee, K.; Kim, K. Hakai, an E3-ligase for E-cadherin, stabilizes δ-catenin through Src kinase. *Cell. Signalling* **2017**, *31*, 135–145.
(52) Banno, A.; Garcia, D. A.; van Baarsel, E. D.; Metz, P. J.; Fisch, K.; Widjaja, C. E.; Kim, S. H.; Lopez, J.; Chang, A. N.; Geurink, P. P.; Florea, B. I.; Overkleeft, H. S.; Ovaa, H.; Bui, J. D.; Yang, J.; Chang, J. T. Downregulation of 26S proteasome catalytic activity promotes epithelial-mesenchymal transition. *Oncotarget* **2016**, *7*, 21527–41.
(53) Aghajanian, C.; Blessing, J. A.; Darcy, K. M.; Reid, G.; DeGeest, K.; Rubin, S. C.; Mannel, R. S.; Rotmensch, J.; Schilder, R. J.; Riordan, W.; Group, G. O. A phase II evaluation of bortezomib in the treatment of recurrent platinum-sensitive ovarian or primary peritoneal cancer: a Gynecologic Oncology Group study. *Gynecol. Oncol.* **2009**, *115*, 215–20.
(54) Rosenberg, J. E.; Halabi, S.; Sanford, B. L.; Himelstein, A. L.; Atkins, J. N.; Hohl, R. J.; Millard, F.; Bajorin, D. F.; Small, E. J.; B, C. a. L. G. Phase II study of bortezomib in patients with previously treated advanced urothelial tract transitional cell carcinoma: CALGB 90207. *Ann. Oncol* **2008**, *19*, 946–50.
(55) Hicke, L.; Riezman, H. Ubiquitination of a yeast plasma membrane receptor signals its ligand-stimulated endocytosis. *Cell* **1996**, *84*, 277–87.

DOI: 10.1021/acs.jproteome.7b00046
J. Proteome Res. XXXX, XXX, XXX–XXX

cancers

MDPI

Article

Heat Shock Protein 90 Chaperone Regulates the E3 Ubiquitin-Ligase Hakai Protein Stability

Andrea Díaz-Díaz [1], Daniel Roca-Lema [1], Alba Casas-Pais [1], Gabriela Romay [1], Giovanni Colombo [2], Ángel Concha [3], Begoña Graña [4] and Angélica Figueroa [1,*]

[1] Epithelial Plasticity and Metastasis Group, Instituto de Investigación Biomédica de A Coruña (INIBIC), Complexo Hospitalario Universitario de A Coruña (CHUAC), Sergas, Universidade da Coruña (UDC), 15006 A Coruña, Spain; andrea.diaz.diaz@sergas.es (A.D.-D.); Daniel.roca.lema@sergas.es (D.R.-L.); alba.casas.pais@sergas.es (A.C.-P.); Gabriela.Romay.Cousido@sergas.es (G.R.)

[2] Istituto per la Ricerca e l'Innovazione Biomedica (IRIB)—CNR di Palermo, Via Ugo La Malfa 153, 90146 Palermo, Italy; giovanni.colombo@community.unipa.it

[3] Pathology Department and A Coruña Biobank from Instituto de Investigación Biomédica de A Coruña (INIBIC), Complexo Hospitalario Universitario de A Coruña (CHUAC), Sergas, Universidade da Coruña (UDC), 15006 A Coruña, Spain; angel.concha.lopez@sergas.es

[4] Clinical Oncology Group, Instituto de Investigación Biomédica de A Coruña (INIBIC), Complexo Hospitalario Universitario de A Coruña (CHUAC), Sergas, Universidade da Coruña (UDC), 15006 A Coruña, Spain; Begona.Grana.Suarez@sergas.es

* Correspondence: Angelica.Figueroa.Conde-Valvis@sergas.es

Received: 17 December 2019; Accepted: 12 January 2020; Published: 15 January 2020

Abstract: The E3 ubiquitin-ligase Hakai binds to several tyrosine-phosphorylated Src substrates, including the hallmark of the epithelial-to-mesenchymal transition E-cadherin, and signals for degradation of its specific targets. Hakai is highly expressed in several human cancers, including colon cancer, and is considered as a drug target for cancer therapy. Here, we report a link between Hakai and the heat shock protein 90 (Hsp90) chaperone complex. Hsp90 participates in the correct folding of its client proteins, allowing them to maintain their stability and activity. Hsp90 inhibitors specifically interfere with the association with its Hsp90 client proteins, and exhibit potent anti-cancer properties. By immunoprecipitation, we present evidence that Hakai interacts with Hsp90 chaperone complex in several epithelial cells and demonstrate that is a novel Hsp90 client protein. Interestingly, by overexpressing and knocking-down experiments with Hakai, we identified Annexin A2 as a Hakai-regulated protein. Pharmacological inhibition of Hsp90 with geldanamycin results in the degradation of Hakai in a lysosome-dependent manner. Interestingly, geldanamycin-induced Hakai degradation is accompanied by an increased expression of E-cadherin and Annexin A2. We also show that geldanamycin suppresses cell motility at least in part through its action on Hakai expression. Taken together, our results identify Hakai as a novel Hsp90 client protein and shed light on the regulation of Hakai stability. Our results open the possibility to the potential use of Hsp90 inhibitors for colorectal cancer therapy through its action on Hakai client protein of Hsp90.

Keywords: Hsp90 chaperone; E3 ubiquitin-ligase Hakai; targeted therapy; colon cancer

1. Introduction

Hsp90 (90-KDa heat shock protein) is a molecular chaperone involved in the correct folding of a selected group of proteins, named as client proteins, allowing them to maintain their proper conformation and the preservation of their activity [1]. The regulation of Hsp90 client proteins not only plays a crucial role in several cellular processes, such as cell cycle control, apoptosis and cell

survival, but also contributes to the development of pathological conditions, such as neurodegenerative and infectious disease or cancer [2]. Indeed, many client proteins of Hsp90 are oncogenes, mutated or overexpressed, which are important for tumor malignant progression [3]. The activation of Hsp90 client proteins occurs in an ATP-dependent manner [4]. The small-molecule inhibitor geldanamycin (GA), a benzoquinone ansamycin antibiotic, occupies the ATP binding-pocket of Hsp90, specifically interfering on the association with its client proteins. The general described dissociation between Hsp90 and their client proteins results on the degradation of the clients by the ubiquitin-dependent proteasome pathway [5–7]. However, new findings provide evidence of an autophagy-dependent mechanism [8]. A quantitative high-throughput analysis of the Hsp90-client proteins interactions reveals that only 7% are transcription factors, 30% are human ubiquitin-ligases and 60% kinases [1,9]. Therefore, it is reasonable to assume that additional E3 ubiquitin-ligases that associates to Hsp90 await to be elucidated.

Hakai is a new class of the three families of RING-finger type E3 ubiquitin-ligases that contains a novel domain called HYB (Hakai pTyr-binding) whereby it interacts with the tyrosine-phosphorylated substrates inducing their ubiquitination and degradation [10,11]. So far, the best-characterized substrate for Hakai is E-cadherin. Hakai interacts with the Src tyrosine-phosphorylated E-cadherin, inducing its ubiquitination and degradation, which in turn causes the alteration of cell–cell contacts [12,13]. E-cadherin is the best-characterized member of the adherens junctions and its loss at cell–cell adhesions is a well stablished hallmark of the epithelial-to-mesenchymal transition during tumor progression and metastasis [14,15]. Hakai is not only involved in the regulation of cell–cell adhesions but also in regulating cell proliferation, cell motility and invasion [16,17]. Importantly, Hakai is highly expressed in colon and lung cancer compared to human healthy tissues [18–20]. Additional target proteins for Hakai, such as Cortactin or DOK1, have been identified, however, the functional significance is still unknown [10]. Recently, we employed an iTRAQ approach and found differentially regulated proteins in epithelial MDCK cell lines stably expressing Hakai compared to non-transformed MDCK cells. Interestingly, several membrane-binding proteins, including Annexin A2, were confirmed to be decreased in Hakai-overexpressing cells while other proteins, such as Hsp90 chaperone, were slightly increased [21].

In this paper, we were interested to understand the meaning of the link between the E3 ubiquitin-ligases Hakai and Hsp90 chaperone complex. Here, we demonstrate that the E3 ubiquitin-ligase is a novel client protein for Hsp90. Pharmacological inhibition of Hsp90 with geldanamycin disrupts this interaction, and induces Hakai degradation via lysosome, which in consequence is accompanied by an increased expression of E-cadherin and Annexin A2. Importantly, geldanamycin reduces Hakai-induced cell migration, further underscoring the possible impact of Hsp90 inhibitors in tumor progression by its action on Hakai stability.

2. Results

2.1. Hsp90 Chaperone Interacts with Hakai

In a proteomic study conducted for the search of interacting proteins with Hsp90, Taipale and collaborators showed that, far from expected, more than 100 proteins were E3 ubiquitin-ligases [1,9]. However, only few of these interactions have been demonstrated, such as the interaction with the E3 ubiquitin ligases Cullin-5 or CHIP, [22,23]. Given that we have previously shown a regulation of Hsp70 and Hsp90 chaperones in Hakai stably expressing MDCK epithelial cells compared to non-transformed epithelial cells [21], we decided to evaluate whether Hakai could be among the E3 ubiquitin ligases interacting proteins with these chaperones. In a first experiment, we immunoprecipitated endogenous Hakai using several different cell lines, including HEK293T, ACHN, HT29 and HCT116 (Figure 1, Supplementary Figure S4). Co-immunoprecipitation of Hakai and Hsp90, but not Hsp70 was detected in all four cell lines tested.

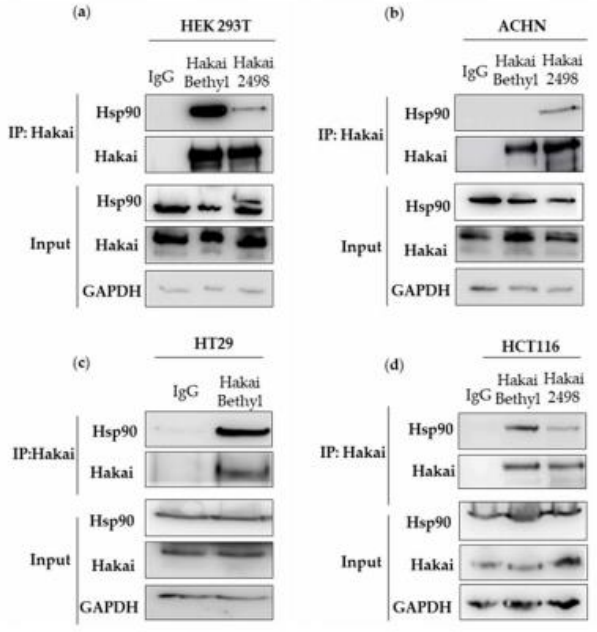

Figure 1. Hakai interacts with heat shock protein 90 (Hsp90): Co-immunoprecipitation of Hakai and Hsp90 was performed in different cell lines: (**a**) HEK293T. (**b**) ACHN. (**c**) HT29. (**d**) HCT116. Hakai immunoprecipitation was performed by employing two different rabbit polyclonal Hakai antibodies indicated in material an methods: one from Bethyl (Bethyl Ab) and one kindly provided by Dr. Fujita (Hakai-2498). GAPDH signal was used as protein loading control.

Moreover, the analysis of Hakai interactome in HCT116, by employing endogenous Hakai immunoprecipitation following by nano-flow liquid chromatography (LC) coupled to a triple TOF Mass Spectrometer, also identified Hakai and Hsp90 proteins in Hakai immunoprecipitation samples compared to IgG control sample, further confirming the interaction between these two proteins. However, no effect on Hsp90 protein levels was detected when Hakai was transiently transfected in HEK293T cells in a concentration-dependent manner (Supplementary Figures S1a and S10) neither in a time-dependent manner (Figure S1b, Supplementary Figure S10). Similarly, we neither detected any effect on Hakai expression by transiently transfecting increasing amounts of Hsp90 (Supplementary Figures S1c and S10). Since we previously demonstrated that Hakai is highly expressed in human colon cancer tissues compared to healthy colon tissues, we also analyzed the possible co-localization by using HT29, LoVo and HCT116 colon cancer cell lines. Endogenous Hakai is highly detected in the nucleus and less intense signal is observed in the cytoplasm, where it is described to exert its E3 ubiquitin-ligase activity. Hsp90 is clearly localized throughout the whole cytoplasm where co-localization with Hakai is slightly detected in HT29 and Lovo cells, with an enriched signal detected in perinuclear areas (Supplementary Figure S2).

2.2. Interaction between Hsp90, Hakai and Annexin A2

It is generally reported that chaperone-interacting E3 ubiquitin-ligases induce the degradation of the chaperone client proteins that have not been correctly folded [22–24]. Therefore, it is reasonable to assume that additional E3 ubiquitin-ligases are involved in the degradation of HSP90 clients. Given the interaction confirmed between Hakai and Hsp90, our findings led us to ask whether Hakai may also participate in the regulation of other Hsp90 client proteins. Annexin A2 was one of the proteins

detected in a proteomic study that turned out to be downregulated in Hakai-overexpressing MDCK cells compared to non-transformed MDCK epithelial cells [21]. In addition, it has been reported that Annexin A2 co-immunoprecipitates with Hsp90 [25]. Annexin A2 is a calcium-binding protein reported to be implicated in membrane and vesicle trafficking [26]. Considering these premises, we further analyze the possible interaction between these three proteins. Endogenous interaction of Hsp90 with Hakai and Annexin A2 was confirmed in HCT116 cells. Immunoprecipitation of endogenous Hakai co-precipitated with endogenous Hsp90 (Figure 2a, Supplementary Figure S5). Endogenous Annexin A2 also co-precipitated with endogenous Hakai (Figure 2b, Supplementary Figure S5). Conversely, immunoprecipitation of Annexin A2 also co-precipitated with endogenous Hsp90 (Figure 2c, Supplementary Figure S5). These results confirm that Hakai, Hsp90 and Annexin A2 form an interacting protein complex, either mediated by a direct or indirect interaction.

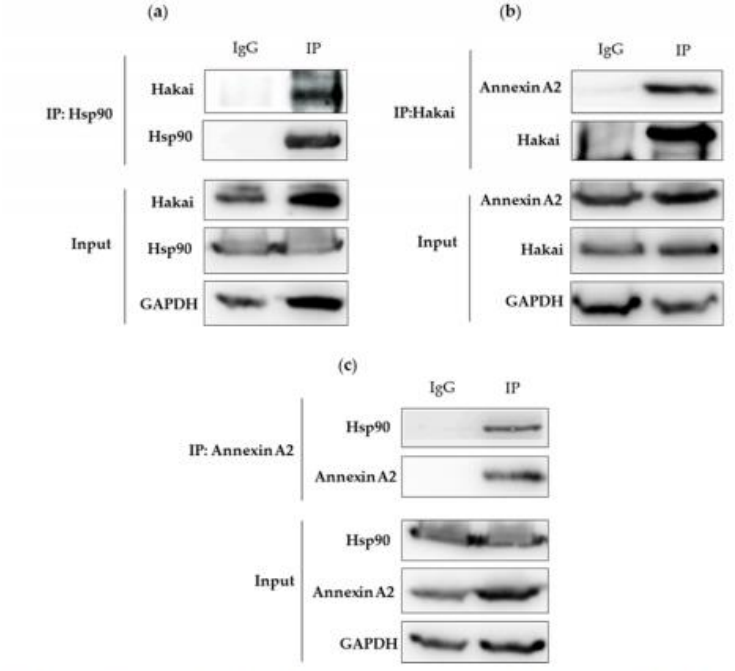

Figure 2. Hakai, Annexin A2, and Hsp90 interact with other: The whole cell extracts of HCT116 cell line cells were prepared and subjected to a co-immunoprecipitation assay. Subsequent western-blotting analysis was performed by using Hakai, Annexin A2, or Hsp90 antibodies **(a)** Hakai is specifically detected in anti-Hsp90 immunoprecipitates. **(b)** Annexin A2 is specifically detected in anti-Hakai immunoprecipitates. **(c)** Hsp90 is specifically detected in anti-Annexin A2 immunoprecipitates. GAPDH signal was used as protein loading control.

2.3. Hakai Regulates Annexin A2 Protein Expression

In order to understand the meaning of the interaction between Hakai, Annexin A2 and Hsp90, first, we decided to confirm the previous proteomic study on which Annexin A2 was downregulated in stably Hakai-overexpressing MDCK cells compared to normal cells [21]. On one hand, it is reported that Hakai interacts with Src tyrosine-phosphorylated substrates, an on the other hand, Annexin A2 is tyrosine-phosphorylated by Src kinase [12,27]. We carried out a transient transfection of Flag-Hakai together with Src and HA-ubiquitin in HEK293T cells to favor the activity of the ubiquitin-mediated degradation system. Besides, co-overexpression of Hakai with Src favors the increase of Hakai levels

[12,16]. As expected, Annexin A2 protein expression was significantly reduced by Hakai overexpression, while Hsp90 protein expression was not affected (Figure 3a, Supplementary Figure S6). Moreover, silencing Hakai protein levels by transiently transfecting two different Hakai siRNAs statistically significant increased Annexin A2 expression in HEK293T (Figure 3b, Supplementary Figure S6) and in HCT116 cells (Figure 3c, Supplementary Figure S6), without affecting Hsp90 protein expression. Moreover, this upregulation of Annexin A2 in HEK293T cell line was accompanied with an increase protein levels of the best-described substrate for the E3 ubiquitin-ligase Hakai, E-cadherin [12,16]. These data suggest that Hakai may act as an E3 ubiquitin-ligase for Annexin A2 protein, inducing its degradation.

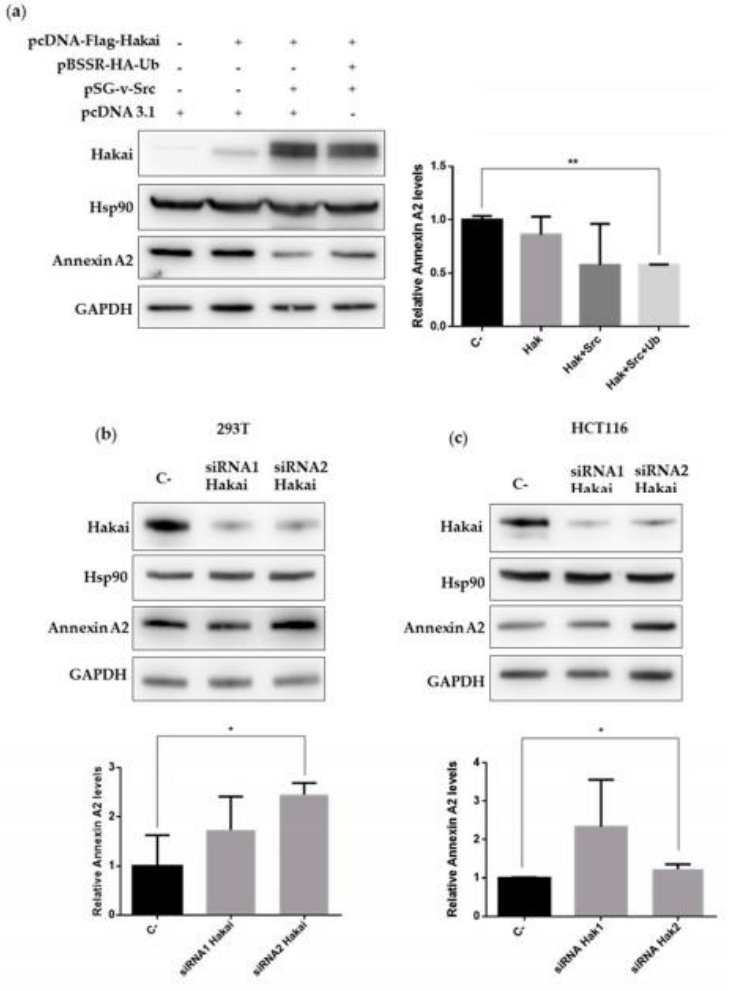

Figure 3. Hakai regulates Annexin A2 expression levels: (**a**) HEK293T cells were transiently transfected with pcDNA-Flag-Hakai (4 μg), pBSSR-HA-ubiquitin (3 μg) and pSG-v-Src (3 μg) plasmids for 48 h. Cells were harvested and the levels of endogenous Annexin A2 levels and Hsp90 were determined by western blot analysis (left panel) and quantified by densitometry (right panel). The effect of the indicated transfected siRNA-Hakai on Annexin A2 and Hsp90 levels were tested in

293T cells (**b**) and HCT116 (**c**). Whole-cell lysates were subjected to western-blotting 72 h after transfection (top) and protein expression was quantified by densitometry (bottom) using GAPDH as loading control for normalization. Relative quantification of Annexin A2 expression levels was graphically represented as Mean ± SEM for two independent experiments for panel a and three for panel b and c (* $p < 0.05$, ** $p < 0.01$, *** $p < 0.001$).

2.4. *Hsp90 Inhibitor Geldanamycin Induces Downregulation of Hakai Protein via Lysosome*

Geldanamycin is probably the best described Hsp90 inhibitor so far and acts by blocking its ATP binding site, preventing the correct folding of the client proteins that, in consequence, often turns into the degradation through proteasome [28,29]. Given the previously detected interaction between Hsp90, Hakai, and Annexin A2, we decided to study whether geldanamycin may affect these protein interactions. As shown, the described interaction between Hakai, Hsp90 and Annexin A2 was completely disrupted in presence of geldanamycin when using Hakai or Annexin A2 antibodies for the immunoprecipitation assays (Figure 4, Supplementary Figure S7). Given that Annexin A2 is proposed as a potential new substrate for the E3 ubiquitin-ligase Hakai and that geldanamycin disrupts the interaction between Hakai and Hsp90, it is open the possibility that Hakai might be a direct client protein for Hsp90 chaperone. In order to test whether geldanamycin could downregulate Hakai, we used two different concentrations of geldanamycin Hsp90 inhibitor (10 μM and 20 μM) and we treat two different cell lines, HEK293T and HCT116 cells for 16 and 24 h. The cells were collected and subjected to western-blotting analysis. As shown, geldanamycin treatment decreases Hakai protein levels in both cell lines tested, while an increase of Annexin A2 was detected (Figure 5a, Supplementary Figure S8). Furthermore, we found that treatment with geldanamycin did not decrease Hakai mRNA levels supporting that Hsp90 inhibitor downregulates Hakai at the post-transcription level (Figure 5b, Supplementary Figure S8). Moreover, we tested the effect of Hsp90 inhibitor on the downregulation of Hakai by transiently transfecting Flag-Hakai together with v-Src, and HA-ubiquitin in HEK293T cells. Hakai levels were drastically reduced in presence of geldanamycin compared to non-treated control transfected conditions, accompanied by an increase of Annexin A2 protein levels (Figure 5c, Supplementary Figure S8). These data confirm that geldanamycin is able to downregulate both endogenous and ectopically expressed Hakai while it upregulates Annexin A2. Finally, the effect on Hakai and Annexin A2 protein levels was tested by combining geldanamycin treatment together with two different siRNA Hakai oligos. HCT116 cells were transiently transfected with the indicated siRNA Hakai oligos for 72 h and treated with 10 μM geldanamycin for 24 h. Reduction of Hakai expression levels was accentuated when combining geldanamycin treatment together with the previously tested siRNA Hakai oligos, leading to almost Hakai completely disappearance (Figure 5d, Supplementary Figure S8). On the contrary, Annexin A2 levels were significantly increased. Altogether, these data demonstrate that geldanamycin Hsp90 inhibitor induce Hakai protein downregulation via post-transcriptional mechanism and support that Annexin A2 is a new substrate for the E3 ubiquitin-ligase Hakai protein.

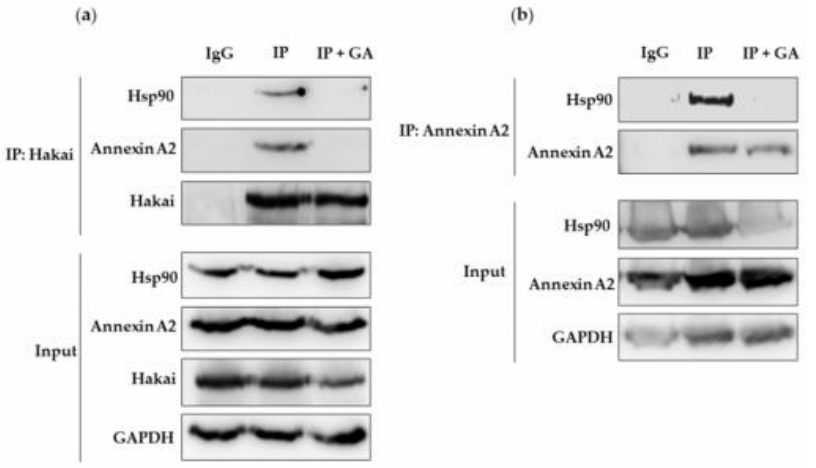

Figure 4. Geldanamycin treatment disrupts Hakai, Hsp90 and Annexin A2 interaction: HCT116 cell line was treated with 10 μM geldanamycin for 24 h. **(a)** Immunoprecipitation was performed by using Hakai antibody. Subsequent western blotting-analysis was performed using Hakai, Annexin A2, or Hsp90 antibodies. **(b)** Immunoprecipitation was performed by using Annexin A2 antibody and western blotting analysis was performed using Hakai and Hsp90 antibodies. GAPDH was used as protein loading control.

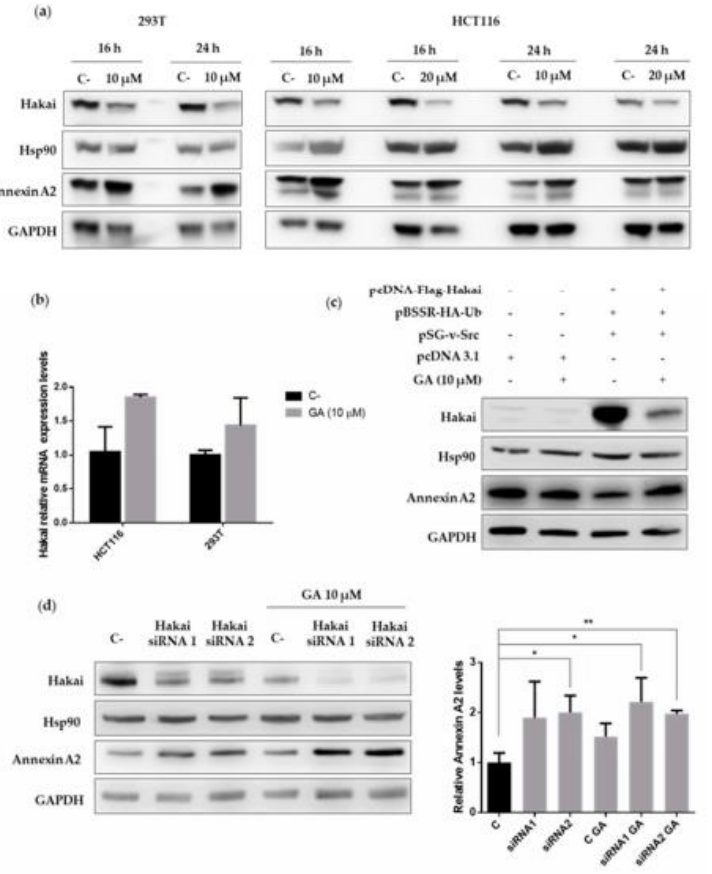

Figure 5. Geldanamycin reduces Hakai protein expression accompanied with an increase of Annexin A2: (**a**) HEK293T and HCT116 cells were treated with geldanamycin at the indicated times and concentrations. Cell lysates were collected and subjected to western blot analysis with the indicated antibodies. (**b**) HCT116 and HEK293T cell lines were treated with geldanamycin for 24 h at the indicated concentration. Cells were collected and subjected to mRNA extraction followed by RT-qPCR. Levels of Hakai mRNA normalized to control (HPRT) mRNA were measured and graphically represented as Mean ± SEM for three independent experiments (* $p < 0.05$, ** $p < 0.01$, *** $p < 0.001$). (**c**) HEK293T cells were transiently transfected with pcDNA 3.1 (10 μg) empty vector or pcDNA-Flag-Hakai (4 μg), pBSSR-HA-ubiquitin (3 μg) and pSG-v-Src (3 μg) plasmids for 48 h. Cells were treated with 10 μM geldanamycin 24 h after transfection. Cells were collected and protein levels were evaluated by western-blotting with the indicated antibodies. (**d**) HCT116 cells were transfected with Hakai siRNA-1 and siRNA-2 oligos for 72 h and treated with 10 μM geldanamycin for the last 24 h of transfection. Cell lysates were collected and protein expression was evaluated by western- blotting with the indicated antibodies. Relative quantification of Annexin A2 expression levels was graphically represented as Mean ± SEM for three independent experiments (* $p < 0.05$, ** $p < 0.01$, *** $p < 0.001$).

As previously mentioned, Hakai is an E3 ubiquitin-ligase for E-cadherin that plays a role on the epithelial–mesenchymal transition program. Given the effect of geldanamycin on Hakai expression,

we also analyzed the effect of geldanamycin on the cell phenotype. HCT116 epithelial cells were treated for 24 h with geldanamycin with the indicated concentrations showing a more epithelial phenotype under the treatment. Indeed, HCT116 loses the mesenchymal phenotype accompanied by decreasing cellular protrusions (Figure 6a). Moreover, we also analyzed the localization of Annexin A2 and E-cadherin by immunofluorescence. Annexin A2 expression was increased in presence of the geldanamycin showing a statistically enriched pattern in cytoplasm and cell membrane (Figure 6b).

On the other hand, we also observed a three-fold increase expression of E-cadherin at cell–cell contacts in presence of geldanamycin (Figure 6c). All these data support that Hakai is downregulated by geldanamycin inhibitor, which in consequence may influence the upregulation of E-cadherin and Annexin A2 proteins, and further reinforce the hypothesis of Hakai being an Hsp90 client protein.

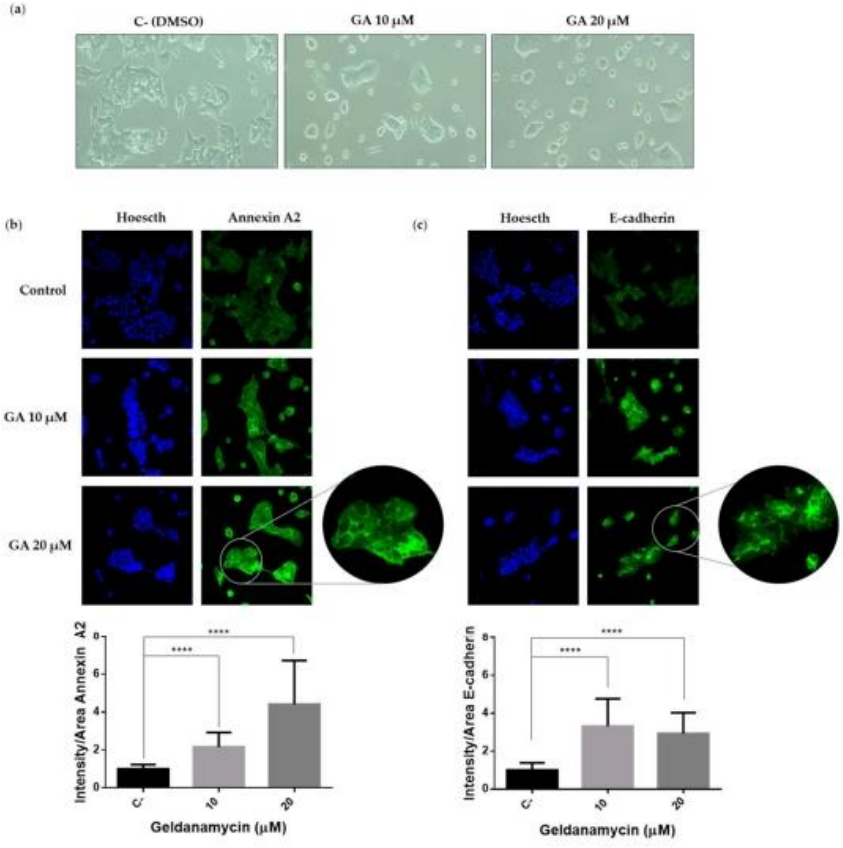

Figure 6. Geldanamycin induces an epithelial-like phenotype accompanied by an increase expression of E-cadherin and Annexin A2: HCT116 cell line was treated at the indicated concentrations of geldanamycin (GA) for 24 h. (**a**) Images of HCT116 were taken by optical microscopy. (**b**) Representative immunofluorescence images of Annexin A2 are shown (upper panel) and fluorescence intensity quantification is represented (lower panel). (**c**) Representative immunofluorescence images of E-cadherin are shown (upper panel) and fluorescence intensity quantification is represented (lower panel). Images were taken with confocal microscope by employing 40X magnification objective. A zoom image of 80X magnification was included. Annexin A2 and E-cadherin were stained in green, and cell nuclei were counterstained with Hoechst. Quantification of intensity/area was represented as Mean ± SEM (* $p < 0.05$, ** $p < 0.01$, *** $p < 0.001$, **** $p < 0.0001$).

Then, we further investigated the possible mechanism of Hakai degradation under geldanamycin treatment. First, we analyzed the effect on Hakai protein expression of proteasome inhibitor MG132 and the lysosome inhibitor chloroquine (CQ). As shown, Hakai protein expression was increased in presence of chloroquine while no effect was observed in presence of MG132 (Figure 7a, Supplementary Figure S9), further indicating that Hakai may be degraded in a lysosome-dependent manner. Besides, Hakai levels increase was accompanied by a downregulation of Annexin A2, supporting the previously obtained results that suggest that Annexin A2 is as a new possible target protein for Hakai E3 ubiquitin-ligase. Next, we analyzed the mechanism by which Hakai is degraded in absence of Hsp90 function. In order to better detect Hakai downregulation under geldanamycin treatment, HEK293T cells were transiently transfected with Hakai, Src and Ubiquitin for 48 h and treated in presence or absence of geldanamycin and chloroquine for 24 h and protein lysates were analyzed by western blot. As shown, chloroquine lysosome inhibitor efficiently prevented Hakai degradation induced by geldanamycin (Figure 7b, Supplementary Figure S9). Accordingly, Annexin A2 was upregulated under geldanamycin treatment while this effect was reverted in combination with chloroquine inhibitor. Moreover, the well-described substrate for the E3 ubiquitin-ligase Hakai, E-cadherin, was also regulated in a similar manner than Annexin A2. All these data support that Hsp90 inhibitor geldanamycin induces downregulation of its client protein Hakai in a lysosome-dependent manner. Moreover, Hakai substrate E-cadherin was also regulated in a similar manner than Annexin A2. All these data support that Hsp90 inhibitor geldanamycin induces downregulation of its client protein Hakai in a lysosome-dependent manner. Moreover, E-cadherin and Annexin A2, were also affected by geldanamycin treatment, suggesting the involvement of Hsp90 chaperone in the regulation of Hakai specific substrates.

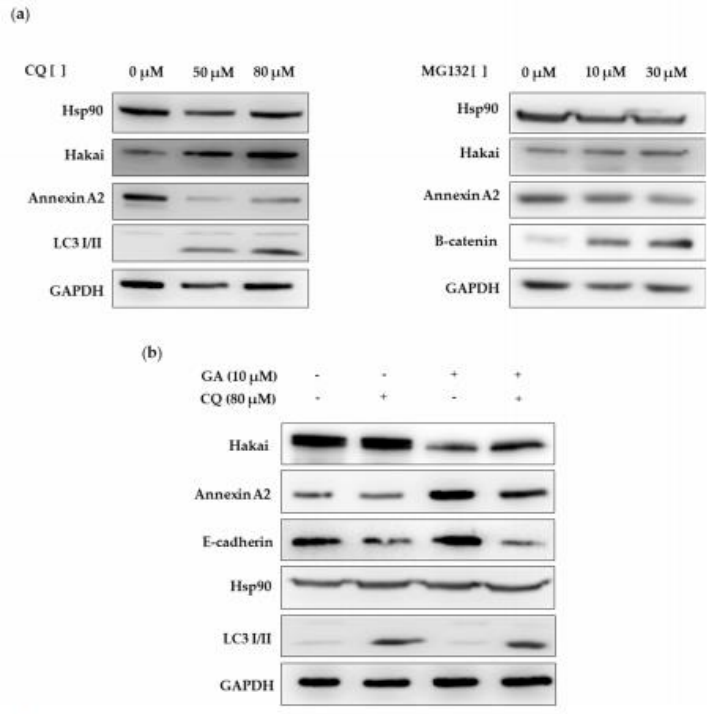

Figure 7. Geldanamycin increases Hakai protein degradation in a lysosome-dependent manner: **(a)** HEK293T cells were treated with chloroquine (left panel) and with MG132 (right panel) for 24 h at the indicated concentrations. Cell lysates were collected and evaluated by western blot analyses with

Hakai and Annexin A2 antibodies. (**b**) HEK293T cells were transiently transfected with pcDNA-Flag-Hakai (4 μg), pBSSR-HA-Ubiquitin (3 μg) and pSG-v-Src (3 μg) for 48 h. The day after transfection, cells were treated with chloroquine and geldanamycin at the indicated concentrations for 24 h. Cell lysates were collected and protein expression was evaluated by western blot analyses using the indicated antibodies. Chloroquine treatment-induced Hakai protein levels recovery during geldanamycin treatment. LC3 I/II levels was used as a positive control in chloroquine treatment and β-catenin as positive control in MG132 treatment.

2.5. Downregulation of Hakai May Partially Account for the Pharmacological Anti-Migratory Effect of Geldanamycin Hsp90 Inhibitor

HSP90 is required for the stability and function of numerous oncogenic proteins, and its specific inhibitors display multiple anticancer effects [30–32]. On the other hand, Hakai is considered an oncogenic protein that was reported to be overexpressed in various cancers such as colon and lung cancer [16,19,20], furthermore, Hakai knockdown inhibits cell migration [33]. Therefore, we decided to test whether Hsp90 geldanamycin inhibitor may indeed influence the migratory effect driven by Hakai. Transwell migration assay was performed in HEK293T by transiently transfected with pcDNA 3.1 or pcDNA-Flag-Hakai. HEK293T cells transfected with pcDNA-Flag-Hakai would strongly increase cell migration compared to cells transfected with an empty vector (Figure 8). This migratory capability induced by Hakai overexpression was drastically reduced in presence of geldanamycin. herefore, our results support that geldanamycin treatment affects Hakai-mediated cell migration by reducing Hsp90 activity and consequently affecting Hakai-induced migration capacity.

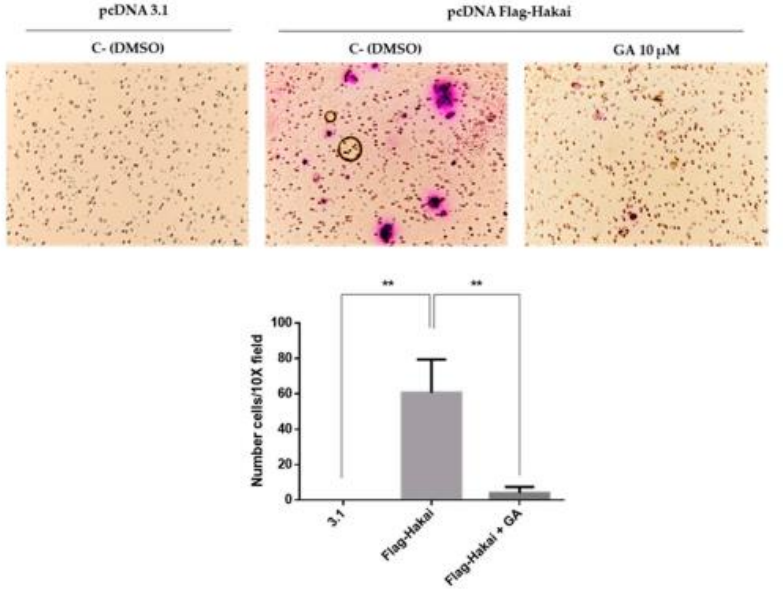

Figure 8. Geldanamycin reduces Hakai-induced cell migration: HEK293T cells were transiently transfected with 8 μg of empty vector pcDNA 3.1 or pcDNA-Flag-Hakai for 54 h and motility was evaluated by transwell migration assay in presence or absence of 10 μM geldanamycin. Cells were seeded into migration transwells 48 h after transfection and let to migrate for 16 h in a gradient concentration of FBS (1–30%). Then cells were fixed and stained as indicated in methods. Images were obtained by optical microscopy with an objective of 10X magnification. Representative images taken using the 10X objective are shown (**upper panel**) and quantification of migrating cells is shown

(bottom panel). Results are represented as as Mean ± SEM of triplicates (* $p < 0.05$, ** $p < 0.01$, *** $p < 0.001$).

2.6. Hsp90 Is Highly Expressed in Colorectal Cancer Samples Compared to Adjacent Normal Epithelial Tissues

The results described thus far suggest a link between Hsp90 and Hakai using an in vitro model. We previously demonstrated that Hakai expression levels are correlated to colorectal tumor progression, being proposed as a novel biomarker for colon cancer progression. Indeed, Hakai expression is gradually increased according to clinical TNM Classification System from UICC in adenoma and in different TNM stages (I–IV) from colon adenocarcinomas compared to human healthy colon tissues [20]. In order to ascertain whether Hsp90 might be involved in colorectal cancer *in vivo*, we investigated Hsp90 expression in human colorectal cancer patient samples. We performed immunohistochemistry experiments in samples of colorectal cancer patients, including healthy tissue, adenoma, and TNM stages I to IV of colorectal cancer. Hsp90 expression, but not Hsp70 (Supplementary Figure S3), is highly increased in carcinoma samples (TNM stage I–IV) compared to healthy epithelial tissue and adenoma (Figure 9). The changes in Hsp90 expression during colorectal cancer progression further support a pathological role for Hsp90 during tumor progression. Taken together, our studies reveal that Hsp90 is a critical regulator of Hakai protein expression and we propose that its influence on Hakai-regulated genes may, at least partially, impact in tumor progression.

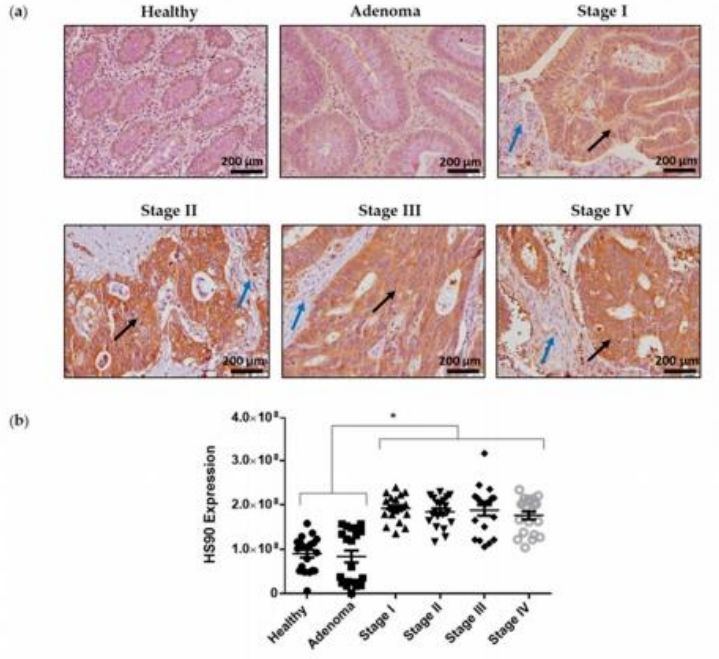

Figure 9. Hsp90 expression levels in colorectal cancer human samples: **(a)** Representative images of Hsp90 immunoreactivity in normal colonic mucosa, adenoma and colorectal cancer (TNM stages I–IV). Images were obtained with 20× objective. Scale bar 125 µm. **(b)** Statistical quantification of Hsp90 staining intensity in epithelial cancer cells at different colon cancer stages and in adenoma and normal colon tissue. A total of 30 human colon samples were analysed including: different TNM stages (I–IV) from colon adenocarcinomas, colon adenoma compared to human colon healthy tissues (normal

colonic mucosa, n = 5; adenoma, n = 5; colorectal cancer, n = 5 of all stages) Scale bar, 200 μm. Black arrows show tumoral tissue and blue arrows show stromal tissue. Five photographs of each tissue were quantified and data are represented as scatter plot. Results are represented as Mean ± SEM for signal intensity scoring per area. Analysis was performed by employing Kruskal-Wallis with Tukey correction test (* $p < 0.05$; ** $p < 0.01$; *** $p < 0.001$).

3. Discussion

Hsp90 chaperone has been widely described to be implicated in cancer progression by regulating client proteins described as hallmarks in cancer disease. Most of the Hsp90 client proteins are implicated in cellular processes such as regulators of cellular proliferation, proteins of oxidative stress or proteins implicated in cellular differentiation between others [2]. Interestingly, a recent study show that more than a hundred E3 ubiquitin-ligases interact with Hsp90 and therefore many of them awaits to be elucidated [1,9]. In this study, we have shown that the E3 ubiquitin-ligase Hakai is a novel Hsp90-interacting protein (Figure 1). It is generally established that the interaction between Hsp90 and their client proteins results on the degradation of the clients by the ubiquitin-dependent proteasome pathway [5–7]. Indeed, pharmacological inhibition of the folding activity of Hsp90 is coupled to the action of different E3 ubiquitin-ligases, such as Cullin-5 and CHIP, that signal for ubiquitinization and degradation of the specific Hsp90 client proteins that have not been correctly folded [22,34]. Although this is the best-described mechanism, we demonstrate that Hakai is a novel client protein for Hsp90 (Figure 5). So far UHRF1 was the only reported E3 ubiquitin-ligase described as a client protein for Hsp90 [35]. Our results underscore that pharmacological inhibition of Hsp90 by geldanamycin results in the degradation of Hakai in a lysosome-dependent manner (Figure 7). A major challenge for future study is to identify the exact ubiquitin-ligase that mediates Hakai degradation upon pharmacological inactivation of Hsp90. To our knowledge, this proteasome-independent mechanism of degradation under Hsp90 geldanamycin inhibition was only previously described for IκB kinase. In this work, authors demonstrate that Hsp90 client protein IκB kinase (IkK), an essential activator of NF-kB, is degraded by autophagy when inhibiting Hsp90 with geldamacyn [8].

In previous work from our lab, we demonstrated that Annexin A2 is downregulated in Hakai-overexpressing MDCK epithelial cells compared to non-transformed MDCK cells [21]. Moreover, it has been previously shown an interaction between Annexin A2 and Hsp90 in vitro an in vivo in diabetic rat's aorta [25]. Based on these reported results, and given the interaction confirmed between Hsp90 and Hakai in different cell lines, we were also interested in determining the possible relationship between Annexin A2, Hakai and Hsp90. As shown in Figure 2, by immunoprecipitation we confirmed an endogenous interaction between Hakai, Hsp90 and Annexin A2 in HCT116 cell line (Figure 2). Annexin A2 belongs to annexin family and is involved in the dynamic organization of membrane microdomains and the formation of membrane-cytoskeleton and membrane-membrane contacts [36]. Annexin A2 is tyrosine-phosphorylated by Src kinase [27] and, as previously mentioned, Hakai interacts with Src tyrosine-phosphorylated substrates inducing their ubiquitination and degradation, turning Annexin A2 into a potential substrate for Hakai. Transient overexpression of Hakai, Src and ubiquitin significantly downregulates Annexin A2 expression levels, and Hakai silencing give rise to an upregulation of endogenous Annexin A2 expression (Figure 3). These data confirm the direct regulation of Annexin A2 by Hakai, and suggest Annexin A2 could be a novel substrate protein for its E3 ubiquitin-ligase activity. Furthermore, the inhibition of Hsp90 with geldanamycin completely disrupted the interaction between Hakai, Hsp90 and Annexin A2 (Figure 4), while a decrease Hakai expression and an increase of Annexin A2 expression is observed. Moreover, a recovery of an epithelial phenotype in HCT116 cell line after geldanamycin treatment was observed, accompanied by an increase of Annexin A2 in cell membrane and E-cadherin at cell–cell contacts. Finally, geldanamycin reduces Hakai-induced cell migration. All these data support that the effect of the inhibition of Hsp90 by geldanamycin regulates Hakai client protein stability and, in consequence, E-cadherin Hakai-substrate and Annexin A2 are increased, which may partially account for the pharmacological the anti-migratory and the reversion of the EMT. This data

are according to previously reported results on which ganetespib treatment or HSP90 knockdown downregulated molecular pathways associated with EMT and motility [37].

Despite the broadly described role of Annexin A2 as a poor-prognosis marker during cancer progression, it has recently been reported to be induced for degradation by other oncogenic E3 ubiquitin-ligases, such as TRIM65 [38,39]. Furthermore, Annexin A2, involved in the membrane-cytoskeleton dynamics, was demonstrated to play a role in the recovery of E-cadherin at adherens junctions due to its effect on actin cytoskeleton [40], further supporting the above-explained phenotype observed during geldanamycin treatment. On the other hand, it was shown that geldanamycin stabilizes E-cadherin through the degradation of Hsp90 client protein ErbB2, responsible of increasing β-catenin-E-cadherin association and thus, contributing to the maintenance of the epithelial phenotype [41]. These results suggest that geldanamycin might revert EMT process at least partially due to its effect on the stability of Hakai client protein of Hsp90, and in consequence supports Hakai effect on E-cadherin substrate and Annexin A2.

In this study, we evaluated the expression of Hsp90 in different colon adenocarcinoma stages in order to find an implication of this chaperone during tumor progression. Previous findings of our group show that Hakai expression is increased during colon cancer progression and it is considered as a novel biomarker for colon cancer development [20]. We show an increased expression of Hsp90 in human colorectal cancer samples compared to adenoma and to adjacent healthy tissue but no differences were detected between TNM stages I to IV, further suggesting the role of Hsp90 in the acquisition of tumor malignancy in colon cancer. This data are according to the correlation between Hsp90 expression and poor outcome in patients with colorectal cancer [42]. Given that Hakai oncogene is also aberrantly highly expressed in colorectal cancer [10,13,20,43], and the demonstrated interaction between Hsp90 and Hakai *in vitro*, future investigations on the role of Hsp90 and Hakai in vivo await to be elucidated. Promoting the degradation of Hsp90 oncogenic client proteins by inhibiting Hsp90 is considered as a promising new anticancer strategy [44,45]. Since the appearance of the first generation Hsp90 inhibitors, such as geldanamycin and radicicol, many derivative compounds have been developed and studied for cancer treatment and subjected to clinical trials [29,46]. Although Hsp90 inhibition has been widely studied for the treatment of different types of cancer, Hsp90 inhibition-based monotherapy has not yet reached the expected results due to different resistance mechanisms. So far, for colorectal cancer only combined therapies using Hsp90 inhibitors with chemotherapeutic agents have been successful [47]. Given that one of the drug resistance mechanisms is based on an induced EMT, the development of Hakai inhibitors together with Hsp90 inhibitors could be an attractive strategy for therapeutic interventions.

4. Materials and Methods

4.1. Plasmids, Antibodies, and Inhibitors

pcDNA-Flag-Hakai, pBSSR-HA-Ubiquitin, and pSG-v-Src were previously described (Fujita et al., 2002), pcDNA 3.1, pEGFP-C1 and pEGFP-Hakai were provided by Dr. Fujita (Institute for Genetic Medicine, Hokkaido University, Japan), and pcDNA-Flag-HA-Hsp90 was kindly provided by Dr. Paweł Bieganowski (Mossakowski Medical Research Centre Polish Academy of Sciences, Poland). For western blot Hakai antibody (36-2800, Invitrogen, Carlsbad, CA, USA) was used at 1:1000. Hsp90 antibody (sc-13119, Santa Cruz, Dallas, TX, USA) was used at 1:1000. Annexin A2 antibody (sc-28385, Santa Cruz, TX, USA) was used at 1:500. LC3 A/B antibody (4108, Cell Signaling, Leiden, The Netherlands) was employed at 1:1000. E-cadherin antibody (610182, BD Trans Lab, Franklin Lakes, NJ, USA) was employed at 1:1000. β-catenin antibody (Cell Signaling, Leiden, The Netherlands) was employed at 1:1000. GAPDH antibody (39-8600, Invitrogene) was used at 1:10,000. Mouse and rabbit secondary antibodies (NA934V, NA931V, GE Healthcare, Chicago, IL, USA) were used at 1:10,000. For immunofluorescence Hakai and Hsp90 antibodies were used at 1:100 concentration, Annexin A2 antibody (sc-47696, Santa Cruz, Dallas, TX, USA) was used at 1:50 and E-cadherin antibody (610182, BD Trans Lab, Franklin Lakes, NJ, USA) was used at 1:100. Alexa fluor 568-conjugated and Alexa fluor 488-conjugated antibodies (A10042, A11001, Thermofisher, Whaltham, MA, USA) were used at

a concentration of 1:200. For immunoprecipitation, Hakai antibody (A302-969A, Bethyl, Montgomery, TX, USA), Hakai-2498 (provided by Yasuyuki Fujita), Annexin A2 (sc-47696, Santa Cruz, Dallas, TX, USA) and Hsp90 (sc-28385, Santa Cruz, Dallas, TX, USA) Protein A-Agarose (sc-2001, Santa Cruz, Dallas, TX, USA) Protein G PLUS-Agarose (sc-2002, Santa Cruz, Dallas, TX, USA), normal mouse IgG (sc-2025, Santa Cruz, Dallas, TX, USA) and normal rabbit IgG (A300-289A, Bethyl, Montgomery, TX, USA) were used.

For immunohistochemistry Hsp90 antibody (ab13492, Abcam, Cambridge, UK) was used at 1:500. Proteasome inhibitor MG132 (Sigma-Aldrich, St. Louis, MO, USA) was added for 6 h using 10 μM and 30 μM. Lysosome degradation inhibitor Chloroquine (c-6628, Sigma-Aldrich, St. Louis, MO, USA), proteasome inhibitor MG132 (M8699, Sigma-Aldrich, St. Louis, MO, USA) and HSP90 Geldanamycin inhibitor (T6343, TargetMol, Wellesley Hills, MA, USA) were employed as indicated in figure legends.

For Hsp90 chaperone activity, HEK293T and HCT116 were incubated with geldanamycin at the indicated times and concentrations. Lysosome degradation inhibition was performed by incubating cells with chloroquine for 24 h at the indicated concentrations. Proteasome degradation inhibition was performed by incubating cells with MG132 for 6 h at the indicated concentrations.

4.2. Cell Culture and Transfection

HEK293T, HCT116, and ACHN cell lines were cultured in Dulbecco's Modified Eagle's Medium (DMEM) (Gibco, Thermofisher). HT29 cell line was cultured in McCoy's Modified medium and LoVo cell line was cultured in F-12K medium (Kaighn's Modification of Ham's F-12 Medium) (Gibco, Thermo Fisher Scientific). All media were supplemented with 10% heat-inactivated fetal bovine serum (FBS) and 1% penicillin/streptomycin. All cell lines were grown at 37°C in a humidified incubator with 5% of CO2. All cell lines were periodically tested for mycoplasma. Transfection experiments were performed by employing Lipofectamine 2000 Transfection Reagent (Thermo Fisher Scientific) and Opti-MEM (Thermo Fisher Scientific) media following manufacturer's protocol. Transfection was performed for 24 or 48 as indicated in figure legends.

4.3. Western Blot Analysis and Immunoprecipitation

For protein extraction, cells were lysed employing 1% Triton X-100 buffer (20 mM Tris-HCl pH 7.5, 150 mM NaCl and 1% Triton X-100) supplemented with 1 mM phenylmethylsulfonyl fluoride and 1× leupeptin/aprotinin mix. Lysis was performed for 30 min at 4 °C and centrifuged at 14,000× *g* for 10 min. Protein quantification was performed by employing Pierce BCA Protein Assay Kit (Thermo Fisher Scientific) following manufacturer's indications. Twenty micrograms of protein sample were loaded in polyacrylamide gels. Western blot protocol was performed as previously described (Cano et al., 2000). Densitometric quantification was performed by using ImageJ Software (National Institutes of Health, NIH). For immunoprecipitation, protein extracts from 100 mm dishes were incubated with 60 μL of Protein A Agarose Beads (for rabbit antibodies) or Protein G PLUS-Agarose (for mouse antibodies) (sc-2001, sc-2002, Santa Cruz, Dallas, TX, USA) for 1 h at 4 °C in rotation for pre-clearing. Hakai-2498 and commercial antibodies or control IgG were incubated onto 60 μL of beads in 500 μL of PBS-Tween 20 1% for 1 h in rotation at 4 °C. Beads were precipitated by centrifugation at 3000 rpm, 2 min at 4 °C and 80 μL of supernatants were collected for input total lysates. Supernatants were incubated for 2 h with beads-antibody complexes at 4 °C on rotation. Beads were washed twice with lysis buffer and samples were prepared for western blotting by adding 40 μL of Laemmli buffer to the immunoprecipitated sample and 20 μL to the input sample.

4.4. Human Samples and Immunohistochemistry

Human colorectal cancer samples were collected by Pathological Anatomy department of Complejo Hospitalario Universitario de A Coruña (CHUAC) under informed consent from the patients. Research Ethics Committee from A Coruña-Ferrol approved their use for investigation according to the standard ethical procedures described in the "Ley Orgánica de Investigación

Biomédica" of 14 July 2007 of the Spanish regulation (ethical protocol code: 2015/024). Paraffin samples were transferred by CHUAC Biobank, included in the Spanish Hospital Platform Biobanks Network. For immunohistochemistry, slides containing sections of tumors were deparaffinized for 1 h at 60 °C in the stove. Once dewaxed, the slides were rehydrated by successive incubations in xylol (10 min), xylol (10 min), ethanol 100° (10 min), ethanol 96° (10 min), ethanol 70° (10 min) and water (5 min). Antigen retrieval was performed by boiling the slides for 15 min using target retrieval solution pH 6.1 (Agilent, Santa Clara, CA, USA). Slides were washed with PBS-T 1% for 10 min and peroxidase blocking solution (DakoCytomation, Glostrup, Denmark) was added for 30 min at RT. Slides were washed and carefully dried and blocked with blocking solution (0.2% BSA/0.1% Triton X-100 in PBS pH 7.6) for 30 min at RT. Incubation with primary antibody was carried out in a wet chamber overnight at 4 °C. Following primary antibody incubation, slides were washed three times for 10 min and incubated with secondary antibody (Dako REAL™ Envision™ Detection System). Slides were washed three times and revealed with diaminobenzidine (Dako REAL™ Envision™ Detection System) for 2 min. Slides were washed with water for 5 min and counterstained with Gill's Hematoxylin for 20 s. Samples dehydratation was performed following the opposite sequence of alcohols for rehydratation. Samples were mounted with the coverslips using DePeX (Serva, Heidelberg, Germany). Pictures were obtained with Olympus microscope employing the objectives indicated in figure legends. Hsp90 postivity was evaluated based on brown-color developed by diaminobenzidine intensity.

4.5. Immunofluorescence Assays

Immunofluorescence was performed as previously described. Briefly were plated in sterile glass coverslips contained in 6-well plates washed twice with PBS-Tween 1%, fixed with PFA 4% for 15 min and permeabilized with 0.5% Triton X-100/PBS for 15 min. After permeabilization, cells were blocked for 1 h with culture medium supplemented with 10% FBS. Primary antibodies were incubated for 2 h at RT. Secondary antibody was incubated at RT for 1 h. Nuclear staining was performed by employing 1:10,000 Hoechst dilution (Life Technologies, Carlsbad, CA, USA). ProLong Gold Antifade Mountant (Life Technologies, Carlsbad, CA, USA) was employed for coverslips mounting. Images were obtained by using confocal microscope Nikon A1R. Immunofluoresce intensity was evaluated by employing ImageJ software (National Institutes of Health, NIH). Intensity of ten different areas for two different replicates were quantified and relativized against the mean control area. Values are the means ± SEM of the staining intensity signal scoring per area. Calibration and quantification of the images were performed with ImageJ software. Statistical analysis was carried out by using unpaired Student's *t*-test at the indicated significance levels.

4.6. RNA Interference

Hakai silencing was performed by employing two different siRNA oligonucleotides: Hakai-1 (CTCGATCGGTCAGTCAGGAAA) and Hakai-2 (CACCGCGAACTCAAAGAACTA). Oligonucleotides were transfected into cells by using Lipofectamine 2000 Transfection reagent (Thermo Fisher Scientific). Transfection reaction was prepared by mixing 2 μL (200 pmol) of 100 μM oligonucleotides with 4 μL and proceeded as for plasmid transfection. Same quantity of Mission Universal Non-coding siRNA (Sigma-Aldrich, St. Louis, MO, USa) was used as a negative control of transfection. Cells were transfected for 72 h.

4.7. Real-Time Quantitative PCR (RT-qPCR)

HCT116 and HEK293T total RNA was extracted using TriPure isolation reagent (Roche, Basel, Switzerland). mRNA levels were analysed in technical triplicates by quantitative RT-PCR, following specifications of reverse retrotranscriptase kit (NZYTech, Lisbon, Portugal). Amplification was performed in a Light Cycler 480 (Roche, Basel, Switzerland) and data was analysed by qBase+ analysis software (Biogazelle, Zwijnaarde, Belgium). Primers used for Hakai were F' TGCTATGACTGTGCATTTTACATGA and R' ACTGCTAATTCGCTGCAC. HPRT was used as

housekeeping using primers F' TGACCTTGATTTATTTTGCATACC and R' CGAGCAAGACGTTCAGTCCT.

4.8. Migration Assay

Cell migration assay was performed by employing 24-well Cell Migration Plate 8 µm (Merck Millipore, Burlington, MA, USA) HEK293T cells were transiently transfected for 48 h as indicated. Cells were starved 18 h prior to assay. After 48 h of transfection, cells were collected and seeded at a confluence of 3×10^5 cells/transwell in a gradient of 1–30% FBS between upper and lower chamber respectively. Cells were let to migrate for 16 h and non-migratory cells were carefully removed from de upper chamber with a moistened cotton swap. Migratory cells were fixed for 20 min with 4% PFA, rinsed with PBS pH 7.4 and stained with crystal violet for 20 min. Finally, transwells were rinsed with PBS pH 7.4 and membrane was removed and mounted onto slides. Migratory cells were photographed with an Olympus BX50 employing a 10× objective.

4.9. Statistical Analysis

Analysis was performed by employing GraphPad Prism 6 Software (GraphPad Software Inc., San Diego, CA, USA). Western blotting statistical analysis was carried out by using unpaired Student's *t*-test at the indicated significance levels. Graphical representations of results are expressed as Mean ± SEM. Statistical analysis for immunofluorescence was carried out by performing comparative student's *t* test. Results are represented as Mean ± SEM for 10 areas of two different photographs. Migration assay quantification was performed by quantifying the number of migratory cells per 10× objective field for three different photographs. Statistical analysis was performed by employing Student's *t*-test and represented as Mean ± SEM for three photographs of one experiment. Human IHQ quantification was performed by using Kruskal-Wallis with Tukey correction test. Significance of both Student's *t*-test and Kruskal-Wallis with Tukey correction is indicated in the figures as * $p < 0.05$, ** $p < 0.01$ and *** $p < 0.001$.

5. Conclusions

In this study, we have demonstrated that the E3 ubiquitin-ligase Hakai is a novel client protein for Hsp90. Although the best-described mechanism for degradation of the Hsp90 clients proteins is through a ubiquitin-dependent proteasome pathway, we have shown that pharmacological inhibition of Hsp90 by geldanamycin results in the degradation of Hakai in a lysosome-dependent manner. Together with the disappearance of Hakai by geldanamycin treatment, a more epithelial phenotype was observed, accompanied by an increase expression of Hakai E-cadherin substrate at cell–cell contacts and Annexin A2 at plasma membrane. More importantly, geldanamycin reduces Hakai-induced cell migration, further underscoring the possible impact of Hsp90 inhibitors on EMT and tumor progression by its action on Hakai stability.

Supplementary Materials: The following are available online at www.mdpi.com/xxx/s1, Figure S1: Concentration-dependent and kinetics assays for Hakai and Hsp90, Figure S2: Co-localization of Hsp90 and Hakai in different colon cancer cells, Figure S3: Hsp70 expression levels in human samples from colorectal cancer patients, Figure S4: Full blots corresponding to Figure 1, Figure S5: Full blots corresponding to Figure 2, Figure S6: Full blots corresponding to Figure 3, Figure S7: Full blots corresponding to Figure 4, Figure S8: Full blots corresponding to Figure 5, Figure S9: Full blots corresponding to Figure 7, Figure S10: Full blots corresponding to Supplementary Figure S1.

Author Contributions: Conceptualization, A.F. and A.D.-D.; formal analysis, A.D.-D. and D.R.-L.; validation, A.D.-D., D.R.-L., A.C.-P., G.C., A.C. formal analysis G.R., B.G. and G.C.; investigation A.D.-D., D.R.-L., A.C.-P., G.C.; data curation, A.D.-D. and A.F.; supervision, A.F.; writing—original draft preparation, A.F. and A.D.-D.; writing—review and editing, all authors.; project administration, A.F.; funding acquisition, A.F. All authors have read and agreed to the published version of the manuscript.

Funding: This work has been supported by Plan Estatal I + D + I 2013–2016, co-funded by the Instituto de Salud Carlos III (ISCIII, Spain) under grant agreements PI13/00250 and PI18/00121 by Fondo Europeo de Desarrollo Regional (FEDER) "A way of Making Europe". The project leading to these results has received funding from

"la Caixa" Foundation (ID 100010434) under the agreement (LCF/TR/CI19/52460016). Also supported by Seed project (NEODIANAR) from Conselleria de Cultura, Educación y Ordenación Universitaria, by PRIS3 project-ACIS, both from Xunta de Galicia and by I.M.Q. San Rafael Foundation from A Coruña,. A.D-D has been supported by FPU contract (FPU014/02837) from Ministerio de Educación, Cultura y Deporte from Spain; A.C-P Casas-Pais by a predoctoral contract (IN606A-2017/013) from Axencia Galega de Innovación (GAIN)-Consellería de Economía, Empleo e Industria from Xunta de Galicia, Spain and D.R-L was supported by Profesor Novoa Santos Foundation and by Diputacion A Coruña.

Acknowledgments: We thank A Coruña Biobank (B.0000796) for providing clinical samples.

Conflicts of Interest: The authors declare no conflict of interest.

References

1. Schopf, F.H.; Biebl, M.M.; Buchner, J. The HSP90 chaperone machinery. *Nat. Rev. Mol. Cell Biol.* **2017**, *18*, 345–360.
2. Hoter, A.; El-Sabban, M.E.; Naim, H.Y. The HSP90 Family: Structure, Regulation, Function, and Implications in Health and Disease. *Int. J. Mol. Sci.* **2018**, *19*, 2560.
3. Drysdale, M.J.; Brough, P.A.; Massey, A.; Jensen, M.R.; Schoepfer, J. Targeting Hsp90 for the treatment of cancer. *Curr. Opin. Drug Discov. Devel.* **2006**, *9*, 483–495.
4. Panaretou, B.; Prodromou, C.; Roe, S.M.; O'Brien, R.; Ladbury, J.E.; Piper, P.W.; Pearl, L.H. ATP binding and hydrolysis are essential to the function of the Hsp90 molecular chaperone in vivo. *EMBO J.* **1998**, *17*, 4829–4836.
5. Schneider, C.; Sepp-Lorenzino, L.; Nimmesgern, E.; Ouerfelli, O.; Danishefsky, S.; Rosen, N.; Hartl, F.U. Pharmacologic shifting of a balance between protein refolding and degradation mediated by Hsp90. *Proc. Natl. Acad. Sci. USA* **1996**, *93*, 14536–14541.
6. Saibil, H. Chaperone machines for protein folding, unfolding and disaggregation. *Nat. Rev. Mol. Cell Biol.* **2013**, *14*, 630–642.
7. Grbovic, O.M.; Basso, A.D.; Sawai, A.; Ye, Q.; Friedlander, P.; Solit, D.; Rosen, N. V600E B-Raf requires the Hsp90 chaperone for stability and is degraded in response to Hsp90 inhibitors. *Proc. Natl. Acad. Sci. USA* **2006**, *103*, 57–62.
8. Qing, G.; Yan, P.; Xiao, G. Hsp90 inhibition results in autophagy-mediated proteasome-independent degradation of IkappaB kinase (IKK). *Cell Res.* **2006**, *16*, 895–901.
9. Taipale, M.; Krykbaeva, I.; Koeva, M.; Kayatekin, C.; Westover, KD.; Karras, GI.; Lindquist, S. Quantitative analysis of HSP90-client interactions reveals principles of substrate recognition. *Cell* **2012**, *150*, 987–1001.
10. Mukherjee, M.; Chow, SY.; Yusoff, P.; Seetharaman, J.; Ng, C.; Sinniah, S.; Koh, XW.; Asgar, NF.; Li, D.; Yim, D. et al. Structure of a novel phosphotyrosine-binding domain in Hakai that targets E-cadherin. *EMBO J.* **2012**, *31*, 1308–1319.
11. Cooper, J.A.; Kaneko, T.; Li, S.S. Cell regulation by phosphotyrosine-targeted ubiquitin ligases. *Mol. Cell Biol.* **2015**, *35*, 1886–1897.
12. Fujita, Y.; Krause, G.; Scheffner, M.; Zechner, D.; Leddy, H.; Behrens, J.; Sommer, T.; Birchmeier, W. Hakai, a c-Cbl-like protein, ubiquitinates and induces endocytosis of the E-cadherin complex. *Nat. Cell Biol.* **2002**, *4*, 222–231.
13. Aparicio, L.A.; Valladares, M.; Blanco, M.; Alonso, G.; Figueroa, A. Biological influence of Hakai in cancer: A 10-year review. *Cancer Metastasis Rev.* **2012**, *31*, 375–386.
14. Ye, X.; Weinberg, R.A. Epithelial-Mesenchymal Plasticity: A Central Regulator of Cancer Progression. *Trends Cell Biol.* **2015**, *25*, 675–686.
15. Aparicio, L.A.; Blanco, M.; Castosa, R.; Concha, Á.; Valladares, M.; Calvo, L.; Figueroa, A. Clinical implications of epithelial cell plasticity in cancer progression. *Cancer Lett.* **2015**, *366*, 1–10.
16. Figueroa, A.; Kotani, H.; Toda, Y.; Mazan-Mamczarz, K.; Mueller, E.; Otto, A.; Disch, L.; Norman, M.; Ramdasi, R.; Keshtgar, M.; et al. Novel roles of hakai in cell proliferation and oncogenesis. *Mol. Biol. Cell* **2009**, *20*, 3533–3542.
17. Rodríguez-Rigueiro, T.; Valladares-Ayerbes, M.; Haz-Conde, M.; Aparicio, L.A.; Figueroa, A. Hakai reduces cell-substratum adhesion and increases epithelial cell invasion. *BMC Cancer* **2011**, *11*, 474.
18. Abella, V.; Valladares, M.; Rodriguez, T.; Haz, M.; Blanco, M.; Tarrío, N.; Iglesias, P.; Aparicio, L.A.; Figueroa, A. miR-203 Regulates Cell Proliferation through Its Influence on Hakai Expression. *PLoS ONE* **2012**, *7*, e52568.

19. Hui, L.; Zhang, S.; Wudu, M.; Ren, H.; Xu, Y.; Zhang, Q.; Qiu, X. CBLL1 is highly expressed in non-small cell lung cancer and promotes cell proliferation and invasion. *Thorac. Cancer* **2019**, *10*, 1479–1488.
20. Castosa, R.; Martinez-Iglesias, O.; Roca-Lema, D.; Casas-Pais, A.; Díaz-Díaz, A.; Iglesias, P.; Santamarina, I.; Graña, B.; Calvo, L.; Valladares-Ayerbes, M.; et al. Hakai overexpression effectively induces tumour progression and metastasis in vivo. *Sci. Rep.* **2018**, *8*, 3466.
21. Díaz-Díaz, A.; Casas-Pais, A.; Calamia, V.; Castosa, R.; Martinez-Iglesias, O.; Roca-Lema, D.; Santamarina, I.; Valladares-Ayerbes, M.; Calvo, L.; Chantada, V.; et al. Proteomic Analysis of the E3 Ubiquitin-Ligase Hakai Highlights a Role in Plasticity of the Cytoskeleton Dynamics and in the Proteasome System. *J. Proteome Res.* **2017**, *16*, 2773–2788.
22. Ehrlich, E.S.; Wang, T.; Luo, K.; Xiao, Z.; Niewiadomska, A.M.; Martinez, T.; Xu, W.; Neckers, L.; Yu, X.F. Regulation of Hsp90 client proteins by a Cullin5-RING E3 ubiquitin ligase. *Proc. Natl. Acad. Sci. USA* **2009**, *106*, 20330–20335.
23. Connell, P.; Ballinger, C.A.; Jiang, J.; Wu, Y.; Thompson, L.J.; Höhfeld, J.; Patterson, C. The co-chaperone CHIP regulates protein triage decisions mediated by heat-shock proteins. *Nat. Cell Biol.* **2001**, *3*, 93–96.
24. Xu, W.; Marcu, M.; Yuan, X.; Mimnaugh, E.; Patterson, C.; Neckers, L. Chaperone-dependent E3 ubiquitin ligase CHIP mediates a degradative pathway for c-ErbB2/Neu. *Proc. Natl. Acad. Sci. USA* **2002**, *99*, 12847–12852.
25. Lei, H.; Romeo, G.; Kazlauskas, A. Heat shock protein 90alpha-dependent translocation of annexin II to the surface of endothelial cells modulates plasmin activity in the diabetic rat aorta. *Circ Res.* **2004**, *94*, 902–909.
26. Bharadwaj, A.; Bydoun, M.; Holloway. R.; Waisman, D. Annexin A2 heterotetramer: Structure and function. *Int. J. Mol. Sci.* **2013**, *14*, 6259–6305.
27. Stebbins, C.E.; Russo, A.A.; Schneider, C.; Rosen, N.; Hartl, F.U.; Pavletich, N.P. Crystal structure of an Hsp90-geldanamycin complex: Targeting of a protein chaperone by an antitumor agent. *Cell* **1997**, *89*, 239–250.
28. Garg, G.; Khandelwal, A.; Blagg, B.S. Anticancer Inhibitors of Hsp90 Function: Beyond the Usual Suspects. *Adv. Cancer Res.* **2016**, *129*, 51–88.
29. Rodina, A.; Vilenchik, M.; Moulick, K.; Aguirre, J.; Kim, J.; Chiang, A.; Litz, J.; Clement, C.C.; Kang, Y.; She, Y.; et al. Selective compounds define Hsp90 as a major inhibitor of apoptosis in small-cell lung cancer. *Nat. Chem. Biol.* **2007**, *3*, 498–507.
30. Fiskus, W.; Verstovsek, S.; Manshouri, T.; Rao, R.; Balusu, R.; Venkannagari, S.; Rao, N.N.; Ha, K.; Smith, J.E.; Hembruff, S.L.; et al. Heat shock protein 90 inhibitor is synergistic with JAK2 inhibitor and overcomes resistance to JAK2-TKI in human myeloproliferative neoplasm cells. *Clin. Cancer Res.* **2011**, *17*, 7347–7358.
31. Ha, K.; Fiskus, W.; Rao, R.; Balusu, R.; Venkannagari, S.; Nalabothula, N.R.; Bhalla, K.N. Hsp90 inhibitor-mediated disruption of chaperone association of ATR with hsp90 sensitizes cancer cells to DNA damage. *Mol. Cancer* **2011**, *10*, 1194–1206.
32. Weng, C.H.; Chen, L.Y.; Lin, Y.C.; Shih, J.Y.; Tseng, R.Y.; Chiu, A.C.; Yeh, Y.H.; Liu, C.; Lin, Y.T.; Fang, J.M.; et al. Epithelial-mesenchymal transition (EMT) beyond EGFR mutations per se is a common mechanism for acquired resistance to EGFR TKI. *Oncogene* **2019**, *38*, 455–468.
33. Zhou, P.; Fernandes, N.; Dodge, I.L.; Reddi, A.L.; Rao N.; Safran., H.; DiPetrillo, T.A.; Wazer, D.E.; Band, V.; Band, H. ErbB2 degradation mediated by the co-chaperone protein CHIP. *J. Biol. Chem.* **2003**, *278*, 13829–13837.
34. Ding, G.; Chen, P.; Zhang, H.; Huang, X.; Zang, Y.; Li, J.; Wong, J. Regulation of Ubiquitin-like with Plant Homeodomain and RING Finger Domain 1 (UHRF1) Protein Stability by Heat Shock Protein 90 Chaperone Machinery. *J. Biol. Chem.* **2016**, *291*, 20125–20135.
35. Hitchcock, J.K.; Katz, A.A.; Schäfer, G. Dynamic reciprocity: The role of annexin A2 in tissue integrity. *J. Cell Commun. Signal.* **2014**, *8*, 125–133.
36. Hayes, M.J.; Moss, S.E. Annexin 2 has a dual role as regulator and effector of v-Src in cell transformation. *J. Biol. Chem.* **2009**, *284*, 10202–10210.
37. Nagaraju, G.P.; Long, T.E.; Park, W.; Landry, J.C.; Taliaferro-Smith, L.; Farris, A.B.; Diaz, R.; El-Rayes, B.F. Heat shock protein 90 promotes epithelial to mesenchymal transition, invasion, and migration in colorectal cancer. *Mol. Carcinog.* **2015**, *54*, 1147–1158.
38. Wei, W.S.; Chen, X.; Guo, L.Y.; Li, X.D.; Deng, M.H.; Yuan, G.J.; He, L.Y.; Li, Y.H.; Zhang, Z.L; Jiang, L.J.; et al. TRIM65 supports bladder urothelial carcinoma cell aggressiveness by promoting ANXA2 ubiquitination and degradation. *Cancer Lett.* **2018**, *435*, 10–22.

39. Chen, G.; Chen, W.; Ye, M.; Tan, W.; Jia, B. TRIM59 knockdown inhibits cell proliferation by down-regulating the Wnt/β-catenin signaling pathway in neuroblastoma. *Biosci. Rep.* **2019**, *39*, doi:10.1042/BSR20181277.
40. Yamada, A.; Irie, K.; Hirota, T.; Ooshio, T.; Fukuhara, A.; Takai, Y. Involvement of the annexin II-S100A10 complex in the formation of E-cadherin-based adherens junctions in Madin-Darby canine kidney cells. *J. Biol. Chem.* **2005**, *280*, 6016–6027.
41. Bonvini, P.; An, W.G.; Rosolen, A.; Nguyen, P.; Trepel, J.; Garcia de Herreros, A.; Dunach, M.; Neckers, L.M. Geldanamycin abrogates ErbB2 association with proteasome-resistant beta-catenin in melanoma cells, increases beta-catenin-E-cadherin association, and decreases beta-catenin-sensitive transcription. *Cancer Res.* **2001**, *61*, 1671–1677.
42. Barrott, J.J.; Haystead, T.A. Hsp90, an unlikely ally in the war on cancer. *FEBS J.* **2013**, *280*, 1381–1396.
43. Chatterjee, S.; Burns, T.F. Targeting Heat Shock Proteins in Cancer: A Promising Therapeutic Approach. *Int. J. Mol. Sci.* **2017**, *18*, 1978, doi:10.3390/ijms18091978.
44. Sidera, K.; Patsavoudi, E. HSP90 inhibitors: Current development and potential in cancer therapy. *Recent Pat. Anticancer Drug Discov.* **2014**, *9*, 1–20.
45. Kryeziu, K.; Bruun, J.; Guren, T.K.; Sveen, A.; Lothe, R.A. Combination therapies with HSP90 inhibitors against colorectal cancer. *Biochim. Biophys. Acta Rev. Cancer* **2019**, *1871*, 240–247.
46. Zhang, S.; Guo, S.; Li, Z.; Li, D.; Zhan, Q. High expression of HSP90 is associated with poor prognosis in patients with colorectal cancer. *PeerJ* **2019**, *7*, e7946.
47. Aparicio, L.A.; Castosa, R.; Haz-Conde, M.; Rodríguez, M.; Blanco, M.; Valladares, M.; Figueroa, A. Role of the microtubule-targeting drug vinflunine on cell-cell adhesions in bladder epithelial tumour cells. *BMC Cancer* **2014**, *14*, 507.

APPENDIX D

AKNOWDLEDGEMENTS

This work has been supported by funds from:

- Ministerio de Educación, Cultura y Deporte from Spain. FPU contract (FPU014/02837) and mobility grant (EST17/00146).
- Instituto de Salud Carlos III (ISCIII, Spain) and Plan Estatal I + D + i. Grant agreements PI13/00250 and PI18/00121 by Fondo Europeo de Desarrollo Regional (FEDER) "A way of Making Europe".
- Obra Social "la Caixa"-La Caixa Capital Risc. CaixaImpulse program (ID 100010434) under the agreement (LCF/TR/CI19/52460016).
- Agencia Gallega para la Gestión del Conocimiento en Salud (ACIS) Xunta de Galicia. Programa de Desarrollo Precomercial de los Resultados de Investigación. Grant agreement Tercer PRIS3.
- Fundación San Rafael.
- Consellería de Cultura, Educación y Ordenación Universitaria. Xunta de Galicia. Acción estratégica CICA-INIBIC. Seed project (NEODIANAR) (ED431E 2018/03).
- Red Gallega de Investigación sobre Cáncer Colorrectal (REGICC). Consellería de Cultura, Educación y Ordenación Universitaria. Xunta de Galicia (ED431D 2017/23).